UNIVERSITY OF SOUTHAMPTON

Faculty of Social and Human Sciences

Geography and Environment Academic Unit

Complex dynamical changes in the trophic status of Erhai Lake, China, based on palaeolimnology and modelling

by

Rong Wang

A thesis submitted for the degree of Doctor of Philosophy

March 2013

UNIVERSITY OF SOUTHAMPTON

ABSTRACT

FACULTY OF SOCIAL AND HUMAN SCIENCES

GEOGRAPHY AND ENVIRONMENT ACADEMIC UNIT

Doctor of Philosophy

COMPLEX DYNAMICAL CHANGES IN THE TROPHIC STATUS OF ERHAI LAKE, CHINA BASED ON PALAEOLIMNOLOGY AND MODELLING

by Rong Wang

Nature ecosystems are always complex, full of uncertainties and nonlinear changes. These changes are sometimes catastrophic, and many ecosystems have already been altered from their natural state as a result of human activities. Therefore, abrupt changes are likely to happen, the consequences of which can be irreversible. It becomes urgent to (i) further understand the features of complex ecological systems, and (ii) to identify yearly warning signals (EWS) to allow prediction of catastrophic transitions. This thesis aims for an understanding of one such example of a complex ecological system, i.e. Erhai Lake, Yunnan Province, China, and to determine the EWS in this ecosystem.

This thesis focuses on the process of eutrophication in Erhai Lake, using two cores from the lake and a training set from Yunnan province, SW China. The study employed multiple techniques including monitoring, palaeolimnological proxies and modelling. The ideas of feedbacks, resilience and thresholds from complex ecological system theory are used to interpret the lake's eutrophication process. Fossil diatom data is mainly employed to calculate the EWS for the lake's ecosystem transition. The conclusions have been supported with a minimal model which is written with STELLA software.

The main findings include: 1. The alternative stable states in the training set may affect the accuracy of diatom-based transfer functions. 2. The resilience of the lake's ecosystem decreased due to the intensification of human activities, and the lake crossed a threshold at around 2001 due to a new positive feedback mechanism. 3. The lake was in a 'flickering' state between 1980-2000. Rising variance could be considered as an indicator of EWS but it was most likely caused

by flickering rather than ‘critical slowing down’ in these noise-induced critical transitions. 4. The minimal model shows that flickering states can be simulated, and the rising variance due to flickering is also likely to predict the critical transitions in the simulated system.

The mutual authentication between palaeo- data and the minimal model can deeply improve the understanding of a complex system, and explanation of complex theories. This work firstly considered the alternative stable states in a training set and presented EWS in a real natural ecosystem. Our findings suggest that rising variance can be seen as a warning signal in a system; therefore, it can be applied for intervention purposes in critical transitions in real ecosystems.

Contents

Chapter 1Introduction ..... - 1 -

1.1 Background ..... - 1 -

1.2 Methodology and thesis structure ..... - 3 -

Chapter 2 Complex ecological systems and eutrophication ..... - 7 -

2.1 Introduction ..... - 7 -

2.2 Complex ecological system ..... - 7 -

2.3 Ecosystem state change ..... - 12 -

2.4 Early warning signals for abrupt change ..... - 15 -

2.5 Palaeolimnology on studies of Environment change ..... - 17 -

2.6 Lake Eutrophication ..... - 19 -

2.7 Methods for studying eutrophication ..... - 20 -

2.7.1 Instrumental data ..... - 20 -

2.7.2 Palaeolimnological proxies ..... - 21 -

2.7.3 Mathematical Model ..... - 23 -

2.7.4 An example of an ecosystem dynamic model: STELLA 30

2.8 Summary 32

Chapter 3 Site Description 33

3.1 Introduction 33

3.2 Yunnan Plateau 34

3.3 Erhai Lake and its catchment 36

3.4 Summary 43

Chapter4 Methods 45

4.1 Introduction 45

4.2 Lake Sediment Data 45

4.2.1 Sediment core sampling 45

4.2.2 Sediment core chronology 46

4.3 Surface sediment sampling 46

4.4 Diatoms 47

4.5 Physical and chemical measurements. 47

4.5.1 Magnetic susceptibility 47

4.5.2 Chemical Elements 48

4.5.3 Total nitrogen (TN) and Total organic carbon (TOC) 48

4.5.4 Grain Size 49

4.6 Instrument Data 49
4.7 Statistical methods 49
4.7.1 Diatoms dataset and Fossil diatoms 49
4.7.2 Mathematical methods for critical transitions 50
4.8 Phosphorus budget model simulations 51
Chapter 5 Instrument and document data 53
5.1 Introduction 53
5.2 The timeline of human activities and the lake response 53
5.3 Historical Climate Data 54
5.4 Population and economic change 55
5.5 Land cover 56
5.6 Water level change 58
5.7 Nutrient inputs to Erhai Lake 60
5.8 Summary 64
Chapter 6 Diatom-Environment Training set 65
6.1 Introduction 65
6.2 The influence of alternative states for the accuracy of diatom-based transfer functions 66
6.3 Environment variables in Yunnan Province 68
6.4 Surface Sediment Diatom Communities in Yunnan province datatset 70
6.5 Statistical analysis for the Yunnan training set 71
6.6 Diatom-based phosphorus transfer functions 74
6.7 Discussions 77
6.8 Summary 81
Chapter 7 Palaeolimnological Results and eutrophication at Erhai .. 83
7.1 Introduction 83
7.2 Palaeolimnlogical Results 83
7.2.1 Chronology 83
7.2.2 Total nitrogen (TN) and Total Organic Carbon (TOC) 87
7.2.3 Metal Elements 89
7.2.4 Magnetic Susceptibility 91
7.2.5 Grain Size 92
7.2.6 Diatom communities from core EH2-1 94
7.3 Discussion 98
7.3.1 The accuracy of grain size from the core of EH2-2 98

7.3.2 Landscape process in Erhai catchment 99
7.3.3 Lake ecosystem change 102
7.3.4 Diatom-inferred TP..... 105
7.4 Summary 107

. Chapter 8 Eutrophication in Erhai Lake: resilience theory and early warning signals for critical transitions 109
8.1 Introduction 109
8.2 Resilience and feedbacks in Erhai Lake 109
8.3 Fold bifurcation and hysteresis in Erhai Lake 113
8.4 Response of the lake to disturbances as a complex system 118
8.5 Early warning signals of critical transitions 119
8.6 Early warning signals caused by flickering state 124
8.7 Conclusions 128

Chapter 9 Dynamical changes in Erhai Lake based on modelling ... 129
9.1 Introduction 129
9.2 Why only crop land is chosen 130
***9.3* Catchment delineation 131**
9.4 Runoff and Erosion 135
9.4.1 Runoff 135
9.4.2 Soil Erosion 138
9.5 Phosphorus erosion from Northern Erhai catchment 139
9.6 Phosphorus dynamics in the lake 141
9.7 Early warning signals for simulated critical transitions 144
9.8 Discussions and conclusions 147

Chapter 10 Conclusions and Future studies 149
10.1 Conclusions 149

Reference 153

Appendix I Lake's environment variables in Yunnan datasets 176

Appendix II Species descriptions in Yunnan datasets 178

Appendix III Modelling equations 184

Contents of Figures

Figure 1-1 The methodology for this thesis.. ..... - 4 -
Figure 2-1 The attraction basin of a system. ..... - 10 -
Figure 2-2 Types of system state changes in natural ecosystems ..... - 13 -
Figure 2-3 Continuum response of an ecosystem to environmental conditions. - 15 -
Figure 2-4 An example of dynamic model under STELLA software. 31
Figure 3-1 39 Surface sample sites in Yunnan Plateau 34
Figure 3-2 Temperature changeduring past 50years in Yunnan Plateau 35
Figure 3-3 Erhai Lake and its catchment. 38
Figure 3-4 Diancang Mt. Vegetation types 39
Figure 3-5 Erhai lake's submerged macrophytes in different observation periods. 41
Figure 3-6 Bathymetrical chart of Erhai lake. 42
Figure 5-1 The timeline of human activity and lake response in Erhai Lake and its catchment.. 54
Figure 5-2 Temperature and precipitation recorded by Dali climate station 56
Figure 5-4 Vegetation cover change in Erhai Lake at 1990, 2002, 2006 57
Figure 5-5 Crop yields in Dali city 58
Figure 5-6 Water level fluctuations in Erhai lake during 1952-2009. 59
Figure 5-7 Water discharge in Erhai lake 60
Figure 5-8 TP and TN concentrations in Erhai Lake during 1992-2009 61
Figure 5-9 Algae concentrations in Erhai Lake between 1995-2005 62
Figure 5-10 Lake secchi depth, COD_{Mn} and dissolved oxygen (DO) 63
Figure 6-1 Two conceptual models for the pattern of estimation errors from a diatom-environment training set that contains alternative states 68
Figure 6-2 Cluster analysis of environment variables 72
Figure 6-3 CCA analysis with 4 environmental variables from 4 cluster groups (a, CCA plot with 39 sample sites and four main environmental variables. 74
Figure 6-4 Plots of observed versus predicted log-transformed TP and of the residuals 76

Figure 6-5 The plots of drivers (TP) against diatom states in Yunnan province... 79
Figure 6-6 The estimation errors in the Yunnan training set 87
Figure 7-2 The percentage of total nitrogen and total organic carbon in EH2-1 .. 88
Figure 7-3 Metal Elements diagram in EH2-1 90
Figure 7-4 Magnetic Susceptibility from EH2-1 92
Figure 7-5 Particle size distribution in EH2-2 93
Figure 7-6 Photos from difference depth of EH2-1 core 96
Figure 7-8 DCA, HDI, and diatom-inferred total phosphorus in Erhai lake during the past 130yrs..... 97
Figure 7-9 Graphs showing sediment accumulation rate (calculated from ^{210}Pb), grain size (>60 μm), *F. crontonensis* and magnetic susceptibility. 101
Figure 7-10 Calibrated TP in Erhai lake during past 130yrs 106
Figure 8-1 A simplified systems dynamic framework for the Erhai eutrophication process..... 113
Figure 8-2 Phase-space plots of dissolved nutrient driving variables TP (mg L^{-1} - blue dots) and TN (mg L^{-1} - orange dots) versus diatom state response (DCA, HDI and diatom concentrations). 114
Figure 8-3 Phase diagrams of diatom assemblages (diatom DCA and HDI) and environmental variables 117
Figure 8-4 Summary diagram of changing system dynamics in the Erhai eutrophication process. 119
Figure 8-5 Potential early warning signals of the regime shift in the trophic state 121
Figure 8-6 Various early warning signal metrics for diatom DCA and HDI data.. 123
Figure 8-7 A graphic model of state change in a fold catastrophe system..... 126
Figure 8-8 Gaussian Kernel Density Estimation for DCA (a-c) and HDI (d-f). ... 127
Figure 9-1 The outline of the phosphorus dynamic model in the catchment and inner lake of Erhai 130
Figure 9-2 Northern Erhai Catchment delineation under ArcSWAT 133
Figure 9-3 Comparison of rainfall and runoff in the model under CN=89. It shows

that runoff is highly correlated with rainfall 135
Figure 9-4 Modelling discharge (black curve) and monitoring discharge (grey curve) in Erhai lake (From Jan-1952 to Dec-1974). 137
Figure 9-5 Water discharge modelling from STELLA Erhai model from 1951 to 2009. 137
Figure 9-6 Sediment yield (t/ha) in the northern part of the catchment. 138
Figure 9-7 Soil erosion from modelling. 139
Figure 9-8 Monthly phosphorus erosion from North Erhai lake catchment. 140
Figure 9-9 Yearly phosphorus erosion from North Erhai lake catchment 141
Figure 9-10 Multi-states in the modelling system 142
Figure 9-11 F statistic from P in lake showed that the threshold was crossed at the simulation time around 2600. 143
Figure 9-12 Plot of phosphorus from the catchment against phosphorus in lake showing fold bifurcations (red curve) 144
Figure 9-13 Early warning signals in modelling results 146

Contents of Tables

Table 2-1 List of ten mathematic models.....- 24 -
Table 3-1 Submerged plant resource and its distribution in Erhai lake..... 40
Table 5-1 Fertilizer Applied per unit land (kg/ha)..... 58
Table 6-1 Environmental variable statistics descriptions..... 69
Table 6-2 The performance of WA model in Yunnan Province training set..... 75
Table 7-1 The Calculation of CRS model dates, sedimentation rates and ^{137}Cs for EH2-1..... 84
Table 9-1 Parameters in STELLA model for crop land in the northern catchment 134
Table 9-2 Runoff curve numbers for hydrological soil-cover complexes 136

DECLARATION OF AUTHORSHIP

I, Rong Wang,declare that the thesis entitled “Complex dynamical changes in the trophic status of Erhai Lake, China based on palaeolimnology and modelling” and the work presented in the thesis are both my own, and have been generated by me as the result of my own original research. I confirm that:

- this work was done wholly or mainly while in candidature for a research degree at this University;
- where any part of this thesis has previously been submitted for a degree or any other qualification at this University or any other institution, this has been clearly stated;
- where I have consulted the published work of others, this is always clearly attributed;
- where I have quoted from the work of others, the source is always given. With the exception of such quotations, this thesis is entirely my own work;
- I have acknowledged all main sources of help;
- where the thesis is based on work done by myself jointly with others, I have made clear exactly what was done by others and what I have contributed myself;
- none of this work has been published before submission.

Signed: ……..

Date:…….

Acknowledgements

I would like to thank my supervisors Prof. John Dearing, Dr. Peter Langdon, and Dr. Jo Nield. It is impossible for me to finish the research without their help. The most important thing I learned from them during my PhD study is how to solve the scientific question like a researcher. Your wealth of experiences in the geography makes me know how to comprehensively consider geography questions and represent them in academic way. Meanwhile, I would like to give my thanks to my supervisors' kindness that gives me a wonderful PhD experience in the UK.

Thanks to those who help me with the studies, especially my previous colleges from NIGLAS. Thanks to Prof. Xiangdong Yang for his suggestions about diatoms research in my PhD. Thanks to Dr. Enlou Zhang for supporting me in the fieldwork, laboratory work and providing his chironomid data in Erhai lake. Thanks to Prof. Ji Shen for providing funding supports for the fieldwork and laboratory work. I would also like to thank Dr. Xu Chen for his help in the laboratory.

I would like to thank Thierry Fonville, Tom Bishop, Kim Davies for proofreading my thesis. Thanks to my friends in Southampton, especially my colleges from PLUS, like Gunnar Mallon, Tom Bishop, Ying Wang, and Hayley Essex, they make my office time extremely enjoyable. I would also like to thank Niladri Gupta for his plenty of help for my life in UK.

I would like to give my best thanks and delicate this thesis to my family. My parents do always support me wherever I am and whatever happened. My wife, Mrs Yue Wang, do always patiently discuss many issues in terms of life and research, and thanks to her patience to listen to my comments in physical geography as an economic geographer.

Thanks to ORSAS award and the School of Geography for providing tuition fee and maintenance fee during my PhD, and I would like to thank to GBCET Chinese Student Awards for supporting my last four months maintenance fee. Thanks to China 973 projects (2012CB956104 and 2010CB950201) for providing funding for

Yunnan field work and laboratory tests.

Chapter 1Introduction

1.1 Background

Most of nature's ecosystems are complex and their changes are nonlinear (Bar-Yam, 2003; Lenton et al., 2008). They have typically been assumed to change in a smooth gradual way, but we now know that sudden shifts to alternative states can occur (Scheffer et al., 2001). Therefore, management policies guided by linear ideas will probably result in wrong decisions. Abrupt changes are the cause of uncertain or negative effects on human well-being (Carpenter et al., 2009) and typically happen without any warning (Scheffer et al., 2009). They are sometimes catastrophic (Carpenter et al., 1999b), and difficult to reverse (Scheffer et al., 2001). Many ecosystems have already been disrupted from their natural background (Vitousek, 1994) as a consequence of human activities. Abrupt changes may happen and the consequences may be unacceptable (Rockstrom et al., 2009). Although it has already been proved to be distributed widely in many ecosystems like lakes, rainforest, coral reefs (Carpenter, 2003; Hirota et al., 2011; Nystrom et al., 2000), the related studies are still in the initial stages (Scheffer et al., 2009). It is now important to reconsider the features of complex ecosystem dynamics, such as thresholds or early warning signals (EWS), for prediction of catastrophic transitions (Carpenter and Brock, 2006; Scheffer et al., 2009). The majority of work on EWS detection is based on modelling (Bailey, 2011; Biggs et al., 2009; Brock and Carpenter, 2006; Carpenter and Brock, 2006) or laboratory work (Carpenter et al., 2011); fewtests (Lenton et al., 2008) have been conducted on real nature ecosystems. This project is designed with a case study from Erhai Lake, China, and EWS is examined within the context of this real ecosystem.

Normally, three types of data are employed to understand the ecosystem dynamics: instrument data (Walker and Meyers, 2004), palaeo- data (Dearing et al., 2010; Last et al., 2001a; Smol et al., 2005), and modelling data (Carpenter et al., 1999a; Sterman, 2002). Each of them contributes in a different manner to complex ecosystem understanding, and each of them has its own advantages and

disadvantages. Monitored data are the most accurate, but usually lack long-term records (Dearing et al., 2010). Palaeo- methods provide long-term perspectives, but the accuracy should be carefully considered. Both palaeo- data and monitored data are always collected from a specific site. Therefore, they only reflect the features of complex ecosystem dynamics in that specific case. Modelling studies can provide more general conclusions for a particular type of complex ecosystem (Scheffer and Carpenter, 2003) as well as different timescale behaviour, but their accuracy is restricted by inputs and human-designed dynamics (or mathematic equations). Therefore, there is a clear necessity for combination of the three methods to fully understand a complex ecosystem (Anderson et al., 2006; Battarbee et al., 2005a). This project defines a way to combine three methods together to elucidate the dynamics of Erhai Lake as well as other similar complex ecosystems.

The purpose of this research is to track eutrophication processes and features of state shifts in Erhai Lake with a combination of palaeolimnology data, instrument data and data from a minimal model that only focuses on a minimal set of mechanisms (Scheffer and Beets, 1994). The related topics of complex ecological system, such as resilience, threshold, feedbacks, EWS, will be firstly studied with palaeolimnogical proxies and monitored data, and then the findings will be tested with the modelling results. The project is trying to answer the following questions:

1. Can we assess alternative stable state theory within palaeo-reconstructions and training sets, and what are the implications of this?
2. How did the lake Erhai become eutrophic? What are the effects of different variables (such as climate, water level, nutrients) on the eutrophication process?
3. How does resilience impact on an ecosystem's function in a real lake ecosystem? How does the resilience disappear in a real ecosystem?
4. Can the regime shifts be predicted? What does the EWS look like in a real ecosystem?
5. Which process provides EWS for predicting regime shifts? Can the indicators of EWS identified from Erhai be used for other systems?

1.2 Methodology and thesis structure

The methodology of this PhD project is described in Fig. 1.1. The research areas are focused on Erhai Lake as well as other lakes in Yunnan province, China. 39 lakes from Yunnan Province were collected for a diatom environment dataset and a diatom-based total phosphorus (TP) transfer function is constructed for inferring historical TP in Erhai Lake. Two cores were collected from Erhai Lake, and proxies including diatoms, chemical elements, magnetic susceptibility, grain size, total organic carbon and total nitrogen are employed to reconstruct the lake's eutrophication process based on ^{210}Pb and ^{137}Cs chronology. Hereafter, the combination dataset of transfer function, palaeo- proxies and monitored data were used to reconstruct Erhai Lake's eutrophication process. Meanwhile, a dynamic system model (the Erhai STELLA model) was written to simulate phosphorus output from the catchment and then phosphorus dynamics in Erhai Lake is also simulated. The results from both palaeolimnology and modelling are then used to analyse the lake's regime shift using complex dynamical systems theory. The early warning signals for presaging regime shifts are then calculated, and different indicators are discussed. Finally, the thesis gives suggestions for management and future studies.

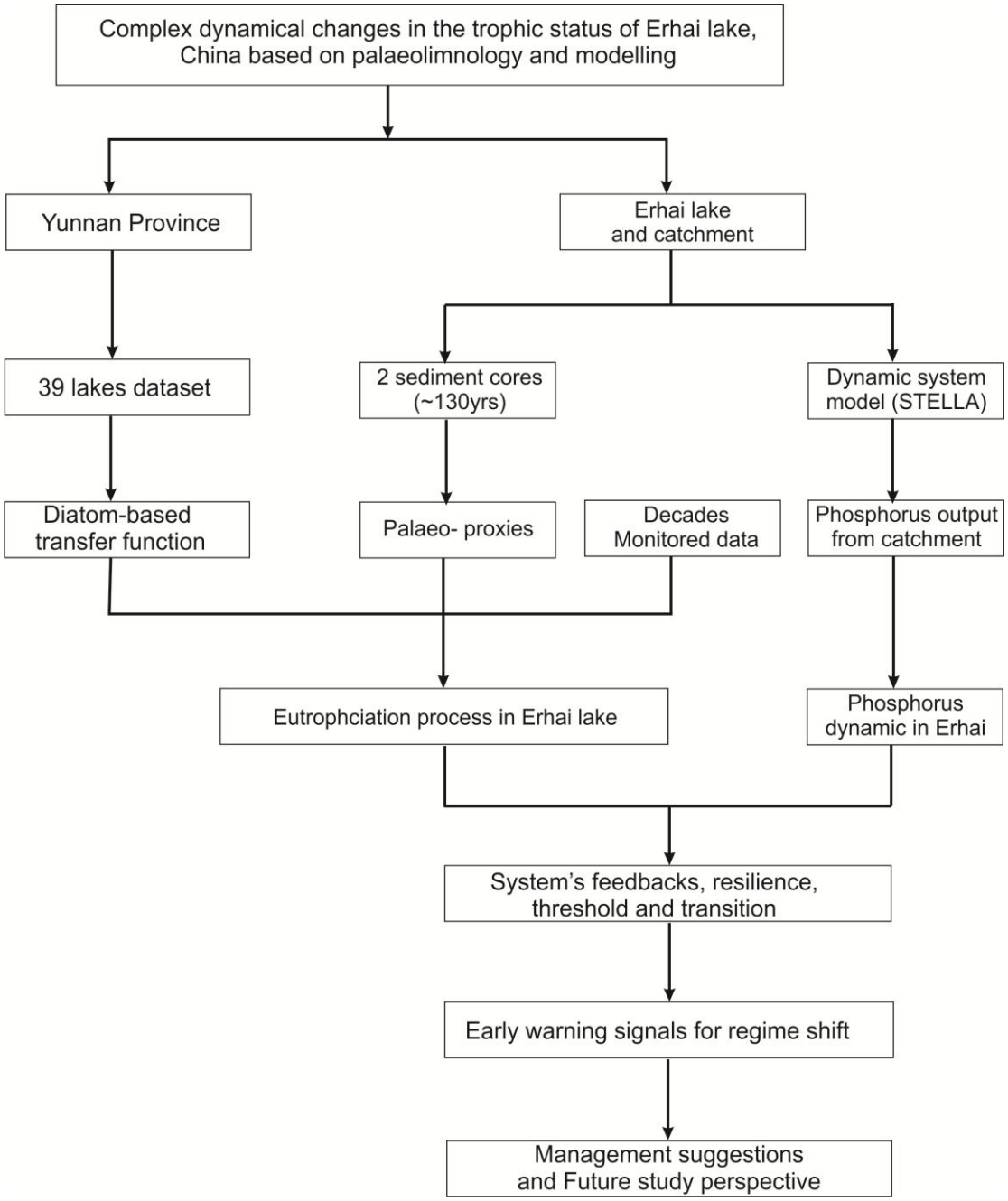

Figure 1-1 The methodology for this thesis. There are three main components: Yunnan diatom environment training set (the left of this diagram); palaeolimnological proxies (the middle of this diagram); STELLA modelling (the right of this diagram). The common purpose is to understand the system's dynamic and then detecting early warning signals for regime shits (the bottom of this diagram).

The structure of this thesis is organized according to the methodology shown in Figure 1.1. Ten chapters will be included. Chapter 2 will introduce the complex

dynamic ecosystems, lake eutrophication, diatom environment training-sets and modelling. The advantages and disadvantages of different methods for studying Lake Eutrophication will be illustrated. The research area will be described in Chapter 3, in which the environment of Yunnan province and Erhai Lake will be described separately. Chapter 4 will give details of techniques used within this thesis including the techniques for data collection, sample collection, measurement of palaeolimnology proxies and modelling techniques. Before introducing the results of the training set and palaeolimnolgical proxies, Chapter 5 will show all the collected data from instruments and documents. Hereafter, the diatom environment training set and TP transfer function will be discussed in Chapter 6. The palaeolimnological results will be shown in Chapter 7, in which all the proxies will be introduced and the TP reconstruction results will also be shown. The lake eutrophication will be discussed with the help of palaeolimnolgical proxies. The eutrophication process in Erhai Lake will be connected to different human activities from both the lake itself and the surrounding catchment area. The theory of complex ecosystems will then be further introduced in Chapter 8 in order to understand the ecosystem's shift, and early warning signals will be detected with these data. In Chapter 9, a minimal model is employed to simulate the phosphorus dynamic in Erhai Lake, and then EWS indicators will be calculated. The results will be compared with the conclusions from Chapter 8. In the last Chapter, answers to the questions posited in the above sections will be presented and the future studies will be suggested in this chapter.

Chapter 2 Complex ecological systems and eutrophication

2.1 Introduction

The planet is suffering from massive pressures from human activities, more than probably any time before (Hirota et al., 2011; Holland et al., 2006; Parry and Intergovernmental Panel on Climate Change. Working Group II., 2007). As a result, there is concern about possible future changes, particularly abrupt regime shifts in complex ecosystems (Scheffer, 2009). Such transitions are sometimes catastrophic, irreversible and without visible warnings, so the related topics of regime shift, including dynamic features, feedbacks, resilience and early warning signals (EWS), are becoming major research priorities. A lake ecosystem is a typical example of a complex ecological system (Holland, 1992; Levin, 1998) and a nonlinear dynamical system (Lansing, 2003; Levin, 2003) in which the interactions among components are complex, and feedbacks in the system maintain the functions through the system's resilience (Walker et al., 2004b). The abrupt changes in many lake ecosystems (Scheffer and Jeppesen, 2007), such as algal blooming, demonstrates the urgency of understanding the dynamics of complex ecological systems and detecting EWS. Different approaches such as instrumental observations, mathematical models and palaeolimnological proxies, play very important but different roles in understanding the complex ecological systems. In this chapter, the types of main ecosystem changes will be reviewed and the main features of a complex ecological system will be discussed. The purpose of this chapter is to introduce the theory behind complex ecological systems and the common methods employed in their study. Lake eutrophication will be introduced as an example of the changing of a complex ecological system.

2.2 Complex ecological system

A complex ecological system is an ecosystem that contains different interactive components (Manson, 2001) and a change of one component may change the ecosystem's patterns (Pascual et al., 2002), structures, behaviour (Swenson et al.,

2000), and functions. The behaviour of a complex ecological system is not just simply the sum of all of its components, but has nonlinear relationships between the drivers and the ecosystem state. This nonlinear dynamic change is one of the most important features for an ecosystem, and it makes the prediction of the ecosystem difficult. For instance, the growth of algae may increase suddenly when the concentration of a nutrient in the lake reaches a certain level (Scheffer, 1998). In this case, the relationship between nutrient supply and algae is nonlinear, and the lake ecosystem is stable before reaching the certain nutrient level. This is the system's tipping point where a small perturbation will lead to large changes in the system (Gunderson, 2000). Before the tipping point, the system has a certain function and a similar pattern, and the system's resilience keeps it stable. The resilience concept was originally introduced to ecology by Holling (1973) to better understand nonlinear dynamic ecosystems (Gunderson, 2000). Resilience is one of many important properties for an ecosystem. It can maintain the patterns of ecosystem components like organic and inorganic components, and allows the ecosystem to provide a sustainable level of service to the human populace. It is necessary to point out that the ecological stable state had previously been confused with the equilibrium point of a state (Holling, 1973). The ecological stable states are dynamic and have the ability to absorb external perturbations (Walker et al., 2004b). Holling (1973) gave the definition for ecological resilience: "*Resilience determines the persistence of relationships within a system and is a measure of the ability of these systems to absorb changes of state variables, driving variables, and parameters, and still persist*" (p. 17). Obviously, the extent of 'absorption' is a good way to monitor the magnitude of an ecosystem's resilience. In another word, the recovery rate of an ecosystem after perturbations can be used to infer the ecosystem's resilience (Holling, 1973). However, resilience as measured by recovery time from disturbance is always called "engineering resilience" (Holling, 1973; Peterson et al., 1998), and seems to be more meaningful for either single or global equilibrium conditions (Gunderson, 2000). The engineering resilience has limited implications in real ecosystems because the recovery time is highly dependent on the magnitude of perturbations. In real world application, the state of an ecosystem is not stable at any one point but has a dynamic equilibrium at different times. Larger perturbation may not

cause obvious fluctuations in ecosystem states when an ecosystem has a high resilience. Walker et al.(2004a) used another definition for ecosystem resilience: '*the capacity of a system to absorb disturbance and reorganize while undergoing change so as to still retain essentially the same function, structure, identity, and feedbacks*'. This definition highlights that a resilient system is able to maintain a function/set of functions despite perturbations. The concept of an attractor basin can be used to understand and illustrate the link between thresholds and resilience (Fig. 2-1). The resilience of an ecosystem is expressed as an attraction basin in Fig. 2-1. The ball represents the state of an ecosystem and a perturbation may move the ball away from the equilibrium state (the basin bottom), and the return time from this perturbation is its engineering resilience. Obviously, the engineering resilience cannot be employed to explain the system change with an alternative state. Therefore, the width of the attraction basin is suggested to represent the resilience of an ecosystem (Beisner et al., 2003). The ball can cross the basin border and enter an alternative state by two means. Firstly, a large perturbation such as a fire, hurricane, or drought event (Scheffer, 2009) may push the ball across the border even though the resilience is high (Fig. 2-1b) (Folke et al., 2004). Secondly, a slow process such as nutrient enrichment in lake will decrease the resilience of attraction basin (Fig. 2-1c), implying that a smaller forcing may trigger the ball to shift to the alternative attractor basin.

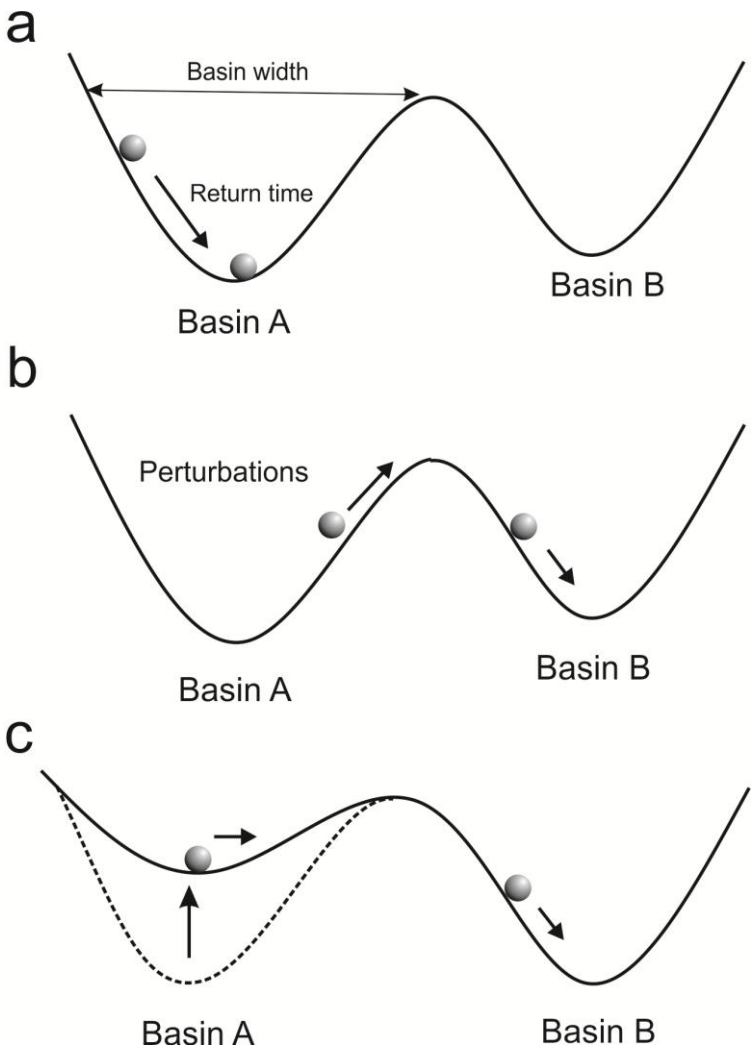

Figure 2-1 The attraction basin of a system: a. Engineering resilience is defined by the time of the system's return back to equilibrium state, and the definition of ecological resilience is the basin width; b. Under high resilience, a fast variable change or large external perturbation may be needed to shift the system to an alternative stable state; c. When a slow process in an ecosystem decreases the ecosystem's resilience, only a small forcing may trigger the shift of the ecosystem state.

The strength of feedbacks in the system should play a very important role in maintaining the system's resilience. Two types of feedback loops have always been considered, i.e. positive feedback loops and negative feedback loops. Positive feedbacks amplify changes and negative feedbacks tend to reduce fluctuations (Nyström et al., 2012). Take the lake system for instance, an increase in the number of algae will reduce the nutrients available so that algal growth in

next time step will be limited. There is then a negative feedback loop between algae and nutrients. In shallow lakes, a positive feedback exists among macrophytes, phytoplankton and zooplankton (Scheffer, 1998), and the macrophytes play a very important role in the feedback (Carpenter, 1981). The macrophytes provide cover for zooplankton from fish, and a high abundance of zooplankton limits the growth of phytoplankton so that the macrophytes have good light conditions for growth (Scheffer, 1998). In deep lakes, the situation is different due to stratification; for example, vertical gradients of temperature, oxygen or light. The role of macrophytes in deep lakes does not seem as important as in shallow lakes, but the vertical profile of oxygen becomes important for the state of the lake. In the summer, the oxygen in the epilimnion (surface layer) is near saturation but there is little or no oxygen in the hypolimnion (deep layer). The living phytoplankton supply oxygen within the epilimnion layer, but the decomposition of these organisms remove oxygen deeper in the water column. A positive feedback among light, phytoplankton and oxygen should be considered because algae growth will increase the turbidity so that light penetrates less deeply, and more organic material falls into the hypolimnion. Bacterial metabolism of this organic material during the summer can reduce hypolimnetic oxygen concentrations to zero. Meanwhile the anoxic condition in the bottom of the lake will increase the phosphorus releasing from the lake sediment; another positive feedback loop among phytoplankton- phosphorus recycling -and anoxic conditions will then become important for the lake's state. The negative feedback maintains the stability of an ecosystem state and keeps the drivers at a certain level (Jeppesen et al, 1997). In contrast, positive feedback loops destabilize the ecosystem and attract the system to the alternative basin (Nyström et al., 2012). The shifts between the two feedbacks in an ecosystem may eventually trigger the abrupt change of the system state. New feedbacks may prevent the altered ecosystem from reverting immediately to the original state (Nyström et al., 2012) so that lags in recovery will appear. This type of response is also called a hysteresis (Scheffer et al., 2001). Hysteresis is important for ecosystem management because it indicates that an abrupt change is difficult to reverse and needs more effort for recovery. It will be introduced in detail in next section.

2.3 Ecosystem state change

Different types of equilibriums between environmental drivers and ecosystem states can be found in natural ecosystems (Scheffer, 2009). Fig. 2-2 highlights three types of relationships between the states and drivers. Fig. 2-2a shows a linear relationship, i.e. the state change is linearly responding to environmental condition change. There is no threshold or tipping point in such a linear responding system. The system state has a little change if a small forcing occurs in the system. In another words, only large perturbations in the environment can cause large changes in the system state. The system can recover on a similar timescale if the environmental conditions change back. This type of relationship is normally considered on a short-term scale or under a limited range of environment conditions, such as the relationship between forest cover and precipitation, and it seems to be unsuitable for long-term scale or full range of environment conditions (Schneider, 2004).Fig. 2-2b shows another type of ecosystem change, i.e. step change ecosystem. This type of ecosystem contains a tipping point that is also called a threshold, and the system will change abruptly around this point even if it is disturbed by only small perturbations. Although small perturbations may cause large shifts in the ecosystem, the recovery of the ecosystem will demonstrate little time-lag or hysteresis if the environmental conditions revert. Therefore the threshold in this ecosystem can be termed a non-catastrophic threshold, which means, for management, that such an ecosystem is easily reversible. In Fig. 2-2c, if the equilibrium of the ecosystem state is folded, not all the states on the equilibrium line are stable. As shown by the arrows in Fig. 2-2c, the dotted equilibrium line is unstable and any small disturbance may trigger a shift to below or above stable equilibrium state, i.e. the solid line. The connections between stable state and unstable state are called fold bifurcation points (i.e. points F1 and F2 in Fig. 2-2c and d). It is also called a catastrophic bifurcation because the environmental conditions must be reversed far beyond the level of the tipping point to recover the previous stable state. Therefore, hysteresis exists in the ecosystems. The ecosystem may shift suddenly when bifurcation points have been crossed (such as Fig, 2-2c) or when an external forcing pushes the ecosystem across the border of an attraction basin (Fig. 2-2d). The deterioration of lake water quality is a good example for this type of change. An extreme

temperature spike or hurricane (James et al., 2008; Scheffer et al., 2001) can cause water quality deterioration (Fig. 2-2d), and long-term nutrient enrichment can also trigger the state of algal blooming (Fig. 2-2c)

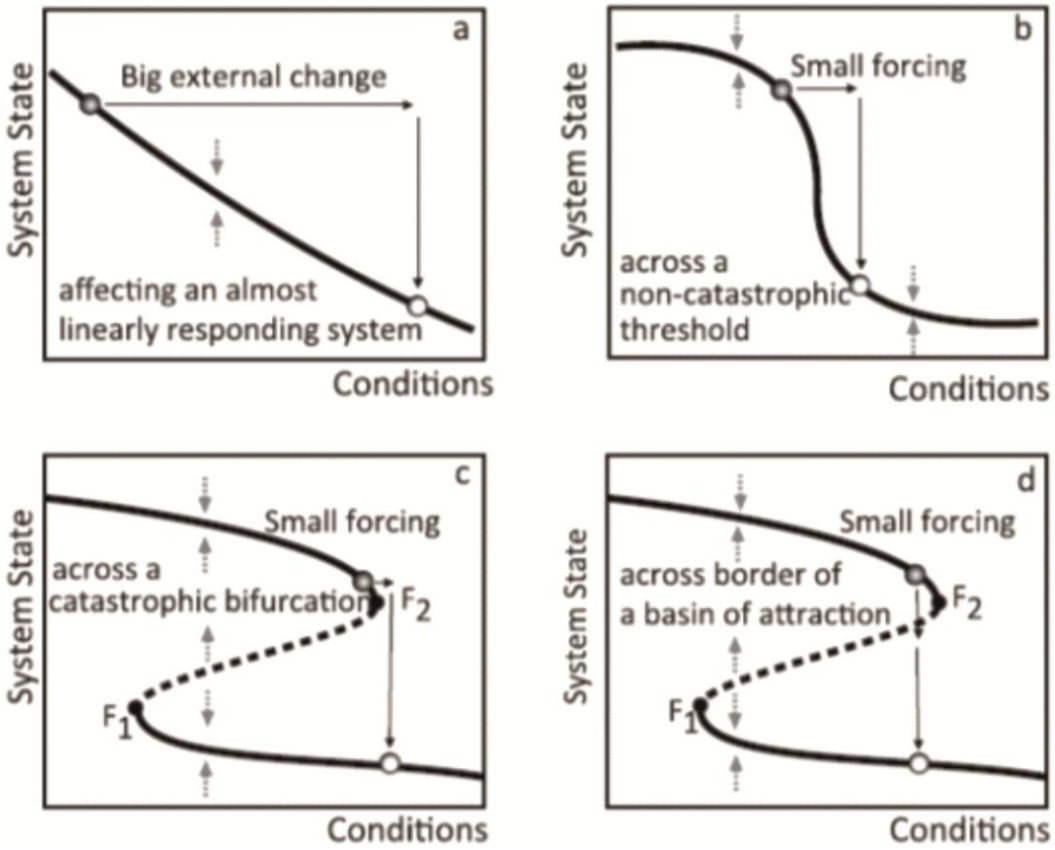

Figure 2-2 Types of system state changes in natural ecosystems (Scheffer et al., 2001). The lines indicate the equilibrium points between the ecosystem states and the environmental conditions. A solid line means a stable equilibrium and a dotted line means an unstable equilibrium. The system state will approach to a stable equilibrium as the arrows show: a) the relationship between environment conditions and system state is linear, only large external changes can cause a big shift in the state; b) step change, the relationship between environment conditions and system state is nonlinear, and it has a tipping point (circles). The system state will abruptly change while the conditions cross the tipping point. The states can revert according to the same trajectory, so it is also a called non-catastrophic threshold change; c) catastrophic bifurcation change; the difference between c and b is that c needs more efforts to reverse the altered ecosystem state; d) is also a catastrophic bifurcation change, but it also shows that a big disturbance can

cause the system to cross the threshold far before the tipping point (Fig 2-1b), while c shows that small perturbations can trigger the system to the alternative stable state (Fig. 2-1 c)

Theoretically, all types of ecosystem changes can be observed in a continuously evolving ecosystem. The response of an ecosystem to environmental conditions may be smooth or linear at the initial state before moving to a catastrophic response (Scheffer, 2009). Fig. 2-3 shows a conceptual model of the possibilities of the evolution of an ecosystem. At the initial stage the change of environment conditions does not impact the state of the ecosystem, and the ecosystem is quite stable. As the drivers strengthen, the ecosystem may experience a linear response, and followed by a catastrophic response. The point between the two states is called a cusp point (Scheffer, 2009), where an alternative attractor may start to affect the ecosystem state (van Nes and Scheffer, 2005a). The ecosystem will enter the alternative stable states when the alternative attractor totally controls the ecosystem.

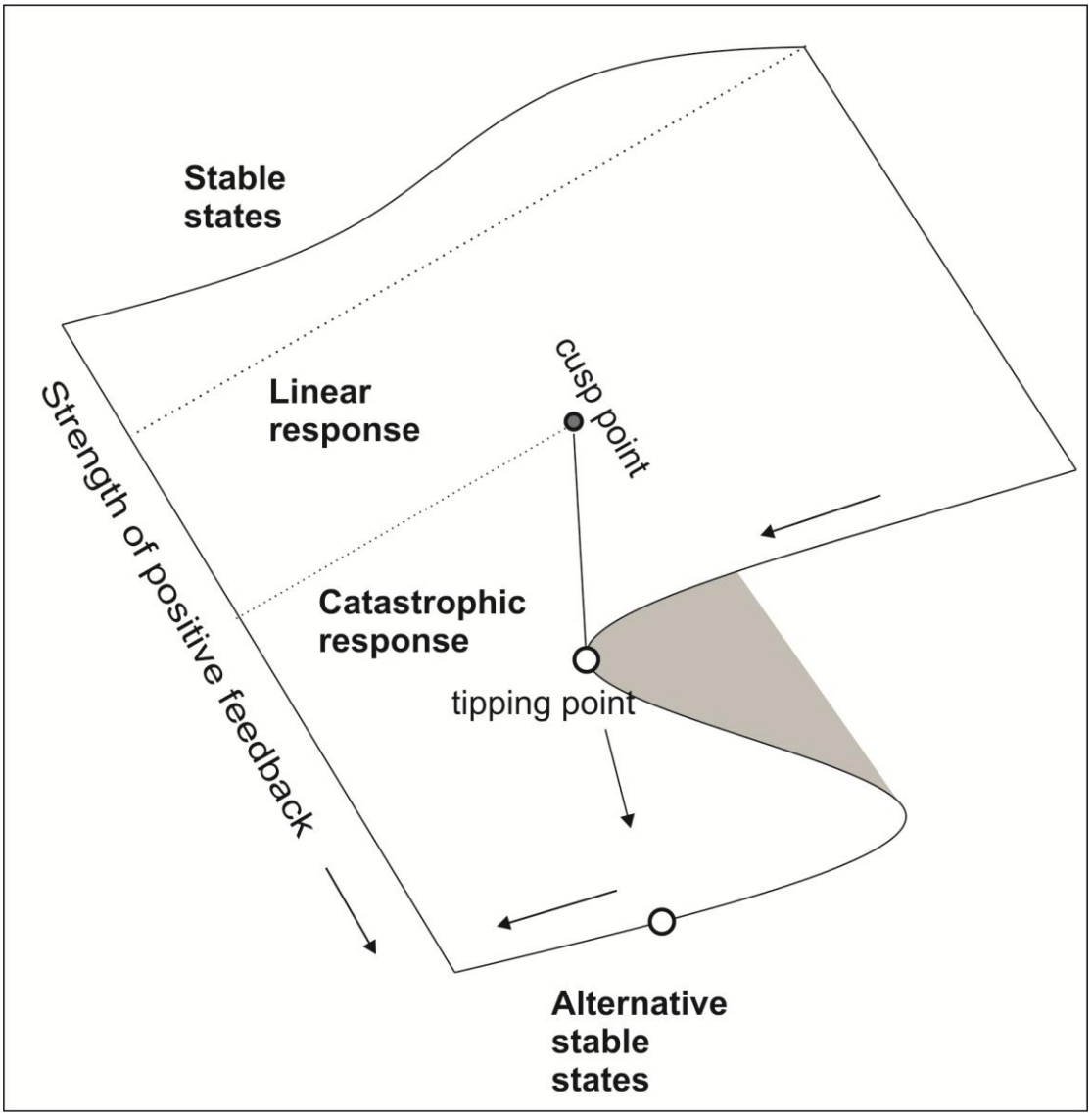

Figure 2-3 Continuum response of an ecosystem to environmental conditions (modified from Scheffer (2009)). The evolution of an ecosystem experiences different types of changes in different stages. This figure shows the type of an ecosystem changes from an almost non-response stage (very stable state), to catastrophic response stage.

2.4 Early warning signals for abrupt change

One main purpose for understanding the nature of ecosystem change is to predict abrupt changes so that we can avoid negative impacts and accelerate positive impacts (Scheffer, 2009). Recently, many published studies have tried to find EWS, which are mainly based on critical slowing down (CSD) theory. It refers to the increasing time that an ecosystem takes in order to return to an equilibrium

point following a perturbation when the ecosystem is near a tipping point (Scheffer et al., 2009; Wissel, 1984). In other words, recovery rate for a system approaching tipping points becomes slow. Some leading indicators are explored for warning of catastrophic shifts, such as recovery rate (van Nes and Scheffer, 2007), lag-1 autocorrelation (Dakos et al., 2008; Lenton et al., 2008; Scheffer and Carpenter, 2003), variance (Brock and Carpenter, 2006; Carpenter and Brock, 2006; Drake and Griffen, 2010), skewness (Guttal and Jayaprakash, 2008) and flickering (Scheffer et al., 2009). The first three of them are related to CSD theory: 1) One model study suggests that the recovery rate after small experimental perturbations can be used to warn us that the system is approaching a tipping point (van Nes and Scheffer, 2007). However, in real systems, the recovery time from perturbations is difficult to measure, so this method is not feasible in real ecosystems. 2) As the system's recovery rate becomes slower and slower, the ecosystem state should become more and more similar to its previous state. Therefore, correlation between adjacent states should increase when the system is approaching a tipping point. The calculation of lag-1 autocorrelation for a time-series data provides a straightforward way to detect the CSD before catastrophic transitions, so that it becomes one of the important leading indicators for critical transitions. 3) The ability of the system to absorb the impacts of exogenous forcing becomes lower as system resilience decreases. The same disturbance may cause much larger deviations in the ecosystem state, which means that state variability will increase as the system approaches a tipping point (Carpenter and Brock, 2006). Therefore, rising variance is also one of the probable leading indicators for impending abrupt change in an ecosystem. 4) Skewness is another important leading indicator for abrupt change: "*As one approaches a regime shift, the landscape picture of the ecosystem dynamics exhibits a pronounced asymmetry around the stable state, in addition to flattening of the potential landscape, i.e. decrease in curvature"*(Guttal and Jayaprakash, 2008). This indicator has also been the subject of modelling studies (Drake and Griffen, 2010; Guttal and Jayaprakash, 2008) but skewness change in the real ecosystem is rarely studied. 5) Flickering is the phenomenon which describes brief excursions between attractors (Brock and Carpenter, 2010). This is unlike critical slowing down where the perturbations come from endogenous processes.

Flickering has only been shown in models (Brock and Carpenter, 2010; Carpenter and Brock, 2006). In most applications, flickering has been considered to be a process between two stable states (Brock and Carpenter, 2010), but has also been considered as a leading indicator for catastrophic shifts (Scheffer et al., 2009). Rising variance can also be considered as an indicator for abrupt change due to system flickering (Carpenter and Brock, 2006; Scheffer et al., 2009). Statistically, flickering can be detected in frequency distributions with bimodality (Carpenter and Brock, 2006; Scheffer et al., 2009). However, most of these studies are based on mathematical models (Carpenter and Brock, 2006; Chisholm and Filotas, 2009; Guttal and Jayaprakash, 2008) or manipulated ecosystems (Carpenter et al., 2011) and discussions of leading indicators are rare in real ecosystems (Dakos et al., 2008; Lenton, 2011; Lenton et al., 2008).Furthermore, the techniques for calculating leading indicators with modelling data and real data are not well unified. For instance, in modelling, the autocorrelation calculation can be based on large datasets, the scale of which is impossible to collect in real world conditions. Alternatively, the autocorrelation calculation in the experimental data has to rely on the slide of time series data. Therefore, in the strict sense, the conclusions from high resolution modelling results cannot be easily verified by the low resolution experimental data. At least the calculation of the leading indicators should be consistent, and therefore, future analysis with modelling data should consider its applications within the real world.

2.5 Palaeolimnology on studies of Environment change

Lake's sediment has been considered as a lake's ecosystem's memory (Smol, 2008).'Because lakes and their sediments collect and integrate regional and local environmental signals, they are often used as sentinel ecosystems (Carpenter and Cottingham, 1997)'. Sediments provide a history book of our environmental sins (Smol, 2008). Itrecords extend time-scales. Smol (1992) argued that palaeolimnolgy is also an important tool for effective ecosystem management, because it can provide long-term environmental data. Paleolimnological approaches allow us to view present and predicted future changes against a historical backdrop. The great leap forward in palaeolimnology came as

Hutchinson with some of his students (e.g. Hutchinson & Wollack, 1940; Deevey, 1942; Livingstone, 1957) and Pennington (1943) began to explore ideas of lake evolution using stratigraphical analysis of sediments. Palaeolimnology has developed rapidly over the last two decades, which should thanks to the three key developments, i.e. accurate methods for dating recent sediment (like ^{210}Pb and ^{137}Cs (e.g. Appleby et al., 1986)), coring techniques and numerical techniques (like transfer function, multivariable analysis) (Battarbee, 1999).

Paleolimnolgical proxies can be used to study environment history including eutrophication, conductivities, temperature, soil erosion, acidification (Battarbee et al., 2005b), climate change, and sedimentary process. For example, on studies of climate change, it can be used to reconstruct past variability in effective moisture, and past variability in temperature (Batterbee, 2000). Lakes also host many microcrustaceans (like pelagic and benthic), organisms whose remains are preserved in lake sediments and which offer the potential to quantify past food-web structures (Jeppesen et al., 2001). Therefore, palaeolimnology can also provide information about lake's ecosystem function change, like Bennion et al. (1996) indicated that fossil diatoms could predict epilimnetic phosphorus concentrations change while lake became eutrophication. Biodiversity can also be assessed with palaeolimnologcial proxies (Sayer et al., 1999). It affords an alternative means of reconstructing temporal trends in biodiversity and provideshigh resolution (often annual to decadal) time-series, which typically extend far beyond available historical biotic records. Palaeolimnology methods can also contribute in the lake's restoration. The potential of palaeolimnological methods for establishing reference conditions and restoration targets for lakes has been recognized for some time, and has received renewed interest in recent years with the introduction of the EU Water Framework Directive (Bennion et al., 2010). It can provide baseline and reference condition for lake's restoration.

Significant progress in diatom-based palaeoenvironmental reconstructions has been made during the last decade due to the development of quantitative methods (Birks, 1998). Clear correlations have been established between species composition and pH (e.g. Gasse & Tekaia, 1983; Birks et al., 1990), salinity (e.g.

Cumming & Smol, 1993), nutrient content (Bennion, 1994) and ionic composition (e.g. Gasse et al., 1983; Fritz et al., 1993). Modern calibration datasets have been established for a mumber of regions. For example, a dataset of 282 modern diatom samples from Africa has been used to create transfer functions for conductivity, pH and ionic ratios (Gasse et al., 1995). In the northern Great Plains region of North America, a salinity transfer function has been developed from a 66 lake dataset. Like Korhola et al. (2000) used cladoceran and chironomid assemblages as quantitative indicators of water depth in subarctic Fennoscandian lakes. Mourguiart et al. (1998) employed an ostracod-based transfer function to reconstruct Holocene palaeohydrology of lake Titicaca, Bolivia. Seppä and Birks (2001) employed pollen-based climate reconstructions to quantitively reconstruct July mean temperature and annual precipitation trends during the Holocene in the Fennoscandian tree-line area.

2.6 Lake Eutrophication

Lake eutrophication is the term used to describe the natural or human-induced enrichment of nutrients in lakes. The most common impact to lakes' ecosystems is the growth of harmful algae, and the consequent decrease in the clarity of their water; it is notably one of the most visible examples of human impact on the biosphere (Smith, 2003; Smith and Schindler, 2009). The most important impacts by eutrophication are water quality deterioration, degraded fisheries and modified aquatic ecosystems (Johnson and Carpenter, 2008; Johnson et al., 2010).It is a costly economic problem (Dodds et al., 2009), resulting in high water-treatment costs and damage to the tourism industry. Attempted remediation techniques include bio-fertilizer use, planting of submerged macrophytes and construction of a biological isolation belt around lake, but few examples have found great success. A lake is a typical complex ecosystem, which contains obvious alternative stable states, feedbacks and resilience. It has already been confirmed that lakes have alternative states (Scheffer et al., 1993) - for example a clean state with high transparency and good water quality, and turbid states with higher opacity and bad water quality. Shallow lakes with low nutrients are characterized by clean water, and are dominated by submerged macrophytes, piscivorous fish and high

abundances of zooplankton in the ecosystem. Negative feedback loops among these components organize the ecosystem and maintain the lake in its clean state. The alternative turbid state is characterized by cloudy water with a high concentration of algae, few submerged macrophytes, and a fish community dominated by planktivores. The growth of algae restricts the growth of submerged macrophytes. Thus positive feedback among phytoplankton, bottom water anoxia and dissolved nutrients re-organizes the lake's ecosystem. The oxygen content in the hypolimnion layer of deep lakes plays a similar role as a part of positive feedback mechanisms (See section 2.2). Many factors can cause the eutrophication of a lake, such as high temperatures (Genkai-Kato and Carpenter, 2005) or run-off of chemical fertilizers (Carpenter et al., 1998b)and sewage (Jeppesen et al., 2003). Undoubtedly, human activities have become one of the most important factors causing lake eutrophication, which is called "cultural eutrophication". This has become the primary water quality issue for most of the freshwater in the world. Lake eutrophication causes the lake's ecosystem to collapse in a very short time period. It is characterized by blooms of noxious algae, excessive growths of aquatic macrophytes, episodes of anoxia, dominance of zooplankton by small, inefficient grazers, and dominance of the fish biomass by benthivores (Carpenter et al., 1998a).

2.7 Methods for studying eutrophication

2.7.1 Instrumental data

Obviously, we still do not understand complex ecological systems very well and the lack of knowledge about their dynamics has led to the failure of ecosystem restoration activities (Suding et al., 2004). Ecosystem dynamics can be assessed through collection of three primary types of data: instrumental data, mathematical model, and palaeolimnolgical data. The main purpose of eutrophication studies are to investigate the reasons for lake eutrophication and to inform management strategies (Schindle, 1974), specifically including nutrient sources (Daniel et al., 1998), nutrient transfer in the catchment (Heathwaite et al., 2003), nutrient dynamics within lakes (Carpenter, 2003), lake reference conditions (Bennion et al.,

2004) and lastly the consequences of eutrophication (Carpenter et al., 1998a). Monitoring of water quality provides the most widely used data on lake eutrophication. It provides the most direct way to understand eutrophication as well as complex ecological system. It is the approach with the least ambiguity and can provide the most robust results. However, the observation scales are always limited, considering the necessity of long term studies on complex ecological systems (Dearing et al., 2010). Additionally, even if there is enough instrumental data, a model is still necessary to simulate the complex system's mechanisms. The mathematic model and palaeolimnological proxies may provide a good supplemental way to study lake eutrophication.

2.7.2 Palaeolimnological proxies

Lake sediment can provide many proxies for inference of environmental change over long time scales (Last et al., 2001a). These proxies can be simply classified as biological proxies (such as diatoms, chironomids, pollen, ostracods, plant macrofossil) and abiotic proxies (such as loss-on-ignition, grain size, magnetic susceptibility, isotopes and the chemistry of metals). The interpretation of environmental variables through lake sediments are not just for the lake but also for the catchment and regional environmental change. For instance, grain size and magnetic susceptibility can reflect soil erosion and flooding in the catchment, while chironomid assemblages (Heiri et al., 2003) and oxygen isotopes (Moore et al., 2001) can be used for regional temperature reconstructions. Each individual proxy is pertinent to at least one environmental process or variable (Last et al., 2001a). However, there are often discrepancies among the environmental interpretations of different palaeo-indicators. This is mainly due to the fact that each proxy contains assumptions or shortcomings. For instance, biological proxies such as diatoms have a problem of preservation (Flower, 1993; Flower and Ryves, 2009; Ryves et al., 2001), the sedimentation process affects the interpretations of metal elemental analysis, bacterial magnetite influences interpretations of magnetic susceptibility (Gibbs-Eggar et al., 1999; Snowball, 1994) and training sets have to face the problem of analogy. Therefore, studies commonly employ a range of proxies, permitting interpolation of the different

assessments of environmental change to improve accuracy (Birks and Birks, 2006).

Plenty of proxies in the lake sediment provide us with good tools for studying lake eutrophication. Indicators such as organic carbon, phosphorus elements and the ratio of C/N have always been employed to infer the eutrophication process (Schelske and Hodell, 1995). Biological proxies such as fossil diatoms (Battarbee, et al., 2005; Smol and Stoermer, 2010) and chironomids (Langdon et al., 2006) reveal the biological response to nutrient enrichment in the lake and provide reference conditions for designing management policies (Bennion et al., 2004). These studies are based on the development of statistical analysis. For instance, indirect statistical analysis (Jongman et al., 1995) such as Principle Component Analysis (PCA) and Detrended Correspondence Analysis (DCA) are used to interpret the relationships between environmental variables and diatom species, so that a qualitative description of the eutrophication history can be provided. The developments of the training set and transfer function make the biological proxies widely applicable in the studies of environmental changes. In the initial stage, a modern analogue approach was used, i.e. it was assumed that the same biological communities have the same environmental background between modern and historical assemblages (Flower et al., 1997; Overpeck et al., 1985). A disadvantage of this approach is that the relationship between biological communities and environment may be not constant and a large dataset is needed. A better way is to calculate the species' tolerance and optimum value for a specific environmental variable using a training set that permits a quantitative reconstruction (ter Braak et al., 1993). For example, the diatom is widespread in almost all aquatic ecosystems with tens of thousands of species existing globally (Smol., 2000), and is one of the most significant biological indicators used in palaeoenvironmental reconstructions (Battarbee et al., 2001). It is very sensitive to environmental change and is preserved relative well in sediment owing to its silica valves. Many researchers have demonstrated that diatom is a suitable proxy for eutrophication (Bigler et al., 2007; Holland and Beeton, 1972; Yang et al., 2008). The transfer function models, such as Weighted Average (WA) model (Braak and Looman, 1986) and Weighted Average – Partial Least Square

(WA-PLS model) (ter Braak and Juggins, 1993; ter Braak et al., 1993), are always constructed based on linear or unimodal distribution between diatoms and environmental variables (Birks, 1998). Although multiple stable states can be identified in lake ecosystems, it seems that little discussion has taken place about the possibility of multiple analogies in the training sets until recently.

2.7.3 Mathematical Model

Mathematical models are an important part of complex system studies because they can not only simulate the mechanisms of the complex systems but can also predict the future. In mathematical models, the relationships among components are expressed by mathematical equations. Some mathematical models try to include as many components as possible; these models are very complex in both structure and equations, such as the most models listed in Table 2-1. These models simulate the process quantitatively, and perform well in some specific purposes after careful calibration and validation, such as erosion (Coulthard et al., 2002). Although many complex models can simulate several processes at the same time, few conclusions can show well-validated model outputs simultaneously. In fact, the understanding of complex ecosystems is limited, when using only complex models. Table 2-1 also lists the disadvantages of ten models. Scheffer and Beets (1994) introduced the problems of using a complex ecological model for understanding the complex dynamic ecological system; for instance, one can always generate a good fit by tuning the model parameters. They pointed out that a minimal model is sometimes more useful than using the complex model to understand the rules of a dynamic complex system.

Table 2-1 List of ten mathematic models

MODELS	PURPOSE	SUBMODELS	PARARMETERS	INPUTS	OUTPUTS	TYPE	DISADVANTAGE
PROFILE (Sverdrup and Warfvinge, 1993)	Critical load of acidity, Soil weathering rate	Soil solution equilibrium, Cation and N uptake, Nitrification, Mineral weathering, Cation exchange	Precipitation rate, air temperature, Runoff, Deposition, uptake, Soil property, Mineral composition	rainfall, temperature, soil texture, and so on	Critical load of acidity, Weathering rate and so on	Kinetic / Steady -state/ mass balance	Steady-state soil chemistry model exclude process, only nature process, No physical weathering
SAFE(Sverdrup et al., 1995)	Long-term weathering	The same as PROFILE	The same as PROFILE	Temp., Precipitation, uptake, nutrient cycling, soil parameter.	Historical Weathering rate, Lake chemistry and so on	Kinetic / Dynamic/ mass-balance	Nature process, Initial condition, No physical weathering
ALLOGEN (Boyle, 2007a; Boyle, 2007b)	Long-term weathering/ acidification	PROFILE for Silicate, Wollast (1990) for Calcite	Same as weathering submodel in PROFILE	Average climate, pCO2, soil-water DOC, initial mineral	Weathering, acidification	Process-based/mass-balance	No physical weathering; weak on hydrological impacts
INCA-P (Wade et al., 2007; Wade et al., 2002, 2004)	P on water quality/aquatic ecology in river	GIS interface (boundaries and land-use of each), land-phase hydrological model, land-phase P model, in-stream P model	Land use and livestock numbers, Fertiliser practice, River networks, Reach networks, Reach boundaries, and Inputs	Hydrology, Air temp. Rainfall, Actual Precipitation, land management, flow rate and SRP of sewage	P fluxes and concentrations/TP/SRP/Chl a and so on	Dynamic, mass-balance	Data required: Daily or monthly
Export Coefficient Model (Bennion et al., 2005; Johnes, 1996; Johnes and Heathwaite, 1997)	Trophic statue in Lake or Stream	$L = \sum_{i=1}^{n} E_i (A_i (I_i)) + p$	Land use, Fertilisers, livestock, human population and wastes, nitrogen fixation and atmospheric deposition nutrients	Time series change in Parameters	Loss of nutrients in a catchment	Empirical model	The accuracy of coefficient and ignore nature process

Table 2-1 Continuous

MODELS	PURPOSE	SUBMODELS	PARARMETERS	INPUTS	OUTPUTS	TYPE	DISADVANTAGE
MAGIC (Cosby et al., 2001; Cosby et al., 1995; Wright et al., 1986)	Recent acidification (long-term but just past 200yr)	Soil-water Cation Exchange, Inorganic Aluminum, Inorganic Carbon, Ionic Balance	Thermodynamic equilibrium constants, Selectivity coefficients, Aluminium solubility constant, Base cations, Strong acid anions, Inorganic Al species, Inorganic carbon species, Dissociation of water, Exchangeable cation, Base saturation, pCO_2	TEMP, pCO_2, Organic Acid, Catchment Discharge and Flow, Atmospheric Deposition, Sources and Sinks of Ions/Organic Carbon and Nitrogen, Decomposition, Mineralization, Plant Nitrogen Uptake, Nitrification and Denitrification	Monthly and annual average concentrations of the major ions in water body	Process-based model	Only nature process, and too many inputs
CAESAR (Coulthard et al., 2002; Coulthard and Van De Wiel, 2006)	Erosion, deposition and landscape evolution	Hydrological model, Discharge routing, Fluvial erosion/deposition, Slope processes, Vegetation cover	Topography, sediment distribution, vegetation pattern, roughness	Rainfall, inflow hydrography, sediment inflow	Flow and sediment hydrographys, topography, inundation, grain size, erosion, deposition maps	Cellular model	Not suitable for large area
WASP (EUTRO) (Di Toro et al., 1983) (http://www.epa.gov/athens/wwqtsc/html/wasp.html)	interpret and predict water quality	Phytoplankton Kinetics, Periphyton Kinetics, Phosphorus Cycling, Nitrogen Cycling, Dissolved Oxygen Balance, Sediment Diagenesis	Dissolved Oxygen, CBOD, Ammonia, Nitrate, Organic Nitrogen, Orthophosphate, Organic Phosphorous, Algae, Benthic Algae, Detritus, Sediment Diagenesis, Salinity	Temperature, Water velocity, Light extinction	DO, BOD, nutrients, phytoplankton, periphyton and so on	dynamic compartment-modelling	Not suitable for long-term model

Table 2-1 Continuous

MODELS	PURPOSE	SUBMODELS	PARARMETERS	INPUTS	OUTPUTS	TYPE	DISADVANTAGE
AQUATOX(Park et al., 2008; Park et al., 1997)	Ecological risk assessments for aquatic ecosystems		Nutrients, Detritus, Plant, Invertebrate, Fish, Site Characteristics, Water Volume Data, Water temperature, Wind, Light, pH, Inorganic Solids (stream only), Chemical, Inflow, Point Source, None-point Source,	Water volume, Temperature, Wind, Chemical inflow, Point Source, None-point Source and any time-series elements	Physical, Chemical, Biological of water body	Mechanistic model	Data is too complicated, not suitable for long-term model
QUAL2K (http://epa.gov/athens/wwqtsc/html/qual2k.html)	River and stream water quality model		pH, Conductivity, Inorganic Suspended Solids, Dissolved oxygen, BOD5, Alkalinity, Ammonia nitrogen, Nitrate nitrogen, Temperature	All water quality variables	Conventional Pollutants (Nitrogen, Phosphorus, Dissolved Oxygen, BOD and so on), pH, Periphyton, Pathogens	Mechanistic model	Not suitable for long-term model

A minimal model is a type of model that only contains some specific mechanisms (Scheffer and Beets, 1994). It does not contain all the processes of the ecosystem, and it may not be suitable for simulating any real complex system, but it provides general rules about the dynamic of complex ecosystem. Some minimal models show great success in understanding complex dynamical changes in the ecosystem, such as the predator-prey model (Noy-Meir, 1975), and fold bifurcation model (Carpenter, 2005; Scheffer et al., 2001). These models describe the interactions among the main mechanisms and conclude the important laws of complex ecosystems (Scheffer and Beets, 1994; Van Nes and Scheffer, 2005b). However, it is possible for us to oversimplify the models - the validity of a minimal model should be carefully discussed (Van Nes and Scheffer, 2005b). Sometimes, the validations of the minimal model are done with the help of other minimal models through hypothesis testing. Such a method may be helpful, but may cause more confusion for those readers who are not familiar with modelling techniques. A better choice would be by means of real data, such as instrumental data, manufactured experimental and palaeo- indicators. For example, a simple model is employed by Lenton (2011) and Scheffer et al (2003) to demonstrate the characters of EWS in the complex dynamic system, and the conclusions are validated with palaeo-proxies from glacial and limnology samples. Another example is a whole lake experiment, with a simple model to test the lake's ecosystem critical transitions (Carpenter et al., 2011; Carpenter and Brock, 2006).

In practice, although the modelers know the importance of validating their models, some tests are impossible due to data limitations. The combinations of minimal models with other methods such as palaeolimnological data might be a good choice to make minimal models more acceptable (Anderson et al., 2006).

There are many purposes of eutrophication modelling such as for ecological risk assessments (AQUATOX in Table 2-1), lake ecosystem services (Dobson et al., 2006). Normally, the models focus on two aspects of the lake eutrophication process. One is the simulation of nutrients (i.e. phosphorus and nitrogen, like INCA-P in Table 2-1), and another one is the biological response to eutrophication in the lake (such as algae and zooplankton, like WASP in Table 2-1). For the latter

type, it has already suggested that it is not suitable for long term simulation owing to the existence of many uncertainties in the dynamics of the complex system, which may affect results. For the first type of model, the focus is generally on phosphorus and nitrogen supply. Only phosphorus will be introduced in the following text for two reasons. First, it has been proven that the phosphorus is the main limiting factor for eutrophication in many lakes in China (Jin et al., 2005a; Yang et al., 2008). Second, the phosphorus is the limiting nutrient for our case lake, i.e. Erhai Lake (World Bank, 2007).The phosphorus models can be divided into three types: process-based models, export coefficient models, statistical models or empirical models (Adler et al., 2010). Process-based models simulate P transfers in catchments through equations that characterize biophysical processes, like runoff and adsorption. The catchments in these models are always divided into cells containing information related to soils, land use, and topography. Two examples of this are the Annualized Agricultural Nonpoint Source (AnnAGNPS) pollution model (Bingner et al., 2009; Young et al., 1989) and the Soil and Water Assessment Tool (SWAT) (Abbaspour et al., 2007; Arnold et al., 1996; Huang et al., 2009; Kim et al., 2009; Saleh et al., 2000). The AnnAGNPS has been widely applied in different regions, including the United States (Odum, 1969; Shrestha et al., 2004; Wang et al., 2005a; Yuan et al., 2006; Yuan et al., 2007) and China (Huang and Hong, 2010; Ma et al., 2009; Tian et al., 2010; Wang et al., 2005b). SWAT is a continuous and distributed model; it simulates plant growth, agricultural management, and pond and reservoir routing. It will not generalize the watershed as a single cell size in AnnAGNPS, but adopts conceptualized Hydrologic Response Units (HRUs) (Arnold et al., 1996). In the recent version of the SWAT model (ArcSWAT), the HRUs are defined by land cover, soil and slope. Nutrients outputs from each HRU are simulated and then the summation of the HRUs is used for each sub-basin (Arnold et al., 1996). The model is widely used for non-point source pollution from agricultural areas (Engel et al., 1993; Lam et al., 2010; Lin et al., 2009; Radcliffe et al., 2009; Yu et al., 2007).

Another type of phosphorus simulation model is called an export coefficient model (Adler et al., 2010), such as the Generalized Watershed Loading Functions (GWLF) model (Haith and Shoemaker, 1987). This type of model is originally

developed to predict nutrient loading in eutrophic water (Beaulac and Reckhow, 1982). The catchments are always categorized according to land use in export coefficient models and a different P export coefficient is assigned for each type of land use (Johnes, 1996; Mattikalli and Richards, 1996). Therefore, the export coefficient models need less data than process-based models (Johnes, 1996), but rely on extensive previous research to sufficiently characterize the coefficient relationships. The model is suitable for small catchments, but impossible to apply to larger catchments (Johnes, 1996). It has also been widely used to predict P loading of receiving water bodies (Beaulac and Reckhow, 1982; Hanrahan et al., 2001; Howarth et al., 1991; Johnes and Burt, 1990; Lee et al., 2000; Lee et al., 2001; Ning et al., 2002; Schneiderman et al., 2002; Swaney et al., 1996).

The third type of model is the statistical or empirical model (Adler et al., 2010). These models are based on empirical relationships between P outputs and other environmental variables, such as runoff (Ditoro, 1984). The accuracy of these models is restricted by the existence and quality of the original data and therefore it is not used often. These models also assume equilibrium or linear conditions and are not suitable for modelling over relatively long timescales when catchment and environmental conditions are changing rapidly. Although plenty of studies have already done to simulate complex ecological phenomena like lake eutrophication, a full comprehension of all dynamics remains an elusive goal. Only a few complex mathematical models, like CAESAR (Coulthard et al., 2002; Coulthard and Van De Wiel, 2006), consider the key features of complex ecological system, such as feedbacks, at the initial stages of modelling programming. Another issue is that not all the models concentrate on an ecosystem's dynamic. A dynamic model should focus on the ecosystem's ratio change so that the ecosystem's states change can be simulated indirectly, such as in SWAT. However, many models, such as export coefficient models, simulate the system state change with mass balance. In the following section, a good modelling platform, STELLA, will be introduced for simulation of dynamic ecosystems.

2.7.4 An example of an ecosystem dynamic model: STELLA

Many scientists do not employ modelling techniques to understand complex ecosystems because of the complexities of programming. STELLA is a system thinking software which can provide a valuable tool to simulate dynamic ecosystem change in nature or society (isee Systems Company, http://www.iseesystems.com/). It provides an icon-based platform for modellers to write differential equations easily into a model. It is convenient to show the dynamic change in a complex system with STELLA software, and enables time-saving for coding and debugging the model (Korhola et al., 1998).

Stock, convector, and flow are the basis components for STELLA. An example is the population size, which is determined by birth and death (Fig. 2-4). Stock represent a reservoir of material (Mourguiart et al., 1998), and it connects with flow. In the example, the population is the stock, which increases due to birth and decreases because of death. The flow component represents the amount of stock change (increase and decrease). Generally, the size of stock is determined by the discrepancy between flow in and flow out; therefore, the stock's changing rate, which is the core of a dynamic system, can be simulated. The convector (birth rate and death rate in the example) provides the parameters for the flow. One of advantages is the parameters provided by convector can be expressed in the way of graphical (Fig. 2-4). Therefore, the relationship between parameters can be well described, and the discrete series data can be expressed as continuous series data in the model.

STELLA has been widely used in simulation nature dynamics or society dynamics such as climate change (Smol, 1992), eutrophication (Bennion et al., 1996; Higgins et al., 2005), population dynamics (Arquitt and Johnstone, 2004; Maclsaac et al., 1991), energy crisis (Lei and Wang, 2008; Lin and Liu, 2010), and societies (Patterson et al., 2004). Many ecological–economic models employ STELLA as the program software (Grasso, 1998; Higgins et al., 1997; Hofmann, 1991; Mourguiart et al., 1998).

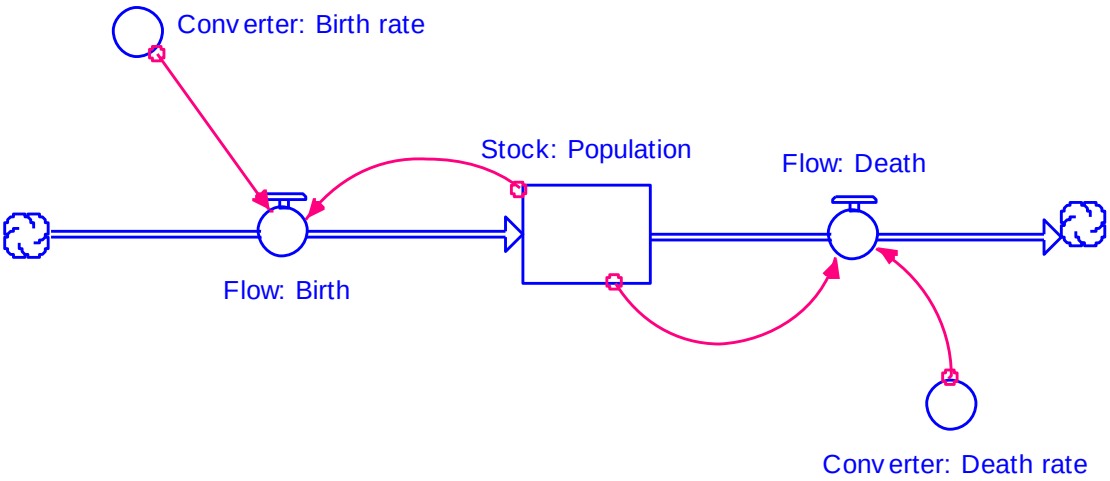

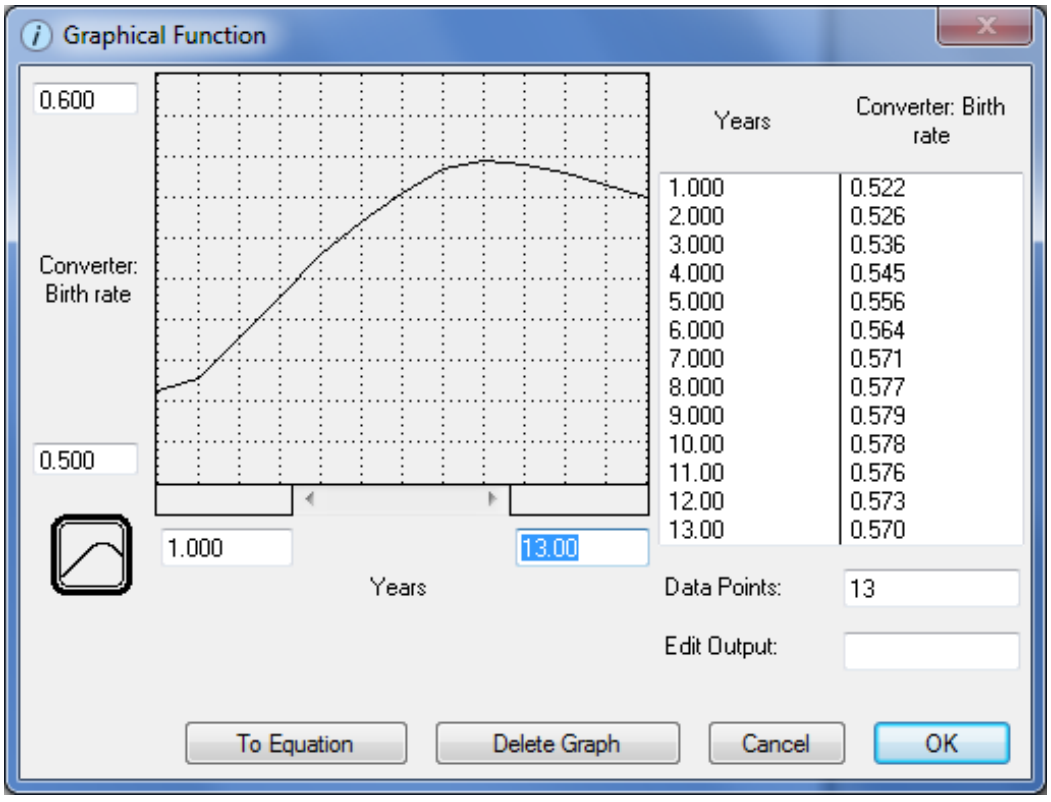

Figure 2-4 An example of dynamic model under STELLA software (the top figure is the basic components in a STELLA model, and the following figure is an example of graphical function, which shows the birth rate change according to year); the population size of the top figure depends on the balance between birth and death, and the direction of arrow decides the outflow (death) or inflow (birth). The death or birth rate is decided by both a stock and a converter.

2.8 Summary

Many global ecosystems are currently experiencing major changes. Not all natural systems change linearly with environmental variables; some systems change abruptly, sometimes in a catastrophic and irreversible manner. These abrupt ecosystem deteriorations have a negative impact on ecosystem services for human wellbeing. Scientists from different disciplines have contributed to the comprehension of complex ecological systems, but most of these theories based on modelling, such as early warning signals, have not been proofed by case-studies from real ecosystems. A lake ecosystem is a typical complex ecological system, and its eutrophication has become a serious problem for human wellbeing. This thesis will choose a eutrophicated lake, Erhai lake in China, as a case study of a complex ecological system. The theory of complex ecological systems will be tested with palaeolimnological data and modelling.

Chapter 3 Site Description

3.1 Introduction

This chapter will describe the research areas including Yunnan plateau where the surface lake samples for the diatom-environment training sets were collected and Erhai Lake, where two cores were collected for palaeolimnological and modelling analyses. Yunnan Plateau is a region with high biodiversity, complex geographical characteristics, and which has been considered a 'hotspot' region for global warming research (Xu and Wilkes, 2004). During recent decades, intensification of human activities coupled with regional warming has caused many environmental issues, including lake eutrophication (Jin et al., 2005b; Wu et al., 2004), biodiversity decline (MacKinnon et al., 1996; Xu and Wilkes, 2004), soil erosion (Barton et al., 2004), and drought (Qian and Zhu, 2001). Sustainable management has already been considered as one of the most important emerging considerations for local government. However, due to continuous increases in population, intensified agricultural activities, deforestation, and regional warming, many ecosystems are still deteriorating (Jin et al., 2005b; Xu and Wilkes, 2004). Erhai Lake suffered obvious eutrophication after the middle of 1990s because of increased nutrient input from agriculture and sewage (Jin et al., 2005b). Several large changes in the ecosystem occurred sequentially, such as the extinction of indigenous species (Du and Li, 2001; Wu and Wang, 1999), algal blooming (Li, 2001; Pan et al., 1999), and soil erosion in the catchment. The environment of the Yunnan Plateau and Erhai Lake will be introduced in this chapter, with a focus on the geomorphology, climate, vegetation, and biodiversity.

3.2 Yunnan Plateau

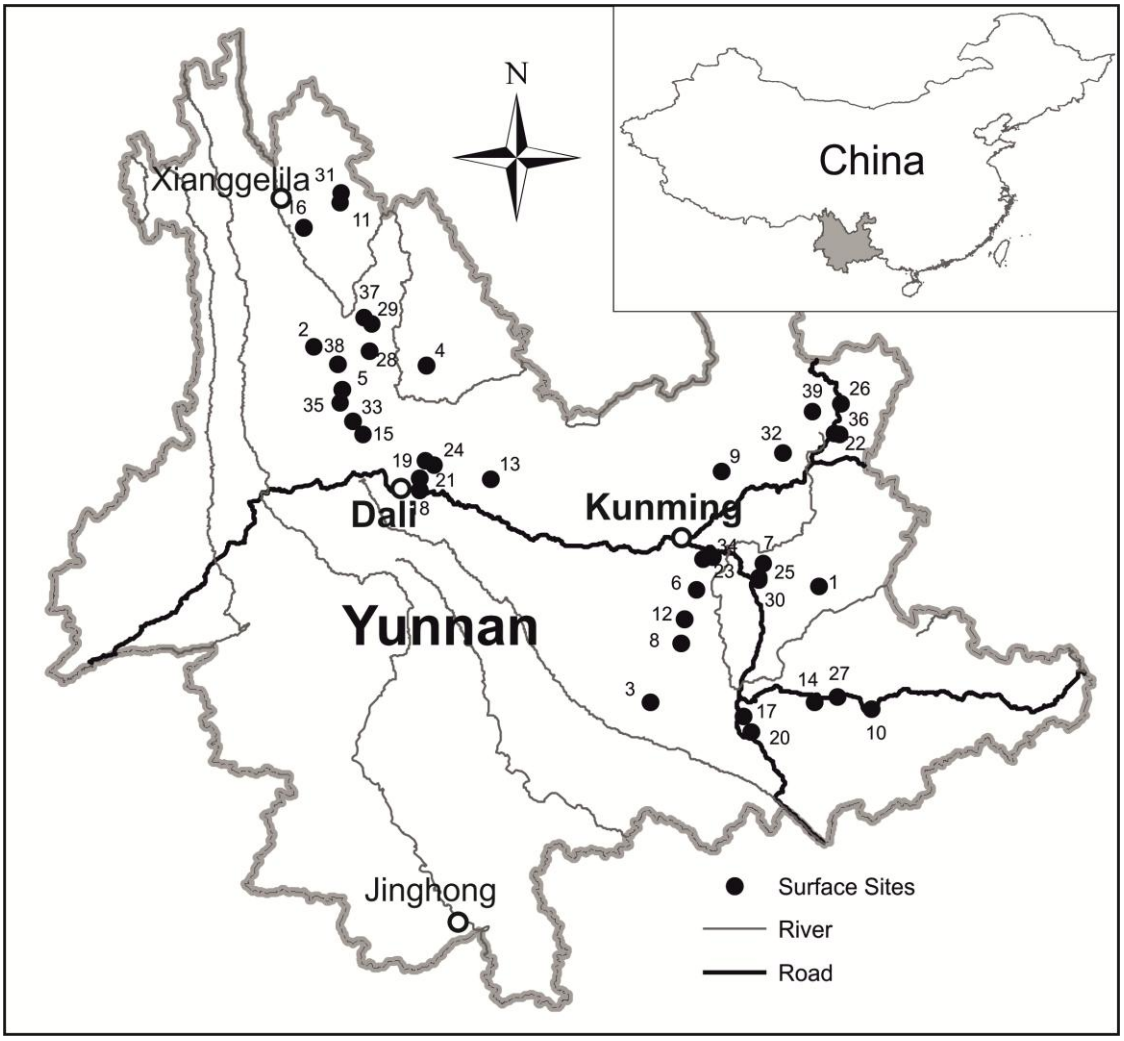

Figure 3-1 39 Surface sample sites in Yunnan Plateau (the names of the sites can be found in appendix I with the corresponding code for each lake)

Yunnan Plateau is an expansive upland region that interconnects the Qinghai-Xizang Plateau and Eastern Plain of China. The region is mountainous with average elevations of 1,500~2,000 m. The sources for many rivers and tributaries are located here, including Yangtze River, Nujiang River (Salween River), Lancang River (Mekong River). The climate is strongly affected by interactions between the summer monsoon from the Indian Ocean and the winter monsoon from Northern China. Most precipitation falls in summer and average annual precipitation is around 1,000-1,500 mm. The average January temperature ranges from 4° to 10°C, with the average July temperature from 19° to 25°C. The

soils are dominated with red earths and yellow earths. This region has undergone regional warming over the last 50 years (Xu and Wilkes, 2004), as shown by two curves of temperature change from two weather stations (Fig. 3-2) (Chen and Xie, 2008).

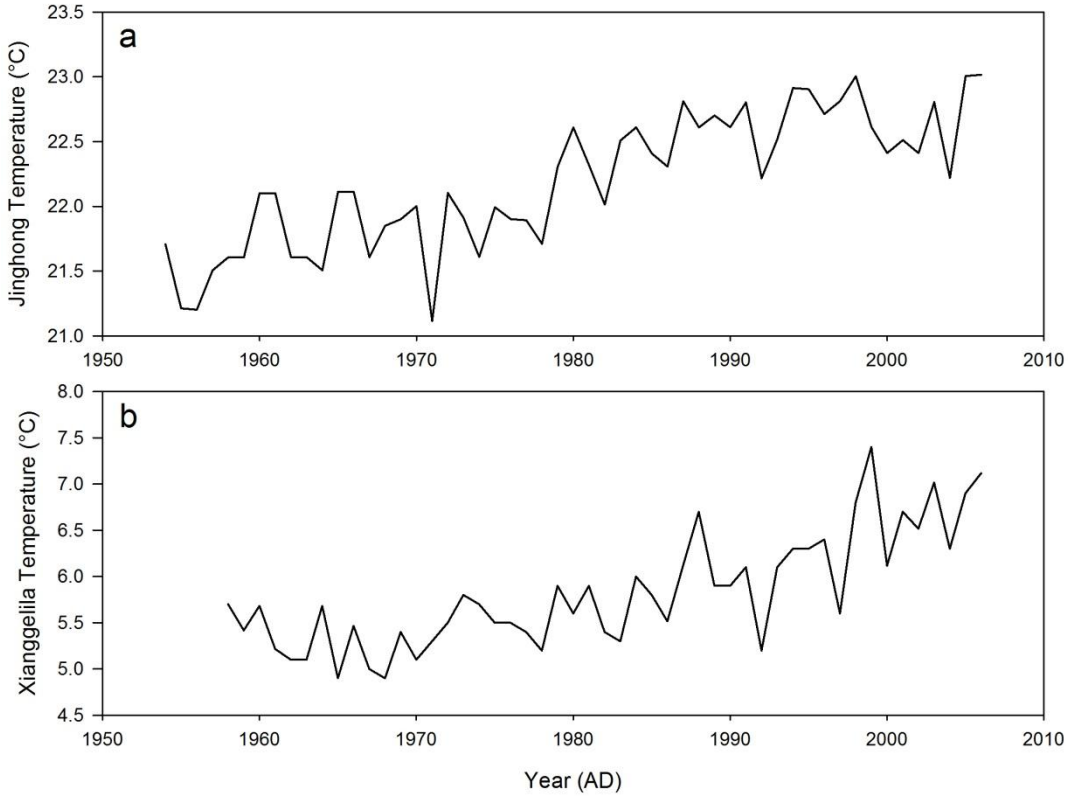

Figure 3-2 Temperature changeduring past 50years in Yunnan Plateau(Chen and Xie, 2008) (a, Jinghong annual average temperature; location: altitude, 582 m, 22°N, 100°47'E; b, Xianggelila annual average temperature; location: altitude, 3276.1 m, 27.83°N, 99.7°E. The sites of Jinghong and Xianggelila are shown in Fig. 3-1)

Characteristic vegetation over much of the Yunnan Plateau consists of seasonally humid, evergreen-broadleaved forest and Pinaceae (*Pinus yunnanensis*). The dominant taxa belong to the Fagaceae family (*Castanopsis* spp., *Lithocarpus* spp., and *Cyclobalanopsis* spp.). The crop and economic vegetation includes rice paddy, wheat, tobacco, and soybeans are also wildly spread in this area. The species richness here is high and has been designated as a global biodiversity 'hotspot' by

WWF/IUCN (MacKinnon et al., 1996). The biodiversity of this region, however, is currently decreasing, likely due to global warming and intensified pressures of human activities. The survey conducted by Xu and Wilkes (2004) showed that the biodiversity loss in the northern west of Yunnan Plateau was mainly driven by land use and land cover change, which included logging, NTFP collections (non-timber forest product collections), agricultural activities, over-grazing, forest fire and an increase in pests (Jianchu Xu and Andreas Wilkes, 2004).

Yunnan Plateau is one of the five densest lake regions in China (Wang and Dou, 1998). Some important cities and agriculture areas are adjacent to lakes; for example, the capital of Yunnan province, Kunming, is surrounded by Dianchi Lake, Dali city is near to Erhai Lake and several cities are adjacent to Fuxiang Lake and Xinyun Lake. The lakes provide important ecosystem services to residents, including clean water, food, irrigation, and pollution purification. Meanwhile, as rapid population growth continues, often resulting in land over-exploitation and irrational managements, the balance of some lakes' ecosystems are changing, often leading to algal blooming (Jin et al., 2005b), intensification of soil erosion (Barton et al., 2004), declining biodiversity (Xu and Wilkes, 2004) and diminishing wetland area(Yan et al., 2005). Eutrophication is one of the most serious environmental issues for sustainable use of lake ecosystem services. The governments are now paying greater attention to conservation of natural recourses, and implementing policies such as banning the logging of natural forests, prohibiting fisheries, reconstructing wetlands, and establishing conservation areas, but the altered lake ecosystem is still problematic. Lakes such as Dianchi Lake (in the capital city Kunming), Xinyun Lake (lake code 12), and Erhai Lake (lake code 15) still suffer serious algal blooming, even after management intervention. The lake sites for this research are illustrated in Fig. 3-1.

3.3 Erhai Lake and its catchment

Erhai Lake (25°36'-25°58'N, 100°05'-100°18'E) is one of the largest tectonic lakes in Yunnan Province, with an altitude of 1,974 m. The lake is located in Dali Bai

Autonomous Prefecture. Its surface area is ~256 km^2 with the catchment area ~2250km^2. It provides important water resources for residents in the catchment, where more than 800,000 people live, of whom about 65% are dependent on agriculture or fishery. As shown in Fig. 3-3, Erhai Lake is located between Chicken Foot Mountain and Diancang Mountain. The distance between north and south is around 42 km with the widest area around 9 km. Xiaguang (also called Dali city) is the biggest city in the area, with ~500,000 people. The main water supply for Erhai Lake is from precipitation through river systems in the catchment, where most of rivers originate from Diancang Mountain. The river system in the west of the catchment, locally called 'the Erhai 18 creeks', is important for both agriculture and human settlement. Many villages are located at the sides of these rivers (Fig. 3-3) and the Miju River is the most important water supply. It is located at the north of the catchment, with a length of 22.3 km, and provides ~0.5 billion m^3 water every year, which is about 57% of the water discharge of Erhai lake (Wang, 2000). The main output river is the West Erhe River, which flows through Xiaguang. The discharge rate of West Erhe River is ~30 m^3/s. The inflow volume of Erhai lake was around 0.62 billion m^3, and the outflow volume was around 0.69 billion m^3atthe end of 1980s. The unbalance of inflow and outflow caused the continuous decline in depth of Erhai Lake at the end of 1970s. The important reasons for the declining water level include the digging of the basin of West Erhe River for a hydroelectric power station (Yan et al., 2005; Yan et al., 2008), which also decreased the base level of the lake so that its water level suddenly declined at the end of 1970s. Considering on the linear population rise and agricultural development, the growing water demands in the catchment are another important reason for lake's historically low level after the 1970s.

Figure 3-3 Erhai Lake and its catchment (Photo by author, 2009).

Mean annual temperature is around 15 °C, and mean annual precipitation is around 977 mm in the catchment. The rainy season is from June to August; around 800 mm precipitation falls during this period. The annual average temperature has increased since the1970s (data from China Meteorological Administration and the detailed data will be shown in Chapter 5). The distribution of precipitation varies within regions. According to the surveys taken by Hydrology and Water Resources Branch Bureau of Dali, the precipitation differs in 4 regions, i.e. west region (Cangshan Mountain), east region (Chicken Foot Mountain), north region (Miju River) and the lake region. The West region has the highest precipitation because of the effects of DianCang Mountain. The annual precipitation is around 1200 mm here and increases with altitude. The East region has relatively low precipitation, which is only around 730 mm. The long term average annual precipitation of Miju River region and Erhai lake area is 778 mm and 998 mm respectively (Li, 2008). The records of drought in Yunnan province showed that there were severe droughts in 1931, 1943, 1979, 1987, and 2010 (Original from He likun, 2010, Yunnan Archives). The crop yields during these periods decreased dramatically. The evaporation of the surface of Erhai lake is ~1,100-1,500 mm per year, which declined with the temperature increasing after 1960s mainly as a result of increased cloud cover (Huang et al., 2010).

The land cover of Erhai lake catchment is mainly dominated by forest, which occupies around 53% of the area. Crop land is the second largest land cover in the catchment, which dominates around 19% area and is always distributed below the height of 2,200 m. The land cover is typical for the altitude distribution in Diancang Mt. and Chicken Foot Mt (Fig. 3-4). Most of the natural Cangshan *Abies* had already been logged during the period of Big Leap Forward (1958-1961) and Cultural Revolution (1966-1976), and it now only exists above 3,300 m. Most of lower area is dominated by Huashan Pine plantation and mixed coniferous broad-leaved. The erosion of Chicken Foot Mountain is serious, and the vegetation is mainly dominated by *Pinus yunnanensis* (>2,300 m), and mixed coniferous broad-leaved (<2,300 m). The agricultural land is mainly distributed at the northern part of the catchment and alluvial plain of Diancang Mountain, and it typically supports a double-cropping system of rice, wheat, legumes and tobacco plants.

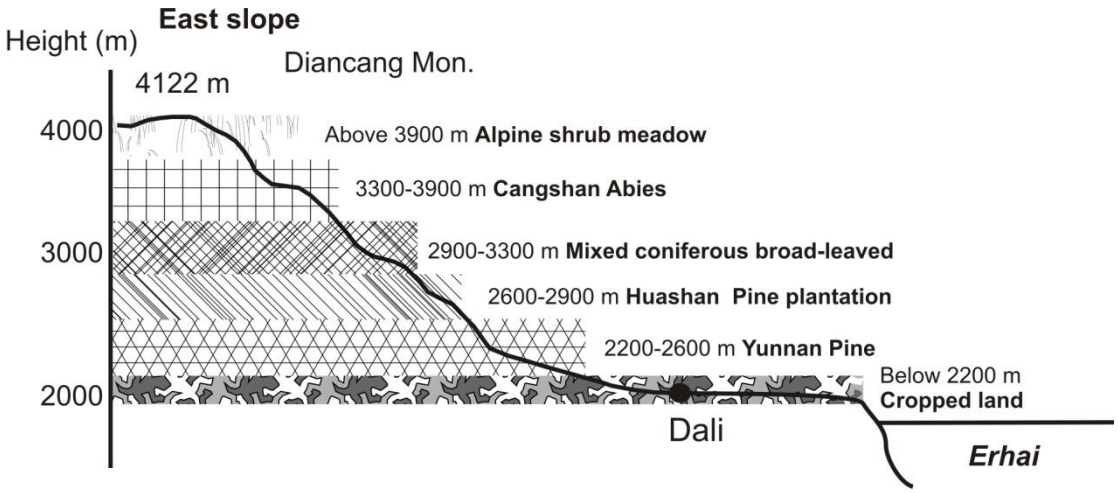

Figure 3-4 Diancang Mt. Vegetation types (The data are from Yunnan Dali Cangshan Mountain Protection Authority)

There are four towns surrounding the lake, which contain 52 villages. Around 8,802 tons of sewage is produced in these villages. Although the construction of a sewage disposal system has been undertaken, still around 75% of the sewage flows into the lake (report from www.yunnan.cn, 14/4/2011). Records show that the nutrients including total phosphorus (TP) and total nitrogen (TN) are increasing from the start of 1990s and hence the lake has been subject to be eutrophication

(Pan et al., 1999). In 2003, TP was ~30 μg/l and the cyanophyta concentration was around $2x10^8$ per litre, and a serious algal blooming occurred. The state of lake shifted from clear to turbid, and the secchi disc depth (SD) decreased from 3.5 m at 2001 to about 1.5 m at 2003 (Detailed data will be shown in Chapter 5).

Table 3-1 Submerged plant resource and its distribution in Erhai lake (after Hu et al. 2005).①*Vallisneria natans*②*P. maackianus*A. Benn.③*Zannichellia palustris* L. ④*Myriophyllum spicatum* Linn.⑤*Hydrilla verticillata*

Distinct	Area (hm^2)	Area %	Macrophytes	Biomass /t	Biomass%
North	2837.5	29.55	①②③	99682.48	25.17
East	967.5	10.08	①②④⑤	27449.8	6.93
Central	3341.25	34.8	②①⑤	141133.75	35.63
SW coast	2456.25	25.58	②①③⑤	127792.29	32.27

The distribution of submerged macrophytes is consistent with depth (Fig. 3-5) (Hu et al., 2005; Li and Shang, 1989). The lake can be divided into four main parts as listed in Table 3-1. The biodiversity of submerged plants is reducing, but the whole biomass of submerged plants is increasing due to nutrient enrichment in the lake (Hu et al., 2005).Fig. 3-6 shows the bathymetric contour of the lake. The deepest part is in the northern basin, where two sediment cores were collected at 2009. The deepest part is around 20 m. The southern lake basin is much shallower, where the deepest depth is around 10 m.

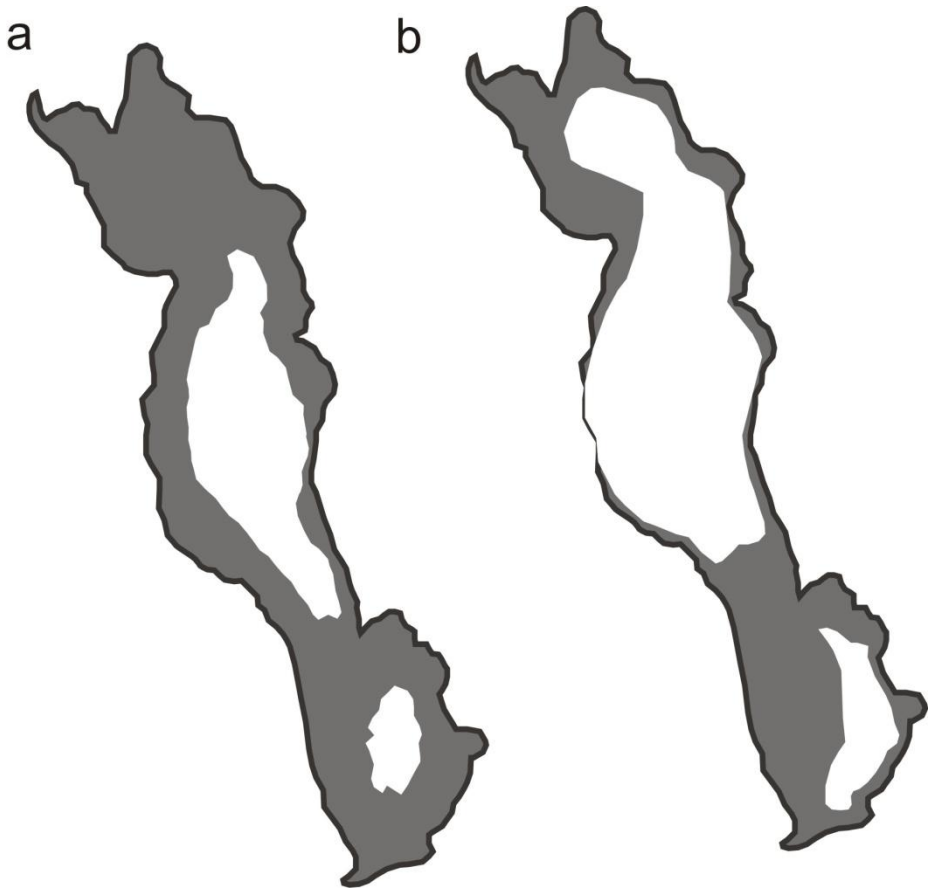

Figure 3-5 Erhai lake's submerged macrophytes in different observation periods. a, observations from Hen Li & Yuming Shang (1989) at the end of 1970s to the beginning of 1980s (the distribution diagram was draw based on the observations at 1975, 1977, 1982, 1983); b, observations from Hu Xiaozhen et al., (2005) at 1998. It indicates the dynamic of the submerged macrophytes dynamic in the lake ecosystem

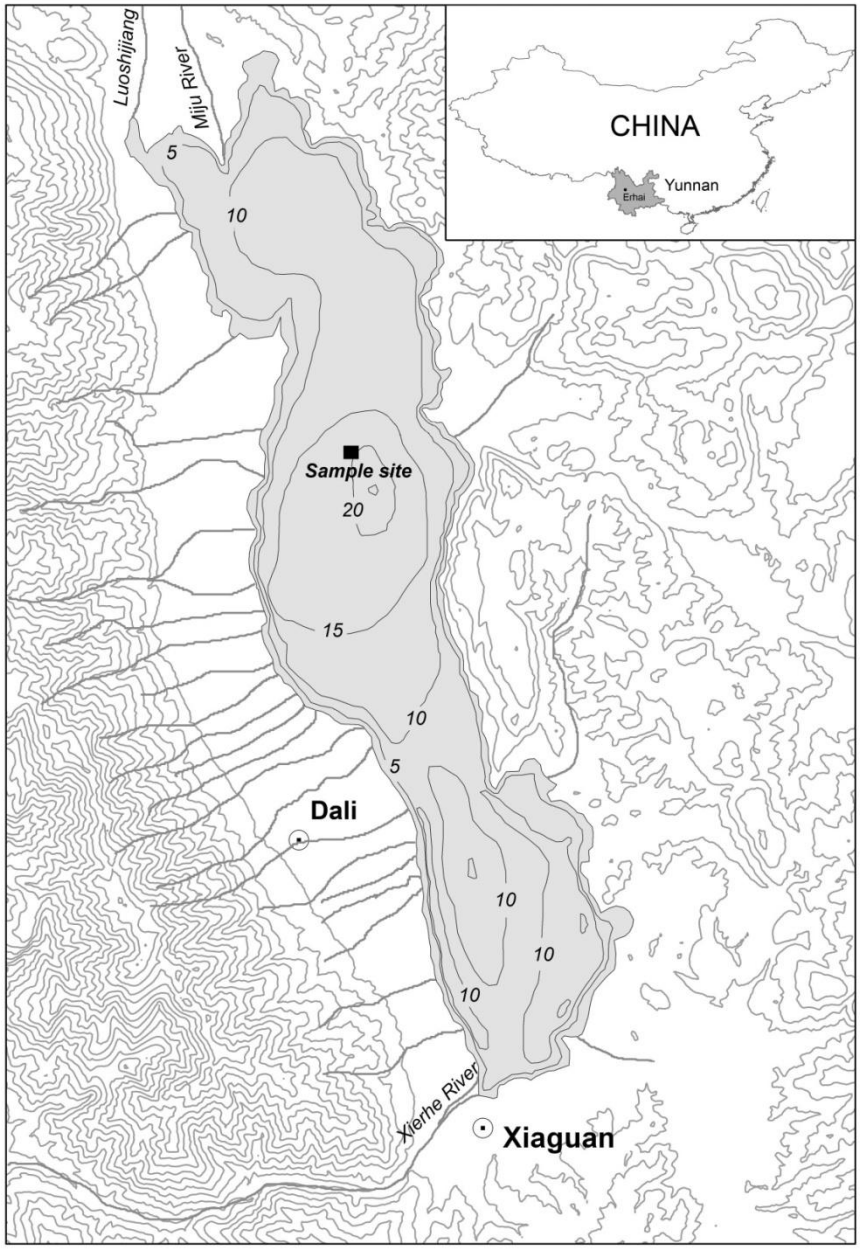

Figure 3-6 Bathymetrical chart of Erhai lake. Many rivers are inflowing into the lake, mainly from the Northern and Western catchment. The most important inflow is the Miju River in the North. Only one river is an outflow, which is located at the southern catchment near the most important city i.e. Xiaguan, with a population of ~500,000.

Several models have been constructed in the Erhai catchment for watershed management (Guo et al., 2001; Huang et al., 1999). An environmental system dynamics model, named ErhaiSD, was introduced by Guo et al. (Guo et al., 2001).

Feedbacks were considered with respect to different aspects of the social, economic, agriculture, and aquatic sub-systems. Simulation outputs correspond well with measured data, and were used to provide suggestions for the lake and its catchment management (Guo et al., 2001). Another modelling study based on hybrid GIS technology was applied to Erhai lake for water pollution control planning (Huang et al., 1999). The Hydrological Simulation Program Fortran (HSPF) was employed for the hydrological cycle and the USLE equation was used to simulate soil erosion in the watershed. HSPF includes many interactive relationships, including agriculture, industry, in-lake net-cage fish culture, tourism, forestry, stone excavation, in-lake navigation, in-lake fishing, lime/brick production, and water supply. An inexact-fuzzy multi-objective linear programming (IFMOP) model was developed to form an environmental decision support system for management or planning (Huang et al., 1999).

3.4 Summary

In conclusion, both Erhai Lake and Yunnan Plateau are currently seriously affected by human activities and climate change. Therefore, an understanding of the interactions between ecology and society is important for designing good management policies. However, the area is well studied during past decades, and the wealth of data is helpful for us to understand the complex ecological system. This chapter provides a general introduction to the lake and catchment. The detailed historical data including water level change, climate change, population and economic growth, algal growth and lake water quality change will be introduced in Chapter 5.

Chapter4 Methods

4.1 Introduction

This chapter will discuss the methods underlying the analysis of critical transitions and lake eutrophicationin Erhai Lake. A range of environmental proxies have been analysed from Erhai lake sediments, and instrumental data collected to co-explain the system dynamics with the palaeolimnological proxies. The analytical techniques for sampling lake sediments, including chronology, magnetic susceptibility, and analysis of diatoms, grain size, chemical elements, and total organic carbon/total nitrogen, will be presented, followed by discussion of statistical methods for assessing lake eutrophication, regime shifts, and early warning signals. The modelling techniques are also introduced in this chapter. The palaeolimnological proxies (i.e. chronology, magnetic susceptibility, grain size, chemical elements, and TOC/TN) were measured at Nanjing Institute of Limnology and Geography, Chinese Academy of Science. The training set diatom slides were also prepared in the Nanjing institute, but the identification was conducted in the Palaeoecology Laboratory at the University of Southampton (PLUS).

4.2 Lake Sediment Data

4.2.1 Sediment core sampling

Two short cores (EH2-1, EH2-2) (Fig. 3-5) were collected from the centre of Erhai lake with a Kajak gravity corer in the summer of 2009. The samples were sliced in field with a vertical resolution of 0.5 cm. They were then kept at low temperature (<4 °C) until further analysis. Samples from EH2-1 (64 cm, 128 samples) were used for measuring radioisotopes, diatoms, magnetic susceptibility, chemical elements, total nitrogen (TN) and total organic carbon (TOC). The samples from EH2-2 (57 cm, 114 samples) were used for measuring grain size. All 128 samples were analysed, but only samples with ^{210}Pb dating were employed in this thesis, which means the top 64 samples (32 cm) were used. This is no dating ion EH2-2

were performed, therefore, it assumes that a given depth has the same age for both cores so that only the top 32 cm of EH2-2 are used in this thesis.

4.2.2 Sediment core chronology

EH2-1 was used for ^{210}Pb and ^{137}Cs measurement. The activities of ^{210}Pb, ^{226}Ra and ^{137}Cs were measured with gamma spectrometry, using a well-type coaxial low background intrinsic germanium detector (Ortec HPGe GWL series). Supported ^{210}Pb in each sample was assumed to be in equilibrium with the *in situ* ^{226}Ra, and unsupported ^{210}Pb (^{210}Pbexc) was estimated by subtracting ^{226}Ra activity from the total ^{210}Pb activity. The onset of ^{137}Cs activity in the core and peak values derived from atmospheric nuclear weapon testing was used to testify the ^{210}Pb chronology. The dates of samples were calculated with CRS model (constant rate of supply) (Appleby, 2002), and the uncertainties of the dates were also calculated with the methods from Appleby (2002).

4.3 Surface sediment sampling

In order to develop a diatom training set for the region, surface sediments and water samples from 39 lakes in Yunnan Province were collected in the summers of 2005 and 2007. The deepest parts of the lakes were chosen for sampling using a Kajak gravity corer, and the uppermost 0.5 cm samples were taken as representative of the contemporary diatom communities of each lake. Water samples (~2 litres) were collected from the surface of the lakes. Measured chemical variables included pH, conductivity, potassium (K^+), sodium (Na^+), calcium (Ca^{2+}), magnesium (Mg^{2+}), chloride (Cl^-), sulphate (SO_3^{2-}), total nitrogen (TN), total phosphorus (TP), nitrate (NO_3-N), silicon (Si), chlorophyll-a (chla). pH and conductivity were measured in field, using a HANNA EC-214 pH-meter and HI-214 conductivity-meter. Details of the measurements of Chla, total suspended solids (TSS), TN and TP can be found in Zhang et al.(2007), and analytical techniques for the measurement of chemical elements can be found in Yang et al.(Yang et al., 2003). The water depth was determined using a portable echo sounder. Secchi depth (SD) was measured using a standard transparency disc, and the lake's depth was used instead of SD in the lakes where the bottom could

be seen. The lakes' surface areas were calculated with Google Earth Pro, and the ratio of lake surface area to depth was used as one of the physical characteristics.

4.4 Diatoms

Diatoms sample preparations followed standard procedures (Battarbee et al., 2001). For fossil diatoms, at least 300 valves were counted from each sample, and the diatom communities were expressed as a percentage of each species compared with the total number of valves counted per sample. For diatoms in the environment training set, at least 500 valves were counted from each lake and diatom communities were also expressed as percentages. Only the species with abundances greater than 1% and which appeared in more than 2 lakes were retained for final statistical analysis. Nomenclature and taxonomy mainly follows Krammer and Lange-Bertalot (1988a, b, 1991a, b, 2000), and the current equivalence taxonomy referred to Algaebase (http://www.algaebase.org/).

4.5 Physical and chemical measurements.

4.5.1 Magnetic susceptibility

Samples for magnetic susceptibility testing were measured with Bartington MS2 magnetic susceptibility instrument after being freeze-dried and ground. The sub-samples were packed into pre-screened 10 ml polystyrene sample pots. The magnetic susceptibilities were read under dual frequency (470 Hz=Xlf, 4700 Hz=Xhf). Xfd% and Xfd can be calculated by Xlf and Xhf (Dearing et al., 1996). Percentage frequency dependent susceptibility (Xfd%) is calculated based on the equation of (Xlf -Xhf/Xlf) x 100, and the mass specific dual frequency dependent susceptibility (Xfd) is calculated based on the equation of $\chi fd = (Xlf-Xhf)/\rho$ (where ρ is the sample bulk density). The effects of organic matter and calcium carbonate dilutions are removed with the following equation: Y=X*(1/(1-Z)). Where, X is original magnetic susceptibility, Z is organic matter, calcium carbonate or their summary, Y is the calibrated magnetic susceptibility.

4.5.2 Chemical Elements

The standard EPA method 3052 was employed for metal element (Al, Ba, Be, Ca, Co, Cr, Cu, Fe, Li, K, Mg, Mn, Na, Ni, P, Pb, Sr, Ti, V, Zn) analysis (USEPA, 1996) (*inductively coupled plasma-atomic emission spectrometry (ICP-AES)*). A representative weighed sediment sample (~125 mg) was placed in a Teflon nitrification tank with 6.0 ml conc. HNO_3, 0.5 ml conc. HCl and 3.0 ml HF. The sealed tank was then placed in a microwave oven (Berghof MWS-3 Digester) and nitrified at 180±5 °C for 15 minutes. The residue was then transferred into a Teflon breaker and dissolved with 0.5 ml $HClO_4$at ~200 °C before dilution to 25 ml with double-distilled de-ionized water. The solution was then analysed for metal elements by inductively coupled plasma-atomic emission spectrometry (Leeman Labs, Profile DV). The accuracy of the analytical determination was established using the reference material GSD-9, supplied by the Chinese Academy of Geological Sciences. The analytical results for all elements were found to be in agreement with the certified values, with accuracy better than 93%. The dilutions from organic matter were also removed with the same method as magnetic susceptibility. Calcium carbonate will be represented by Ca content value multiplied by 2.5 (according to the chemical formula of $CaCO_3$).

4.5.3 Total nitrogen (TN) and Total organic carbon (TOC)

Around 2 g of wet sediment was chosen for TOC (C% in organic matter of sediment) and TN (N% in sediment) measurement. The samples were placed in 50 ml of 5% HCl overnight to remove carbonates. The samples were then rinsed with deionised water, and oven dried at 40 °C. The sediments were ground into a fine powder, and sieved with an 80 µm mesh. TOC and TN were measured using a FlashEA 1112 Elemental Analyser linked to a Thermo Delta Plus Advantage mass spectrometer. In the following chapters, TOC and TN means C% in organic matter of sediment and N% in the sediment respectively in the absence of specific annotation. For organic dilution discussion, the organic matter in lake sediment will be represented by TOC value divided by 0.6.

4.5.4 Grain Size

Particle size spectra of EH2-2 were determined using a Malvern automated laser optical particle-size analyzer (Mastersizer-2000) after removal of organic matter and carbonate minerals by 10% H_2O_2 and 10% HCl treatment. There was no chronological data for this core. The dating of each depth in EH2-1 was applied to EH2-2, therefore, the particle size results cannot be used for high resolution comparison even though two cores were close to each other. In this thesis, particle size could only be used for understanding the rough trends of hydrological change, and was not used for core comparisons. The particle sizes are expressed in terms of percentage, and median particle size and average size are also given.

4.6 Instrument Data

Modern instrumental water quality data, including nutrient concentrations, algae concentrations, chemical oxygen demand (COD), secchi depth (SD), water level, have been collected from publications and local environmental management institutes. Such environmental data are collected every month, and the monthly average data are used in this thesis. Data on population, agricultural activities, fertilizer consumption and economic data were collected from Yunnan province and the Dali Autonomous Yearly Book, which is a statistical yearbook provided by Dali Autonomous Statistical Bureau. Climate data including temperature and precipitation (1950-2010) were collected from Dali weather station and provided by the China Meteorological Administration.

4.7 Statistical methods

4.7.1 Diatoms dataset and Fossil diatoms

The statistical descriptions of environment variables in the training set were conducted using the C2 software package (http://www.staff.ncl.ac.uk/staff/stephen.juggins/software/C2Home.htm). The values of minimum, maximum, mean, median, and standard deviation were

included in order to describe the environment variables in the dataset. All the environment variables were then normalised by a log(x+1) transformation to reduce discrepancies between measurement units and reduce the effect of extreme values (Lepš and Šmilauer, 2003). Diatom data were square root transformed with rare species down-weighted to stabilize variance before analysis. The detrended correspondence analysis (DCA) was firstly used to identify the gradient length within the diatom data and hence decide whether unimodal analyses would be appropriate (ter Braak, 1987). Partial canonical correspondence analysis (CCA) was then employed to test the significance of each environment variable, and the significant variables were chosen for further analysis according to the p-values in Monte Carlo permutation tests. Only the variables with p-values < 0.05 were chosen. The DCA and CCA analyses were completed in CANOCO Version 4.5 (ter Braak and Šmilauer, 2002). The cluster analysis of environmental variables was used to help classify the variables so that the appropriate variables for diatom distribution could be selected and autocorrelation effects could be reduced. The environmental variables were plotted with lakes and diatom species in the dataset in order to examine the properties of lakes and diatoms species patterns in Yunnan province. The DCA axis 1 score of fossil diatom assemblages cannot just represent the past diatom communities in Erhai lake but also represent diatom communities in the training set as it can find the main dissimilarity or gradients in diatom communities. It will be used to represent the lake's state change in this thesis. It should be noted that the 'DCA' will mean the DCA axis 1 score unless otherwise noted. Meanwhile, Hill's diversity index N2 (Hill, 1973)(HDI) was employed to calculate diatom diversity in each sample.

4.7.2 Mathematical methods for critical transitions

Both DCA and HDI data are linearly interpolated to annual intervals to obtain equidistant time series data (Dakos et al., 2008). In order to get the stationary data, single exponential smoothing methods in Minitab is used to filter out long-term trend impacts. Early warning indicators, including variance, autocorrelation, skewness, will calculated based on the smoothing residuals. Standard deviation

(SD) of the residuals is calculated to represent the variances before critical transitions. Autocorrelations are calculated based on lag-1.All the indicators' calculations are based on the moving window on half-size of time series data. Different moving window size (1/4 time series, and 1/3 time series) are also calculated to further test the signal of rising variance before the tipping point. In order to check the hypothesis of tipping point, sequential F statistics is employed (Andersen et al., 2009). F statistics are conducted with strucchange packages in R. Due to a very short period after assumed transitions at 2001, the most recent 20year data will be employed to test the hypothesis, and the slide width for F calculation is 4 years. Bimodality can be detected by frequency distributions of system states. Due to the limitation of the data, in this thesis, bimodality of the ecosystem state will be estimated by Gaussian Kernel density estimation, which is an alternative way to estimate the probability density of the lake's ecosystem state. The estimations are based on sliding windows in time series data, and the window size will be chosen as 20yr. The calculation of Gaussian Kernel density estimation is calculated with the R function of 'density'.

4.8 Phosphorus budget model simulations

A phosphorus output model from crop land in Northern Erhai catchment was written using STELLA software. Like the CREAMS model (Knisel, 1980), runoff volume is estimated with SCS (USDA Soil Conservation Service) curve number. Soil loss caused by rainfall is estimated through Universal Soil Loss Equation (USLE) (Wischemier and Smith, 1978). Its improvement method MUSLE (Williams, 1975) is used to simulate soil erosion in this thesis. Phosphorus cycling in the soil mainly refers to phosphorus cycling in the EPIC model. The detailed equations of phosphorus are found in Jones et al. (1984a). A differential equation (Carpenter et al., 1999b; Scheffer et al., 2001) is employed to simulate P dynamic in the lake. The catchment delinearations are based on GIS and ArcSWAT models. All simulation data is input into Excel for further analysis.

Chapter 5 Instrument and document data

5.1 Introduction

In chapter 3, the general background of Erhai lake was introduced. Many previous studies show plenty of data about human activities and eutrophication in Erhai lake. These data are buried in different types of publications. In consideration of the huge importance of these instrumental data, a chapter is separated to show all these secondary data together.

The purpose of this chapter is to: list the instrument and document data that will be used in the analyses within this thesis; provide an initial insight into human activities in Erhai lake catchment; and assess the eutrophication statue through instrumental data. In this chapter, the history of the lake's water quality, water level, and algal concentrations will be shown, as well as the historical changes in the lake's catchment, including factors such as land cover, fertilizer consumption, economic, population growth, and climate change.

5.2 The timeline of human activities and the lake response

Significant human activities and lake response are shown in Fig. 5-1. In 1949, the foundation of the People's Republic of China fundamentally changed the lifestyle of people living in Erhai catchment. Deforestation was initiated in 1958, and lasted around 23 years before the Diancang Mountain provincial conservation area was established in 1981. With respect to cropland systems, massive amounts of chemical fertilizers started to be used from the 1980s. This increased the nutrient supply to the lake, which has been considered to be the most important non-point nutrient pollution source for eutrophication in Erhai Lake (Li, 2001; Pan et al., 1999; Wang et al., 1999; Yan et al., 2005). Other important influential activities included the building of a hydropower station in West Erhe River from the end of the 1970s, the exotic fishes introduced from 1961 (Du and Li, 2001), and the cage fisheries in the 1990s. The lake's ecosystem changed along with the human activities. For example, the local fish started to become extinct in the middle of the 1970s due to

exotic fish invasion (Du and Li, 2001). It had been argued that the decline in water levels was responsible for the lake's ecosystem state change (Hu et al., 2005; Li, 2001; Wu and Wang, 1999). The first algal blooming was recorded in 1996, and continuous algal blooming has been recorded since 2002. Many efforts have already been undertaken to protect the Erhai Lake ecosystem, including the establishment of conservation areas, removal of fish cages and reconstruction of wetlands around the lake, but the lake's water quality is still in decline.

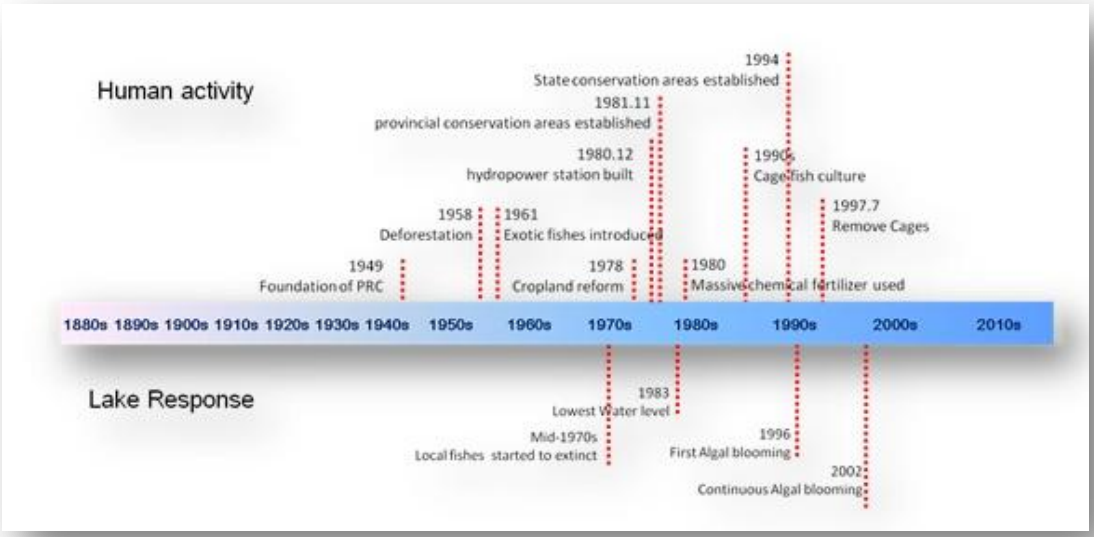

Figure 5-1 The timeline of human activity and lake response in Erhai Lake and its catchment. The main human activities are drawn on the top of diagram according to time. The lake's responses are listed on the bottom of this diagram and obvious responses are from the middle of 1970s.

5.3 Historical Climate Data

The climate data, including daily temperature and precipitation between January 1951 and November 2010, were collected from the China Meteorological Administration. The nearest weather station is at Dali which is located at Xiaguan. The annual precipitation and temperature are shown in Fig. 5-2. The change of mean precipitation over past 60 years is not obvious, which is around 1000 mm per year. For temperature, it declined before 1970s, and remained quite stable between 1970s and 1990s. However, one of the main features is that the temperature increased after the 1990s (Fig 5-2). The temperature fluctuation in

Erhai area is local as two other climate stations noted that the temperature started to rise after 1950s (Fig. 3-2)

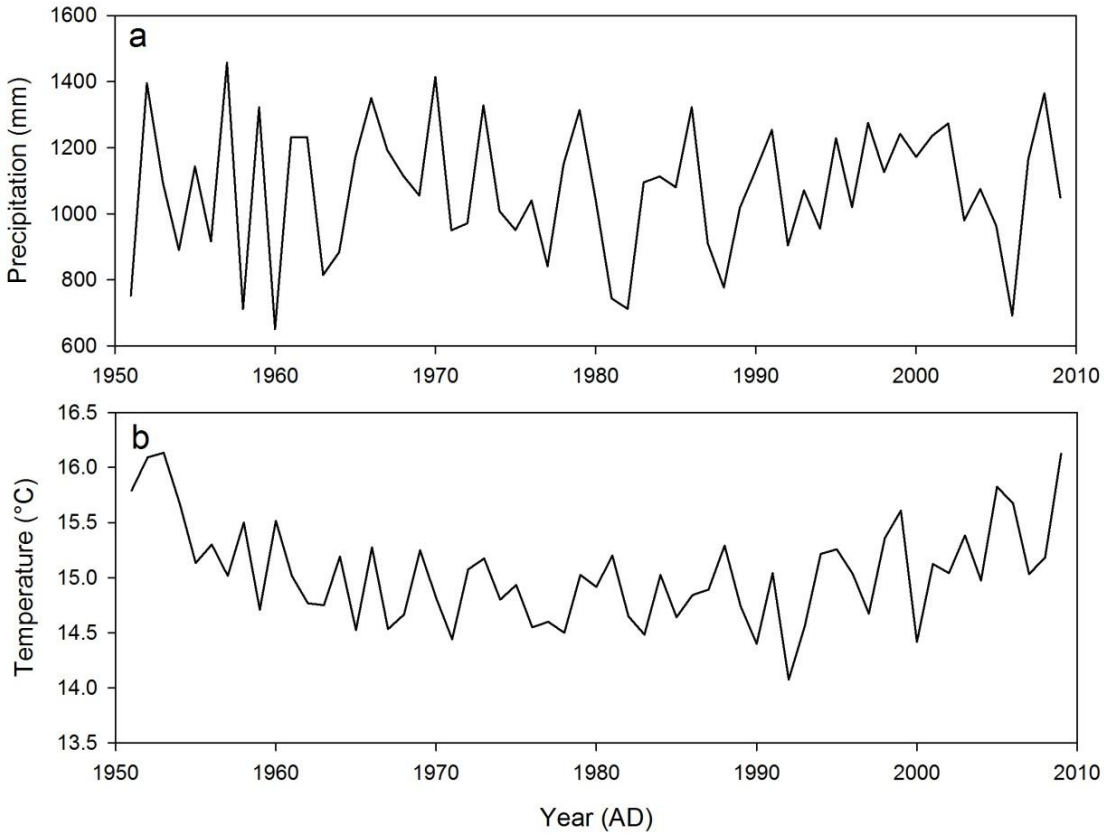

Figure 5-2 Temperature and precipitation recorded by Dali climate station (a, annual precipitation of Dali climate stations, and it shows the amount of precipitation over past 60years are quite stable; b, average monthly temperature for last 60years, which shows a little rising of local temperature after 1990s)

5.4 Population and economic change

The imprint of human activities in the catchment and lake started from around 3,000 years ago (Dearing et al., 2008), with documentary records starting around 2,000 years ago (Elvin, 2002). Recently, human activities surpassed any historic periods in terms of rapid economic growth and population (Fig. 5-3). The GDP (Gross Domestic Product) of Dali City increased from 4.8 million Yuan in 1985 to 98.8 million Yuan in 2007. The population increased from 0.4millionin 1985 to 0.6 million in 2007. During this period urbanization grew rapidly, while the percentage

of agriculture population decreased from 19% in 1985 to less than16% in 2007.

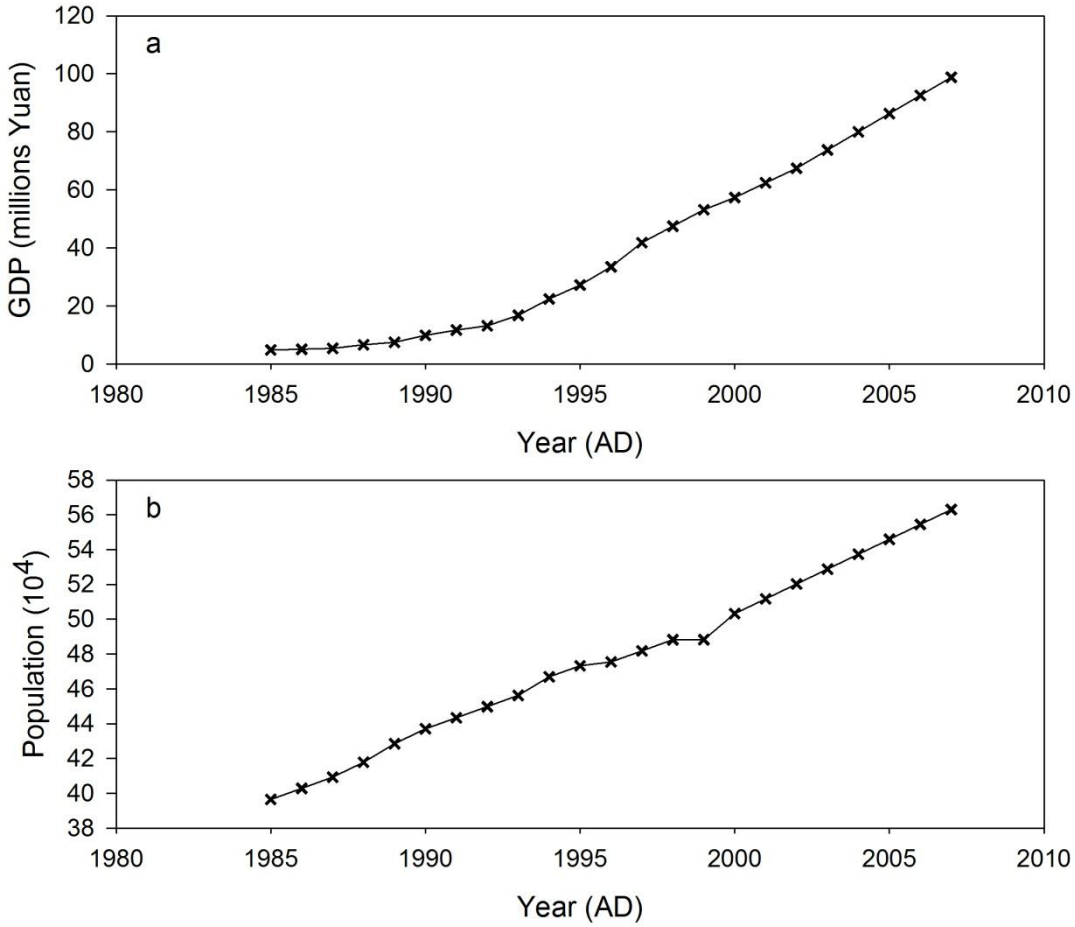

Figure 5-3 Population growth and economic growth in Dali city(Data original from Dali Municipality Yearly Book).

5.5 Land cover

The pressures from population and economic change induce the changes of land cover in the catchment. As shows in Fig. 5-4, forest cover has decreased since 1990, and barren land and urban land use increased. The forest cover in the catchment was around 61.7% in 1990, and declined to 53.4% in 2006. Many decreased forest areas are not transformed into crop land, but are used as infrastructure for human wellbeing, like house and road. The areas of town/village increased from 2.4% in 1990 to 6.8% in 2006. The environmental deterioration in the catchment could also be detected from the land cover change. In Fig. 5-4, the

percentage of barren and grass land increased from 13.9% in 1990 to 18.9% in 2006, which meant around 120 km^2 in the catchment was turned into barren or grass land during 1990-2006.

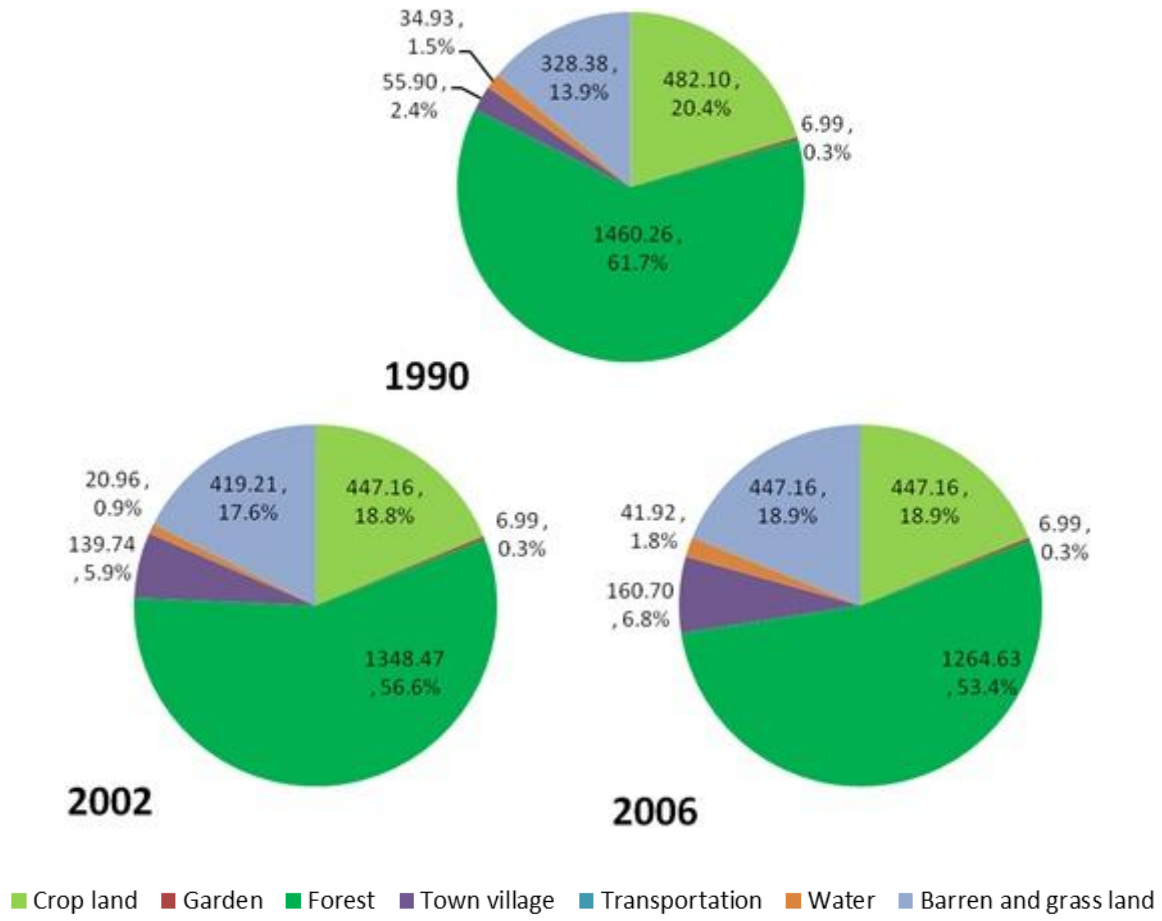

Figure 5-4 Vegetation cover change in Erhai Lake at 1990, 2002, 2006(Data collected from Institute of Environment and Sustainable Development in Agriculture, CAAS)

However, the crop yields are still increasing (Fig. 5-5). The main reason is that agricultural methods are changing with economic growth, and more chemical fertilizer is being consumed. Fertilizer consumption is increasing sharply in both Dali city and Eryuan county (Table 5-1). The quantity of chemical fertilizer used in Dali city was around 423.95 kg/ha in 1999, but it increased to 970.06 kg/ha by 2005. In Eryuan county, the applied chemical fertilizer was around 323.35 kg/ha at 1999, and it increased to 646.71 kg/ha by 2005. The data showed that around 23,547 t chemical fertilizers were used in 2005, which was 48% more than in 1999

(Data collected from Institute of Environment and Sustainable Development in Agriculture, CAAS). Consequently, crop production increased significantly from 3,268.7 kg/ha in 1952 to 7,820.9 kg/ha in 1996 (Fig. 5-5).

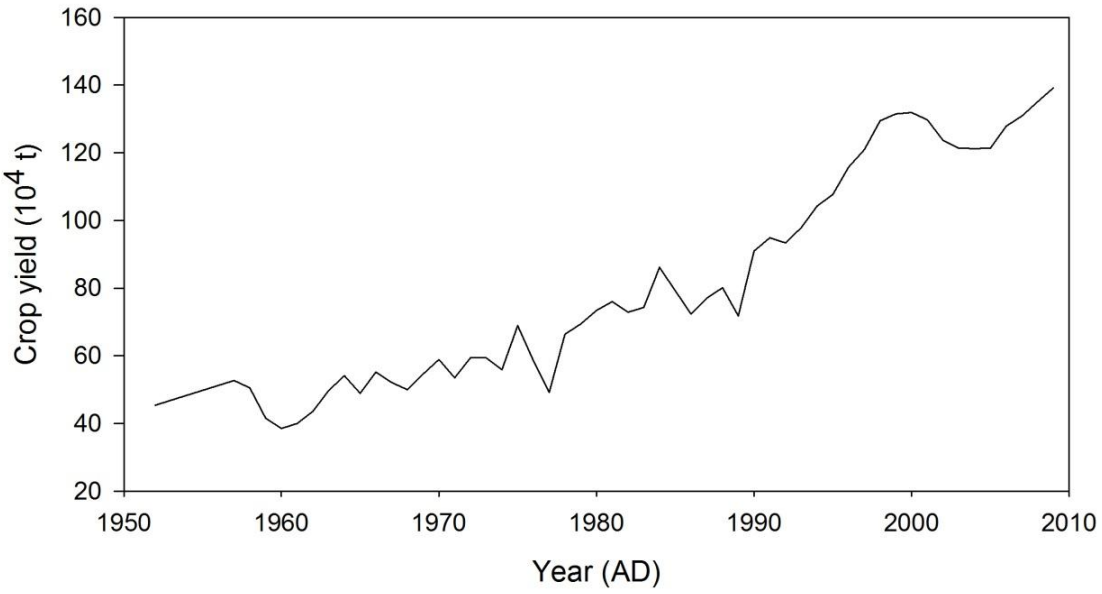

Figure 5-5 Crop yields in Dali city. The crop yields have increased threefold over the past 60years (data collected from Yunnan Province Yearly book)

Table 5-1 Fertilizer Applied per unit land (kg/ha)

Year	Dali	Year	Eryuan
1999	423.95	1999	323.35
2002	445.51	2002	495.81
2004	689.82	2004	524.55
2005	970.06	2005	646.71

5.6 Water level change

Fig. 5-6shows the water level fluctuation during the period 1952-2009.These data indicated that the lake level was stable before 1973, but decreased quickly during 1973-1982, experiencing its lowest water level at 1982. The main reason for the decline of water level was the digging of West Erhe River for a hydrologic power station (Yan et al., 2005) and the drought in 1982 (Fig. 5-2).Furthermore, the

increasing water demands within the catchment cannot be ignored. It could be due to increased irrigation in the catchment. Fig. 5-7 shows that the lake's water budgets and its inflow and outflow volumes decreased after the 1960s, but the decreased rate for inflow was larger than the outflow volumes. The water budget was at a 0.75 $\times 10^8$ m^3 deficit during 1980s (Fig. 5-7). Therefore, the increased water demands in the catchment are likely one of the most important reasons for water level declines. It is noteworthy that the lake's water level increased after 1998, and the value was almost similar to the lowest water level in 1976. Meanwhile, the highest water level was kept at around 1,974 m a.s.l.

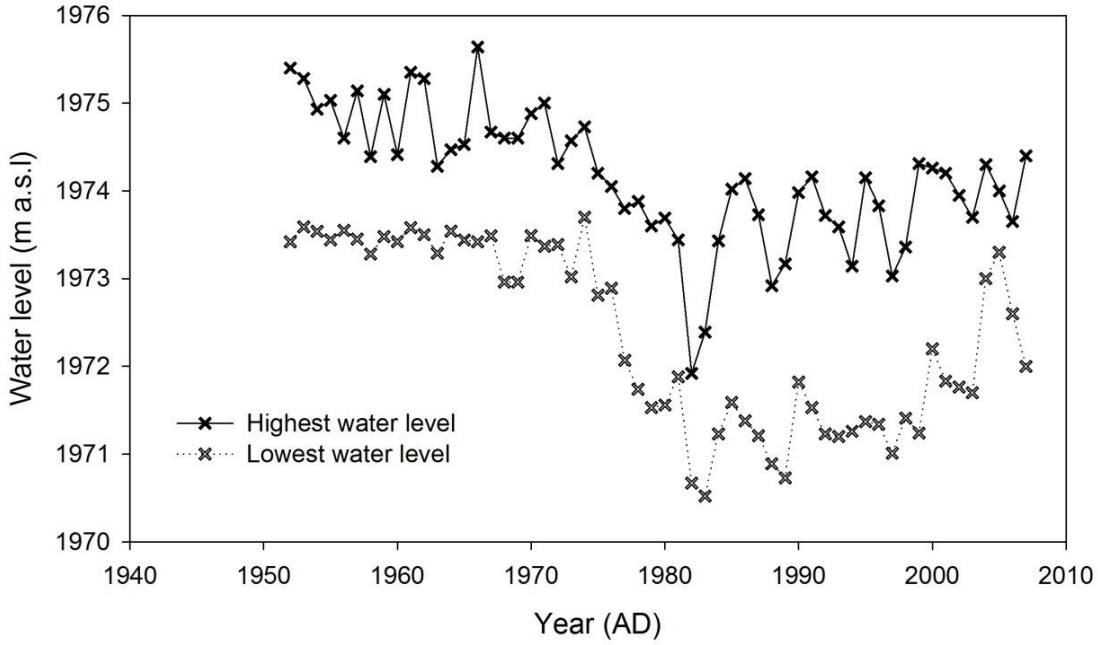

Figure 5-6 Water level fluctuations in Erhai lake during 1952-2009.

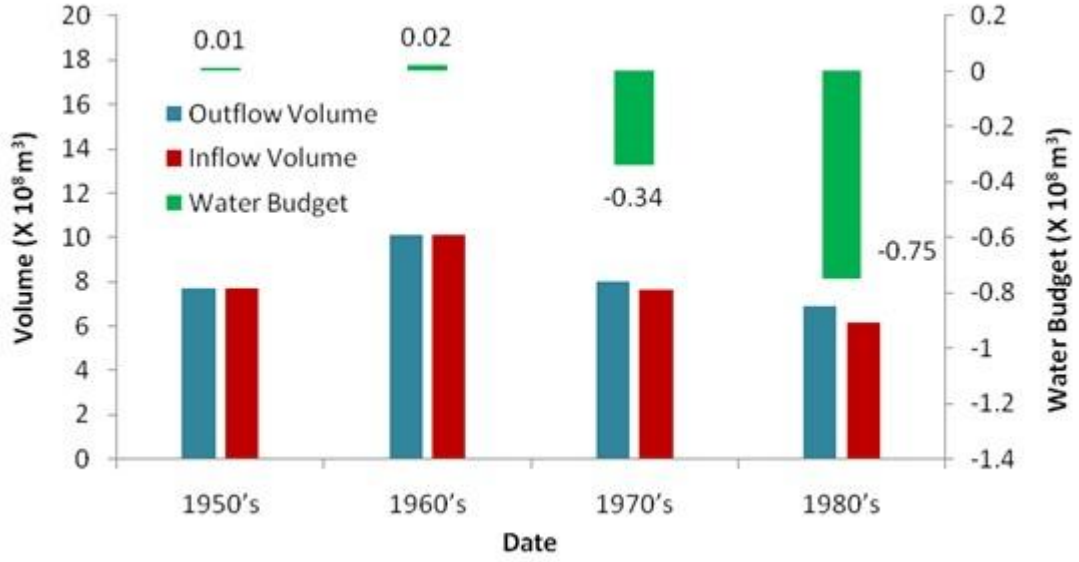

Figure 5-7 Water discharge in Erhai lake

5.7 Nutrient inputs to Erhai Lake

With the development of society and economy, especially urbanization and agriculture improvement, increased nutrients import into the lake. The main nutrient source is from non-point pollution which dominated (around 90% of inputs) in 1999 and the major non-point pollution is from agriculture (Yang and Ni, 1999). The records show that nutrient concentrations (TP, TN) (Fig. 5-8) gradually increased since 1992 AD. At 1992 AD, TP was around 0.015 mg/l, and the lake was mesotrophic (Yan et al., 2005). It became eutrophic after 1996 AD, when TP was greater than 0.35 mg/l. The nutrient enrichment induced the algal growth in the lake (Fig. 5-9). The main algae were Cyanophyta and the content was only 215×10^4 per litre in 1995, but it increased to 2,025 $\times10^4$ per litre by 2003, when a serious algal blooming was recorded. The concentrations of Chlorophyta and Bacillariphyta also increased with the nutrient enrichment. TP decreased after 2003 AD, but TN remained at high levels. There are no detailed studies about the effects of management on nutrient reduction. A widely accepted reason is the sewage disposal practices and the reconstruction of wetland around the lake. The enrichment of nutrients caused the degradation of the lake's water quality. COD_{Mn} increased since 1993, but have declined after 2005 (Fig. 5-10a). High correlation between COD_{Mn} and TP indicates that the limiting nutrient for Erhai Lake should

be P rather than N. The dissolved oxygen in the lake declined from 1997, reaching its lowest level between 2006-2008, but seems to have improved recently (Fig. 5-10b). The lake's clarity kept at a high level at above 3 m before 2001, but suddenly declined to around 1.5 m after (Fig. 5-10c).

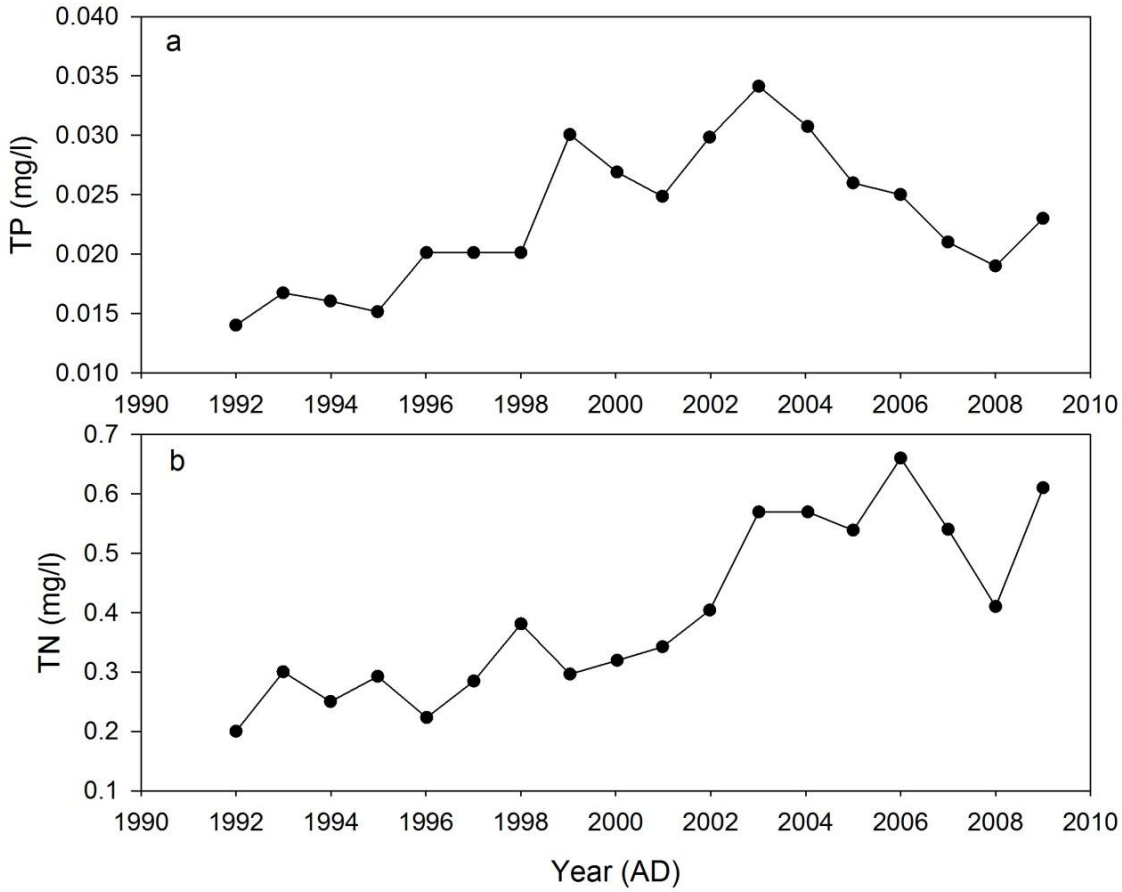

Figure 5-8TP and TN concentrations in Erhai Lake during 1992-2009, TP shows an increase before 2003 but decreases afterward (Data collected from Institute of Environment and Sustainable Development in Agriculture, CAAS, and Environmental Monitoring Station of Dali Prefecture)

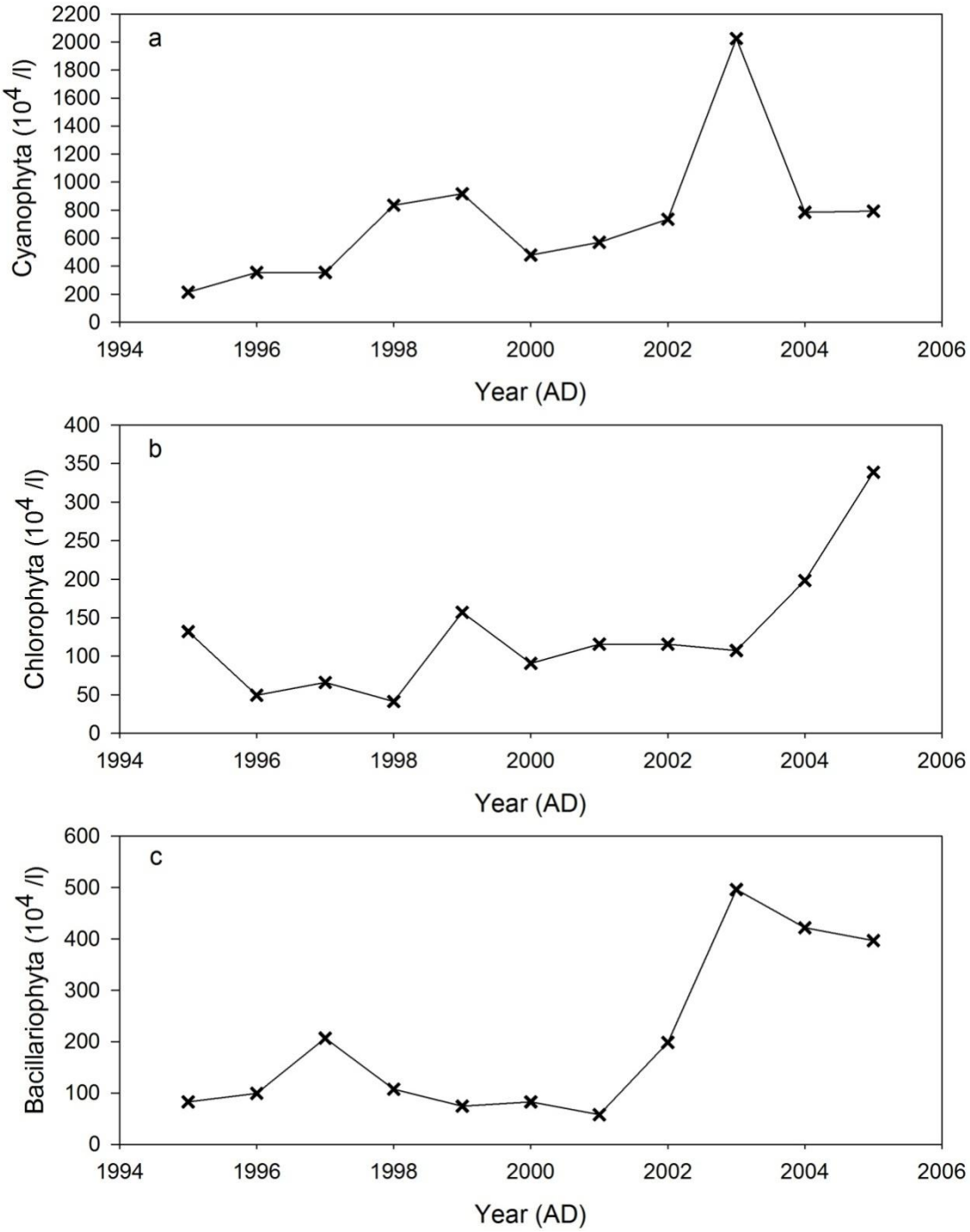

Figure 5-9 Algae concentrations in Erhai Lake between 1995-2005. a, the concentration of Cynophyta between 1995-2005 shows a continuous rise and with a peak value in 2003; b, the concentration of Chlorophyta between 1995-2005 shows big increasing after 2003; c, the concentration of Bacillariophyta between 1995-2005 shows step change after 2001, and reaches at a high value after 2003.

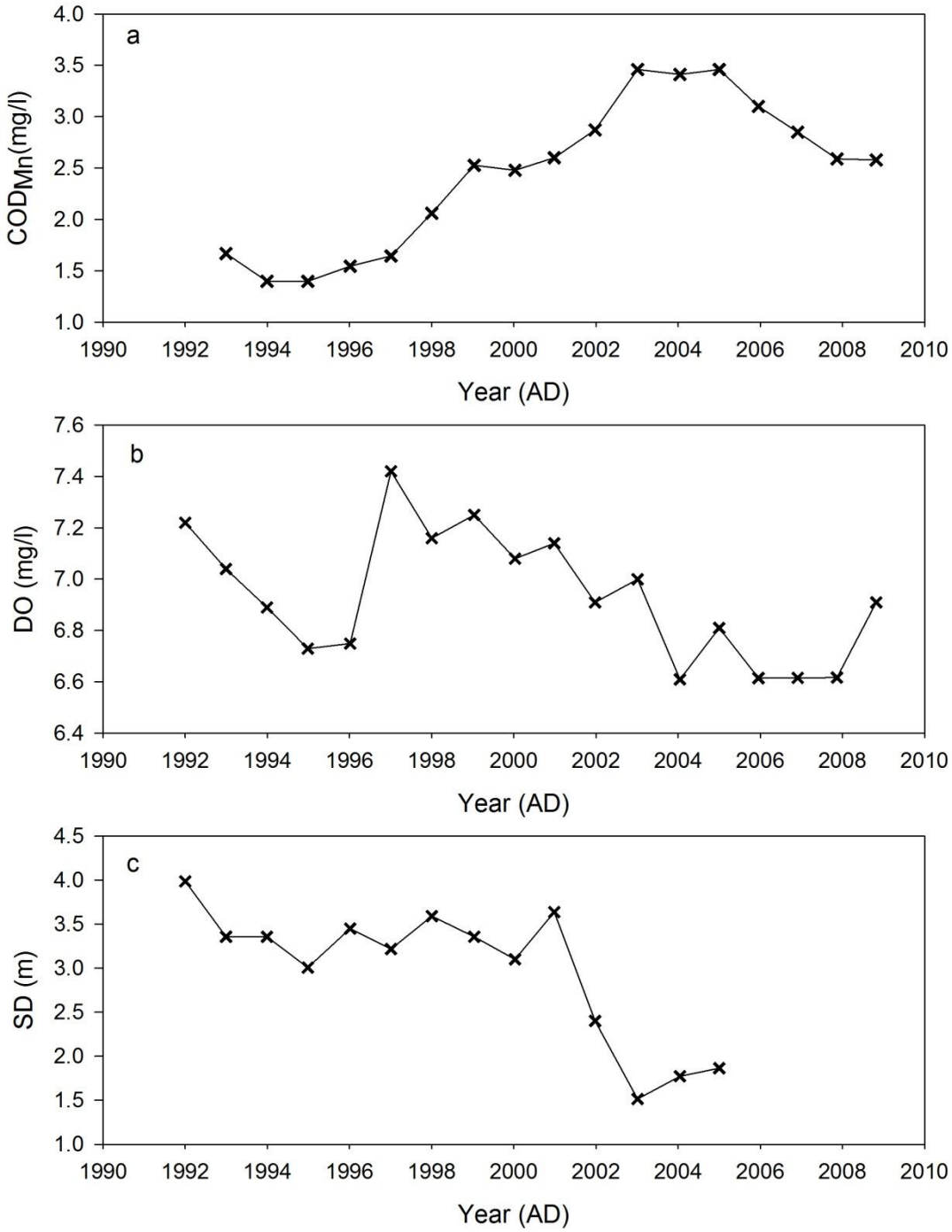

Figure 5-10 Lake secchi depth, COD_{Mn} and dissolved oxygen (DO). a, COD_{Mn} in the lake surface water shows that the water quality deteriorated at least from 1994, and reached a high value after 2003; b, dissolved oxygen (DO) in the surface water of Erhai lake. It decreases between 1997-2007, with only a slight rise in 2009; c, SD shows the clarity change of Erhai lake. The SD was high and stable before 2001, but declined sharply afterward.

5.8 Summary

The instrument and document records show that Erhai lake was starting to become eutrophic around the 1990s, and changed from a clear to turbid state after 2002. Many factors could be responsible for the lake's eutrophication, such as agricultural activities, deforestation, fertilizer consumption, declining water level, regional warming, and population growth. Due to a lack of long term monitoring data, it is still difficult to track the lake's eutrophication process. To fully understand the lake's eutrophication process, long term analysis using palaeolimnological proxies will be presented in the following chapters.

Chapter 6 Diatom-Environment Training set

6.1 Introduction

Diatoms have been used to quantitatively reconstruct environments such as temperature (Rosen et al., 2000; Vyverman and Sabbe, 1995; Weckstrom et al., 1997), pH (Birks et al., 1990; Smol and Stoermer, 2010), total phosphorus (Bennion, 1994; Yang et al., 2008), and conductivity or salinity (Fritz et al., 1991; Gasse et al., 1995; Wang et al., 2011; Yang et al., 2003). A calibration training set is needed for a transfer function between environment variables and indicators. The relationships are usually interpreted by some well-known methods, such as partial least square (PLS) (ter Braak and Juggins, 1993), Canonical correspondence analyses (ter Braak, 1986) and Weighted average-Partial least square (WA-PLS) (ter Braak and Juggins, 1993). The techniques used are either linear (such as PLS) or unimodal (such as CCA and WA-PLS). Undoubtedly, these methods have contributed significantly to reconstructing past environmental change. However these reconstructions are based on some assumptions. For instance, the fossil diatoms have the same ecological characteristics as the diatoms in the training set; and that the environmental variable of interest is at least monotonically related to an ecologically important determinant in the system studied (Birks et al., 2010). Although the assumptions are very important for the accuracy of the reconstructions, they are not well tested in many literatures. Some studies emphasised the importance of testing the assumptions before conclusions can be reached(Birks et al., 2010). Some possible uncertainties are discussed in previous studies, such as species habitat selection (Sayer, 2001) and the impacts from spatially structured environments (Telford and Birks, 2009). The aim of addressing these uncertainties is to illustrate and overcome the potential discrepancies of transfer functions. In fact, the interactions between environmental variables and indicators are always dynamic in nature(Scheffer, 1998), and more than one state may exist in the real ecosystem (Carpenter et al., 1985). Linearor unimodal methods cannot describe multiple states in an ecosystem. In the present study, the possibility of multiple states in the training set will be considered in order to reveal the potential reconstruction errors for diatom-based transfer functions.

Firstly, this chapter will demonstrate the possible reconstruction errors resulting from a training set using a conceptual model. As a result of the focus on lake eutrophication within this study, all of the discussions take place in the context of the relationship between the diatoms and TP. Secondly, the compilation of a training set derived from 39 lakes in Yunnan province (Fig. 3-1) will be discussed in this chapter. The features of the lakes will be introduced, which include 23 environment variables and surface diatom communities. The purposes of this chapter are: 1. Elucidating the relationship between diatoms and environmental variables in Yunnan province, so that it can provide a reference for historical water quality change in Erhai lake based on fossil diatom assemblages; 2. Considering the idea of alternative states in the training set to show its influence on the accuracy of diatom-based transfer functions.

6.2 The influence of alternative states for the accuracy of diatom-based transfer functions

The bias of diatom-based transfer function at the ends of the gradient is always large, and the species optima always result in inaccurate estimates so that the reconstructions are always high or low in a maximum or minimum of the TP gradient. The effect is what is known as the ‘edge effect’ (Hall and Smol, 2010). To acquire a robust transfer function and reduce the impacts of uncertainties, a large dataset is required so that a broader range of environmental variables can be covered (Hall and Smol, 2010). Obviously, it indicates that the lakes in the middle of the TP gradients may have a better reconstruction. If we consider the set of all possible calibration lakes, diatom communities may not be arranged on a simple gradient for a given state of a variable. There may be a step-change in community structure at a threshold value of the variable. A transfer function assuming a simple linear relation would be inaccurate. Further, it is possible that multiple stable states may be sampled, with different lakes observed in either state. In this case, while variable values may be quite similar, diatom communities are very different. The issue is not that individual diatom taxa are necessarily occurring at

different TP values, but that the switch from an open water state to a turbid state involves a major habitat switch and/or seasonality change creating different diatom assemblages that are not necessarily sensitive to TP fluctuations. One of the key weaknesses of transfer functions is that the optima are calculated without regard to the community context in which the taxa occur at the different sites. Therefore, as discussed in the previous section, the relationship between diatoms and environmental are one fold in most of training set, i.e. there is no alternative stable state in the training set. As introduced in chapter 2, it is highly possible that there are multiple states between environment and biology. . The question is: can we still have strong reconstruction results when there are multiple states represented in the training set? A simple conceptual model was created to address this question.

Fig. 6-1 shows conceptual models for the estimation errors in a diatom-environment training set that contains alternative states. Two types of multiple states system are examined: fold bifurcation (Fig. 6-1a) and step change (Fig. 6-1b). Two equilibrium states, i.e. state 1 and state 2, exist between diatom and environmental variables (TP). In Fig. 6-1a, two states can exist simultaneously under one TP value between two bifurcation points (F1 and F2); for instance, D1 and D2 can exist simultaneously under P0. If linear methods are used for transfer function construction, the relationship between diatoms and inferred TP will probably be changed to the grey curve in Fig. 6-1a. Therefore, if this relationship is used for TP reconstruction based on fossil diatoms, the reconstructions will be overestimated in state 2 and underestimated in state 1 (like the horizontal arrows in Fig. 6-1). The similar estimation errors also exist in the step change condition (Fig. 6-1b).

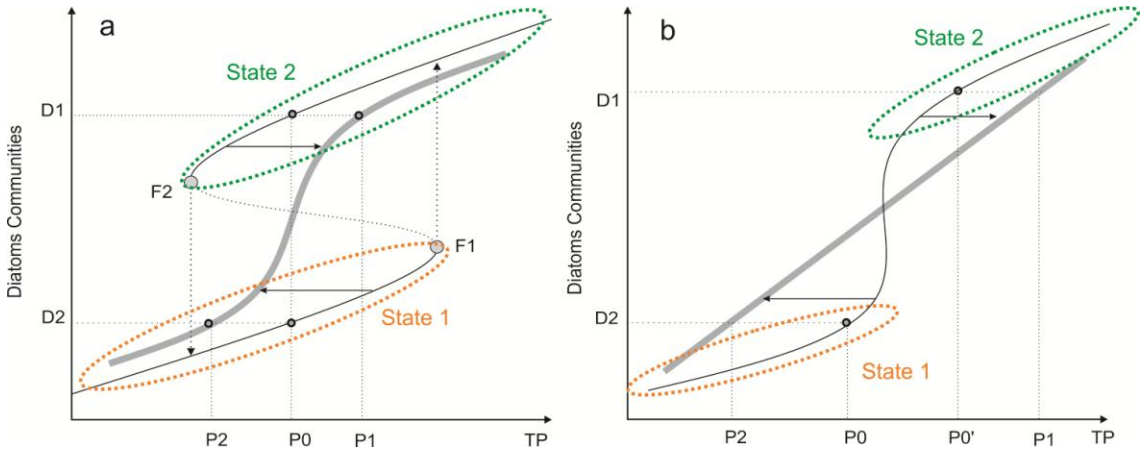

Figure 6-1 Two conceptual models for the pattern of estimation errors from a diatom-environment training set that contains alternative states (state 1 and state 2). Two equilibrium states existed in the dataset, and the relationship (solid curves) is assumed as (a) fold bifurcation and (b) step change between diatoms and environment (TP). The wide-grey curve represents the transfer functions between diatoms and TP.

6.3 Environment variables in Yunnan Province

23 environment variables were collected from the 39 lakes. Statistical descriptions are listed in Table 6-1 and detailed data are listed in Appendix I. The lakes covered a large area of Yunnan Plateau (Fig. 3-1), and the altitudes ranged from 1,291 m a.s.l (Changqiaohai Lake) to 3,827 m a.s.l (Laojunshan Lake). A high standard deviation (614.5 m a.s.l) indicates that the lakes are spread out across a large range of elevations. Most of the lakes are shallow, and only 3 lakes are 20 m deep or more (i.e. Yangzonghai, 20 m; Qingshuihai, 21 m; Fuxianhu, 110 m). Most of the lakes ranged from 1 $km^2$to 30 km^2 in size and 11 lakes are smaller than 1 km^2. Two lakes (Erhai lake, 249 km^2; Fuxianghu, 211 km^2) had extremely large surface areas. The ratio of area to depth (A/D) is calculated to further describe the morphometric of the lake, which shows that many small but deep lakes exist in this dataset. All lakes are alkaline (with pH>7) which reflects the geology in Yunnan Province. Most of the lakes are turbid and only 7 lakes have Secchi depths (SD) higher than 2 m; Cibi Lake is the most transparent. The SD are strongly and negatively affected by TSS in the lake (Pearson coefficient was -0.52, $p<0.001$), and the lakes with high nutrients have relative low SD. This may suggest that the

clarities of the lakes are related to nutrient pollution. TP and TN are significantly correlated with the coefficient around 0.44 ($p<0.001$), and 10 lakes have a TP in excess of 50 µg/l. All of these lakes are located in the valley and with intense human activities in the catchment. Qiantunshuiku has the highest TP value (1,248.3 µg/l). However, the content of chlorophyll (Chla) in Qiantunshuiku Lake is low (~1.7 µg/l). The second highest value is 329.5 µg/l in Tinghu Lake, which is much smaller than Qiantunshuiku Lake. The standard deviation of TP is high (Table 6-1). Six lakes including Erhai Lake belong to a meso-eutrophic category as their TP values are among 30-50 µg/l, while the other 23 lakes could be classified as oligotrophic. The salinity was negatively correlated with altitude (r^2=-0.47, $p<0.001$), which indicates that the lakes on the plains have, in general, higher salinity.

Table 6-1 Environmental variable statistics descriptions (A/D means the ratio of area/depth of each lake; Min. means minimum of each variable; Max. means maximum of each variable; Var. means variance; λ1 and λ2 eigenvalues of CCA axis 1 and axis 2)

FullName	Min.	Max.	Mean	Median	SD	P-value	λ1	Var.of species	λ1/λ2
Depth (m)	1.0	110.0	9.3	4.7	17.22	**0.001**	0.204	5.5	0.48
Area km^2	0.2	249.0	19.2	2.2	51.30	**0.002**	0.26	5.8	0.6
A/D	0.01	27.98	2.11	0.40	4.75	**0.016**	0.161	4.3	0.43
pH	7.20	9.73	8.58	8.65	0.51	0.369	0.102	2.7	
Longitude (°N)	23.44	27.91	25.50	25.69	1.19	0.045	0.14	3.7	
Latitude (°E)	99.64	104.40	101.98	102.78	1.68	0.103	0.103	2.8	
Altitude (m)	1291	3827	2066	1954	614.49	0.181	0.181	4.8	
SD (m)	0.20	6.14	1.28	0.90	1.18	**0.003**	0.174	4.7	0.42
NO3-N (mg/l)	0.01	2.06	0.28	0.08	0.50	0.519	0.094	2.5	
Na^+(mg/l)	0.40	132.80	10.20	3.80	21.38	**0.001**	0.278	7.4	0.84
K^+ (mg/l)	0.10	15.20	3.11	2.10	3.52	**0.001**	0.278	7.4	0.84
Mg^{2+} (mg/l)	0.60	49.10	13.78	11.90	10.33	**0.006**	0.164	4.4	0.44
Ca^{2+} (mg/l)	1.60	58.40	25.70	24.20	14.16	0.124	0.125	3.4	
Cl^- (mg/l)	0.10	43.90	7.77	2.40	10.73	**0.001**	0.245	6.6	0.71
SO_4^{2-} (mg/l)	0.30	204.60	24.83	9.50	37.29	**0.001**	0.206	5.5	0.56

Si (mg/l)	0.26	6.74	1.87	1.46	1.48	0.166	0.119	3.2	
Chla (ug/l)	0.01	133.22	12.23	3.10	28.34	**0.001**	0.224	6	0.66
TN (µg/l)	213.9	4592.5	1201.0	687.1	1092.60	**0.001**	0.217	5.8	0.55
TP (µg/l)	1.7	1248.3	76.6	21.3	201.67	**0.001**	0.214	5.7	0.56
TSS (mg/l)	0.17	57.73	15.22	9.10	14.62	**0.001**	0.217	5.8	0.52
Cond. (uS/cm)	40.00	281.00	226.18	230.00	34.47	0.259	0.118	3.2	
Salinity (mg/l)	6.07	341.42	87.54	68.17	69.22	**0.001**	0.219	5.9	0.63
Do (mg/l)	0.07	11.83	3.70	3.34	2.69	0.045	0.14	3.7	

6.4 Surface Sediment Diatom Communities in Yunnan province datatset

192 different diatom taxa were identified from the 39 lakes. Only 102 of them were chosen for further statistical analysis after removing the taxa with abundances of <1% and in two or less lakes. The common taxa included both littoral epiphytic and benthic taxa such as *Achnanthidium minutissimum* (Kützing) Czarnecki, *Navicula cryptotenella* Lange-Bertalot, *Discostella stelligera* (Cleve & Grunow) Houk & Klee, *Navicula trivialis* Lange-Bertalot, *Nitzschia palea* (Kützing) W. Smith, and planktonic species such as *Staurosirella pinnata* (Ehrenberg) D.M.Williams & Round, *Cyclotella bodanica* var. *lemanica* (O. Müller) Bachmann, *Cyclotella pseudostelligera* Hustedt, *Cyclostephanos dubius* (Fricke) Round, *Cyclotella ocellata* Pantocsek, *Aulacoseira granulata* (Ehrenberg) Simonsen; all of these taxaappeared in more than 20 lakes. The most common taxawas a littoralbenthictaxa*Achnanthidium minutissimum* (Kützing) Czarnecki, which appeared in 35 lakes, and the highest percentage was 38.9%, in Haishaoshuiku. Planktonic taxasuch as *Cyclotella* sp., *Cyclostephanos* sp. were the dominant taxa in this dataset. These taxa typically dominated eutrophic lakes, for example, *Cyclostephanos dubius* had around 50% percentage in Xinyunhu, and *Cyclostephanos tholiformis*Stoermer, Håkansson & Theriot dominated with around 59% of population in Yiliangcaohai and 74% in Yangpai Reservoir respectively. However, some other taxaseemed highly related with salinity in oligotrophic lakes, such as *Cyclotella ocellata* which dominated in Lake Fuxian, Bitahai, Qingshuihai, Yangzonghai, and Erhai. Other planktonic taxa such as *Aulacoseira* spp. with the highest percentage of *Aulacoseira ambigua* (Grunow) Simonsen represented75.9% in Lake Qiluhu that was a eutrophic shallow lake with a high Chla value (84.2 µg/l).

Another planktonic taxa *Fragilaria crotonensis* (Kitton) were important in relation to water quality at Erhai. This taxon had the highest percentage in Erhai Lake, which was around 35%. It was also common in Xinyunhu (~28.8%), which was a lake with a TP of around 271.5 µg/l. Other research also showed that the increase of *Fragilaria crotonensis* was related to lake circulation and stratification (Platt Bradbury, 1988). All species and some statistical descriptions were listed in Appendix II.

6.5 Statistical analysis for the Yunnan training set

The gradient length of the first DCA axis is 3.6 standard deviation (SD) units, which indicates that there is near complete turnover of species in diatom communities (Hassan et al., 2012; Jongman et al., 1995) and that unimodal methods could be employed for ordinations. The first CCA axis shows that around 10.3% of the variance in the diatom data is explained. Partial CCA analysis is employed to test the significance of each environmental variable to diatom communities. 14 environment variables are finally considered to be significant for diatom distributions as their p-values were <0.05 under the Monte Carlo test (Table 6-1). The eigenvalue (λ_1) and explained variance of species for first CCA axis are also listed in Table 6-1. It indicates that Na^+ and K^+ concentrations were the most significant variables for the patterns of diatom communities in Yunnan province, as they provide the highest λ_1 (0.278) and independently explained more diatom distributions (7.4%). TP and TN independently explained 5.7% and 5.8% of diatom distributions in this dataset. It indicates that the cation concentration in the water may be the most important environmental indicator in this training set, but nutrients such as TP and TN are also significant to diatom distribution in Yunnan. In order to reduce the impacts from the co-linearity of the environmental variables in the dataset, a cluster analysis with only significant variables is employed (Fig. 6-2). It gives the relationships among different environment variables. The variables are divided into two main groups according to the correlations among them, i.e. ionic concentrations and nutrients. The dendrogram (Fig. 6-2) shows that all chemical elements, which indicate the state of a lake's ionic content, have high correlations with each other. Another important group is nutrients in lakes, i.e.

TN and TP. The amount of Chla in lakes is highly related to nutrients, and also seems to determine the content of TSS. Other two small groups seem significant different with the two main group. One is the group of depth-SD. Although TSS has a strong negative relationship with SD, they are not in the same group. On the contrary, SD is in the same group with depth, and they have a high positive coefficient (r^2=0.5, p<0.001). It indicates that the deep lakes are always clean. Another group includes area and area/depth, which are related to the lakes' physical characteristics. According to the results of cluster analysis, four variables will be chosen for further analysis. Table 6-1 shows that the most significant of ions is Na^+; therefore, it will be chosen first. Although TN is slightly more significant than TP for diatom distribution in the dataset, TP is still chosen for the further analysis due to the purpose of the thesis which focussed on the relationship between diatom communities and TP. The choice of SD, depth, area, or A/D will not strongly affect the ordination results.

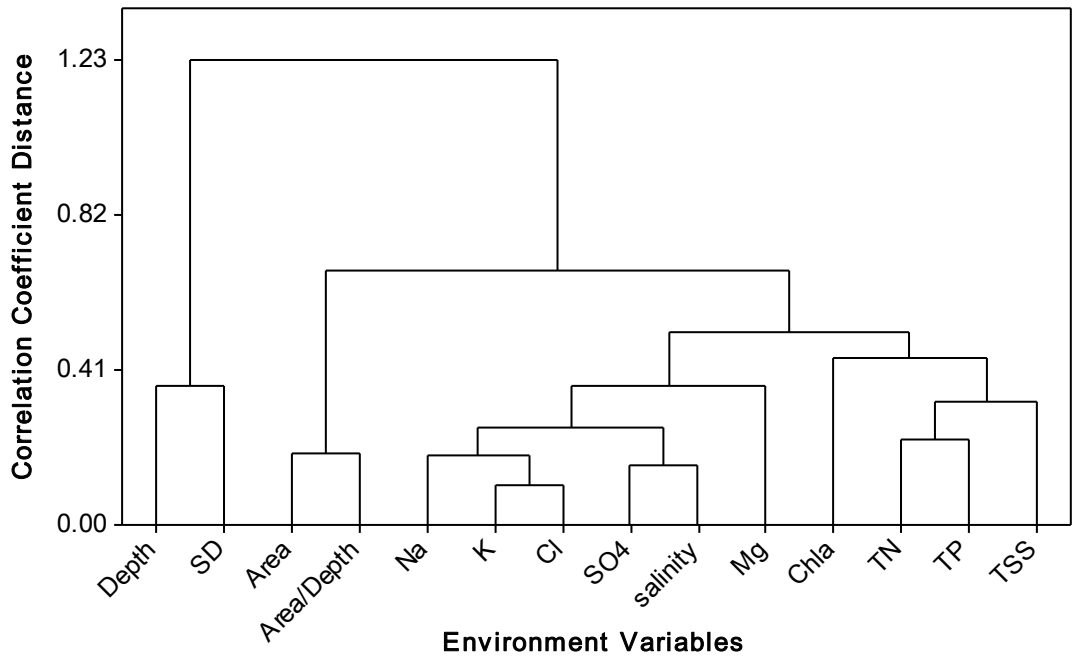

Figure 6-2 Cluster analysis of environment variables

The CCA plots of the selected four environment variables with surface samples and species in the lake are shown in Fig. 6-3. Fig. 6-3a indicates that there are no obvious outliers in the Yunnan dataset. However, two lakes (CB07 and FXHL) are

not similar to the other lakes. Both lakes were deep and have very high SD values (Appendix I). The plot of species with environmental variables (Fig. 6-3b) shows that the taxa of *Cyclotella atomus* (Hustedt), *Fragilaria exigua* (Grunow), *Tabellaria ventricosa* (Kützing), *Stauroneis anceps* (Ehrenberg) and *Eunotia bilunaris* var. *linearis* (Okuno) Lange-Bertalot are dissimilar from other taxa. Most of these species rarely occur in the lakes except *Eunotia bilunaris* var. *linearis* that was around 21.3% of population in Laojunshan but had very low percentages in the other 2 lakes. The species patterns in Fig. 6-3b do not correlate with any environmental variables, which might indicate that the critical factors for species distributions are complicated in Yunnan Province.

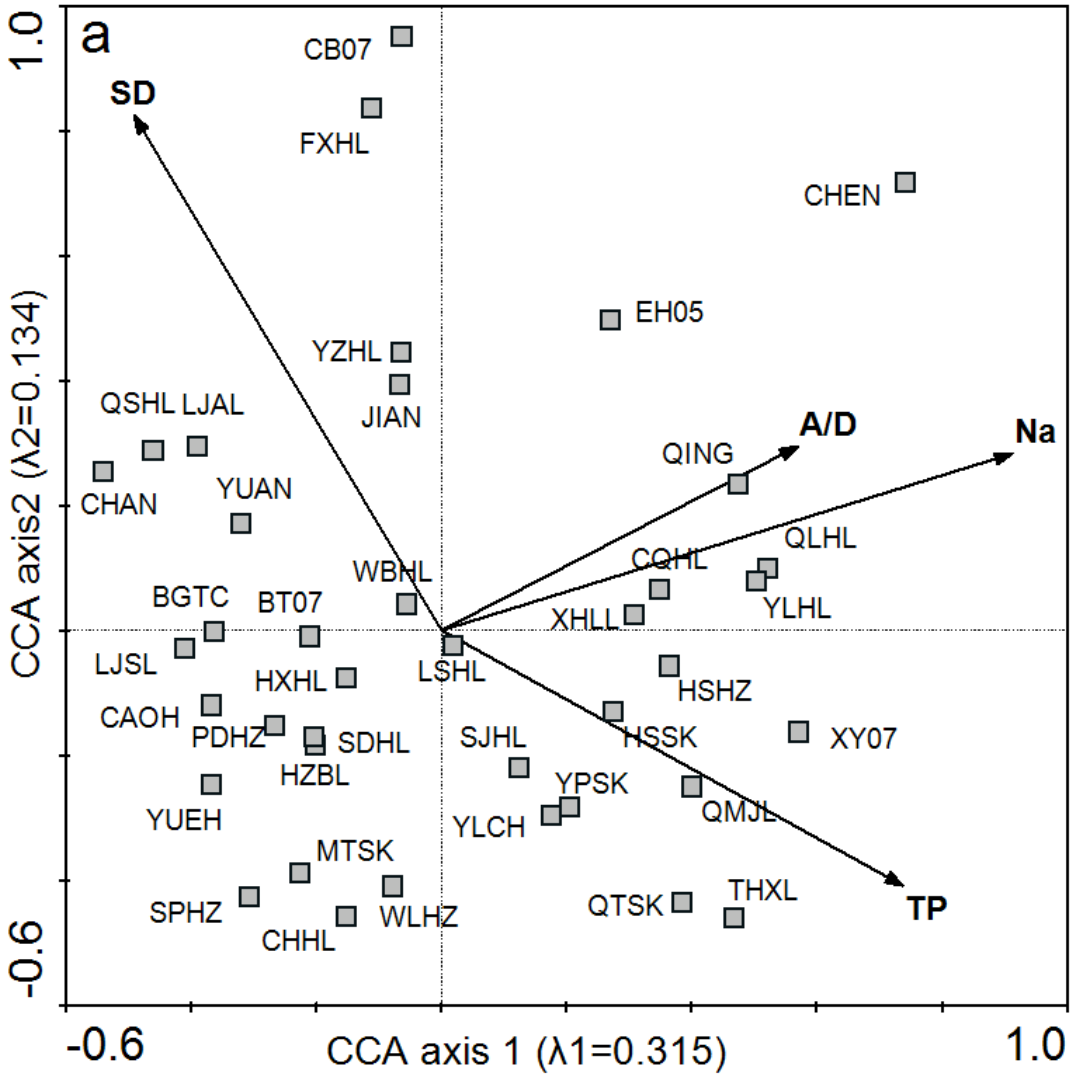

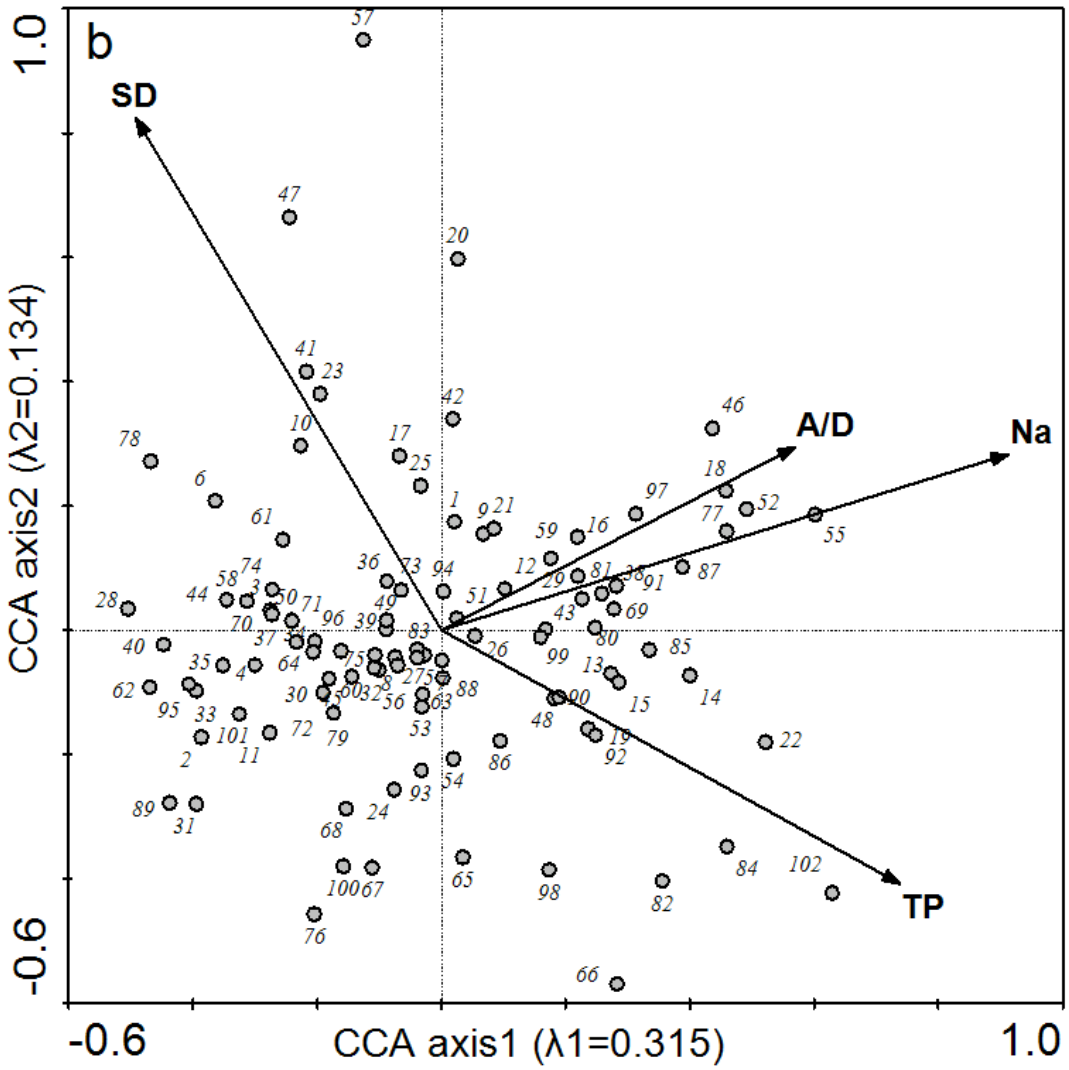

Figure 6-3 CCA analysis with 4 environmental variables from 4 cluster groups (a, CCA plot with 39 sample sites and four main environmental variables. The code of lakes could be found from Appendix I; b, CCA plot with diatom species in 39 lakes and four main environmental variables. The code of species could be found from Appendix II.)

6.6 Diatom-based phosphorus transfer functions

Table 6-1 gives ratios of λ_1/λ_2 in order to choose the environmental variables for transfer functions. The highest λ_1/λ_2 in the four selected variables is Na (0.84) while TP is the second largest variable (0.56). However, only TP transfer function will be discussed here because this thesis will focus on the eutrophication process.

A weighted averaging model with bootstrapping cross validation method is employed to construct a transfer function based on diatoms. The lake of Qiangtunshuiku (QTSK) is deleted from the dataset when the diatom-based TP transfer function is constructed, as it is an obvious TP outlier. The weighted averaging model classical deshrinking (WA_classical) for TP has the highest but still very low predicted coefficients (bootstrapping R^2) which is only 0.44, and the relatively lower RMSEP (0.42) (Table 6-2). Meanwhile, the WA_classical model gives the lowest bootstrapping maximum bias (~0.61). Fig. 6-4 indicates that the predicted TP is mainly linearly related to the observed TP **(**Fig. 6-4a**)**. However, the residuals are very large **(**Fig. 6-4b**)**. Xinyunhu Lake had the largest residuals in the dataset, and TP in Erhai lake is overestimated.

Table 6-2 The performance of WA model in Yunnan Province training set

#	Id	WA_Inv	WA_Cla	WA_{TOL}_Inv	WA_{TOL}_Cla
1	RMSE	0.26	0.30	0.23	0.26
2	R^2	0.74	0.74	0.78	0.78
3	Ave_Bias	0.00	0.00	0.00	0.00
4	Max_Bias	0.38	0.22	0.39	0.24
5	Boot_R^2	0.43	**0.44**	0.40	0.41
6	Boot_Ave_Bias	0.02	0.02	0.02	0.02
7	Boot_Max_Bias	0.71	0.61	0.78	0.73
8	RMSEP	0.41	0.42	0.43	0.44

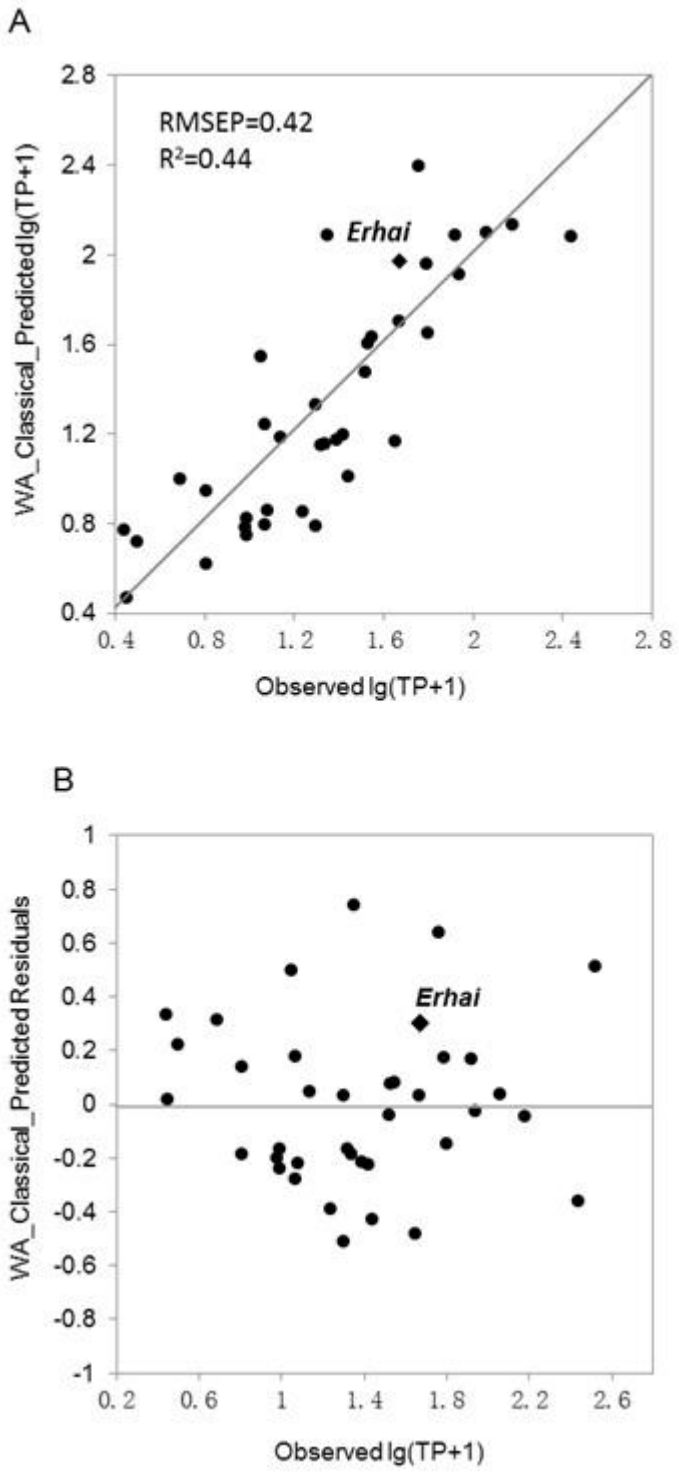

Figure 6-4 Plots of observed versus predicted log-transformed TP and of the residuals. (a, plot of observed conductivity versus predicted TP by WA classical deshrinking; b, is the residuals for the respective model)

6.7 Discussions

The training set is small and the environmental condition is very complex in Yunnan province. The above analysis indicates that nutrient content is not the only significant factor for diatom distribution, and in fact iron concentrations show the highest significance to diatom communities. Other studies (Gausse, 1986; Khelifa, 1989; Gasse, 1987) found quantitative relationships between diatoms and salinity (or conductivity), especially in arid or semi-arid areas such as Africa (Gasse, 1986; Khelifa, 1989; Gasse, 1987), Xizang (Wang et al., 2008), and Australia (Gell & Gasse, 1990). The responses of diatoms to the lake's salinity are always employed to understand the P-E balance (precipitation-evaporation) so that the water level can be reconstructed (Wang et al., 2008) and the impacts of climate change can be estimated. However, most of the lakes in Yunnan province are freshwater lakes, and hence salinization is not a problem for the lakes' ecology. In this training set, both nutrients and ions are the main variables for the patterns of diatoms. Therefore, it is highly possible that there is an interactive relationship between nutrient and ion concentration. There is no further data to test these hypotheses, but the analysis shows that nutrient content is also significant for diatom distribution in the region. Eutrophication is one of the greatest threats for lakes in Yunnan province. Although it is hard to get a robust result, it is still worth trying to explore the relationship between diatoms and nutrients.

Undoubtedly, the transfer function of Yunnan Province is weak, and there are probably many factors contributing to this weakness. Table 6-3 lists a summary of some diatom-based TP transfer functions from other studies. Compared to most of the listed transfer functions, the Yunnan diatom-based TP transfer function is small, and the errors are large (RMSEP=0.42 log(TP)). All the transfer functions with high values of R^2 are corresponding to a large dataset, such as the Northwest Europe dataset (Bennion et al., 1996) and Switzerland dataset (Lotter et al., 1998). In contrary, the performance of small datasets is not as good as large ones; for example, the Southeast England dataset (Bennion, 1994) and Yunnan dataset. However, one should note that most of the better performing datasets have relative simple landscapes or lake geomorphologies. For example, all the lakes in Northwest Europe dataset are small and shallow (Bennion et al., 1996). Relatively

simple environmental backgrounds (or low heterogeneity in other variables) may be a good reason for the good performance of transfer functions in certain small datasets, such as the S.E. China dataset (Yang et al., 2008). The TP range in Yunnan province is large but the heterogeneity in its geography may be the main reason for the weak transfer function. As well as TP, many other environmental variables also determine the diatom patterns in Yunnan Province.

Table 6-3 Summary of diatoms-based TP transfer function in other studies

Location	No. of sites	TP range	Model	R2	$R2_{Jack/boot}$	RMSEP	Reference
Yunnan, China	38	1.7-329.5	WA	0.74	0.44	0.42	This thesis
S.E. China	43	30-550	WA		0.82	0.12	Yang et al., 2008
Ireland	73	0-675	WA-PLS2	0.67			Taylor et al., 2006
Denmark	29	24-1145	WA-PLS3	0.86	0.37	0.28	Bradshaw et al., 2002
Sweden	43	7-370	WA	0.75	0.47	0.24	Bradshaw & Anderson, 2001
Northwest Europe	152	5-1190	WA-PLS2	0.91	0.82	0.21	Bennion et al., 1996
Southest England	30	25-646	WA	0.79		0.28	Bennion, 1994
Switzerland	72	6-520	WA-PLS2	0.93	0.79	0.19	Lotter et al., 1998

The accuracy of the WA method depends largely on reliable estimates of WA coefficients, namely the estimated optima and tolerances, derived from modern diatom distributions in training sets. However, WA estimates of species optima will be biased when the distribution of lakes along the gradient is highly uneven, or when species are not sampled over their entire range. The bias at the ends of the gradient (e.g. at very high or low TP) is caused by truncated species responses, or so-called 'edge effects', resulting in inaccurate estimates of species optima that reduce the accuracy and precision of diatom-inferred TP at high and low values. This has important implications for the reliable estimation of reference lake conditions. Perhaps the best solution to avoid problems associated with edge effects is to sample a sufficient number of lakes along the full environmental gradient. However, as was presented in the conceptual model, it may have larger estimation errors if there are alternative stable states in the training set. If this hypothesis is true, we have to check the patterns of diatoms along the environment gradient before constructing a diatom-based transfer function.

The dataset of Yunnan province is used to prove the idea from the conceptual models. First, it is going to be used to find alternative states in the dataset, and then the pattern of estimation errors will be checked. A plot of drivers against ecosystem states can be employed to detect the existence of multiple stable states (Hirota et al., 2011). Fig. 6-5a showed a plot of diatom communities (DCA) against instrumental TP in the dataset of 38 lakes. First, the correlation coefficient (R^2) is 0.46 ($p<0.01$) which indicates that the linear relationship between TP and diatoms is significant but not strong. Second, the diatom assemblages may have alternative states, as shown by the green lines and the dotted line. Fig. 6-5b shows a plot of diatom-reconstructed TP against diatom communities for each site. The coefficient (R^2) of linear relationship between diatoms and TP obviously increased to 0.77 ($p<0.01$). In conclusion, the alternative states may exist in the training set and it is possible to bias diatoms-based reconstructions.

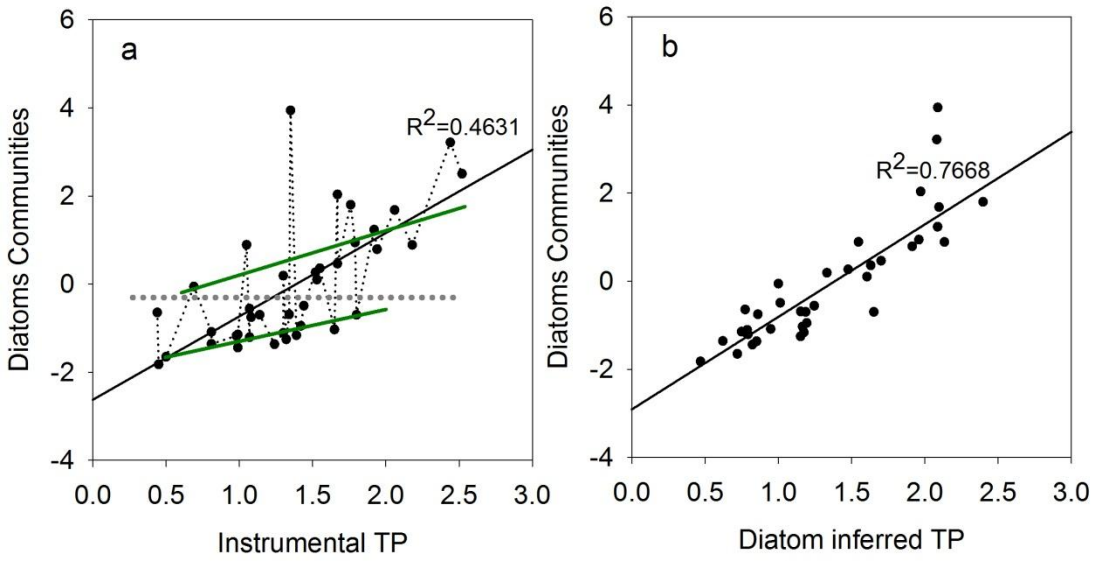

Figure 6-5 The plots of drivers (TP) against diatom states in Yunnan province. a, diatom communities (DCA) against instrumental TP in 38 lakes in Yunnan province to show the possible multiple states in the training set.; b, diatom communities (DCA) against diatom-inferred TP based on 38 lakes in Yunnan province.

Normally, a plot of predicted residuals against instrumental TP (such as in Fig. 6-3) is employed to show a trend of prediction error (ter Braak and Juggins, 1993), for instance, with overestimation at low values or underestimation at the high values

(Kauppila et al., 2002; Keatley et al., 2008; Wang et al., 2011; Yang et al., 2003). In the Yunnan dataset, as shown in Fig. 6-3b, it is not clear whether the predictions are overestimated at low values, and/or underestimated at high values. In the above conceptual models, the samples may be overestimated in one state and underestimated in the alternative state. Fig. 6-6 shows instrumental TP against DCA from the Yunnan dataset and the estimated errors are also added at each sample. Most samples were underestimated in state 1 but overestimated in state 2. The result provides evidence to support the conclusion from the conceptual model (Fig. 6-4).

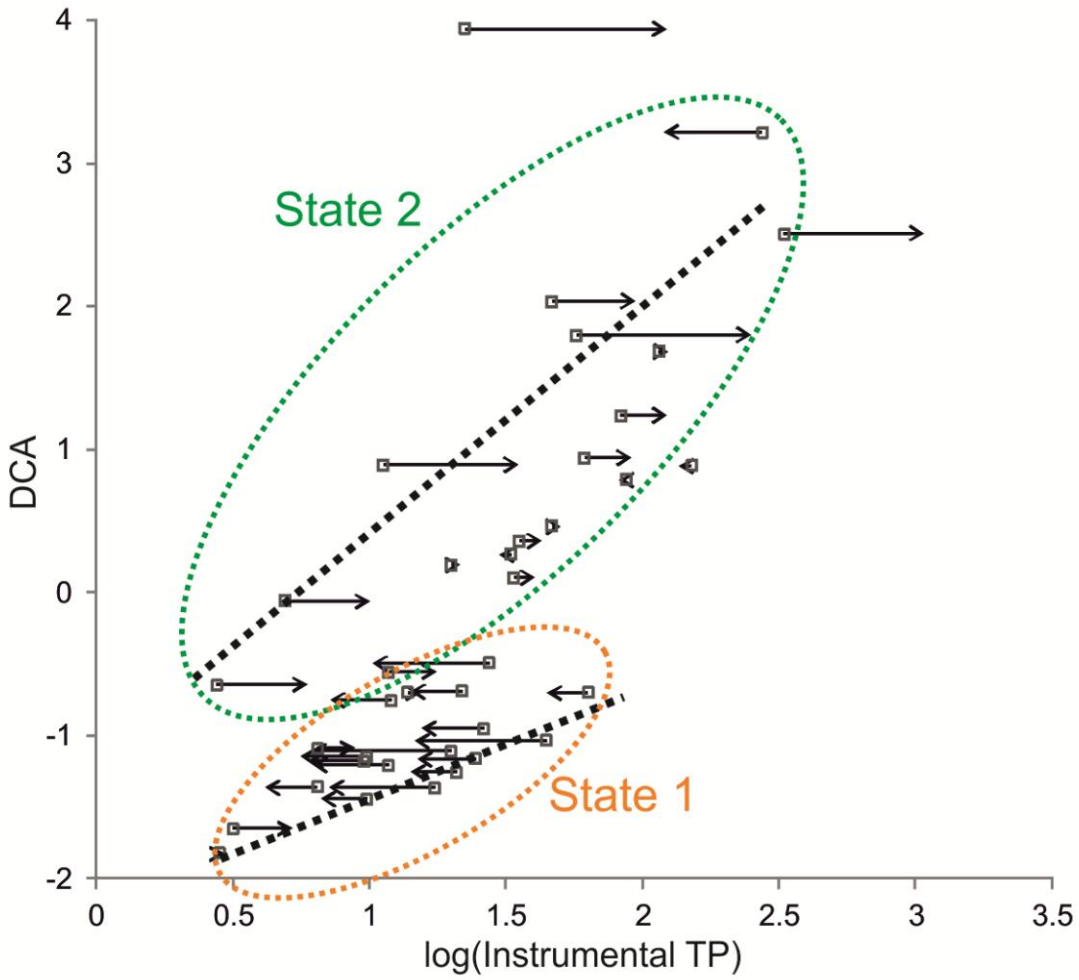

Figure 6-6 The estimation errors in the Yunnan training set. The squares are the instrument TP against diatom DCA in the training set. The arrows mean the estimation error, and the magnitudes are represented by the width of arrows.

It should be pointed out that the evidence for the alternative states in the Yunnan province training set is weak. There is still a lack of proper statistical analysis available for detecting the alternative states in a training set. In additional, there are only 39 lakes in the Yunnan training set. This may be one of the reasons for the weak transfer function as well as the weak evidence for alternative states. However, through the above analysis it is evident that the alternative states should be considered in the training sets.

6.8 Summary

- The environmental variables in the Yunnan dataset covered a large range of gradients. Diatom community patterns are highly related to ionic content in the area of interest, and nutrient concentrations also determine the composition of diatom communities in the lakes.
- Several models were tested to construct the transfer functions for TP, but all models showed a very low correlation between predicted and measured values.
- The estimation errors of the transfer function may be affected by the alternative states in the training set, i.e. the samples may be underestimated in one state but overestimated in the alternative state.

Chapter 7 Palaeolimnological Results and eutrophication at Erhai

7.1 Introduction

Two sediment cores from Erhai lake were analysed to help understand the complex dynamic lake-catchment system. This chapter will focus on these palaeolimnological proxies. The proxies will be introduced separately. The lake's ecosystem change will be interpreted with these proxies. The purpose of this chapter is to track the trajectory of the lake ecosystem change through common palaeolimnological explanations, and describe the reference conditions for the lake's management. Discussions on the complex ecological system, focussing on the lake's feedbacks, resilience and regime shift, will be described and detailed in the next chapter.

7.2 Palaeolimnlogical Results

7.2.1 Chronology

The detailed ^{210}Pb and ^{137}Cs data are shown in Table 7-1.The calculations can be found in Appleby (2002). Unsupported ^{210}Pb were calculated with total ^{210}Pb subtracted from ^{226}Ra. As shown in Fig. 7-1, unsupported ^{210}Pb decayed exponentially with depth. A CRS model (Constant rate of supply) is employed to estimate the date of samples, and a cumulative unsupported ^{210}Pb inventory is calculated using the trapezium rule (Appleby, 2002) with the equilibrium depth set as 32 cm. In order to avoid the influence of total unsupported ^{210}Pb inventory on the dating accuracy, the infinite integrals (below 32cm) with the equation between unsupported ^{210}Pb activity and depth are used to calculate the equilibrium ^{210}Pb inventory. The calculation of all dating errors follows the method of Appleby (2001). The results are shown in Table 7-1 and Fig. 7-1, showing that the errors become larger as depth increase. The highest ^{137}Cs value exists between 16 -18 cm and likely links to the 1963 peak period of global nuclear testing (Appleby, 2002). The

1963 mark and errors are annotated in Fig. 7-1. The result shows that the dating from ^{137}Cs and ^{210}Pb are consistent at 1963 AD, and thus strengthens the reliability of the ^{210}Pb dating. The sedimentation rate calculated from ^{210}Pb dating is shown in Fig. 7-1. It decreases slightly in recent decades, with greater oscillations before c. 1950s. The highest value appears around 1900s, when the sedimentation rate is around three times larger than after the 1960s.

Table 7-1 The Calculation of CRS model dates, sedimentation rates and ^{137}Cs for EH2-1

Depth (cm)	Mass depth g/cm^2	total^{210}Pb (Bq/kg)	^{226}Ra (Bq/kg)	$^{210}Pbex$ (Bq/kg)	^{137}Cs (Bq/kg)	CRS age	errors (±a)
0.5	0.01	1176.8	210.4	966.5	8.1	2009.3	0.1
1.0	0.02	1072.5	93.7	978.8	6.5	2008.8	0.3
1.5	0.03	941.4	123.5	817.9	5.6	2008.3	0.6
2.0	0.05	886.4	106.4	779.9	4.0	2007.8	0.8
2.5	0.06	1172.8	108.5	1064.3	15.7	2007.3	1.1
3.0	0.07	844.6	149.6	694.9	10.7	2006.8	1.3
3.5	0.09	909.4	115.1	794.3	6.2	2006.3	1.6
4.0	0.10	1008.8	125.6	883.1	6.0	2005.6	1.9
4.5	0.12	749.8	123.4	626.5	9.7	2005.1	2.2
5.0	0.13	816.7	154.6	662.2	13.7	2004.7	2.5
5.5	0.15	999.6	108.7	890.9	16.5	2004.1	2.8
6.0	0.17	779.9	136.1	643.8	4.2	2003.3	3.1
6.5	0.19	1147.9	93.8	1054.1	14.8	2002.4	3.5
7.0	0.22	517.2	61.3	455.9	4.6	2001.1	3.8
7.5	0.25	774.3	101.5	672.8	21.6	2000.2	4.2
8.0	0.30	706.4	84.6	621.8	15.1	1998.4	4.5
8.5	0.40	485.0	71.6	413.5	17.4	1995.0	4.9
9.0	0.44	588.5	83.6	504.9	15.6	1993.7	5.4
9.5	0.50	552.7	91.1	461.6	24.0	1991.6	5.8
10.0	0.56	451.4	105.5	345.9	19.6	1989.8	6.2

Table 7-1 Continuous

Depth (cm)	Mass depth g/cm^2	total^{210}Pb (Bq/kg)	^{226}Ra (Bq/kg)	^{210}Pbex (Bq/kg)	^{137}Cs (Bq/kg)	CRS age	errors (±a)
10.5	0.61	469.7	97.8	371.9	19.4	1988.5	6.6
11.0	0.65	453.3	99.0	354.4	19.0	1987.1	7.0
11.5	0.70	494.8	90.9	403.9	14.9	1985.5	7.4
12.0	0.83	349.0	68.7	280.3	25.0	1981.4	7.9
12.5	0.89	361.1	63.0	298.1	19.4	1979.5	8.3
13.0	0.97	272.0	67.0	205.0	18.8	1977.3	8.7
13.5	1.04	320.5	76.0	244.5	20.6	1975.5	9.2
14.0	1.10	258.1	79.5	178.6	25.7	1974.0	9.6
14.5	1.17	280.8	81.7	199.1	22.8	1972.2	10.0
15.0	1.24	235.1	56.6	178.5	23.9	1970.3	10.4
15.5	1.32	238.7	73.2	165.5	26.7	1968.4	10.9
16.0	1.39	211.7	67.9	143.8	29.1	1966.7	11.3
16.5	1.47	200.3	50.6	149.7	17.7	1964.8	11.7
17.0	1.54	264.0	73.3	190.7	26.6	1962.7	12.2
17.5	1.61	163.9	52.4	111.5	22.9	1960.7	12.6
18.0	1.67	260.5	70.0	190.5	29.4	1958.8	13.1
18.5	1.75	257.5	67.7	189.7	11.9	1955.6	13.5
19.0	1.83	192.9	54.5	138.4	11.4	1952.5	13.9
19.5	1.91	152.9	60.2	92.8		1950.1	14.4
20.0	1.99	101.2	52.2	49.0		1948.5	14.8
20.5	2.06	194.3	56.2	138.2		1946.6	15.3
21.0	2.14	150.5	54.6	95.9		1943.9	15.7
21.5	2.22	193.0	56.2	136.8		1940.7	16.2
22.0	2.29	140.3	78.3	62.0		1938.0	16.6
22.5	2.37	136.1	73.6	62.5		1936.0	17.1
23.0	2.45	150.7	70.0	80.7		1933.6	17.6
23.5	2.53	111.1	60.0	51.1		1931.0	18.0

Table 7-1 Continuous

Depth (cm)	Mass depth g/cm^2	total ^{210}Pb (Bq/kg)	^{226}Ra (Bq/kg)	^{210}Pbex (Bq/kg)	^{137}Cs (Bq/kg)	CRS age	errors (±a)
24.0	2.62	100.5	58.2	42.3		1929.0	18.5
24.5	2.70	89.8	52.6	37.2		1927.1	19.0
25.0	2.78	128.9	70.5	58.4		1925.0	19.5
25.5	2.87	95.6	65.0	30.6		1922.7	20.0
26.0	2.95	97.2	81.6	15.6		1921.4	20.5
26.5	3.04	116.0	69.9	46.1		1919.7	21.0
27.0	3.12	122.2	57.2	65.0		1916.3	21.5
27.5	3.22	100.2	56.1	44.1		1912.1	22.1
28.0	3.32	108.3	62.2	46.2		1907.7	22.7
28.5	3.41	76.1	61.0	15.1		1905.0	23.3
29.0	3.48	89.1	62.2	26.9		1903.1	24.0
29.5	3.57	81.9	59.2	22.7		1900.5	24.6
30.0	3.67	72.7	65.5	7.1		1898.7	25.3
30.5	3.75	114.9	70.8	44.1		1895.7	26.1
31.0	3.83	117.9	68.7	49.2		1889.8	26.9
31.5	3.91	75.0	62.5	12.5		1885.4	27.8
32.0	3.99	80.6	63.1	17.5		1882.8	28.8

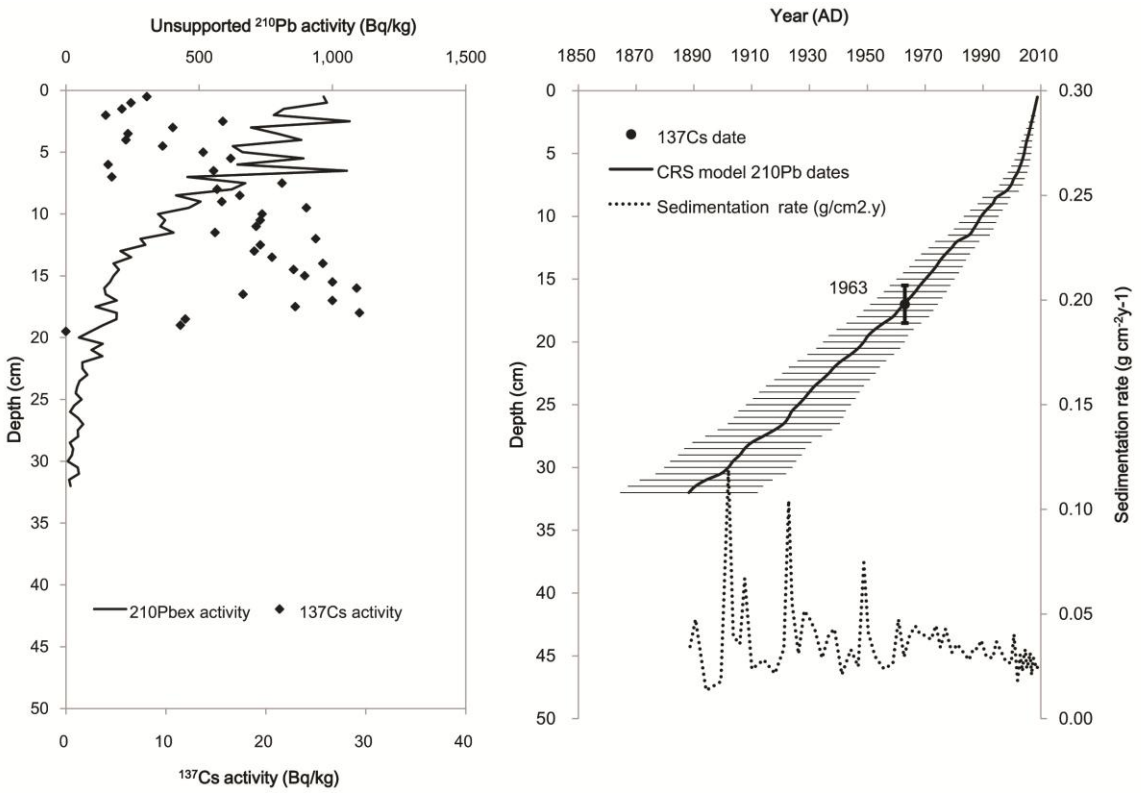

Figure 7-1 The chronology of EH2-1 based on ^{210}Pb and ^{137}Cs. A CRS model is employed to calculate the dates of sediment.

7.2.2 Total nitrogen (TN) and Total Organic Carbon (TOC)

Fig. 7-2 shows the percentage of total nitrogen and total organic carbon in EH2-1. Both TN and TOC decreased slightly before around 1895 AD. The values were quite stable before the 1960s, where TOC was around 1.7% and TN was around 0.2%. Hereafter, both records started to gradually increase until ~2001. TOC increased to 3.5% at 2001 and TN increased to 0.4% at 2001. There was also a peak value at around 1977-1978 in both proxies. The dramatic change in TN and TOC happened at around 2001-2003, when the lake status altered to continuous algal blooming. The transition was rapid, and TN values increased around 2.6 times until 2007 and nearly 2.7 times for TOC. After the dramatic change TOC and TN kept at a relative high value after 2003.

Fig. 7-2 also shows the ratio between TOC and TN, which can be interpreted as a proxy to explain the organic matter source in lake sediments (Kaushal and Binford,

1999; Meyers, 1994). Algae have a C/N ratio between 4 and 10, whereas terrestrial organic matter has a ratio greater than 20 (Meyers, 1994). Therefore, the ratio of C/N could reflect the source of organic matter, i.e., whether the main source of organic matter has come from terrestrial material or algae within the lake (Kaushal and Binford, 1999). The ratio in Erhai Lake is around 9, and is stable during research period. It indicates that the organic matter is mainly autogenic rather than from the catchment. The dramatic increase in organic matter should be consistent with the period of eutrophication after 2003 and corresponds with the algal blooming identified from historical records (Fig. 5-9).

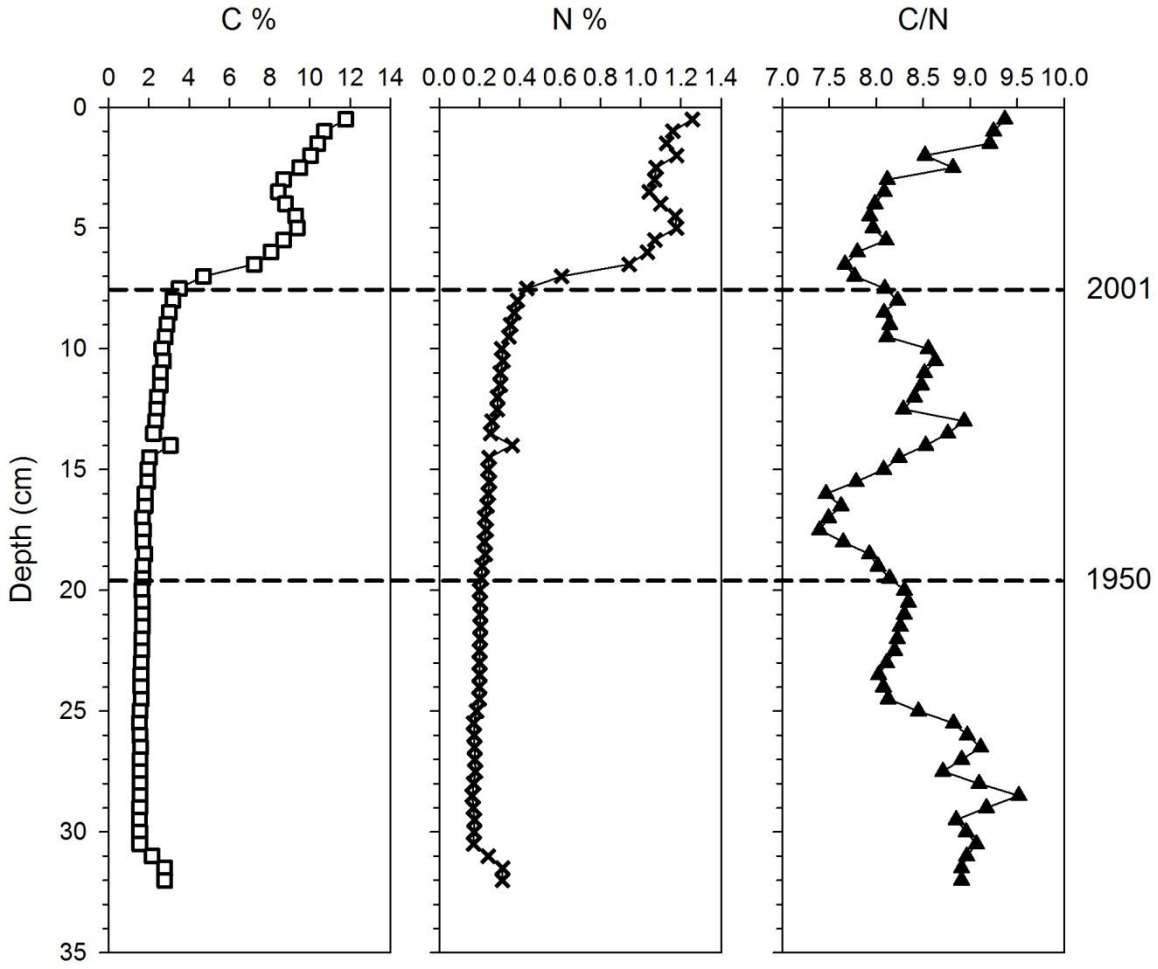

Figure 7-2 The percentage of total nitrogen and total organic carbon in EH2-1. Both indexes increase by about 5-6 times after 2003. The ratio of C and N is also given, and it shows that most of C/N values are less than 9, which indicates the main organic resources are not from the catchment but are autogenic.

The large increase of organic matter in the lake will unavoidably dilute chemical elements eroded from the catchment. In this thesis, the dilution of organic matter was estimated by the equation: $Chem_{after}$=Chem/(1-organic matter %), where the $Chem_{after}$ is the chemical element concentration after calibration, and Chem is the measured chemical element. Only the percentage of organic carbon was measured in the sample, so the content of organic matter was evaluated with C% value divided by 0.6 (Galman et al., 2008; Håkanson and Jansson, 2002).

7.2.3 Metal Elements

The metal elements of EH2-1 are illustrated in Fig. 7-3. The composition changed at around 7 cm (2001). Below 7 cm (before 2001), most elements were stable in terms of trend over time. Fe and Al were the most important elements in the sediment, with concentrations around 100 mg/g and 70 mg/g respectively. Some elements like phosphorus (P) and lead (Pb) gradually increased between around 13.5 cm (1970s) and 7 cm (2001). The composition of elements changed notably at the top of the core, as Ca became dominant having increased from around 20 mg/g below 7 cm to around 70 mg/g at the core top. As the change of metal elements was consistent with the organic change in the lake, the possibility of dilution due to organic matter was considered. As showed in the red lines, the dilution from organic matter did not change the trends of all metal elements. The results suggest that the dilution from organic matter was likely small (Fig. 7-3).

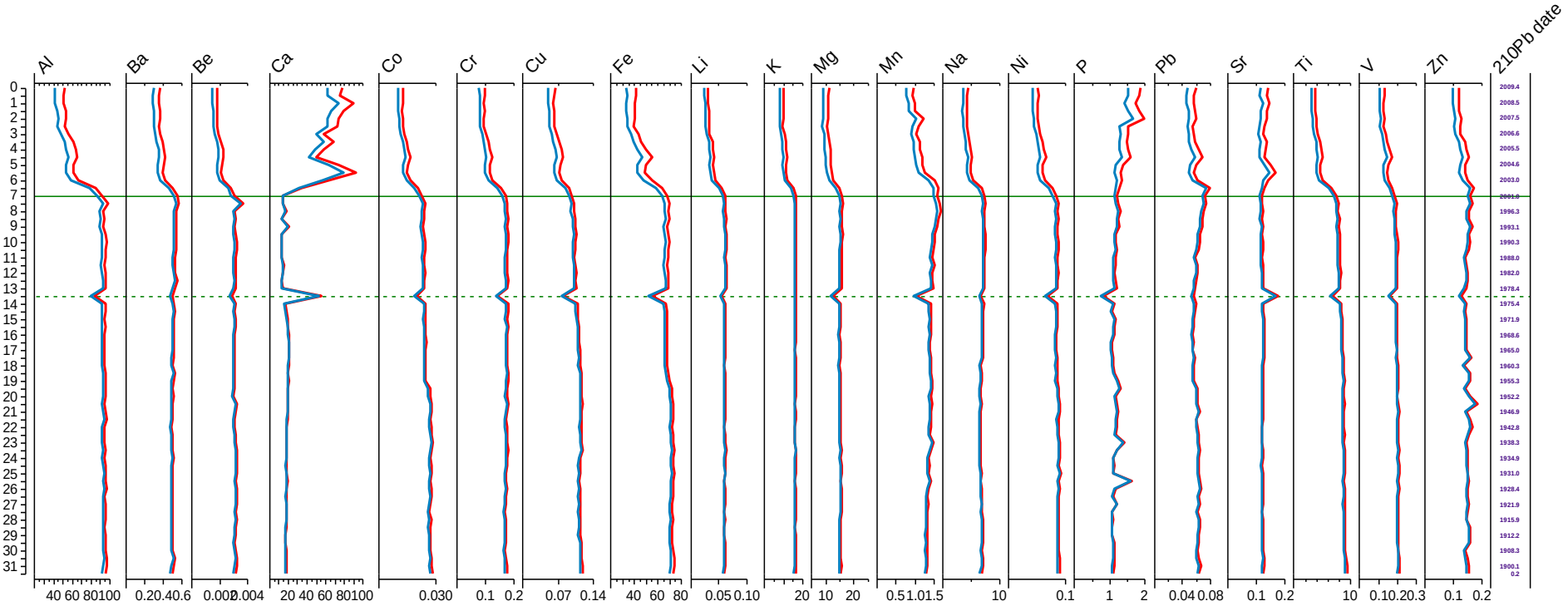

Figure 7-3 Metal Elements diagram in EH2-1 (the unit of all the elements are mg/g; the blue line is the elements content without the organic matter dilution effects removed; the red line is the elements content with the organic matter dilution effects removed)

7.2.4 Magnetic Susceptibility

The magnetic susceptibility in EH2-1 was shown in Fig. 7-4. Magnetic susceptibility decreased since around the 1950s, and had a sharp decline at around 1973. The magnetic susceptibility then declined gradually until around 2001, and rapidly after this time. The change in Xlf and Xhf are similar to Fe in the sediment (Fig. 7-3), and the dilution from organic matter might affect the magnetic susceptibility measurements. Fig. 7-4 also shows the calibrated magnetic susceptibility from organic matter dilution. The results do not show a large difference with the original data, and hence it can conclude that the dilution effect from organic matter on magnetic susceptibility is negligible in the EH2-1 core. The frequency distribution of magnetic susceptibility can be used to represent the soil erosion in catchments (Dearing et al., 2008; Oldfield, 1991). Fig. 7-4c showed the Xfd and Xfd% in EH2-1 core. The Xfd% was stable before 2001-2003, and fluctuated more rapidly afterwards, indicating that the source of sediment was stable before 2001-2003, but may have changed afterwards.

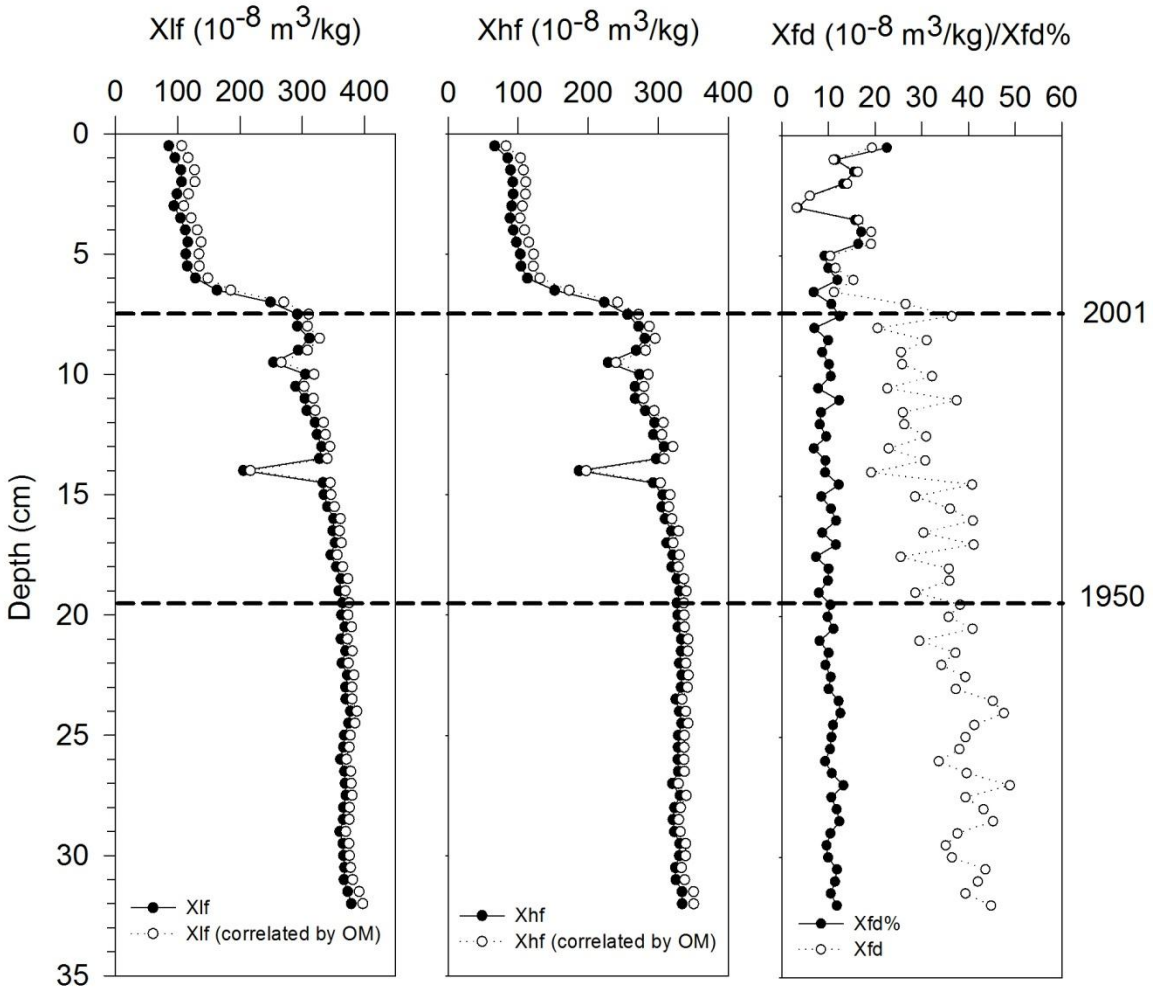

Figure 7-4 Magnetic Susceptibility from EH2-1

7.2.5 Grain Size

The particle sizes from EH2-2 are given in percentages in Fig. 7-5. The results showed that the sediment texture had obviously changed at the depth around 6 cm (~2002), where the composition of clay (<4 μm) and fine silt (4-16 μm) particles decreased, and the percentages of coarse silt (16–64 μm) and sand (>64 μm) increased. Meanwhile, the median and average particle size increased within the top 6 cm. The particle sizes at other depths are consistent.

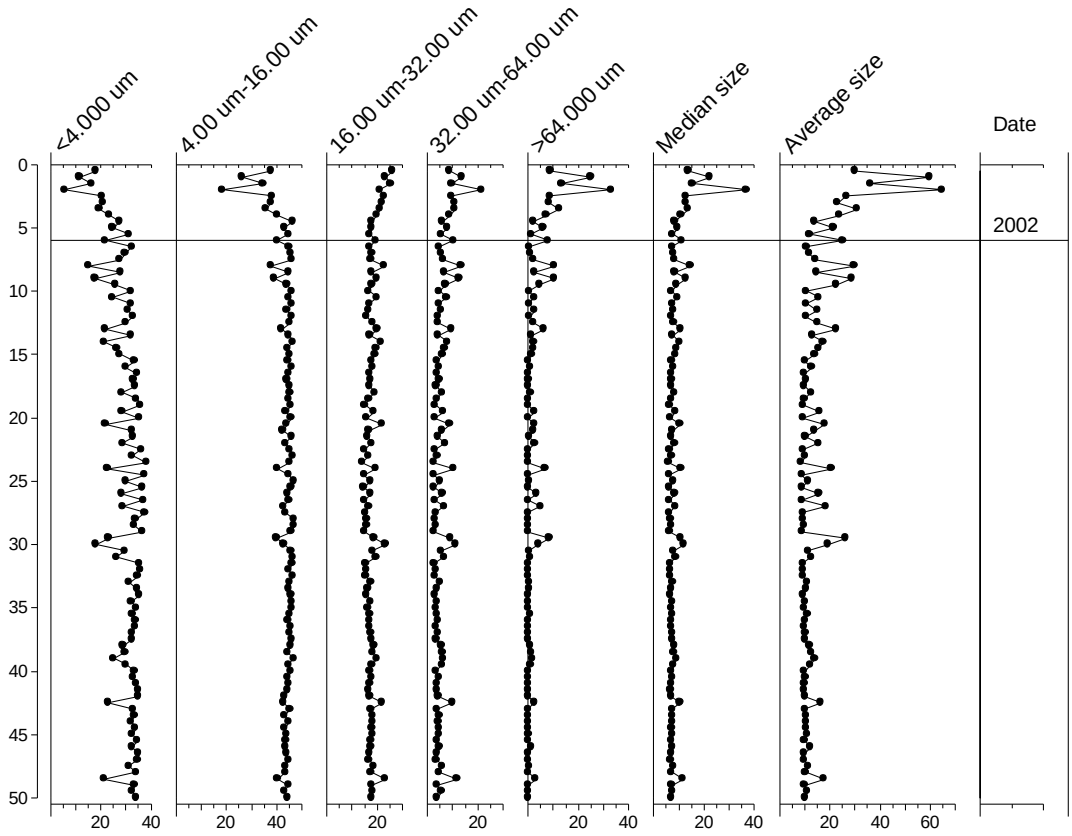

Figure 7-5 Particle size distribution in EH2-2

To check the ratio of the large diatom valves in sediment particles, photos of samples (under microscope) at various depths are shown in Fig. 7-6. Fig. 7-6a and b show images of diatoms and particles in the top of the core. It is clear that the abundance of diatom valves is very high, so the content of particles is lower. In addition, many of the diatom valves are larger than the particles in the sample. In the middle of the core, i.e. 15 cm, Fig. 7-6c, diatom abundance decreased significantly, and particles begin to dominate the slides. The same results can be observed from Fig. 7-6d, which is from the deepest part of the studied section of the core. At this depth, the ratio of diatom valves to particles is small; diatom valves are unlikely to affect the particle size measurement.

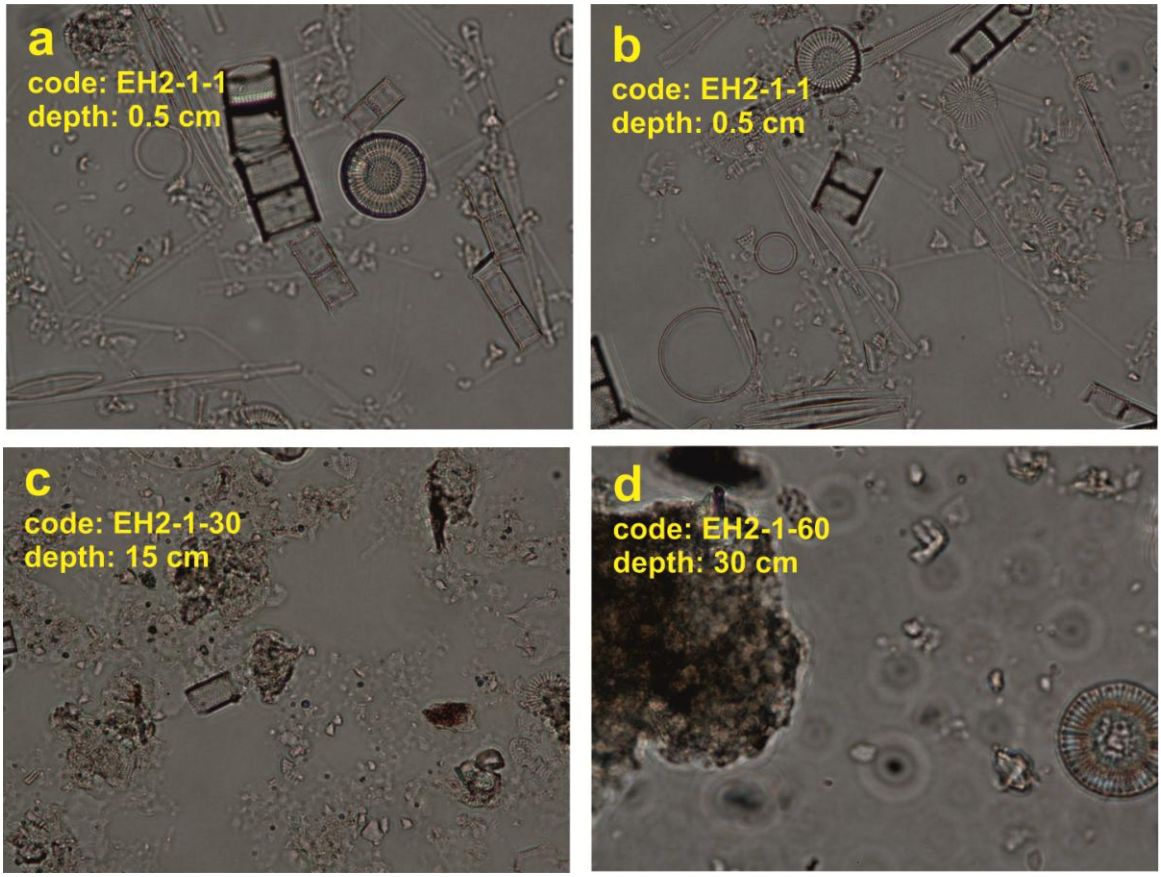

Figure 7-6 Photos from difference depth of EH2-1 core. It can give a first view about the impact of the diatoms to particle compositions in the lake sediment.

7.2.6 Diatom communities from core EH2-1

The full record of diatoms contains 67 species (Fig. 7-7). About 70% of the recent diatom community is dominated by planktonic species, for example *Aulacoseira ambigua*, *Cyclostephanos dubius*, *Cyclotella ocellata*, and *Fragilaria crotonensis*. The community shows major changes centred at7 cm depth (dated ~2001). Below this depth, species such as *Aulacesira ambigua*, *Fragilaria crontonensis* are far less abundant. One notable component of the spring bloom in Erhai is *Fragilaria crotonensis,* which is related to lake circulation and stratification (Platt Bradbury, 1988), and is often used as an indicator of eutrophication (Beeton, 1965; Holland and Beeton, 1972; Liukkonen et al., 1993; Lotter, 1998). This species increased abruptly in abundance from ~17 cm depth (~1960), while other typically eutrophic species, for example *Cyclostephanos dubius* and *Aulacesira ambigua,* increased gradually over the length of the core. Above 7 cm, eutrophic species such as

Cyclostephanos dubius, *Aulacesira ambigua*, and *Fragilaria crotonensis* dominated the communities. *Fragilaria crotonensis* abundance further increased in recent years, while both of the other species decreased.

DCA (Fig. 7-8a) indicates that diatom communities changed gradually since the 1950s, but a critical transition happened at around 2001-2003 when the lake may have shifted to an alternative state with continuous algal blooming. HDI (Fig. 7-8b) did not change gradually before 2001 as the DCA did, but had more fluctuations and suddenly shifted after 2001-2003. The diatom-inferred TP (DI-TP) transfer function based on the WA-classical model from Yunnan Province (Chapter 6) is employed for historical TP reconstruction. The DI-TP shows that TP increased from an original level of around 25 µg/l since the 1960s (Fig. 7-8c). The value reached its highest point between 2001-2003, when DI-TP was around 90 µg/l. The instrumental TP was employed to validate the reconstructions (Fig. 7-8c). The comparisons show that the reconstructions are larger than the instrumental data in terms of magnitude, being on average around 20 µg/l higher, but the trends were quite similar.

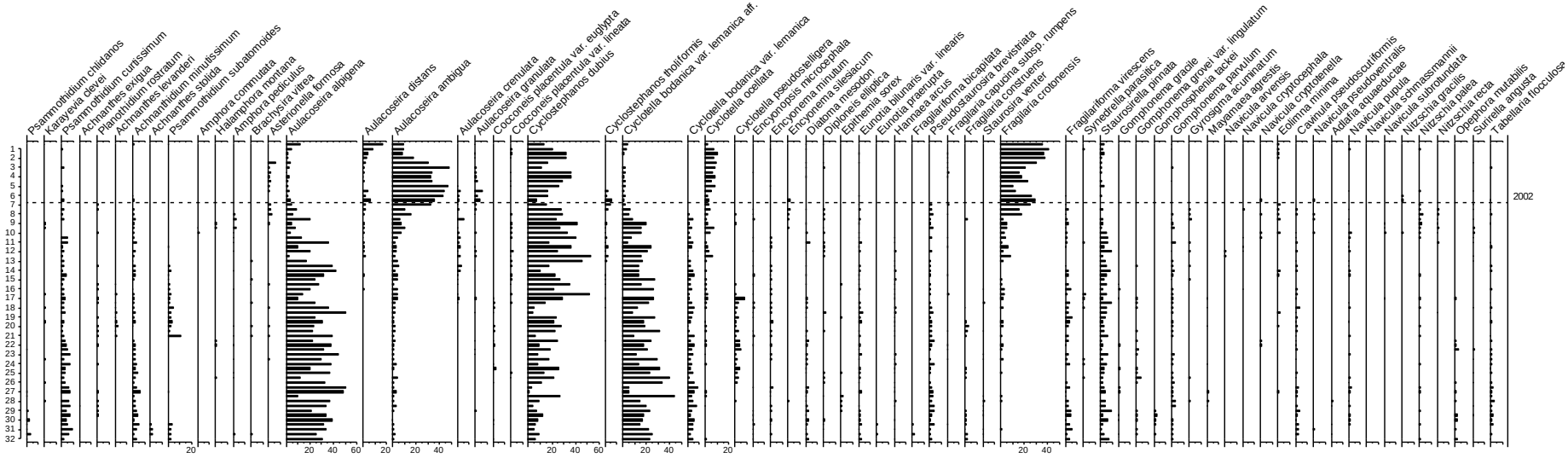

Figure 7-7 Diatom assemblages in EH2-1

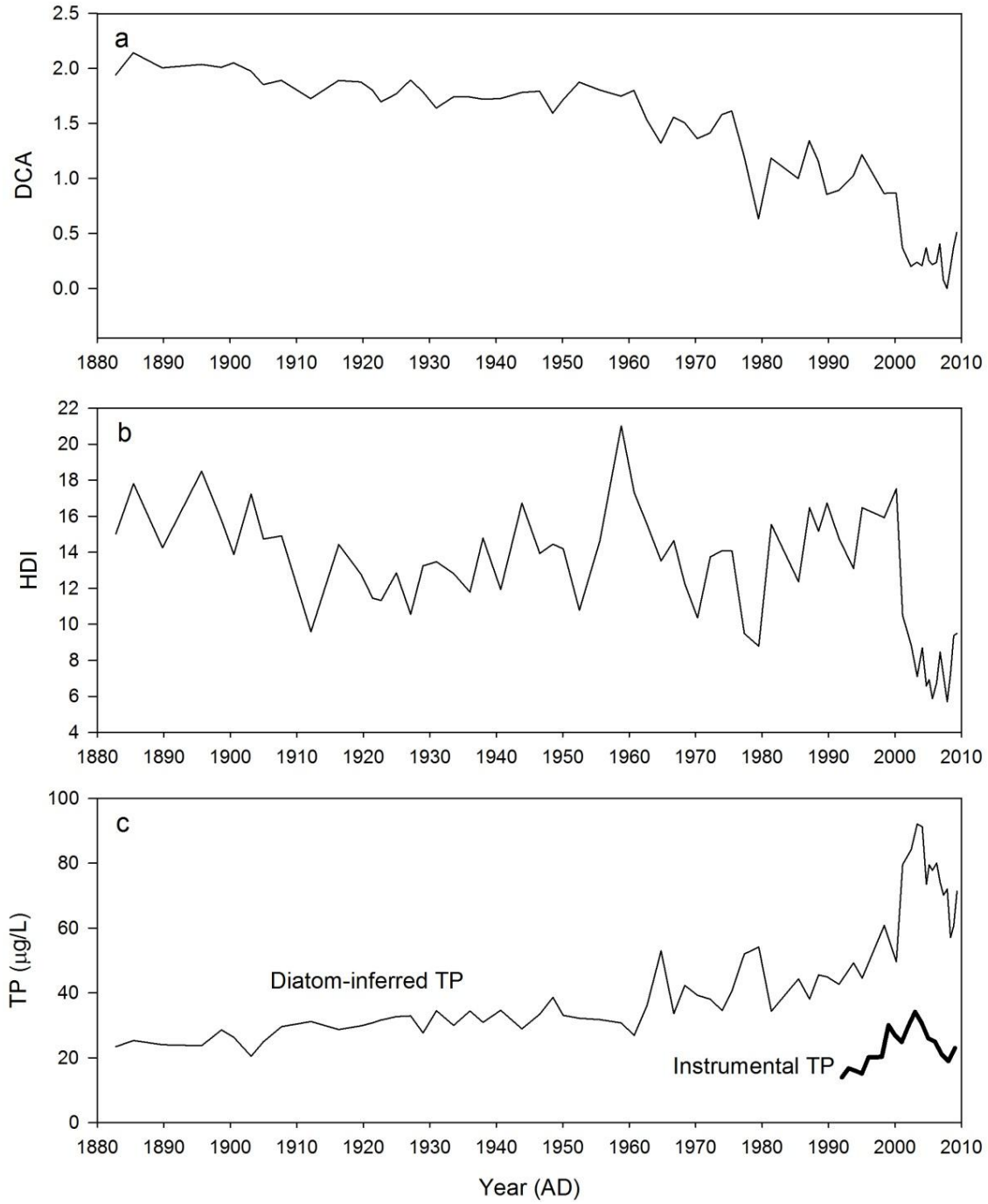

Figure 7-8 DCA, HDI, and diatom-inferred total phosphorus in Erhai lake during the past 130yrs (a, DCA axis 1 score calculated from fossil diatom community; b, HDI (Hill's diversity N2 index) calculated from fossil diatom community; c, the diatom-inferred total phosphorus based on the Yunnan province training set which was introduced in Chapter 6; the instrumental TP since 1991 is also given.

7.3 Discussion

7.3.1 The accuracy of grain size from the core of EH2-2

It should be noted that grain size data were obtained from a neighbouring core, and that there is no ^{210}Pb chronology data for this core. The dataset was calibrated using theEH2-1 core and, assuming the same depth between the two cores, has the same ^{210}Pb chronology. In any case, the grain size data are not used for many comparisons other than to provide a first view of the hydrodynamic changes in the catchment.

Undoubtedly, grain size plays a very important role in understanding environment change with lake sediment, especially the understanding the hydrological properties change of a lake or its catchment (Last, 2001).In theory, a change in the hydrodynamic regime of a lake will be reflected by a change in the deposition rate or pattern of suspended particles. Therefore, it can be used to explain water level fluctuations or river discharges (Last, 2001). The ratio of particle size is always employed as an important proxy for flooding in a catchment (Dearing et al., 2008). However, these explanations ignore the impacts of the internal lake dynamics, such as diatom growth. Grain size pattern in Erhai lake is probably affected by diatom valves. As shows in Fig. 7-5, the average particle size is actual quite stable below 7 cm (~2001 AD), and it had only a slight increase from 15 cm (~1970s) to 7 cm. The abundance of coarse particles increased considerably after 2001, corresponding to the changes in diatom communities in Fig. 7-7. Meanwhile, large taxa, i.e. *F. crontonesis*, started to increase from 1950s, and suddenly began to dominate diatom communities after 2001. Therefore, the bloom of *F. crontonesis* (average size around 60-80 μm) is likely to affect the grain size, making coarse particles more frequent than expected. The photos of Fig. 7-6a show that diatom valves dominate the slides at the top of the core, which confirms this hypothesis. However, Fig. 7-6b and c show that the ratio of the diatom valves to large particles in the deeper samples are low and their influence seems limited. The coarse particles (>60 μm) and the percentage of *F. crontonensis* are compared in Fig. 7-8.Considering the possible impacts of chronological uncertainties, grain size after the 1970s may be strongly affected by the

abundance of *F. crontonensis* as showed by the peaks in T1 and T2. However, the influence before 1970s seems very limited. The obvious evidence is peaks as showed by T3 and T4. Therefore, it can be concluded that the grain size may be strongly affected by the large diatom *F. crontonensis* after 1970s, but can accurately reflect the catchment's hydrological properties before 1970s.

7.3.2 Landscape process in Erhai catchment

The lake's ecosystem should be strongly affected by its catchment. Human activities and the dynamic of environmental variables such as climate sometimes determine the directions of lake ecosystem evolution. Due to the importance of this driver for ecosystem change, it is necessary to know the changes in the catchment before examining the dynamics of a lake's ecosystem. Lake sediment archives preserve several important proxies for us to understand the changes in the catchment, such as coarse particles for flooding, frequency magnetic susceptibility for erosion, and pollen data for deforestation. In Erhai lake, magnetic susceptibility, chemical elements, grain size, and sediment accumulation rate can all be possible proxies to represent the disturbance of the catchment. With the exception of sediment accumulation rate, all other elements have a sharp change at around 7.5 cm (~2001). The content of the main chemical elements, such as Fe, decreased to around half of the previous value, although Ca content increased to around twice as much as before. Affected by the sharp change of chemical elements, magnetic susceptibility changed suddenly at around 2001. This evidence suggests that there might have been a huge disturbance in the catchment at around 2001. However, the accumulation rate calculated by ^{210}Pb chronology suggests that the sedimentary deposition rate became stable after the 1950s. In considering these conflicting observations, and given that there are no reports of widespread disturbances around 2001, it was inferred that the abrupt change in these indicators at around 2001 was mainly controlled by the lake's internal mechanisms. That is to say that the change of deposition conditions appears to have been the most important reason for the change in these indicators in 2001.

Engstrom & Wright (1984) conclude that mineral matters in lake sediment can be used to show that the amount of eroded material from catchment. In contrast, the sediment accumulation rate becomes much stable after 1950s, after which the intensification of human activities increased due to the population growth after the foundation of the P.R.C (Chapter 5). Many human activities, such as deforestation and farming, may enhance erosion in the catchment, but anthropic management activities may also stabilize the catchment and reduce the soil transportation to the lake. Obviously, the transformation of river systems due to agriculture activities plays a very important role. In the Erhai catchment, most of the sediment flows into the lake through its numerous river systems (Fig. 3-5) so the sedimentation rate should strongly relate to the river discharges. Before the 1950s, human activities were relatively small, and comparatively large fluctuations could only indicate the effects of natural environmental changes in the catchment. The stability of sedimentation rate after the 1950s might reflect the increasing management from humans -for example the construction of drainage and farming systems. Further evidence could be found from the comparison between grain size and sediment accumulation rate before the 1950s (Fig. 7-9). The large particles in the lake sediment could be considered as a flooding proxy (Dearing et al., 2008; Last et al., 2001b). Before the 1950s, the comparable peak values (T3 and T4) between sedimentation rate and large sediment particles showed a consistency between high run-off and flooding (Fig. 7-9). Hereafter, the average grain size increased while the river discharge declined (Fig. 7-9). As introduced above, the coarse particle yield is probably affected by the increased quantities of diatom valves after 1970s, and this might be the reason of inconsistency between grain size and sediment accumulation rate. It is noteworthy that magnetic susceptibility measurements show that the soil erosion did not change greatly (Fig. 7-9 d), even when large-scale landscape changes occurred in the catchment during 1950-1980 (Chapter 5). The reason for this inconsistency is not clear, but it is probably due to the small scale of gully erosion in the catchment. Overall, it appears that human activities influence the interaction between Erhai Lake and its catchment. Due to the intensification of human activities, especially the management of river systems after 1950s, the sediment accumulation rate become stable after 1950s. Engstrom & Wright (1984) suggested that in lake sediments, Ca and Mg are principally found in the allogenic fraction, however, this

is in contrast to our findings which will be presented in the next section.

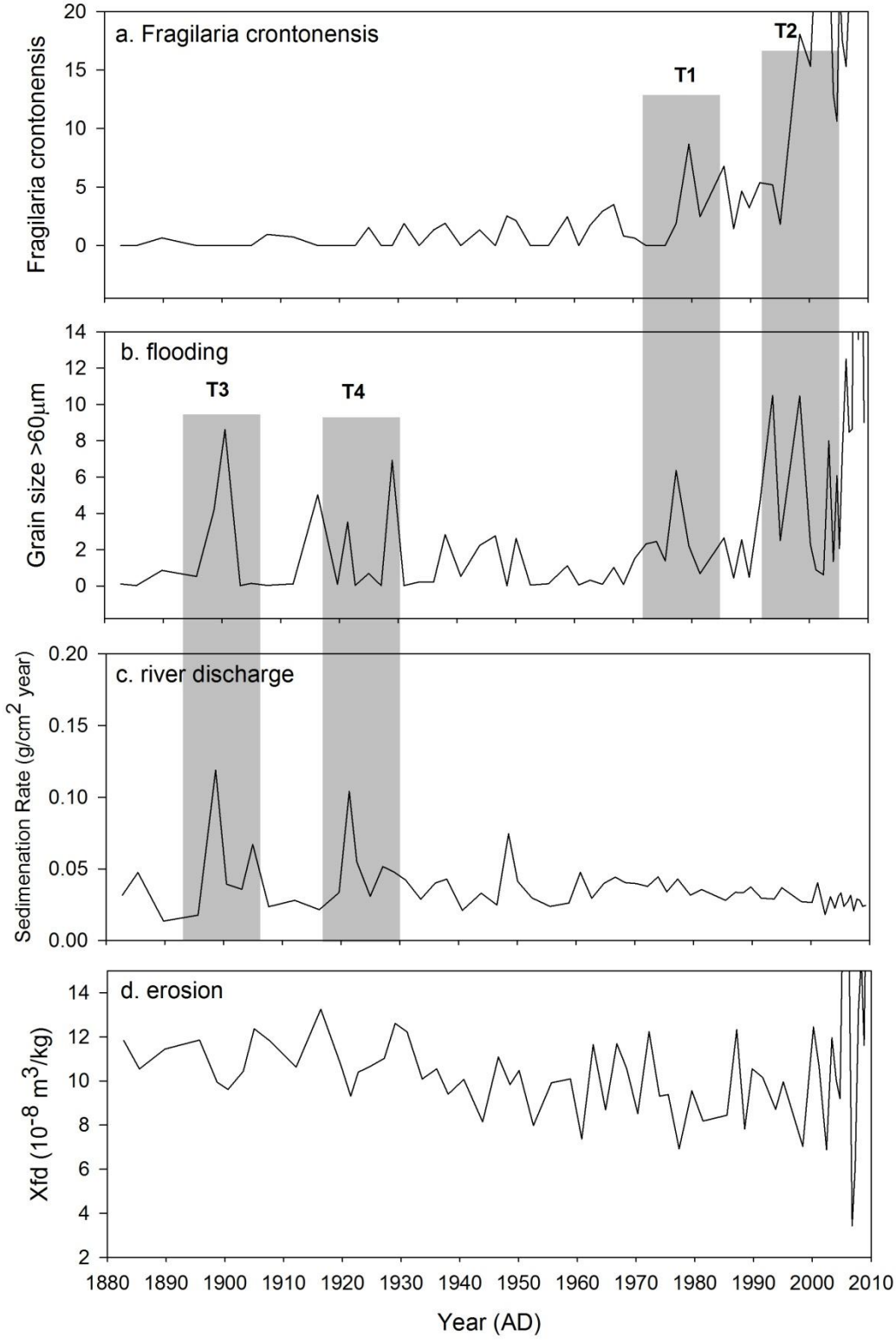

Figure 7-9 Graphs showing sediment accumulation rate (calculated from ^{210}Pb),

grain size (>60 μm), *F. crontonensis* and magnetic susceptibility. After 1970, due to the increase of large *F. crotonensis* in the lake's sediment, the grain size change is related to the diatoms' composition in the sample. The pictures from different slides of the core can confirm this (Fig 7-5 added). Strong correlation between *F. crotonensis* and grain size after 1970s can also prove this hypothesis.

7.3.3 Lake ecosystem change

Undoubtedly, the most obvious change in the lake's sediment composition is the content of calcite ($CaCO_3$) in the lake sediment. The trend of $CaCO_3$(Fig. 7-3) corresponds to the changes of organic carbon (Fig. 7-2). Other studies (Dean, 1999) suggest that the concentrations of organic carbon and $CaCO_3$ in lake sediments are often inversely related. The reverse relationship is not just due to simple dilution of one component by another. The evidence from core data shows that once the organic carbon concentration in the sediments becomes greater than about 12%, the CO_2 produced by decomposition of that organic carbon and production of organic acids lowers the pH of anoxic pore waters enough to dissolve any $CaCO_3$ that reaches the sediment-water interface (Dean, 1999).A long core from Erhai lake (Xiangdong Yang, unpublished data) shows this inverse relationship between TOC and $CaCO_3$ in the whole Holocene. Therefore, the shift of the relationship between TOC and $CaCO_3$ may be a sign of the change of the ecosystem function. In Erhai lake, the evidence shows that most of the elements show stationary or gradually changing trends, and that the trends in Ca and P are similar to TOC, strongly suggesting that all these elements are linked to increased biological productivity as a result of eutrophication. The content of carbonate may be related to contemporary nutritional interactions and photosynthetic regulation (Wetzel, 1970). A possible reason for the abrupt increase of calcite deposition in the sediment may be the rise of the lake's pH because of photosynthetic enhancement during the eutrophication process. The consequence of the rise in pH may include an increase in [HCO_3^-] in the lake, which would increase $CaCO_3$ precipitation to the lake's sediment. There is no obvious change in land use or hydrology that could account for an absolute decrease in detrital fluxes in the period 2000-2003.The reduced percentage values of other elements after 2000

that have mainly detrital origins from the metamorphic and basic igneous geologies in the catchment (Al, Ba, Be, Co, Cr, Cu, Fe, Li, K, Mg, Mn, Na, Ni, Pb, Sr, Ti, V, Zn) are due to the diluting effect of higher absolute fluxes of biological material to the sediment.

As a result of the changing of the ecosystem function, the content of the chemical elements in the sediment has an abrupt change at around 2001 (Figure 7-3). The concentrations of the main elements such as Ca and Fe show that the ecosystem is stable pre-2001. However, other elements such as Pb and P showed obvious changes pre-2001; this might be a strong signal of pollution from human activities. Figure 7-3 shows the content of Pb increasing from around the 1970s to 2000. This may be evidence of pollution from industrial emissions related to industry in the region. Although industry is not the most important economic contributor in Erhai catchment, the government report suggests that it has considerable growth after 1970s (when was the start of China economic reform). Pb from the sediment also indicates that the pollution can trace back to 1970s. Another obvious pollution in Erhai Lake is phosphorus, which is highly responsible for the lake's eutrophication. Since the onset of human activities in the catchment, which may be traced back to around 3000 years ago (Dearing, 2008), agricultural activities are an important source of nutrients for the lake. However, the nutrient supply from the catchment is obviously increased after the wide use of chemical fertilizers since the 1970s. Fig. 7-3 also shows the phosphorus content in the lake sediment slightly increased from 1970s and lasts until recently. The trajectory of phosphorus concentration is different from that of most other elements during the last 130years.Whereas most other elements have an abrupt change at ~2001, the phosphorus content continuously increased during recent decades.

The enrichment of nutrients will unavoidably cause changes in the ecosystem. The documentary evidence shows that algal content was increasing (Fig. 5-9) and that macrophytes were diminishing in number because of intensification of human activities after the 1990s (Pan et al., 1999; Wu and Wang, 1999). Siliceous algae (diatoms) show clearly the trend of the lake's ecosystem. The eutrophic species like *C. dubius* slightly increased from the bottom of the core whereas other, less eutrophic species like *A. alpigenia* suggested a decline after 1950s. Both of the

species are blooming in the summer or fall (Hu et al., 2012) which suggests that nutrient availability for diatoms in summer or fall has increased since the 1950s. Previous research also suggested that the low water level after the 1970s was most likely the main reason for eutrophication (Pan et al., 1999; Wang, 2000). However, according to the diatom community's change during the period of lower water levels (the end of the 1970s), DCA reached a low value at the end of the 1970s but it rapidly recovered from the perturbation (Fig. 7-7a). Other proxies such as chemical elements also suggest that the rapid processes such as water level change did not change the function of the lake ecosystem on a long-term scale, only briefly, from which it was able to recover. The document records show that the lake suffered an algal blooming at 1996, but the lake's state did not shift permanently. This can be confirmed by the steady change in palaeo-indicators, such as TOC, TN and metal element concentration around 1996. Meanwhile, the palaeo- indicators did not show any evidence for an external disturbance occurring in the catchment or in the lake (Fig. 7-9). Therefore, fast variables such as high temperature and drought might be responsible for that algal blooming. The lake ecosystem shifted after a second algal blooming at 2003. The rising organic matter content (Fig. 7-2), the change in chemical element composition (Fig. 7-3) and the shifted diatom compositions (Fig. 7-8) could confirm that the lake's ecosystem transited, and the function of the ecosystem abruptly shifted.

The most obvious changes in diatom communities are the abrupt shifts from *C. dubius* and *A. alpigena* diatoms to *F. crotonensis* and *A. ambigua* and *C. dubius* diatoms. Both *F. crotonensis* and *A. ambigua*bloom in the spring in Erhai lake (Hu zhujun et al. 2012). Therefore, the diatom composition shifts may track changes in nutrient source, which probably shows the release of phosphorus from the lake's sediment in spring. If this assumption (i.e. the blooming of *F. crotonensis* in spring may mean the enhancement of nutrient recycling from lake sediment) is correct, then*F. crotonensis* may indicate the possibility of algal blooming in summer and autumn. However, another possible explanation of the shift in the diatom communities may be the limitation of silica in the lake water rather than phosphorus (Lund, 1950). The hypothesis is that the blooming of spring diatoms such as *F. crotonensis* consumes most available silica in the lake, which will

nutrient-limit the growth of diatoms in summer and autumn. Therefore, the shift in diatom composition may be due to the limitation of silica rather than phosphorus in the lake. This explanation seems to be reasonable for the dynamics of diatom communities. However, the dynamic is still triggered by phosphorus, i.e. the increasing of phosphorus releasing from the lake's sediment is the main reason to cause the limitation of silica in summer or autumn. Therefore, phosphorus should be considered as the initial driver for the dynamic of the diatom communities and for the lake's ecosystem. Other studies show that, in Erhai Lake, diatoms are dominant in spring or early summer (Lv et al., 2010), and that algal blooming events are reported in late summer or autumn (Lv et al., 2010). Therefore, the abundance of *F. crotonensis* might be more sensitive than other species and could be employed as a proxy to predict the possibility of algal blooming.

7.3.4 Diatom-inferred TP

The diatom-based TP transfer function in Yunnan Provinces is weak, but it is difficult to reconstruct TP for Erhai Lake with other training sets due to their lack of analogy with the Erhai system. For instance, the Lower Yangtze River diatom-TP transfer function (Yang et al., 2008) only contains 23 of 67 species found as Erhai fossil diatoms. Here, in order to define the baseline for lake management (Battarbee, 1999; Bennion et al., 2001), the TP reconstruction in Erhai Lake uses the Yunnan province diatom-TP transfer function (Chapter 6), but the reconstructed TP will be calibrated with the instrument TP data. The DI-TP is overestimated at Erhai (also see Chapter 6), but the trend of DI-TP is similar to the instrumental TP (Fig. 7-8c), which is shown by the high linear relationship coefficient between DI-TP and instrumental TP (R^2=0.60). Both TP are plotted in Fig. 7-10. The values at 2000 and 1999 depart from the main trends of the relationship, which may be due to the lack of chronological accuracy. The two data points (1999 and 2000) are not going to be considered in linear regression. The linear regression with rest of TP indicated that R^2 was improved to around 0.87 ($p<0.01$), which means the regression, in terms of trends, is significant between the instrumental TP measurements and DI-TP. Therefore, the equation is employed to calibrate the TP before 1991 when no instrumental data can be used.

The trajectory of lake's TP is shown in Fig. 7-10, and the baseline TP value is around 11-12 µg/l. This could be used as TP target value for management design (Battarbee, 1999; Bennion et al., 2001).

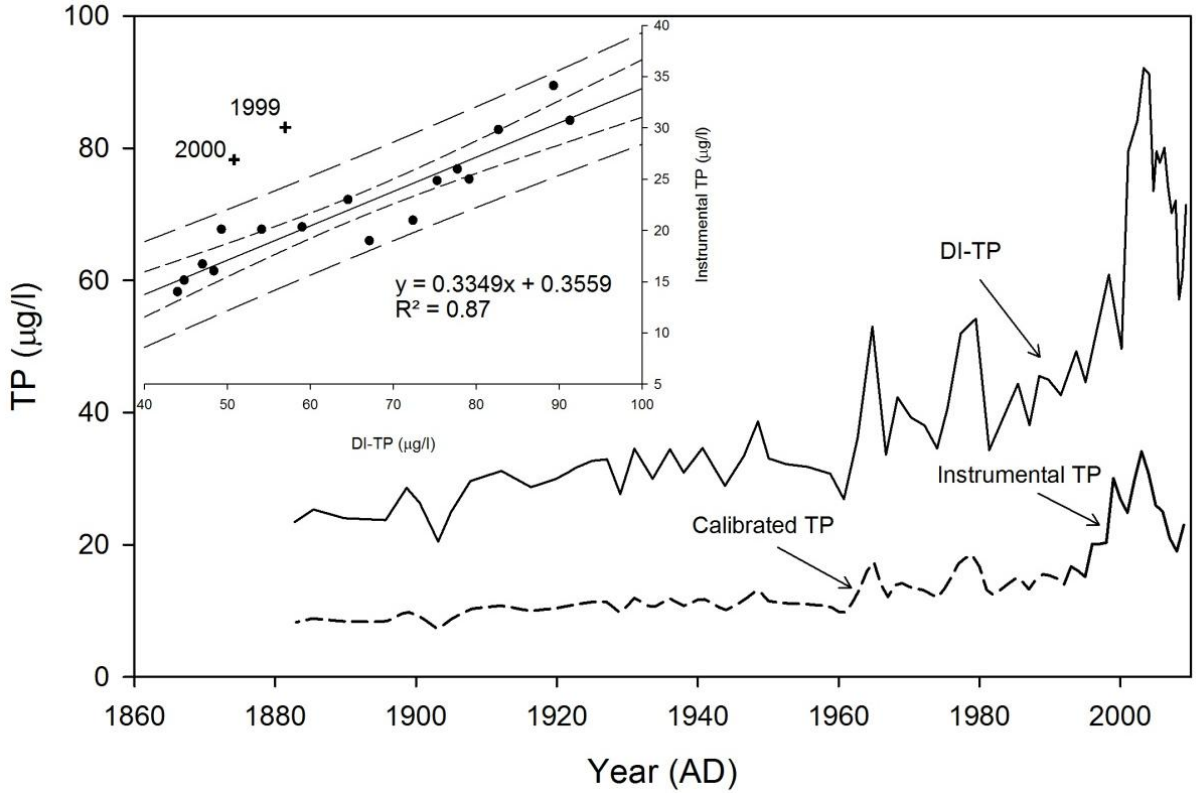

Figure 7-10 Calibrated TP in Erhai lake during past 130yrs. The relationship between instrumental TP and DI-TP is shown at left-top of the figure (DI-TP was annually interpolated). The short dashed line is the 95% confidence interval for regression, and the long dashed line denotes 95% prediction intervals. The calibrated TP before 1991 are calculated with equations provided by the linear regression (in the equation, y is instrumental TP, and x is DI-TP).

There are many possible reasons for thelarge discrepancy between diatom-inferred TP and instrumental TP data. Firstly, the training set is weak in Yunnan province. As introduced in the previous chapter, the diatom distributions in Yunnan province may be affected by strong gradients in temperature landscape, etc., and it is hard to say that the diatom communities can represent the TP gradient in the training set well. Therefore, the estimated errors are large for the diatom-based TP transfer function in Yunnan province. It will unavoidably cause big uncertainties in the TP reconstruction. Secondly, as discussed in the previous chapter, if the training-set lakes lie within a two-fold bifurcation, the lakes may

have large estimated errors even though they are in the middle of the TP gradient in the training set. The reliability of this assumption remains uncertain, and the estimation errors may be also caused by the habitat differences among lakes. Confirmation would require more studies in a larger training set. Thirdly, the shift of diatom communities has an obvious feature of seasonality, and it is probable that the growth of spring diatoms restricts the bloom of the summer or autumn taxa. Therefore, although the shifts are probably triggered by the TP releasing, the silica content in the lake might be the limiting factor so the TP transfer function may not reconstruct the TP well, and large uncertainties are expected.

7.4 Summary

- The dating based on ^{210}Pb and ^{137}Cs is reliable, and provides an important base for following analysis. All palaeolimnological proxies were relatively stable before 2001-2003 when the algal blooming occurred, but quickly changed afterwards.
- The palaeolimnological proxies show that there is no big disturbance at around 2001-2003. The lake's eutrophication is probably controlled by the slow processes, such as nutrient enrichment. Rapid, short-lived processes such as water level decline or temperature fluctuation are not the main drivers for the lake's regime shift.
- The diatom species *Fragiliaria crotonensis* is dominant in the spring of year while the lake is in a state of eutrophication, but its abundance is limited while the lake is not in a state of eutrophication. It can be used as an effective indicator to guild the lake's management and to evaluate the efficacy of this management.
- The diatom-inferred TP is overestimated in Erhai Lake, but the trends are similar to the instrumental TP during the last two decades. Therefore, the equation of linear regression of the relationship is used to calibrate DI-TP. The result suggests that the lake's reference TP value is around 11-12 µg/l.

Chapter 8 Eutrophication in Erhai Lake: resilience theory and early warning signals for critical transitions

8.1 Introduction

As introduced in the previous chapter, a lake's state can be affected by many processes including slow and fast variables. These variables can impact the lake's states in many ways and at different scales (Bayley et al., 2007; Dearing, 2008; Dillon and Kirchner, 1975). Through the analysis in the last chapter, we can only know the trajectory of eutrophication, but we still do not know the reason for the lake's critical transition without big disturbances or visible warning signals. In fact, it has proved difficult to fully understand abrupt ecosystem changes without including the idea of nonlinear responses between system states and drivers (Williams et al., 2011). This chapter will see the lake as a complex ecological system, and the change in resilience and feedbacks will be investigated to explain eutrophication in Erhai Lake. This chapter will also test the EWS theory in real ecosystems, rather than in terms of modelling.

8.2 Resilience and feedbacks in Erhai Lake

From the analysis in Chapter 7, it is clear that Erhai Lake changed into an alternative state at around 2001, and that the transition only took around 1-3 years. However, gradual changes in the lake happened some decades prior to the transition. As shown by palaeolimnological proxies, nutrients and primary production gradually increased from the 1950s (Fig. 7-2). Documentary records showed that significant human activities occurred in the catchment during the period of the Great Leap Forward (1958-1962) and Cultural Revolution (1966-1976), when around 20% of the forest was logged in the Diancang Mountains and alien fish species were introduced to the lake. Some research (Pan et al., 1999; Wang, 2000) noticed nutrient enrichment in the lake after the

1980s, and suggested that algal blooming (Cyanophytes) might happen when nutrient levels reached a certain value (Li, 2001; Pan et al., 1999). A state conservation area was established in 1994 in order to protect the local environment. Meanwhile, several approaches to controlling nutrient loading were implemented, such as the sewage interception project in the catchment and wetland reconstructions around lake. However, the algal blooming (that is, blooms of blue algae observed instrumentally) still occurred in 1996 and 2003, and continuously every year afterwards.

The state change provided good evidence about the loss of the lake's resilience. Instrument data show that TP reached a high level of around 35 µg/l before 1996. However, the lake was still fairly clean and algae concentrations remained at low values (Fig. 5-9). One possible explanation could be the high resilience in the ecosystem. It is noteworthy that macrophytes were abundant in clean water states, at around 800,000 t before 1980 (Wu and Wang, 1999). Meanwhile, the fish community was dominated by local species (Du and Li, 2001). Zooplankton abundance was more than 900 per litre (Wu and Wang, 1999). It is known that macrophytes can prevent zooplankton from being preyed upon by fish (Jeppesen, 1998; Scheffer, 1998). Therefore, high zooplankton abundance likely restricted the growth of algal communities in the lake (Schriver et al., 1995), and the negative feedback between zooplankton and algae probably kept the lake in a clear state (Jeppesen et al., 1997). The density of phytoplankton was only around 64.9×10^4 unit per litre in 1957 (Wu and Wang, 1999). Low density of phytoplankton may indicate that the lake ecosystem was in a high resilience state.

It is difficult to directly estimate the resilience of a lake (Holling, 1973), although perturbations from fast variables in the system, like seasonal water level, may provide a good insight for evaluation of the size of the attraction basin (Carpenter, 2003). The water level declined to its lowest value at around 1978, from a high stable level (Fig. 5-6). Diatom communities showed a rapid response to water level decline in 1979 (Fig. 7-7). The lake recovered after the 1970s, and therefore, it appears that the lake had a high resilience before the 1980s so that the influence from big external perturbations could be suppressed.

From 1980s, DCA fluctuations indicated that the lake became easier to push away from the equilibrium state i.e. clean water attraction basin. As the lake continued to be enriched with nutrients the attractor basin was shrinking and the resilience was decreasing. This was mainly manifested by the increasing fluctuations of DCA after 1970s. The algae concentration was still low and negative feedback between dissolved nutrients and algae is critical to control the algal blooming.

Before the 1980s, the diatom communities are mainly dominated by the summer and autumn taxa, and the spring taxa like *F. crotonensis* have a relatively low abundance. This is probably due to the phosphorus limits in the lake as discussed in Chapter 7. Evidently, the phosphorus release from the lake's sediment in spring is quite small pre-1980s. Therefore, at the beginning, dissolved nutrients originated mainly from the catchment, and lower quantities of nutrients were released from the recycling of lake sediment. Limited nutrients controlled the blue-green algae growth in Erhai Lake. Then, after the 1980s, an evidence of the increase in *F. crotonensis* indicated the gradual release of TP from lake sediment. It indicated that, from this point, the lake ecosystem resilience started to decrease. The most direct evidence for this was the rise in phytoplankton concentrations, which reached 123.6×10^4 unit per litre around 1980 (Wu and Wang, 1999). The sediment recorded the consequences of the loss of the ecosystem resilience; for example, organic matter quantities increased from the beginning of the 1970s.

Extraordinary changes in most palaeo-proxies suggest that the ecosystem's function shifted as discussed in previous chapter. As regards drivers, the external perturbations such as water level and temperature contribute a lot to the lake's ecosystem regime shift at 2001. There was a large lake-level change at the end of 1970s connected with the hydro project (see Chapter 5), a quick response and recovery of diatoms communities to this perturbation could be occurred. Therefore, it can conclude that water level may be a fast and short term driver for lake's ecosystem shift. It should be the reason why lake's ecosystem cannot recovery although the lake's water level raised to the level of around 1979. For lake's ecosystem shifts, temperature may play same role as water level. In contrast, nutrients enrichment may be one of the important slow and long term driver for lake's ecosystem shift. However, the abrupt change in the lake might be

correspondence with the mechanism changes in the lake. As showed in Chapter 7, given the evidence for increasing concentrations of dissolved TP up to 2000 and increasing levels of aquatic productivity up to 2000 and beyond, a relatively low increase in sediment P may be consistent with recycling of P from the upper sediments as anoxia develops. It suggests that the lake's ecosystem function change is mainly due to the anoxia conditions appearance in the lake ecosystem. There are no direct bottom oxygen data to demonstrate the anoxic conditions in the lake. However, indirect data from chironomid head capsules (Zhang, unpublished data, Wang et al., in press), shows that the concentration of these capsules in the lake's deepest part decreased to around 0 at ~2001;this is strong evidence of anoxic conditions (Little, 2000). One of important reason for the reduction of oxygen at the bottom of the lake is the increasing abundance of organic matter (Fig. 7-2). Carvalho et al (2012) also suggests that seasonal changes in temperature and rainfall may have been significant reductions in in-lake phosphorus concentration. As the temperature increasing in recent decade is so obvious that may increase the lake's phosphorus releasing from sediment. Therefore, the deoxygenation process leads to a new positive feedback between bottom water oxygen content, dissolved nutrients in the lake and algal communities (Fig. 8-1). The lake shifted from clean water to turbid with the SD declining by 2 m.

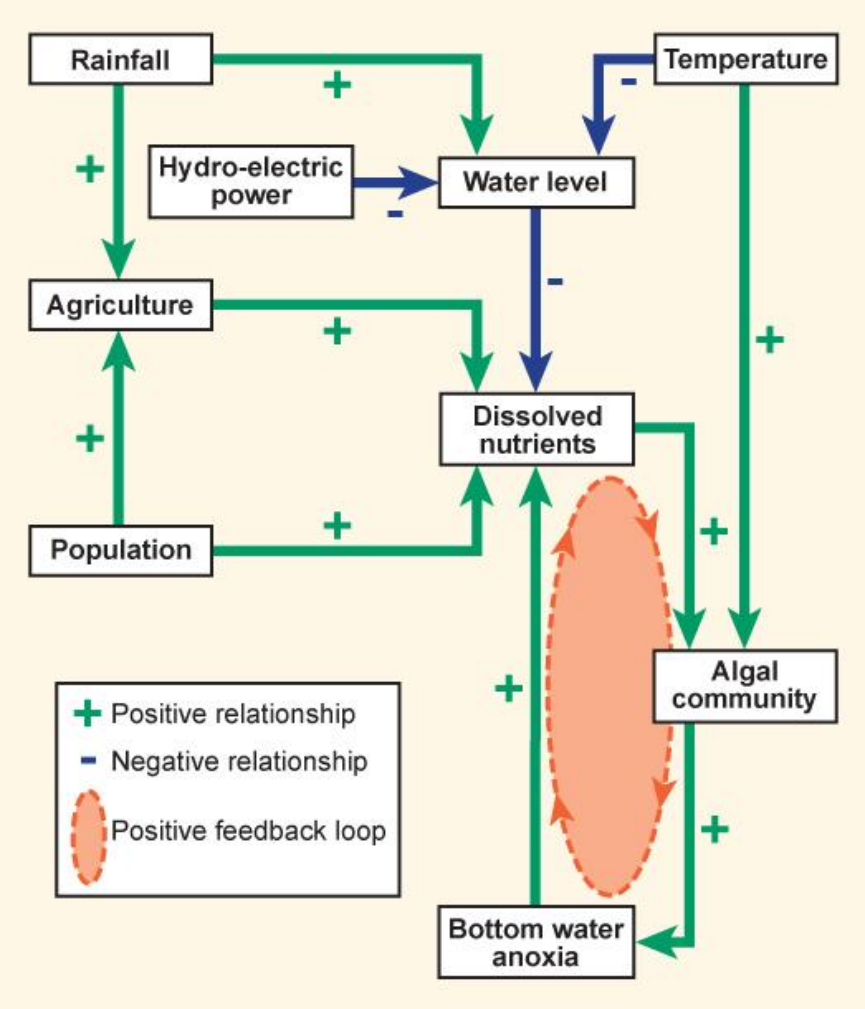

Figure 8-1 A simplified systems dynamic framework for the Erhai eutrophication process. The figure represents the stage of eutrophication equivalent to the fold bifurcation in 2002-2004 when the positive feedback loop (dashed oval) involving recycling of phosphorus from sediments to lake was firmly established. The figure shows the diversity and interconnectedness of major external drivers (bold) of the lake algal community with typical relationships (+ and -) shown for major interactions.

8.3 Fold bifurcation and hysteresis in Erhai Lake

As introduced above, the lake's state shifted as a new positive feedback developed in the lake. In order to stop the on-going water deterioration, many efforts had already been made to reduce the nutrient loading, such as the sewage interception project in the catchment and wetland reconstructions around lake. These efforts can be shown to have changed the TP concentration in the lake, as

monitoring data show that the TP reduced since 2003. Government reports demonstrate that the days of water quality classify II are increasing but the COD do not improve. However, these efforts did not prevent continuous algal blooming in summer and autumn since 2001. The lake is still in the turbid water state even when the TP is lower than pre-2001 (Fig. 8-2). Therefore, there may be hysteresis between drivers and lake states in Erhai. Fig. 8-2 shows phase diagrams between nutrients and phytoplankton, in order to identify hysteresis. The phase diagram between DCA and monitored TP for the period 1992-2005 show clearly two clusters of points, each with approximately linear trends. It is shown that more than one diatom state is possible for a single specific TP (Fig. 8-2a, b). It confirms the existence of hysteresis, which means the lake may stay in a turbid state even when TP is reduced as low as pre-2001. Hysteresis is also found between TP and instrumental Bacillariophyta (Fig. 8-2c), but there is no evidence for hysteresis between nitrogen and algae, as the nitrogen is still increasing after 2001 (Fig. 8-2 d-f).

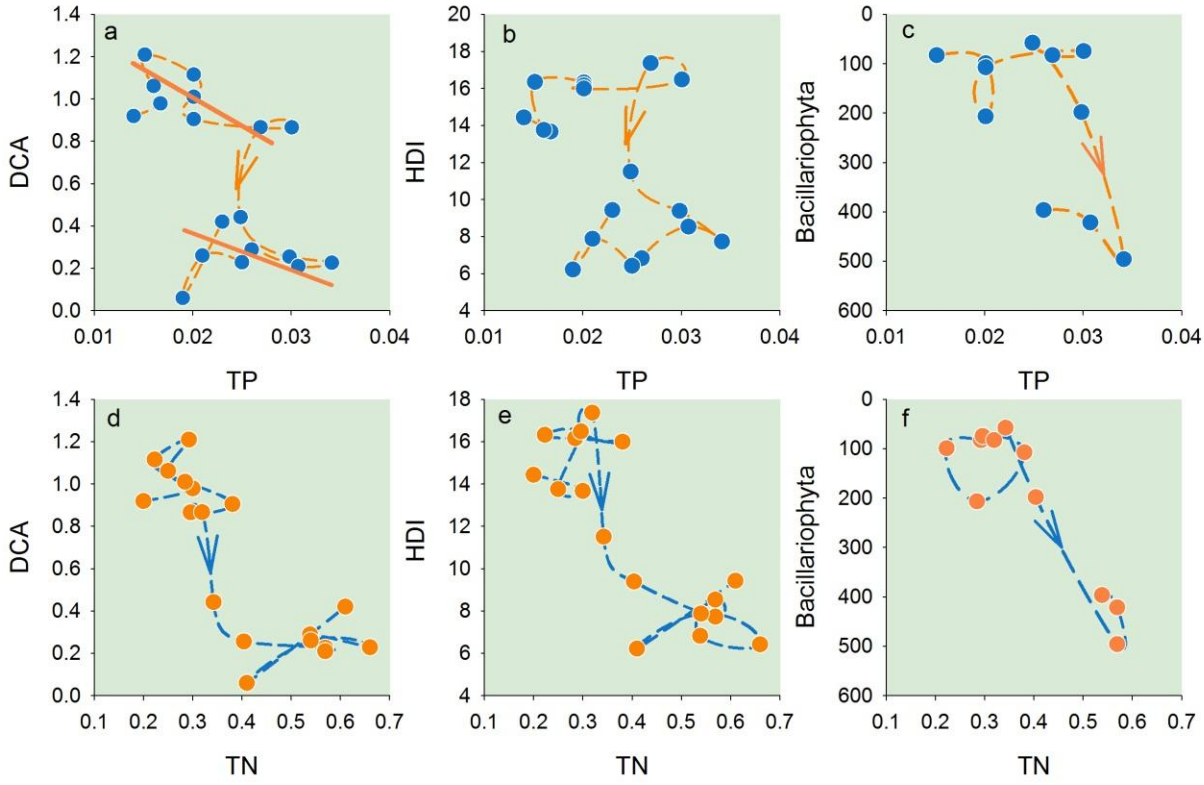

Figure 8-2 Phase-space plots of dissolved nutrient driving variables TP (mg L^{-1} - blue dots) and TN (mg L^{-1} - orange dots) versus diatom state response (DCA, HDI and diatom concentrations). The two orange lines in the plot for TP v DCA (Fig.

8-3a) describe linear clusters of points pre-2002 (upper line) and 2002-2009 (lower line). The lower line indicates that there is more than one value of DCA for declining TP values after 2002, evidence of hysteresis that typifies a catastrophic fold bifurcation.

The monitoring monthly water column TP has a trend of reducing over past years, which suggests some success of the management policies. The water column TP should come from two parts, i.e. catchment erosion and release from the sediment. As discussed before, the oxygen content of the water determines the phosphorus release rate from the sediment. The abundance of spring diatom taxa *F. crotonensis* suggests that the P recycling is still possible to be at a high level. Therefore, the P mitigation in the catchment is probably very significant, so that the sum of phosphorus from sediment recycling and catchment is reducing. However, the reduced P cannot push the ecosystem back to its previous clean states. The main reason for this is probably the shifts of the ecosystem function. Submerged macrophytes play a very important role for water clarity, and the survey's suggests that it gradually lost in the centre of the lake from 1970s (Fig. 3-5). The relationships among the components in the ecosystem are different without submerged macrophytes (Scheffer, 1998). Therefore, the delay of macrophyte recovery might be the main reason for the hysteresis of lake's state recovery. However, the evidence is weak here, especially the macrophyte data in long time scale. The fossil macrophytes may be helpful for these studies in the future.

Until now, the evidence for hysteresis between algae and TP is clear (Fig. 8-2a), and its implication is that management cannot necessarily set the TP target as equal to the critical TP value of the ecosystem transition. However, it is still difficult to use the current evidence to demonstrate that the ecosystem is a fold bifurcation system. It is clear that the ecosystem contains a critical point where the ecosystem shifts from a clear state to a turbid state, but there is insufficient data to confirm that the ecosystem contains another critical point during the lake's recovery. The Erhai case study may satisfy the character of a half fold bifurcation system, however. In any case, the Erhai lake system demonstrates the main features of a fold bifurcation system such as tipping point, alternative stable states,

and hysteresis. The discussions of early warning signals in the following section are based on fold bifurcation systems.

The phase diagram between diatoms (DCA and HDI) and other variables are shown in Fig. 8-3. The water level (both highest water and lowest water level) are linked to clusters of diatoms but the evidence for alternate steady states and hysteresis is weak. These clusters could be related to the sudden decline of water level at around 1979, and the lake's regime shift at around 2001. The diatom responses to climate (Fig. 8-3 e-h) also show no evidence for alternate steady states and hysteresis.

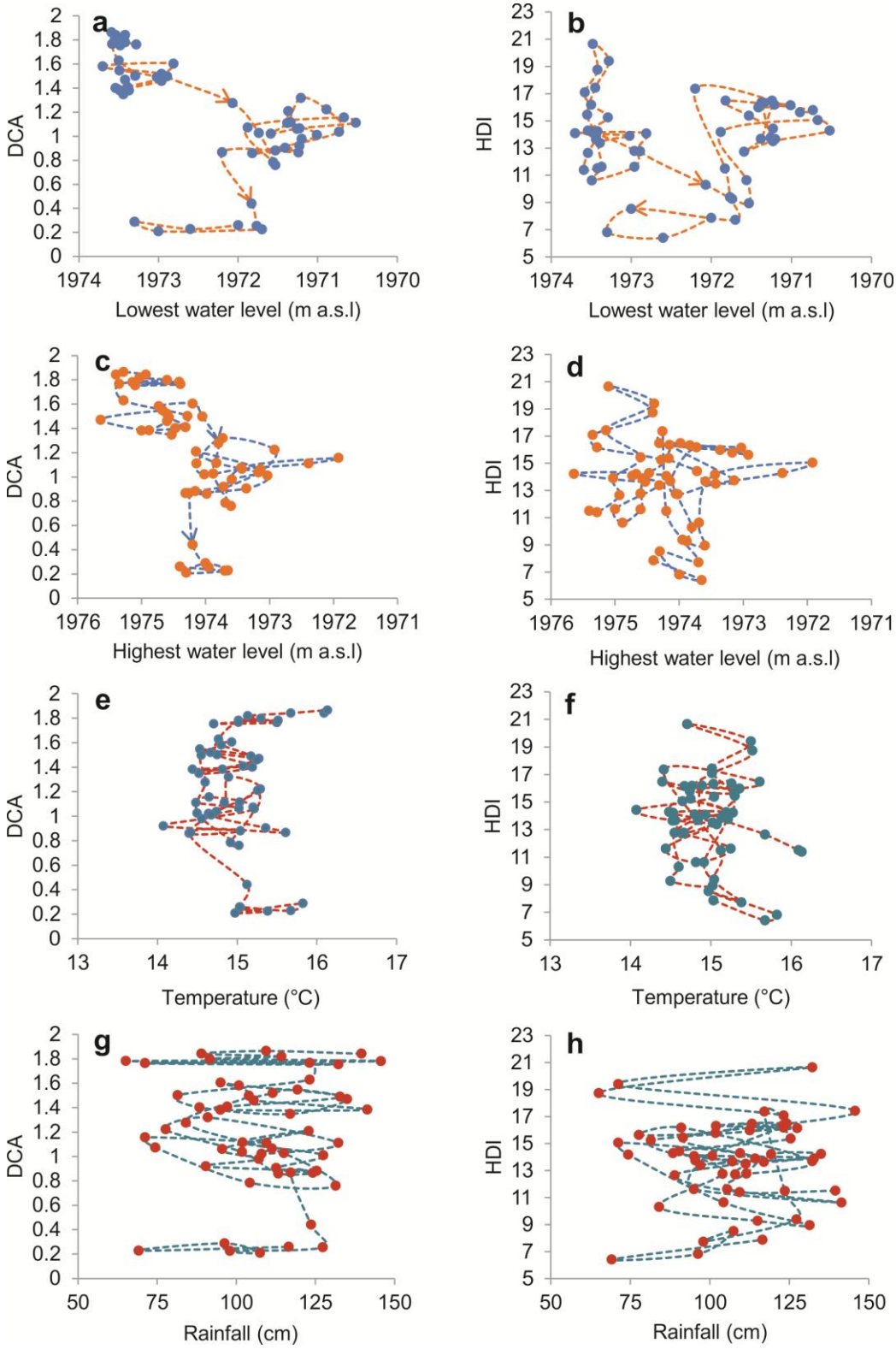

Figure 8-3 Phase diagrams of diatom assemblages (diatom DCA and HDI) and environmental variables (a, b) DCA and HDI versus lowest water level (m. a.s.l.); (c, d) DCA and HDI versus highest water level (m a.s.l); (e, f) DCA and HDI versus mean annual temperature, (g, h) DCA and HDI versus mean annual rainfall.

8.4 Response of the lake to disturbances as a complex system

It would appear, through the above analysis, that the response of the lake to environmental variables is nonlinear. Here, the eutrophication process is plotted with feedback strength and nutrients in a 3-D conceptual figure (Fig. 8-4). The ecosystem was divided into 4 theoretical stages. Before 1960s, in state A, the ecosystem state was stable. It could recover from a large external impact. The basin was wide, and the resilience was high at this stage. Therefore, the response of lake's ecosystem to disturbance was small and the system kept at steady. During stage B, the response of the lake to external disturbance became quicker. But the ecosystem could recover if the strength of disturbance declined. The relationship between lake's state and drivers was fairly linear. In Erhai Lake, water level decline and nutrient enrichment were responsible for the decline in water quality at this stage. However, if the water level or nutrient concentrations returned to the same level as before, the water quality could recover easily. Due to low water level and continuous nutrient enrichment, the resilience became weak and a cusp (Scheffer, 2009) in the lake appeared at around 1980.

Between 1980 and 2001, the lake progressed into a stage termed 'non-catastrophic' or 'reversible threshold response' stage. The resilience of this stage became lower, and the system was fragile. It was observed the short-lived eutrophication events and algal blooms during the period 1980-2000. However, the lake's states were also able to recover in a short time if the disturbance subsided. As a result of the increasing strength of positive feedbacks (Fig. 8-1), the lake approached to the point of fold bifurcation (the boundary of C and D, the small circle in Fig. 8-4), where the lake's regime shifted to an alternative state, i.e. stage D. Through the analysis of a phase diagram, we suggest that the ecosystem state is now difficult to reverse. More work should be done to reducing nutrient loading, and tend plant macrophyte and fish communities to recover the lake's healthy ecosystem.

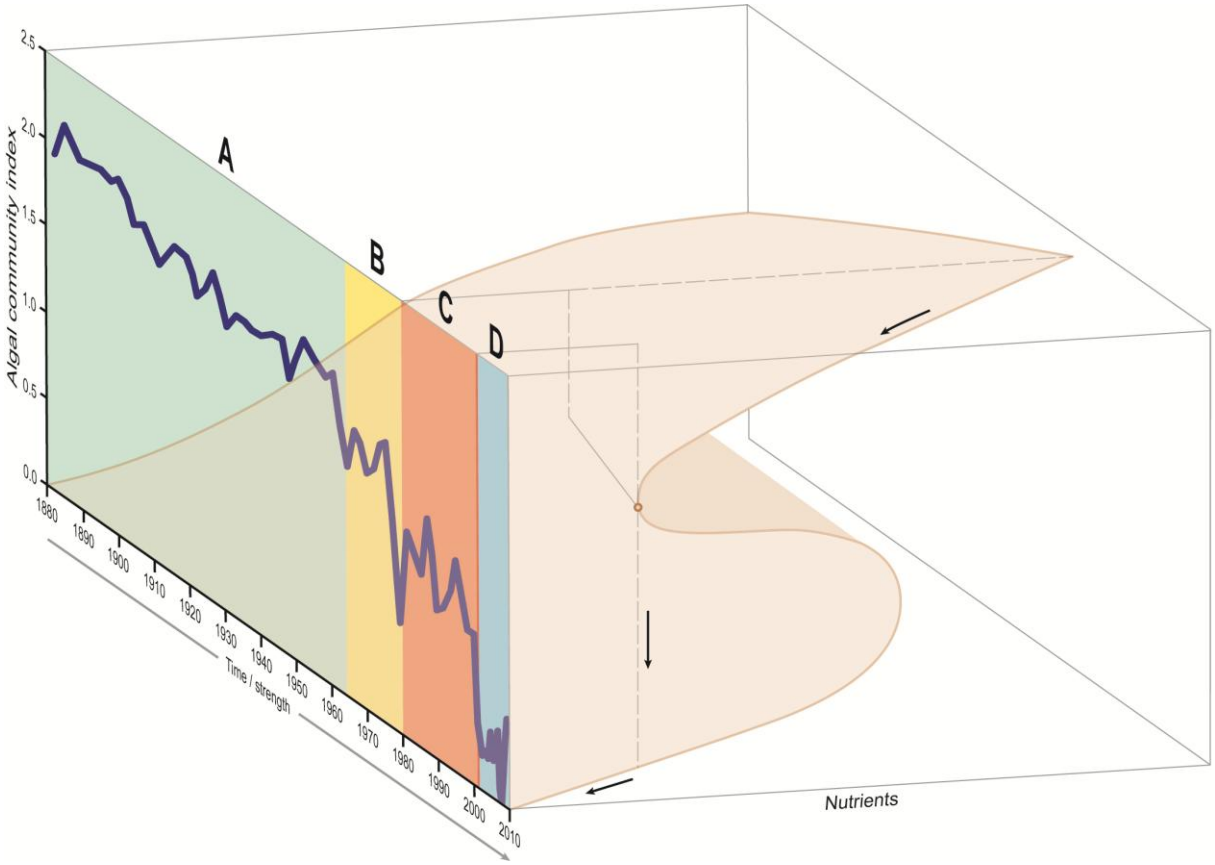

Figure 8-4 Summary diagram of changing system dynamics in the Erhai eutrophication process. The DCA proxy for algal communities and eutrophication (blue line) is plotted as a 2-D image on a timescale 1883-2010. Periods of different system behaviour (A- D) are identified by different colour bands. The linked 3-D schematic (brown) displays the changing relationships between eutrophication and nutrients in phase space as the strength of positive feedback increases along the time axis 1983-2010. The different periods of behaviour are summarised thus: (A) before 1965: relative stability in the first steady state (green). (B) 1965-1980: linear responses to enhanced nutrient loadings (yellow). (C) 1980-2001: non-catastrophic/reversible threshold responses to nutrient loadings and water level fluctuations (orange); 2002-2004: regime shift (boundary C-D) linked to the point of catastrophic fold bifurcation (small circle). (D) 2004-present alternate steady state (grey).

8.5 Early warning signals of critical transitions

The nonlinear dynamic response, especially the hysteresis, suggests that early warning signals (EWS) would be very useful for lake management. Some

indicators from modelling and experiments suggest that it is possible to anticipate critical transitions several decades ahead of transitions based on a theory called critical slowing down (CSD) (Biggs et al., 2009; Brock and Carpenter, 2006; Carpenter and Brock, 2006; Ditlevsen and Johnsen, 2010; Lenton, 2011; Scheffer et al., 2009; van Nes and Scheffer, 2007). The CSD suggests that the system's recovery from perturbation will become slow when it approaches the critical point (Scheffer et al., 2009). Therefore, some indirect indicators such as rising variance and increasing autocorrelation can be employed for prediction of the critical transition (Scheffer et al., 2009).Fig. 8-5 shows the variance (Carpenter and Brock, 2006), skewness (Guttal and Jayaprakash, 2008), and autocorrelation (Dakos et al., 2008; Lenton, 2011) calculated based on the diatom data from Erhai Lake (Fig. 8-5a, f). Residuals started to increase from the 1960s (Fig. 8-5b, g). Variances based on half time-series moving windows increased from around the 1960s when the lake changed from a relatively stable state to a linear response states (Fig. 8-4). The variances obviously increased (Fig. 8-5c, h) after the 1980s when the cusp of lake ecosystem appeared (Fig. 8-4). However, autocorrelation and skewness showed different trends as expectation (Scheffer et al., 2009). Autocorrelation increased pre-1980 and decreased after (Fig. 8-5d, i). Skewness was kept stable before 1980s, and decreased afterwards (Fig. 8-5e, j). In conclusion, rising variance could be considered as a lead indicator for warning of the lake's regime shifts, and could precede the critical transitions by 20 years in this case. Autocorrelation seems to decline when the lake comes close to the threshold. The results are inconsistent with previous modelling studies according to CSD (Scheffer et al., 2009). Rising skewness is not a lead indicator from CSD, but indicates the increasing asymmetry of a system's as it approaches the threshold (Scheffer et al., 2009). The values of DCA skewness were around 0.5 (left-skewed) before 1980, but declined to around -0.7 (right-skewed) at the critical point. This indicates that the system is tending towards asymmetry with the evidence of increased absolute skewness values, but towards an opposite direction (the change from left-skewed to right-skewed). HDI skewness showed similar characteristics (Fig. 8-5).

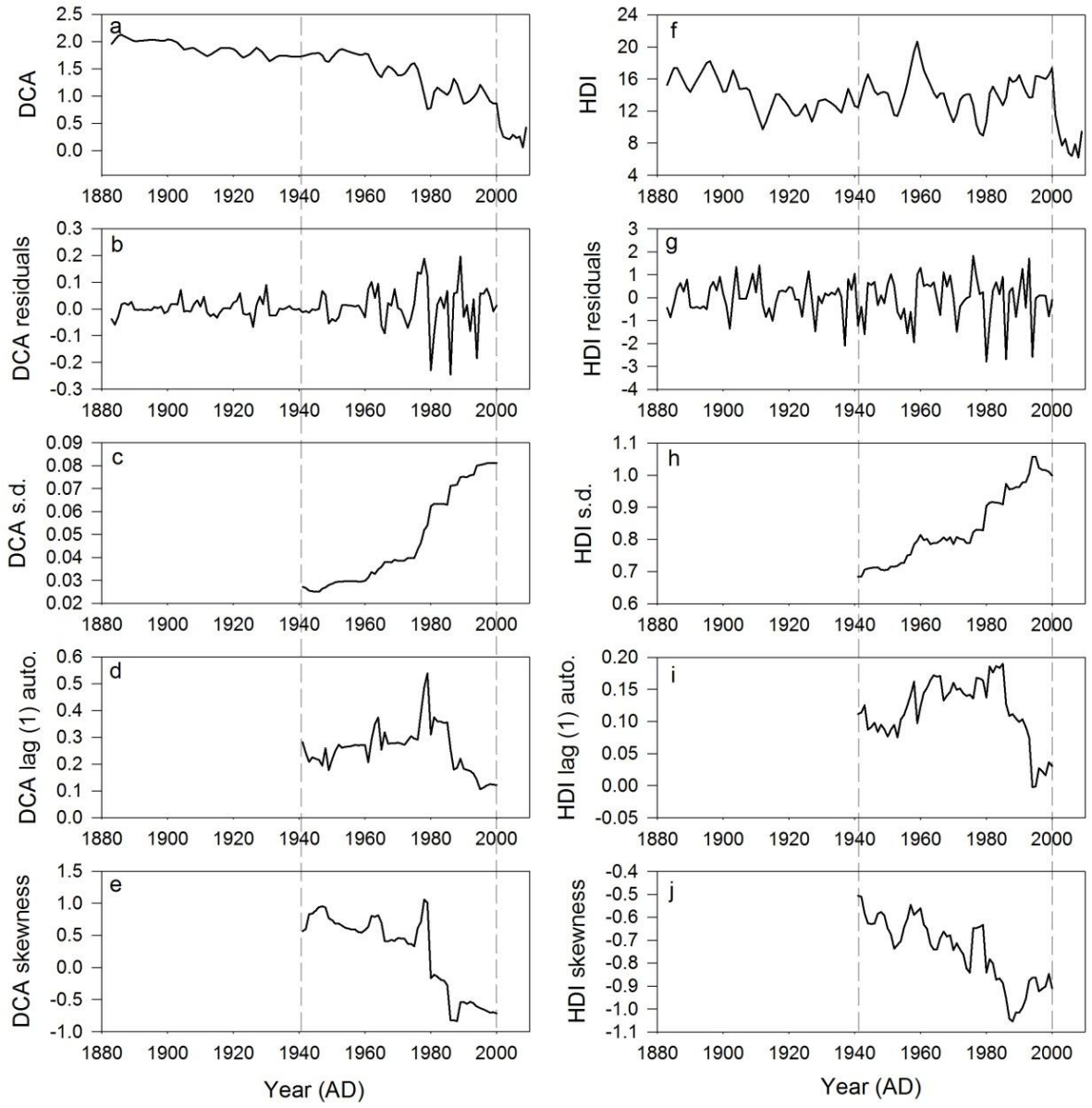

Figure 8-5 Potential early warning signals of the regime shift in the trophic state. (a and f) One-dimensional gradients for sediment diatom composition (DCA line a) and diversity (HDI line f) using interpolated data. (b and g) Residuals from (a and f). (c and h) Variance of (b and g) using standard deviation (SD). (d and i) Skewness of (b and g). (e and j) Lag-1 autocorrelation of (b and g). Plots c-j calculated using a 59 yr (half time series) sliding window (represented by vertical dashed lines) through the period 1883-2000 and plotted to right of the window.

Plenty of processes may affect the patterns of the early warning signals. First, the lake's ecosystem state is represented by DCA. It has proved that the diatoms

communities are sensitive to ecosystem change, but the DCA (DCA axis 1 scores) cannot fully represent the diatoms change. Therefore, it is necessary to check the robustness of statistical analysis for representing diatoms. Second, the techniques for calculation of EWS have not been widely verified, and the techniques such as linear interpolation, half-time series moving windows size and smoothing methods should be carefully used. Third, the conclusions are based on ^{210}Pb dating which has chronological errors, and therefore it is necessary to discuss the impacts from^{210}Pb dating errors. Taking these factors into consideration, further analyses were done to check the robustness of early warning signals (Fig. 8-6). **First**, in the above analysis, the time series data were linearly interpolated into annual intervals before conducting the above EWS calculation. Fig 8-6a, b showed residuals and variances of DCA and HDI based on real data (without interpolation). The rising variance could still be found (Fig. 8-6b) 20 years before the critical transition. **Second**, axis 1 score from Correspondence Analysis (CA) was employed to represent the diatom communities in the lake sediment (Fig. 8-6c). The variance was rising as the lake approaching the threshold change (Fig. 8-6d). The autocorrelation also showed the same features as in DCA, which declined after 1980 (Fig. 8-6d). The discrepancy was in skewness, which declined in DCA but increased after 1980 in CA. It is worth noting that the skewness in CA was around a negative value (around -1) before 1980, but shifted to a positive value (around 1) after 1980. Therefore, different trends due to two different statistical methods does not change the findings about the feature of this system before the critical point, i.e. the system's asymmetry was enhanced and changed towards an opposite direction (but changed from right-skewed to left-skewed in CA). **Third**, the results from different moving window sizes are shown in Fig. 8-6e, f. The sizes of 1/3 and 1/4 of the time series data are chosen to calculate the variances. Fig. 8-6e, f suggests that the rising variance is robust. However, the warning period is highly related to the moving window size. It becomes longer as the window size is reduced, especially in HDI. An alternative method of calculating variance without moving windows should be considered in the future while detecting EWS. **Fourth**, the residuals from the Gaussian kernel smoothing method are showed in Fig. 8-6g-h, and they also show the rising variance before the regime shift with the system becoming less correlated ahead of transition. The last test was conducted for ^{210}Pb errors (±2 standard date errors). The minimum and maximum errors from

^{210}Pb chronology were applied for DCA sequence recalculation, and the residuals based on interpolated annual data are showed in Fig. 8-6i-g. The variance always rises as the system approaches the transition point irrespective of dating errors. Therefore, all tests showed that rising variance was robust in warning of an impending critical transition.

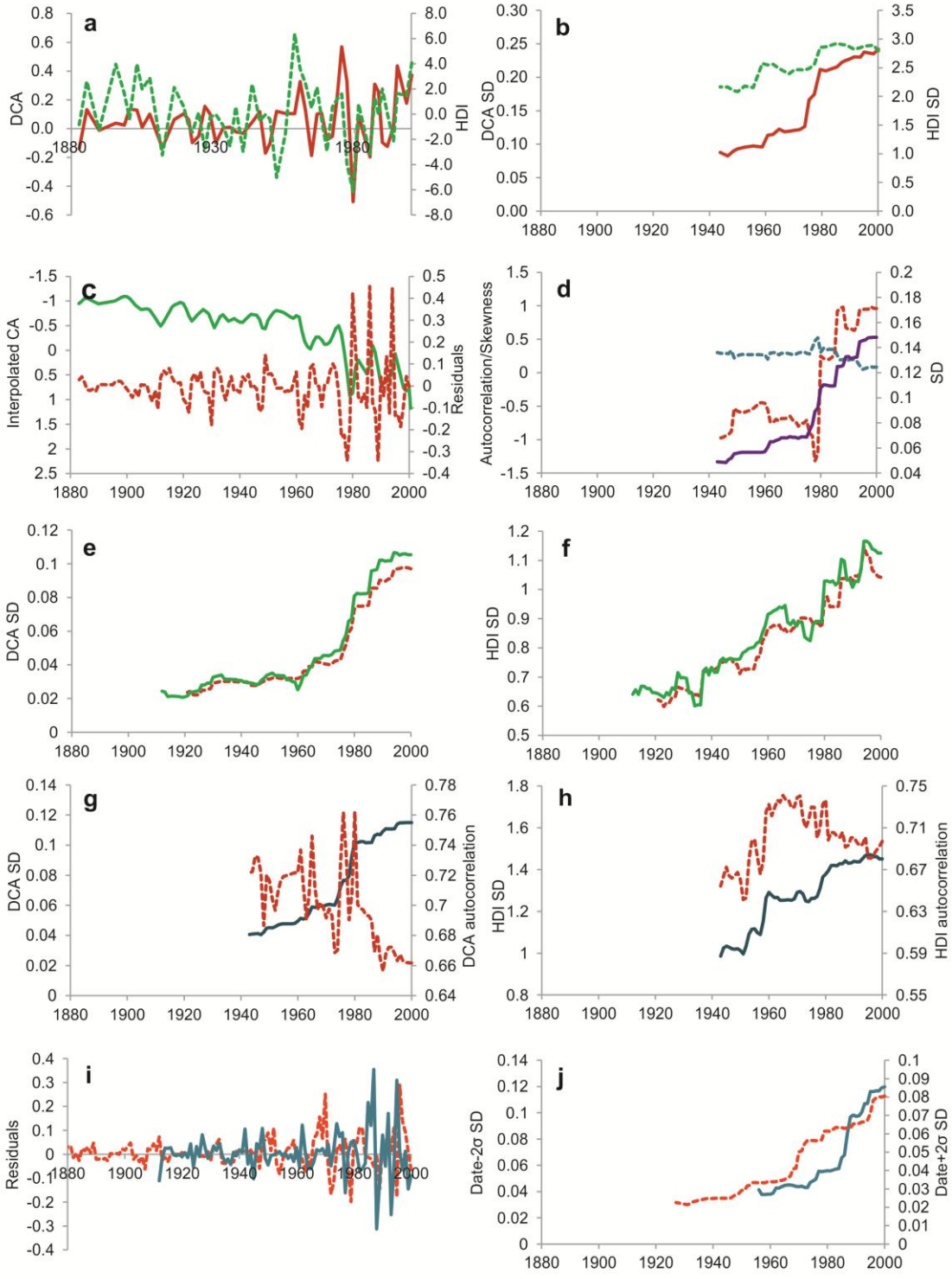

Figure 8-6 Various early warning signal metrics for diatom DCA and HDI data. (a)

DCA (solid red line) and HDI (dashed green line) residuals based on real data without interpolation; (b) DCA (solid red line) and HDI (dashed green line) variance (SD) based on real data without interpolated; (c) Correspondence analysis (CA axis 1) of changes in diatom communities, showing interpolated CA (solid green line) and residuals (red dashed line). Note that the CA axis is reversed; (c) CA variance (SD solid purple line), autocorrelation (dashed blue line) and skewness (dotted red line) for interpolated CA data; (e, f) DCA and HDI variance (SD) using different moving window size (30yr-solid line, 39 yr-dash line); (g) DCA variance (SD) and autocorrelation using Gaussian kernel smoothing method (with 5 as bandwidth); (h) HDI variance (SD) and autocorrelation using Gaussian kernel smoothing method (with 5 as bandwidth); (i) DCA residuals calculated with +2 standard date errors (solid blue line) and -2 standard date errors (dashed red line); (j) DCA variances (SD) with +2 standard date errors (solid blue line) and -2 standard date errors (dashed red line).

In conclusion, early warning signals estimated from de-trended records of algal composition and diversity indices show significant and continuously rising variance from about 1980. Autocorrelation declines linearly for both indices, contrary to expectations. Sensitivity tests indicate that rising variance is a robust finding. However, the lack of corroboration between autocorrelation and variance casts doubt on critical slowing down as the explanation for increased variance (van Nes and Scheffer, 2007). With strong evidence for exogenous drivers, it is possible to reject an alternative explanation for increasing variance in terms of internal noise generated solely by endogenic changes (van Nes and Scheffer, 2007). Thus the rising variance most likely represents the interaction of multiple exogenous drivers and internal thresholds that magnify system responses and induce flickering (Brock and Carpenter, 2010; Carpenter and Brock, 2006).

8.6 Early warning signals caused by flickering state

It is possible that with the increasing human changes, other features (like temperature, water level, nutrients input) that contribute to diatom assemblages are changing rapidly, for example, Dong et al., (2012) suggested that the complexity of climate–nutrient interactions and the roles of the two drivers on

different timescales and at various stages of the lake's history: climate impacts were more pronounced when nutrient concentrations were relatively stable; while nutrients appeared to play a more important role in regulating diatom communities after human activities increasing. Therefore, the signals of rising variance may be caused by drivers' variations. It is different to distinguish the importance of all the drives in this study as most of the system remains a 'black box' which needs more studies in the future. However, if we observe the lake's main drivers like temperature, precipitation, water level, which did not have obvious variation increasing before lake's tipping point at 2001.

According to CSD theory, the evidence from Erhai lake ecosystems do not show early warning signals except the rising variance. It is important to know what is the main reason for the rising variance in this nature ecosystem when it approaches to tipping point.In a model fold bifurcation system, the system approaches a fold bifurcation point (F2 or F1) under the pressure of drivers (Fig. 8-7a). Eventually, the system will swift to an alternative stable state when F2 or F1 are reached. A small perturbation can also trigger the system towards to the alternative basin when the system is near to the fold bifurcation points (F2 or F1). However, a real system always contains exogenous perturbations which may switch the system in advance of bifurcation points during a bistable stage (Fig. 8-7a). As shown in Fig. 8-7b, before bifurcation point F1, there is only one basin in system, and the system is in a stable state (Fig. 8-7b) and exhibits high resilience. As the pressures increase, the system gradually changes to a bistable stage between F1 and F2. At the beginning of this state, the width of the previous basin is large, and the new basin is small, which means the resilience of the previous state is still high. As the strength of the stressors increases further, the resilience of the previous state will decline and the new basin's width will increase (Fig. 8-7c). At this moment, the system may occasionally cross the boundary between the two basins if the perturbation is strong enough (Fig. 8-7a) which is also called flickering (Brock and Carpenter, 2010). During a flickering state, exogenous forces may push the system temporarily across the boundary between the two basins (Fig. 8-7c). As the strength of the stressors increase, the resilience of new basin grows, while that of the former basin is reduced. Exogenous forces eventually push the system into an alternative state (Fig. 8-7d).

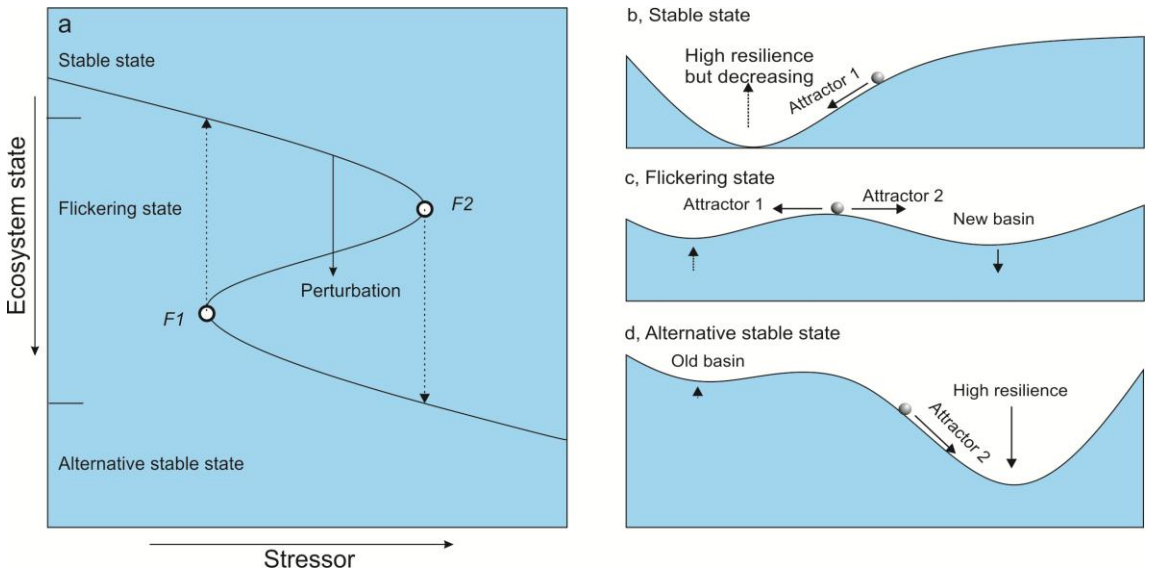

Figure 8-7 A graphic model of state change in a fold catastrophe system; a, fold bifurcation of system states with response of the strength of stressor; b, Stable state. The resilience is high with only one attractor in the system. Slow variables may be decreasing the resilience, but feedbacks in the ecosystem keep the system in a stable state with regards to exogenous forces; c, Flickering state. Slow variables have reduced resilience such that a new attraction basin is appearing. Exogenous forces may push the system temporarily across the boundary between the two basins of attraction; d, Alternative stable state. The resilience in the new basin is high with the old basin disappearing. Exogenous forces eventually push the ecosystem into an alternative state.

Statistically, flickering can be detected in frequency distributions with bimodality (Carpenter and Brock, 2006; Scheffer et al., 2009). It has been used to check the multiple states in other studies (Carpenter and Brock, 2006; Hirota et al., 2011). Here, Gaussian kernel density estimation is employed to check the frequency distribution of DCA and HDI. Fig. 8-8 shows the density distribution in different period of Erhai lake before critical point. For DCA, Fig. 8-8a-b shows unimodal distribution before 1980. Fig. 8-8c shows bimodality in lake's state during 1980-2000. The results suggested that the lake ecosystem has two states during 1980-2000. During this period, the lake was flickering between the two states. Although the unimodal patterns have slight difference, the evidence of flickering in HDI is not as strong as in DCA (Fig. 8-8d-f). Meanwhile, evidence of flickering at

Erhai exists in the form of observed eutrophication events and algal blooms between 1980 and 2000 (chapter 5). Flickering is also supported by evidence for changing skewness that may reflect increasing asymmetry of fluctuations prior to a fold bifurcation (Guttal and Jayaprakash, 2008), and the asymmetry of system changing to an opposite direction as shown above.

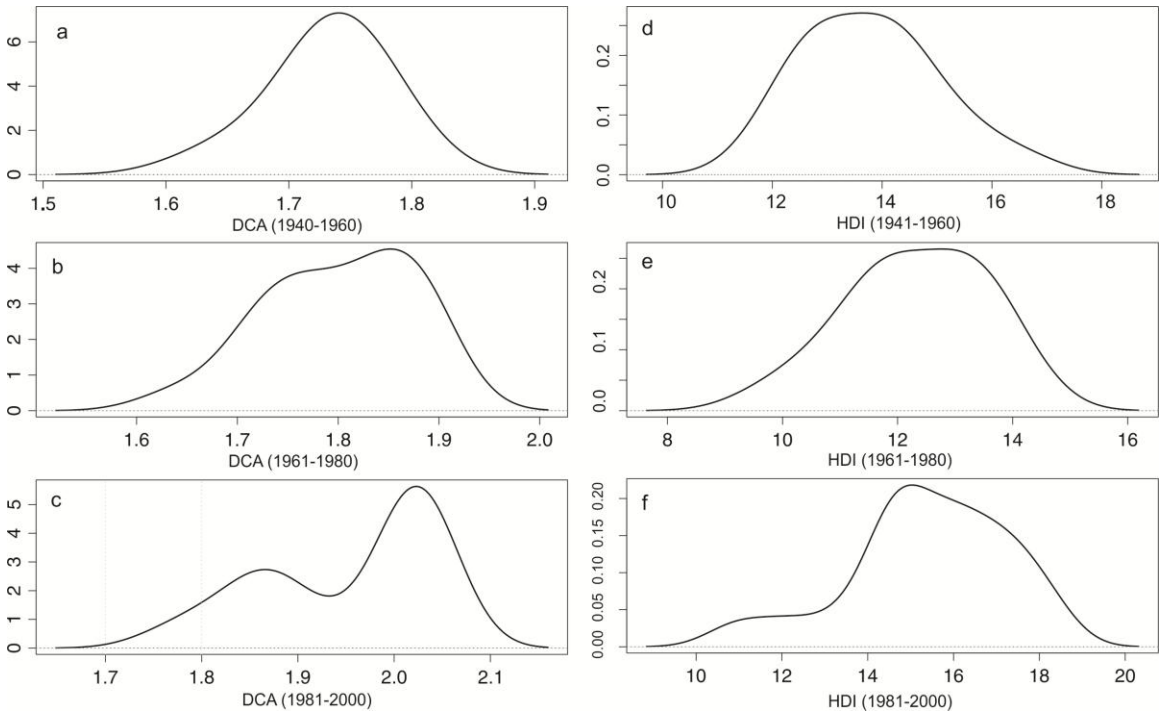

Figure 8-8 Gaussian Kernel Density Estimation for DCA (a-c) and HDI (d-f). The vertical axes mean the density. DCA density estimated based on a bandwidth 0.04, and HDI density estimated based on a bandwidth 0.7. Three ranges of series data were used for kernel density estimation. a and d are the range of 1940-1960 for DCA and HDI respectively. b and e are the range of 1961-1980 for DCA and HDI respectively. c and f are the range of 1981-2000, i.e. when the flickering state was detected.

Therefore, it may be concluded that the early warning signal of rising variance is caused by flickering rather than CSD, which is mainly caused by endogenous drivers. In previous research, CSD theory was employed to find early warning signals. Although the warning indicators from CSD had been previously identified from modelling studies (Scheffer et al., 2009), manipulated ecosystems (Carpenter et al., 2011), laboratory experiments (Drake and Griffen, 2010) and palaeoclimate analyses (Dakos et al., 2008; Lenton et al., 2008). Only modelling

(Scheffer et al., 2009) or laboratory experiments (Drake and Griffen, 2010) show rising variance as well as increasing autocorrelation. The early warning signals from CSD are evidenced well if the transition is approached slowly (Carpenter et al., 2011), but will be challenged if the transitions are induced by noise (Ditlevsen and Johnsen, 2010). It is doubtful whether critical transitions can be anticipated when there is evidence of only one early warning indicator (Ditlevsen and Johnsen, 2010), and it has been shown that early warning signals based on CSD are difficult to detect in non-stationary conditions (Ditlevsen and Johnsen, 2010; Hastings and Wysham, 2010). In contrast to model systems, real environmental systems are commonly impacted by noise, perturbations or external impacts. Therefore, even though CSD is well tested in theory, it may not necessarily be widely used to predict critical transitions in the real world. Our findings suggest that flickering can be seen as a signal of impending transitions even in a noise-induced regime shift. Rising variance caused by flickering, rather than CSD, may be the best metric to use for early warning signals in real, impacted environmental systems.

8.7 Conclusions

- The main reason for Lake Erhai crossing the boundary between clear and turbid water at around 2001 is the rising of new positive feedback (Fig. 8-1).
- As the lake's resilience weakened and feedback strengthened, the lake evolved through various theoretical stages (Fig. 8-2).
- Phase diagram between diatoms and drivers in Erhai lake show strong evidence for a fold bifurcation and hysteresis.
- The lake appears to enter a flickering state between the period of 1980-2000 based on the rising variance, bimodal frequency distribution, short-lived algal blooming and change in skewness.
- Rising variance may be considered as an EWS of critical transitions, but in real systems with large external impacts it may be caused by flickering rather than CSD.

Chapter 9 Dynamical changes in Erhai Lake based on modelling

9.1 Introduction

In Chapter 8, it was demonstrated that rising variance caused by flickering could be considered as an effective indicator for predicting Erhai Lake's critical transition, with a warning period of about 20years before the threshold. The statistics showed that the result is robust. However, there are still some doubts about the critical transitions in this study. The abrupt change of DCA is evidence for the lake's regime shifts. The rising of positive feedbacks should be responsible for the shift, and the flickering is caused by the shrinking of the attraction basin. However, the fluctuation of DCA could also be possible caused by changes in nutrient input. Therefore, there is doubt related to the phosphorus output from catchment. We still do not know whether or not the regime shifts or flickering in the lake are caused by abrupt phosphorus erosion change or fluctuations in the catchment (Andersen et al., 2009). Another doubt is whether this conclusion about EWS only reflects in the particular case of Erhai Lake, rather than a general consequence for other similar systems. In order to explore these issues, a minimal mathematical model is employed to simulate the phosphorus (P) output from Erhai catchment and phosphorus dynamics within the lake.

The outline of the model is presented in Fig. 9-1. The northern part of Erhai catchment is chosen to address the above questions. ArcSWAT was used for the catchment delineation before model implementation. It contains four important components: runoff, soil erosion, P output from catchment, and P dynamics within the lake. The dynamic modelling software STELLA, is used to simulate these processes. This STELLA model is written at the HRUs (Hydrology Response Units) spatial scale, which is then combined for whole subbasins. Details on the individual model components and mathematic equations can be found in Appendix III.

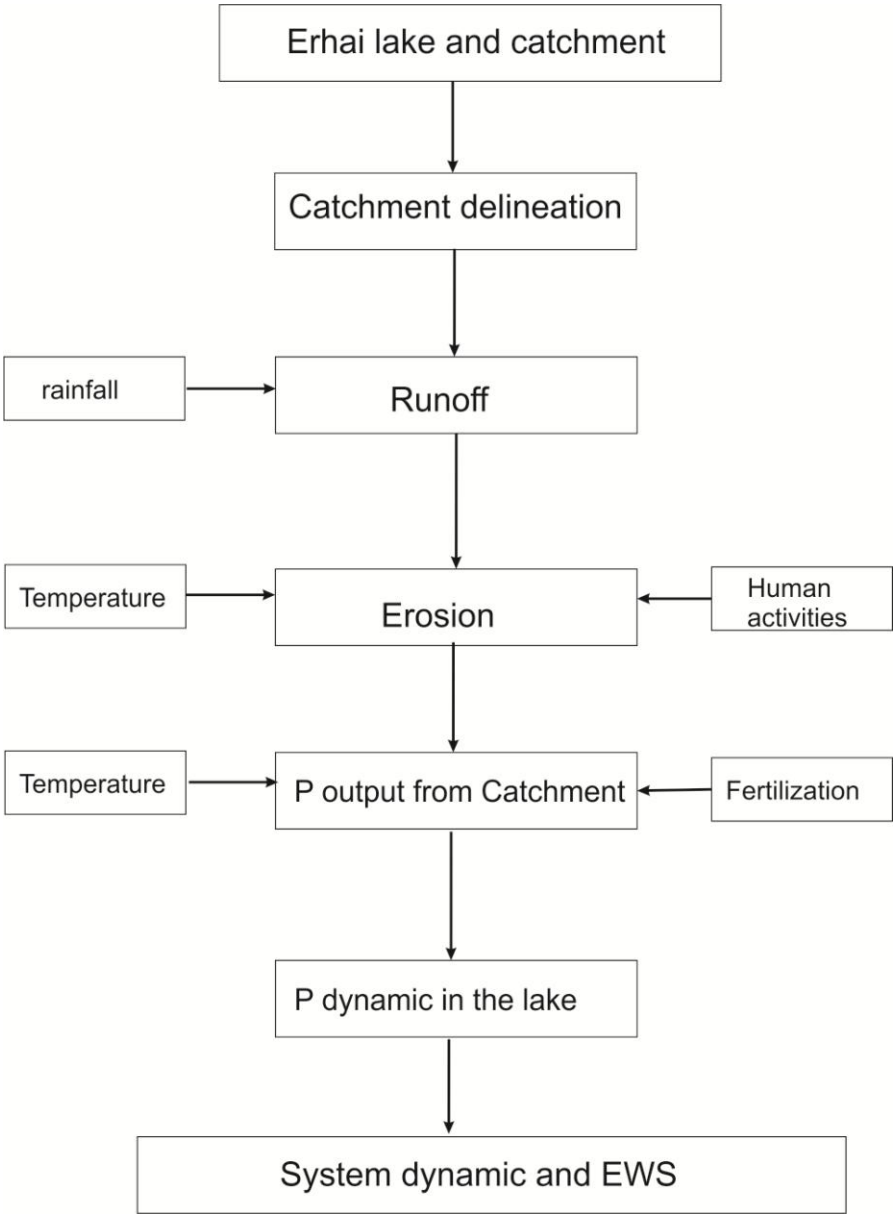

Figure 9-1 The outline of the phosphorus dynamic model in the catchment and inner lake of Erhai

9.2 Why only crop land is chosen

The Erhai catchment is around 2,250 km^2, and the phosphorus erosion is affected by many different factors, such as the relative importance of forest, crop land, barren land, and human sewage influx. The phosphorus transportation is complicated, and is difficult to simulate. Even the most complex model will contain huge uncertainties, and the conclusion may not be better than simple models (Scheffer and Beets, 1994). The purpose of this thesis is to try to simulate a critical

transition and its related early warning signals. Therefore, only the main components are considered in the model. First, concerning the simulation period, the resolution of palaeolimnology proxies does not allow monthly analysis, and only annual discussions are possible. Therefore, the resolution of the modelling is set as annually. Some data like precipitation and temperature can be input into the model on a monthly basis, but the results will be expressed as a monthly average. Therefore, many periodic signals cannot be explained by the model. Secondly, phosphorus is the limiting nutrient for the lake ecosystem (World Bank, 2007).According to Yang and Ni's research (Yang and Ni, 1999), the crop land and sewage are the main source of phosphorus pollution in Erhai catchment (See Chapter 5, section 5.7), Around 90% of the pollution is from non-point pollution, and the main non-point pollution is from agriculture. As introduced in chapter 2, STELLA is not suitable for large area simulation. Therefore, only crop land will be considered in the model. For sewage pollution, it is assumed that it is linearly related to the population size in the catchment. The crop land is primarily distributed in the north and west of Erhai lake. There are more than 18 rivers distributed in the west. It is difficult to focus on so many rivers in a simulation. On the other hand, the main river in northern part of Erhai lake catchment is Miju River. Therefore, in the initial design of the model, only the northern part of Erhai lake is considered. Lastly, regarding the accuracy of the simulation, the purpose of the model is to simulate the dynamic of the lake's ecosystem shifts, and will focus of the discussions of main mechanisms. The model is prone to simulate the trajectory of the eutrophication process rather than give the proper value for lake's phosphorus concentration. Therefore, the final phosphorus dynamics of the inner lake will be based on the normalized phosphorus erosion from the northern part of Erhai lake catchment.

9.3 Catchment delineation

The northern part of Erhai catchment is divided into nine sub-basins. The images for land cover and soil classification from the Landsat program 2005 are used for this purpose. The resolution is 30m. The DEM (digital elevation model) data were extracted from SRTM 90m Digital Elevation by NASA for the topography background of the research area. Soil types are collected from the China Soil Database from the Institute of Soil Science, Chinese Academy of Science.

Catchment delineations are only considered for land cover, soil type, and slope. The area of the northern part of Erhai lake catchment is around 1181 km^2, which means about 46% of the whole Erhai area (2,565 km^2 including lake area) is considered. Five types of land use are chosen, namely Forest land (FRST), grassland (RNGE), Agricultural land (AGRR), undetermined (URMD). Fig. 9-2a show the patterns of these land use types. Only two types of soil were considered in the catchment delineation. There is red soil for forest land and grass land and red-brown soil for crop land (Fig. 9-2b). Five slopes that were classified in the study are as shown in Fig. 9-2c. Most of forest land is located on slopes between 20-45% and most of the crop land is located on slopes between 0-10 %. There is around 689 km^2 (c. 58%) of forested land, 394 km^2 (c. 33%) for grassland, and 98 km^2 (c. 8.3%) for crop**.** Around 259.5 km^2 of crop land is present in the Erhai catchment. This means that the research area is approximately 37.8% of the total land in Erhai catchment.

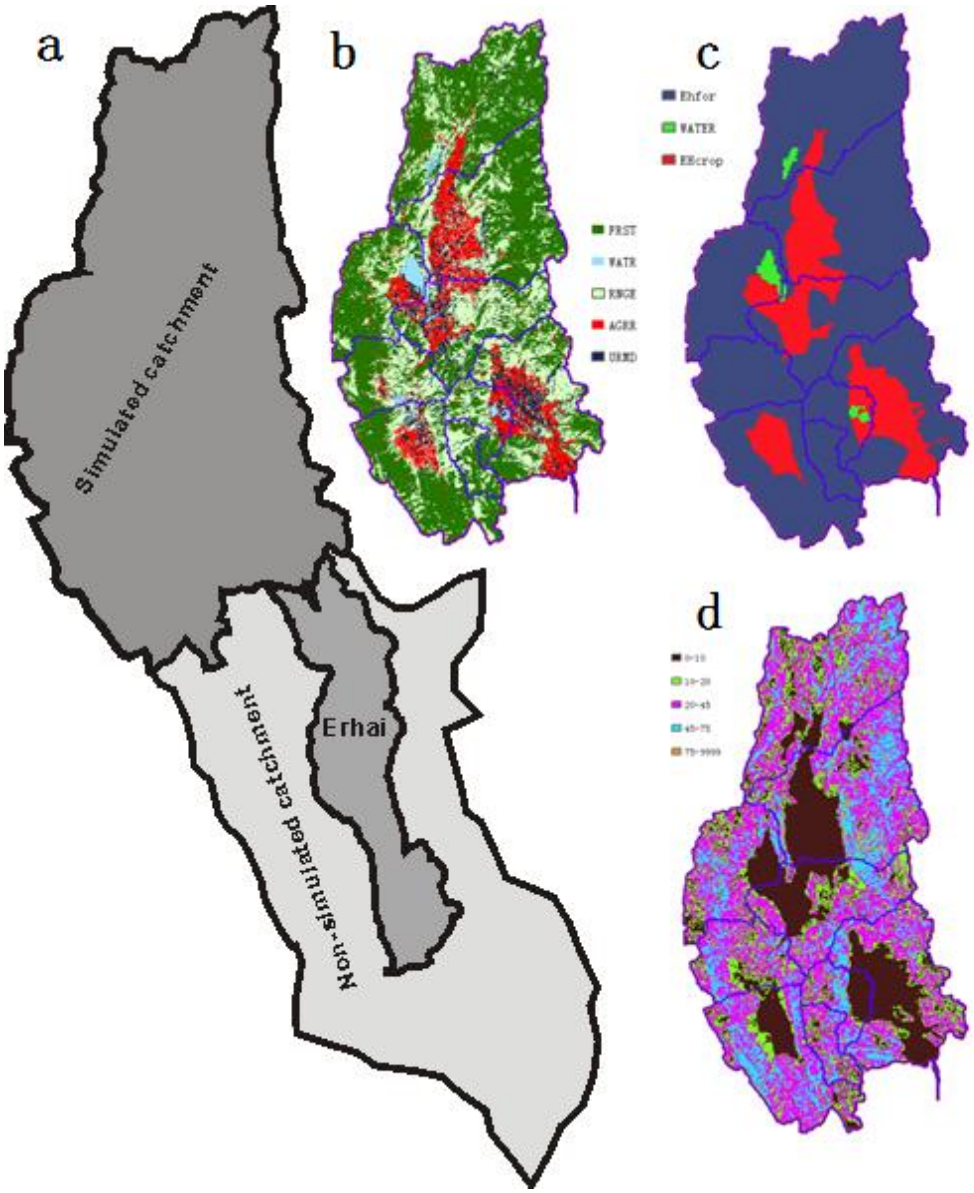

Figure 9-2 Northern Erhai Catchment delineation under ArcSWAT (from left to right: land cover, soil, and slope delineation). Subbasin 1 is selected as an example to test feasibility of STELLA model (a new diagram with whole catchment will replace this one)

The northern part of the catchment is divided into 86 HRUs, of which 18 HRUs are crop land. All HRUs for crop land are listed in Table 1. Most of agriculture are well organized and with straight row for paddy, soy bean, and tobacco. Therefore, in the model the crop lands are aligned in a straight row within the catchment, and experience good hydrological conditions. According to Soil Conservation Service (SCS) (SCS, 1972), the CN (curve number) value (an empirical parameter to predict runoff from rainfall) (Appendix III) is set as 89 for the initial simulation. A

single slope is assumed in each HRU, and the parameters for erosion estimates are also listed in Table 9-1.Another thing should be mentioned here is the influence of different types of crops to models exports. The type of crop lands should impact the phosphorus output, however, the crop types do not considered in this model. First, we need a simplest model, different types of crops will make the model input and mechanism dyanamics become two complex. Secondly, the results will finally compare with palaeolimnological results, which is annually in accuracy. The crops in Erhai catchment do not have obvious fluctuations in annual scale. Therefore, it is unnecessary to input different crops in the model.

Table 9-1 Parameters in STELLA model for crop land in the northern catchment (USLEK, USLEP, USLELS are the parameters for soil loss in Universal Soil Loss Equation (USLE) (Wischemier and Smith, 1978), which is detailed in Appendix III). Apart from CN values, other values were derived from the SWAT model.

Hru code	CN	Hru Area (km^2)	Slope	USLEK	USLEP	USLELS
1	89	33.9018	0.016	0.32	1	0.24
2	89	0.97	0.148	0.49	1	2.26
3	89	0.9047	0.585	0.49	1	11.21
4	89	1.7908	0.038	0.49	1	0.63
5	89	1.2312	0.302	0.49	1	4.03
6	89	15.4865	0.019	0.32	1	0.29
7	89	0.3758	0.576	0.49	1	10.97
8	89	0.4557	0.142	0.49	1	2.12
9	89	0.6076	0.296	0.49	1	3.9
10	89	0.9034	0.041	0.49	1	0.7
11	89	7.4794	0.024	0.32	1	0.35
12	89	0.4573	0.299	0.49	1	3.97
13	89	0.2763	0.147	0.49	1	2.24
14	89	0.1429	0.563	0.49	1	10.62
15	89	29.6177	0.019	0.32	1	0.29
16	89	0.8221	0.14	0.49	1	2.07

17	89	1.854	0.053	0.49	1	0.82
18	89	1.0932	0.303	0.49	1	4.05

9.4 Runoff and Erosion

9.4.1 Runoff

Runoff is initially simulated with CN as 89, which means assigned soil hydrological group is assumed to be D (highest runoff potential) (Radcliffe and Cabrera, 2007). The simulation results are shown in Fig. 9-3. The mean runoff is around 87 mm (Table 9-2), and it is concentrated in summer. The comparison between runoff and rainfall (Fig. 9-3) shows high correlation (R^2=0.99, p<0.001) within expectation. Runoff may be influenced by CN, and so a sensitivity analysis related to CN is performed (Table 9-2). The results show that runoff is insensitive to CN values. Therefore, a CN value of 89 is used for subsequent simulations, as the soil in the catchment is clay-dominated (Soil dataset of Nanjing soil institute, Chinese Academy of Science) and it is in accordance with the description of soil group D (SCS, 1972) (SCS. 1972. Hydrology, Section 4: National Engineering Handbook, U.S. Soil Conservation Service, Washington, D.C., Government Printing Office.)

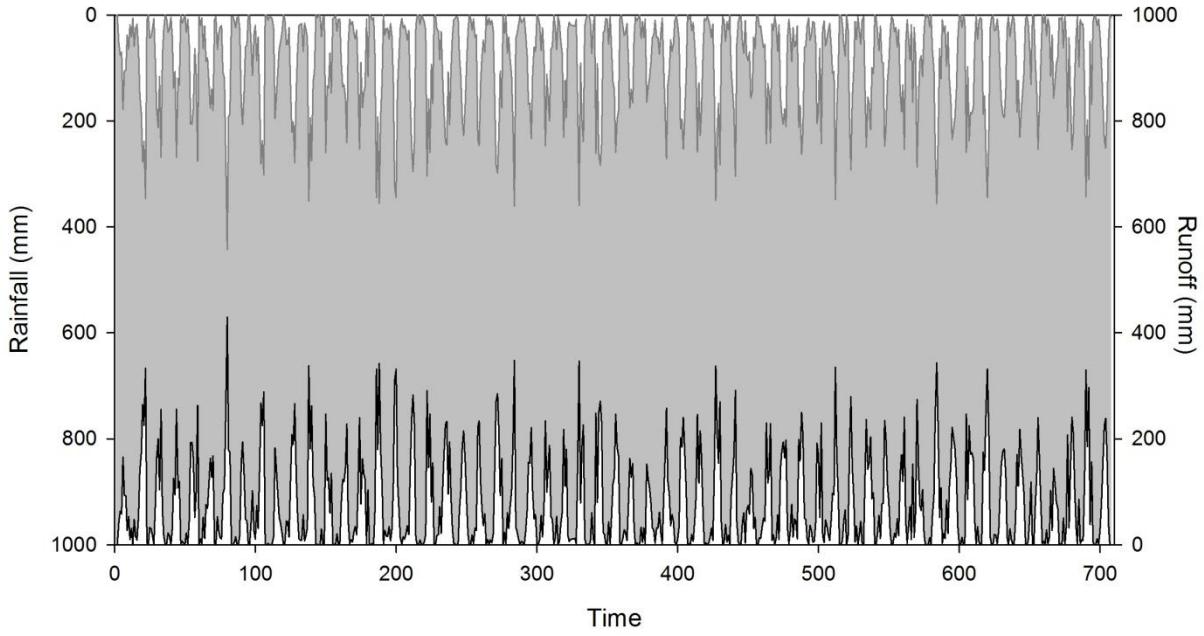

Figure 9-3 Comparison of rainfall and runoff in the model under CN=89. It shows

that runoff is highly correlated with rainfall (The curve in the upper of diagram is rainfall, and the curve in the bottom of diagram is runoff).

Table 9-2 Runoff curve numbers for hydrological soil-cover complexes (which indicates that runoff in this model is not sensitive to CN)

Land Use	Condition	Hydrologic Soil Group	CN	Mean	Standard Deviation	Range
Row crops	Straight row	A	67	88.5	90.10	0-442.09
		B	78	88.1	90.06	0-441.64
		C	85	87.6	89.98	0-441
		D	89	87.0	89.88	0-440.28

River systems are not considered in the model. Therefore, it does not simulate the basin's water storage capacity. Instead, a peak runoff rate is simulated for each sub-basin's water storage capacity. This is in part because we have monitored discharge values from Erhai lake which can be used to calibrate and validate the model. Fig. 9-4 shows them together. The modelling discharge data are consistent with monitored data between 01-1952 and 12-1974. Both are affected by rainfall so their trends correlate well, but their magnitudes vary considerably. The monthly average monitored discharge was approximately 38.4 m^3/s, which is 9.1 times larger than the modelling discharge (4.2 m^3/s). There are a number of reasons for the discrepancy: First, the area of Erhai catchment is around 2,565 km^2, but only around 98 km^2 was considered in the model. Second, water cycles are not considered in the model, and water might be lost through the river network system. Therefore, the monitored discharge is employed to calibrate the modelling discharges. The modelling results were multiplied by a coefficient, α, was multiplied with the modelling results. The value of α is 0.34 according to proportion of the simulation area and the whole lake catchment.

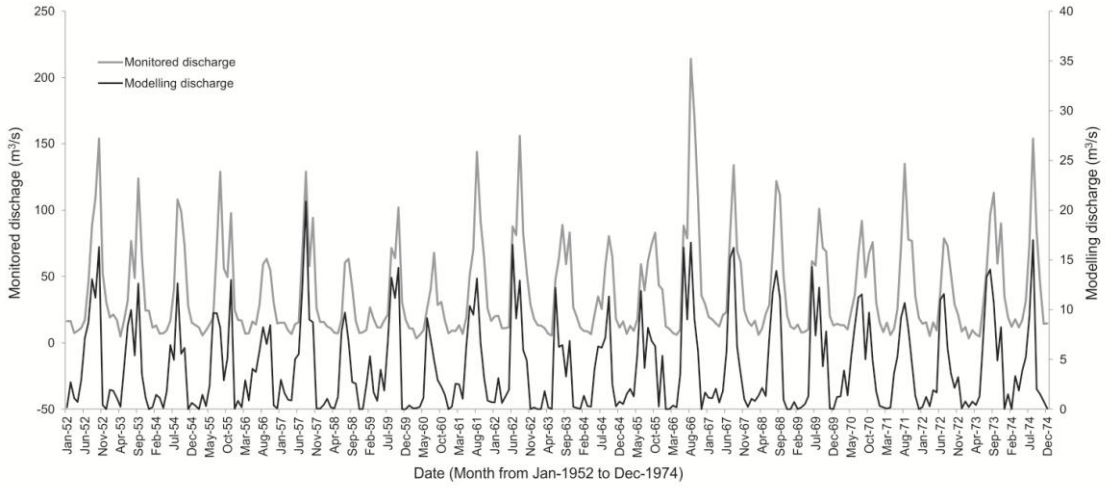

Figure 9-4 Modelling discharge (black curve) and monitoring discharge (grey curve) in Erhai lake (From Jan-1952 to Dec-1974). Monitored discharge was taken from the whole lake on a monthly basis. The modelling discharge is from the STELLA model.

The simulated water discharge in the period 1951-2009 after calibration is shown in Fig. 9-5. The monthly averaged water discharge was approximately 4.3 m^3/s. The moving average shows that the discharge from the northern catchment is highly related to precipitation, and has been steady over the past 60years.

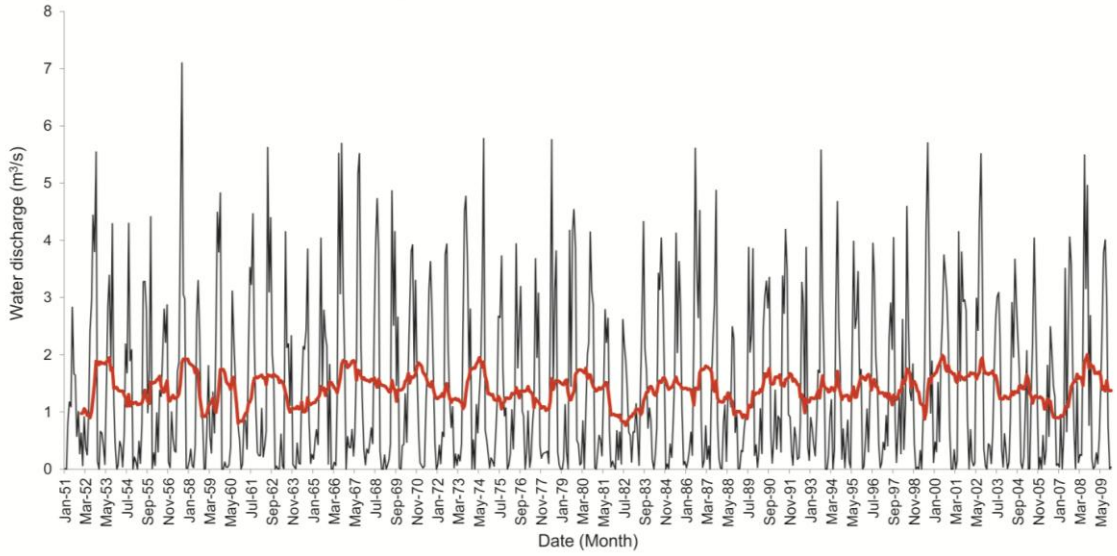

Figure 9-5 Water discharge modelling from STELLA Erhai model from 1951 to 2009. The model results were calibrated with monitored data. The red line is a moving average based on 12 month subsections.

9.4.2 Soil Erosion

Data for crop land erosion during the studied period are not available. Therefore it is impossible to validate the modelling results with continuous monitoring results. However, we collected experimental soil erosion in Eryuan county in 1999 (He et al., 2010), which indicates that the amount of soil erosion is around 95.1 t/ha per month during the period of June-September. This value will be used to calibrate the simulated values of summer soil erosion, i.e. the highest simulated results. In our model, sediment yield is calculated through the empirical equation of Theurer and Clarke (1991) as follows:

$$S_y = 0.22 * Q^{\beta} {Q_p}^{0.95} * KLSCP$$

Where, Sy is the sediment yield (t/ha). β=0.68 in Theurer and Clarke's empirical equation, but here it is employed to calibrate modelling results. P, K, LS were from the SWAT model (Table 9-1). C (cover management) is set to 1 for the value of soil erosion modelled during 2009. The calibrated results show that β=1.35 simulates the soil erosion that matches empirical data. The calibrated sediment yield is also showed in Fig. 9-6.

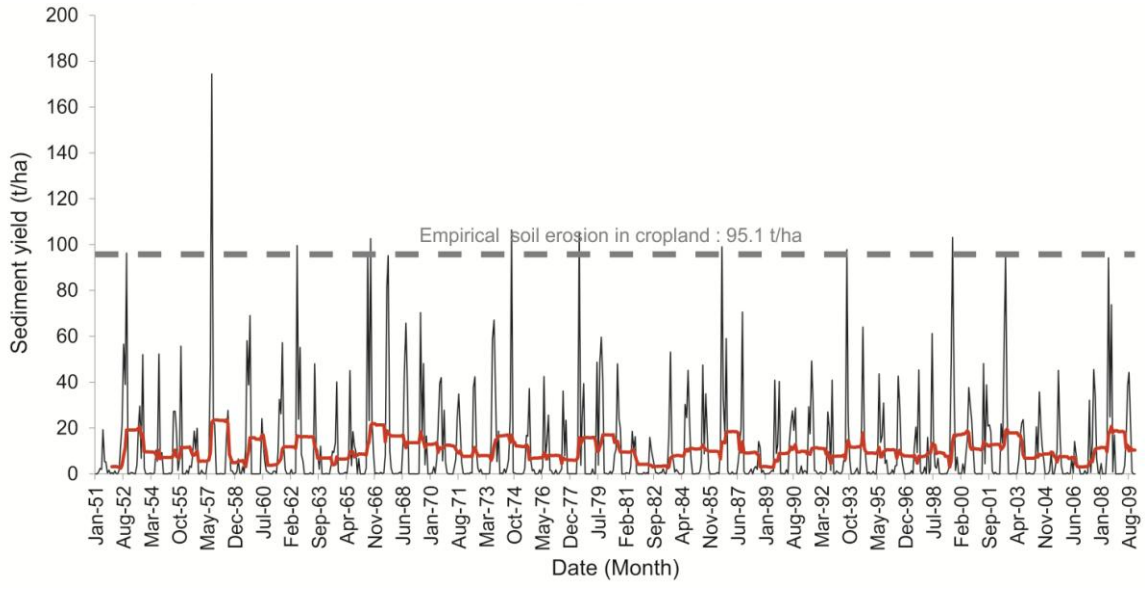

Figure 9-6 Sediment yield (t/ha) in the northern part of the catchment. The dashed line is the empirical soil erosion in cropland from Eryuan county in 1999 (He Shou-jia, 2010).

However, soil erosion is greatly affected by the intensification of human activities,

especially population size increases and the gradual increase in cropland during the study period. Therefore, human activities should be considered alongside soil erosion as a factor. The changes in agricultural practice are likely to have affected soil erosion in the catchment. Ideally, a model should include the details of these changes. However, the model in this thesis is simple, and it cannot represent all aspects phosphorus erosion from the catchment. Only those processes most critical to the aim of modelling the key trend in lake dynamics are included. Furthermore, the changes in agricultural practice may be non-linearly related to the soil erosion or phosphorus erosion, but there are no data to show to which degree this is the case. Therefore, only population size is considered here and is used to define the catchment management (C) coefficient for the catchment soil erosion. Population size at 2009 is set as 1 which is set as C value for 2009; other C values are normalised with the population size divided by population size in 2009. The soil erosion as well as C values are shown in Fig. 9-7.

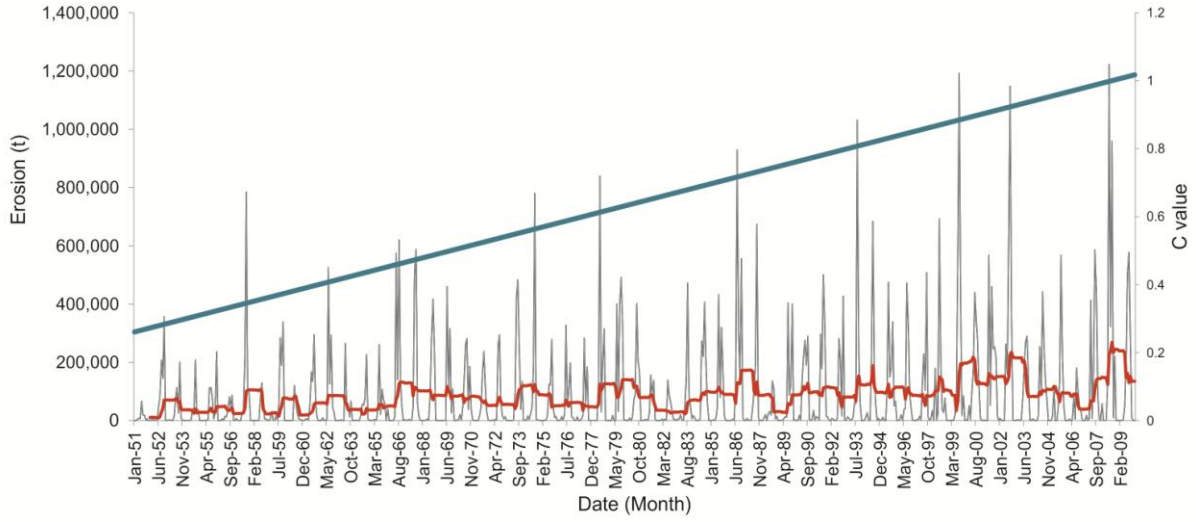

Figure 9-7 Soil erosion from modelling. The grey line is the soil erosion in each month from Jan-1951 to Dec-2009. Red line is 12 months moving average soil erosion. C value of management factor is also showed as blue line.

9.5 Phosphorus erosion from Northern Erhai catchment

Biological phosphorus from cropland in the northern Erhai catchment is shown in Fig. 9-8. P erosion during the summer is much higher, and is around 1,500 t per month for the whole of the simulated catchment. The value is quite low in winter (less than 100 t per month). The reason is due to high rainfall and high

temperatures in the summer. The patterns of phosphorus erosion are linearly related to rainfall in the catchment (Fig. 9-8, left small figure). The relationship between rainfall and phosphorus erosion is not a very strong linear relationship. The main reason could be due to the temperature. Temperature has a positive effect on phosphorus erosion when it is high (Fig. 9-8, right small figure). The linear regression in the figure showed that phosphorus erosion has risen over the past 60years.

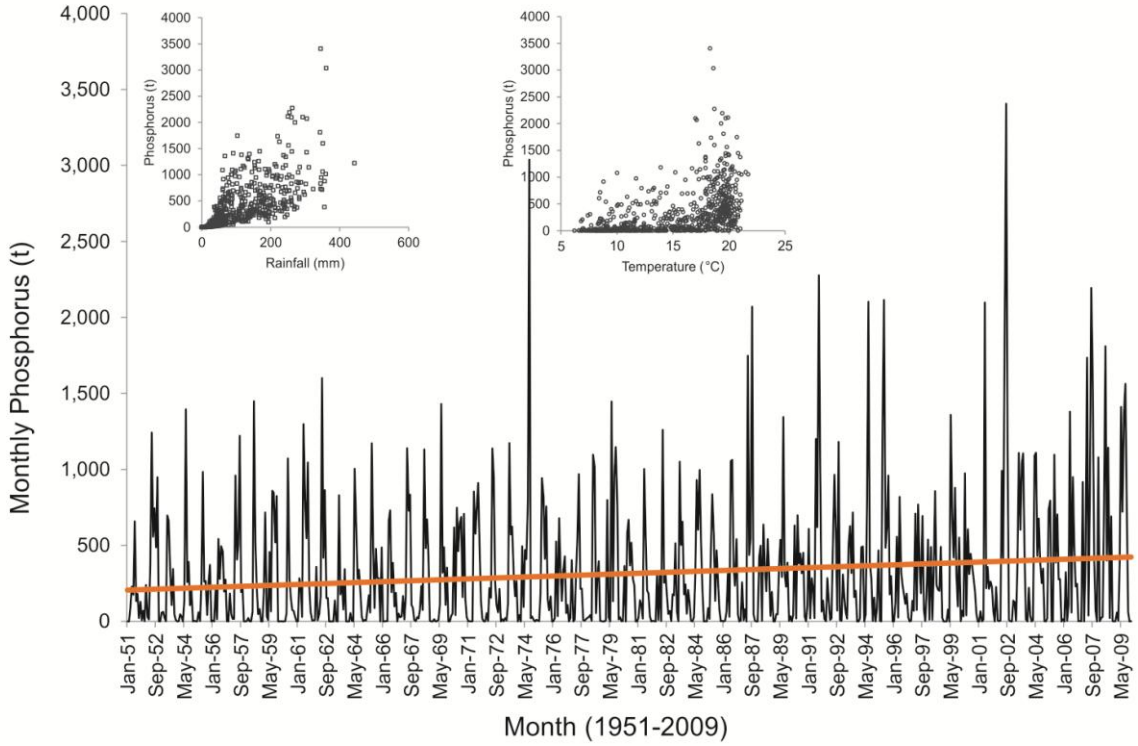

Figure 9-8 Monthly phosphorus erosion from North Erhai lake catchment. The black curve shows monthly phosphorus erosion in the simulated catchment, and the yellow line shows the linear increase of phosphorus erosion. This figure also plotted the modelling phosphorus against rainfall and temperature (inset). The left inset diagram plots phosphorus erosion against rainfall, and the right inset diagram plots phosphorus erosion against temperature. The small diagrams show that the phosphorus erosion in the catchment is much more strongly related to rainfall in the catchment and may be disproportionately affected by high temperature.

In this model soil fertilization and human activities are assumed to increase linearly from the start of the simulation. However, the results actually indicate a

non-linear, periodic change at annual timescales. Therefore, in subsequent modelling, average monthly phosphorus levels at annual intervals are used. Fig. 9-9 shows average monthly phosphorus erosion during the last 60years. Average monthly rainfall is also plotted in Fig. 9-9 to show the possible impacts from rainfall. At this scale, there is only a very low correlation between rainfall and phosphorus erosion. Linear regression shows that phosphorus erosion has increased over the studied period with substantial variability in the phosphorus series. These data are employed as phosphorus inputs to P dynamic model in the lake.

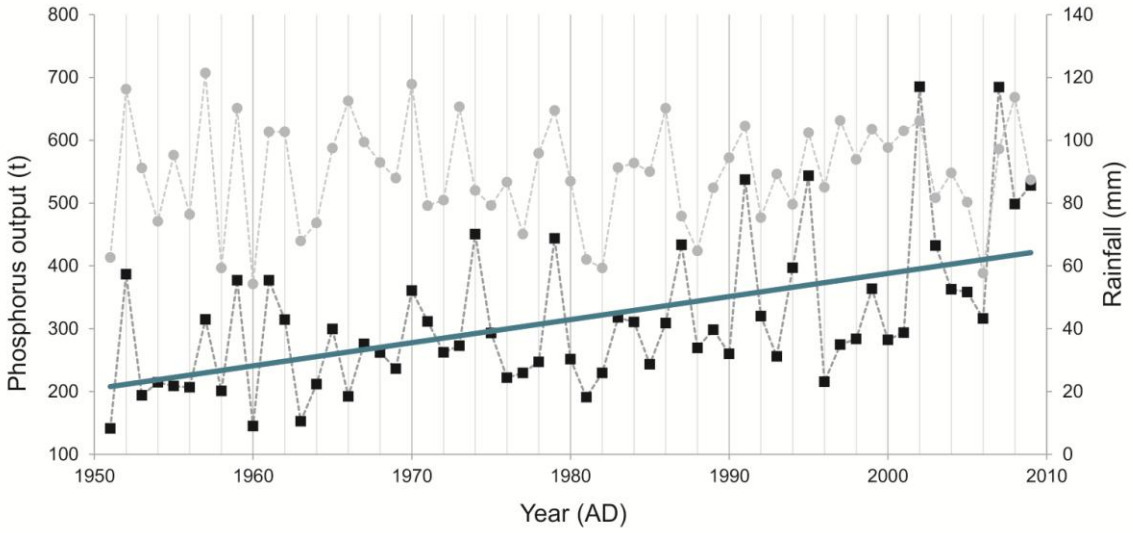

Figure 9-9 Yearly phosphorus erosion from North Erhai lake catchment (black squares are monthly average P output; the blue line is linear regression of P output which indicates the increasing trends of P erosion from catchment during the last 60years; grey circles are monthly rainfall values in the Erhai area calculated for each year)

9.6 Phosphorus dynamics in the lake

Phosphorus erosion from the catchment does not equate to biologically available phosphorus in the lake (Carpenter et al., 1998b). Algal blooming in the lake is not only affected by phosphorus from the catchment, but also by the effects of phosphorus recycling from lake sediment (Carpenter, 2003; Carpenter, 2005). A simple model (Appendix III) shows the dynamic system for eutrophication (Carpenter et al., 1999b; Scheffer et al., 2001). Detailed parameters can be found

from Appendix III. Here, phosphorus inputs use simulated average annual phosphorus from the above model. This model is dimensionless, so the P inputs are normalized to 0-1. All other parameters and their significance are shown in Appendix III. The results are shown in Fig. 9-10.

Before 1974, the data for P (lake) lie below ~0.5 suggesting a steady state (i.e. 1). The model begins to show clusters of data points with values >1 from 1974, suggesting that an alternate state (2) was developing. Between 1974 and 2002, the system periodically shifted from state1 and state 2, where high values in state 2 were always followed by a return to low values in state 1. In other words, the system would recover when the input P (catchment) level was suitably reduced. Then, after 2002, the system permanently shifted to state 2. The F statistic (Fig. 9-11) provides strong statistical evidence of a regime shift (Andersen et al., 2009). Although P (catchment) at around 2006 was lower than many phosphorus values in state 1, the system state was still at state 2 (as the dash line shown in Fig. 9-10), critical evidence that there is hysteresis between the lake's states and phosphorus reduction. To further confirm this hypothesis, a phase diagram between P (catchment) and P (lake) is plotted in Fig. 9-12.

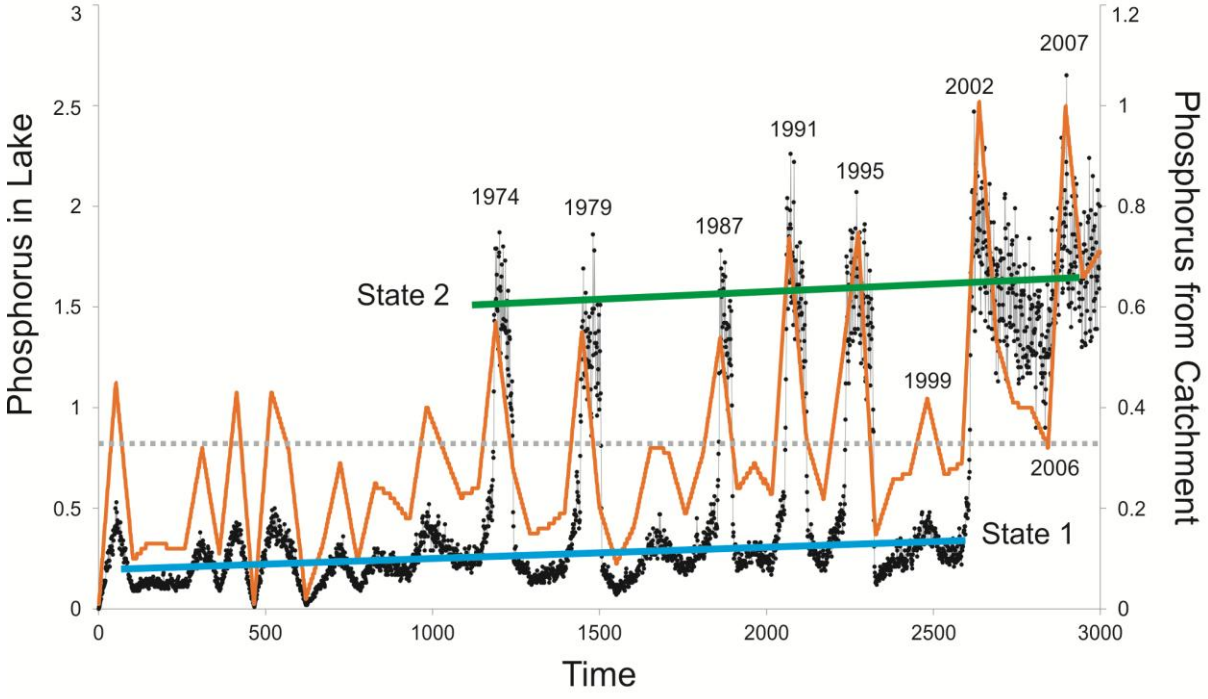

Figure 9-10 Multi-states in the modelling system (the yellow curve is the simulated Catchment P; black dots with a grey line show simulated phosphorus in the lake).

Two lake states (the blue line is state 1 and the green line is state 2) are clearly distinguished after 2002 based on the F statistic curve in Fig. 9-11; The dotted horizon line shows that catchment P values at 2006 were lower than the values at around 1999 and even lower than some peaks pre-1974).

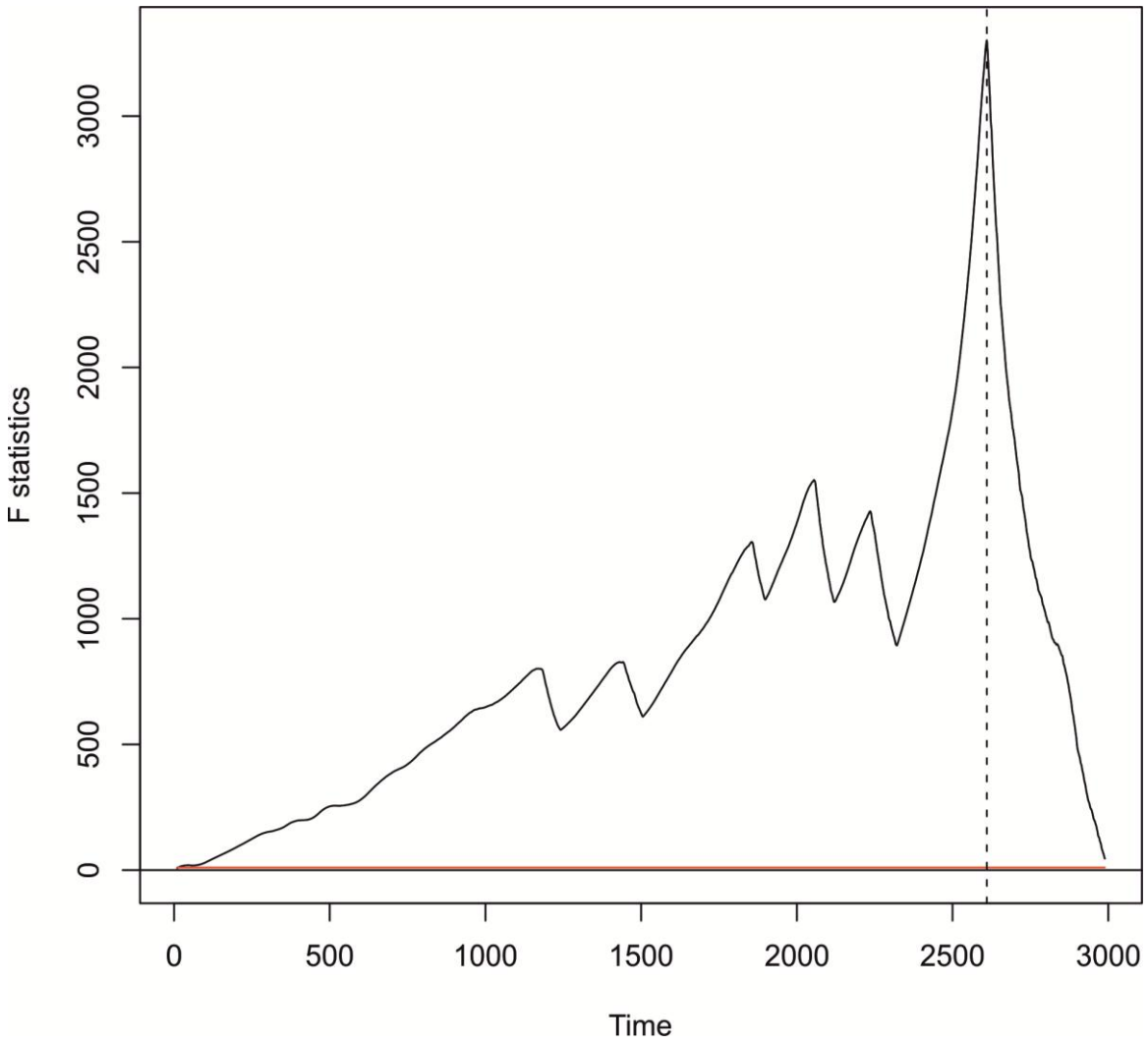

Figure 9-11 F statistic from P in lake showed that the threshold was crossed at the simulation time around 2600 (Dash vertical line threshold crossed in the system; red line showed level of p value at 0.01, higher values p<0.01).

Fig. 9-12 describes a fold bifurcation in the modelling results. The system crossed the first fold point (F1) when the P (catchment) was ~0.6 with the system is in State 2 (Fig. 9-10) when the P (catchment)>0.6. Therefore, the system is in a bistable state between F1 and F2. We can conclude that the system was in a flickering state between P (catchment) 0.2-0.6. Fig. 9-12 implies that the system cannot recover permanently until the P (catchment) is reduced to beyond F2

where the P (catchment) is ~0.2. Such a low mean value was described in the model only before time 1200 (equivalent to the early 1970s), which means that modern P (catchment) inputs are~4 times higher than the safe phosphorus export from the catchment.

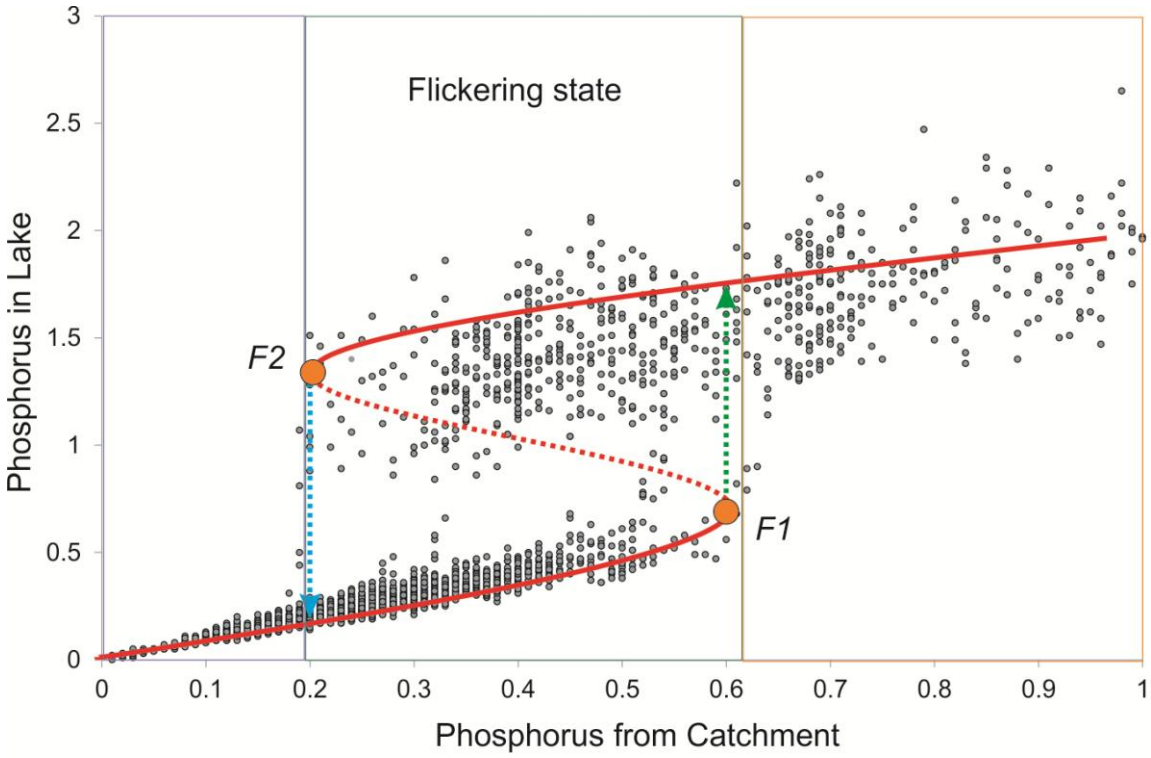

Figure 9-12 Plot of phosphorus from the catchment against phosphorus in lake showing fold bifurcations (red curve). The system enters an alternative state after phosphorus from the catchment reaches around 0.6 (fold bifurcation point F1). The phosphorus from catchment value should reduce to around 0.2 (fold bifurcation point F2) so that the system can recover back to previous state. The flickering state is between F2 and F1, i.e. the simulation time between 1100 and 2600.

9.7 Early warning signals for simulated critical transitions

The model suggests that the lake system was in a bimodal, flickering state between P (catchment) inputs of 0.2-0.6. Three potential warning indicators (i.e. variance, autocorrelation, skewness) are shown in Fig. 9-13. Fig. 9-13b shows that the residuals increased before the lake's switch to an alternative state. SD

was increasing in flickering state (Fig. 9-13c). Therefore, rising variance can be considered as a warning indicator. However, skewness and autocorrelation do not show rising signals as expected for CSD (Guttal and Jayaprakash, 2008; Scheffer et al., 2009). This indicates that rising variance can precede catastrophic transitions due to flickering in a system dominated by exogenous noise. In contrast, autocorrelation and skewness are not early indicators of the catastrophic transition in a flickering system. The model here showed the same conclusion as in Chapter 8, in which the conclusion was based on real data. Therefore, these results improve the robustness of the earlier conclusions. It can be concluded that rising variance is an effective indicator for warning of critical transitions, but that the trajectories of other possible indicators should be examined carefully before concluding about the presence of CSD. These conclusions also tend towards a rejection of critical slowing down before a catastrophic transition which shows flickering behaviour. In many real world situations, where exogenous impacts caused by human activities and climate events are common and even increasing, flickering maybe a more common phenomenon than critical slowing down. Therefore, early warning signals in the form of rising variance may be easier to detect and more common than previously thought.

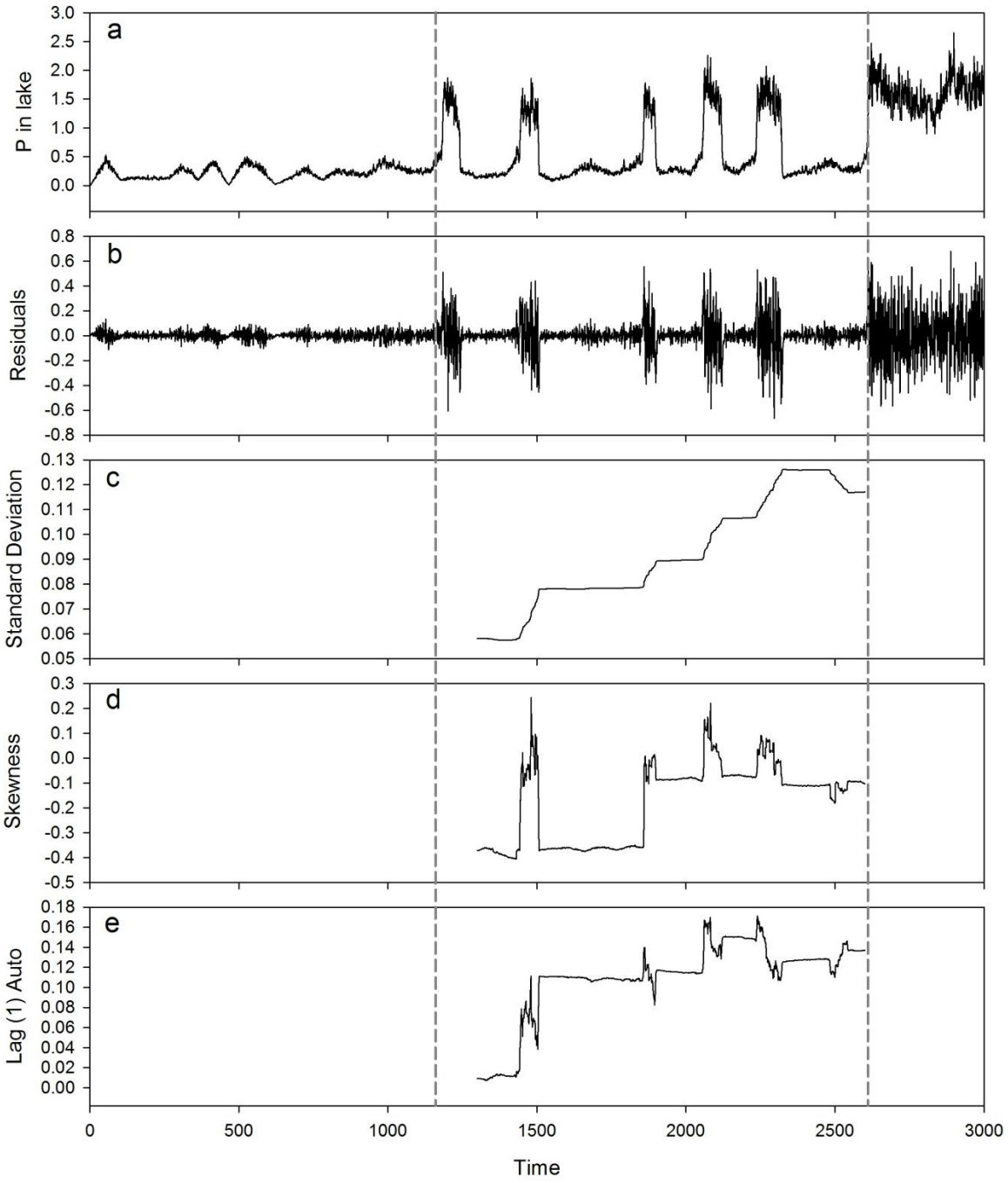

Figure 9-13 Early warning signals in modelling results (The analyses are the same as the EWS detection for diatom data in Chapter 8. a, P in lake from modelling which is driven by the simulated annual P from catchment; b, residuals from single exponential smoothing method; c, standard deviation based on half residuals pre-critical transition, in which is shown the rising variance as the system is in a flickering state; d, skewness calculated based on residuals; e, lag (1) autocorrelation calculated based on residuals)

9.8 Discussions and conclusions

All models employed in this study are very simple and represent an ideal rather than a real world system, for the following reasons:

1) Only cropland in the northern catchment is considered in the models; other types of land use are not considered. For instance, the forest cover in the Diancanshan Mountain was dramatically reduced during the 20th century. Deforestation should have a large impact on soil erosion, which could affect the phosphorus input to the lake. However, previous research suggests that the main phosphorus input is from crop land due to application of synthetic fertilizers (Chapter 3).

2) Many important components such as crop types, fishery, and water consumption are not considered in the model. Therefore, the simulated phosphorus did not reflect the real phosphorus erosion from the catchment nor the real phosphorus transformation in both crop land and lake. Little data can be used to calibrate or validate the simulated results. Nevertheless, limited calibration data has shown that the model is reliable (Fig. 9-4). The trend in the lake's phosphorus increase correlates with previous records (Fig. 9-9, meaning it should be reliable to use in models of the dynamics of Erhai lake system.

3) The important input parameters for the models, such as fertilizer and crop productions, are linearly interpolated throughout the whole study period. Monthly periodical change is ignored, such as changes in fertilization in different seasons. Likewise, no periodic cyclic parameters are considered in the phosphorus dynamicsof the lake, such as temperature, precipitation or macrophyte abundance. Lack of cyclic information is one of the weakest points for the models. Therefore, the models should be more reliable for annual scales rather than in monthly time intervals.

Although the model contains many uncertainties, it also contains the most of important components for the lake's eutrophication process. The model contains

the main phosphorus source (from cropland), phosphorus transport (through soil erosion), and the two most important environment variables for phosphorus input including temperature and precipitation. The phosphorus dynamic model in the lake incorporated the main features of a dynamic system (Scheffer et al., 2001).

The detection of warning signals based on modelling results strongly suggests that rising variance can be considered as a robust warning indicator for critical transitions. Rising variance can be caused by the accumulating effect from residual shocks according to CSD theory (Scheffer et al., 2009) and in that case the noise is internally generated by endogenic changes (Ditlevsen and Johnsen, 2010). In the Erhai model, noise mainly comes from external drivers (i.e. P from catchment). Therefore, rising variance is probably a result of continuous noise and weakened resilience (or attraction basin shrinking). Noise could amplify the deviation away from equilibrium when the system approaches a tipping point. The system might occasionally cross an unstable equilibrium state while in a bistable state (Fig. 8-7) and this phenomenon is known as flickering (Brock and Carpenter, 2010). Lag (1) autocorrelation did not show any increases, and bistability is obvious in the model (Fig. 9-12). Therefore, the rising variance is likely caused by the flickering state rather than CSD in systems with exogenous perturbations.

The same conclusion is obtained from real data in Chapter 8. Here, results from modelling also suggest that flickering precedes critical transitions. Simple models used in this thesis are designed to reflect a common feature for eutrophication, i.e. eutrophication resulting from non-point pollution from agriculture fertilization. Although the model cannot show a detailed eutrophication process in Erhai lake, it represents common features for this kind of complex dynamic system. Therefore, the results may not only be representative of the case of Erhai lake, but may be extrapolated more widely to other natural systems before crossing a threshold.

Chapter 10 Conclusions and Future studies

10.1 Conclusions

Combining landscape and ecological modelling with palaeoenvironmental proxies (Anderson et al., 2006) often uses palaeo-data as inputs to drive a model or to validate the simulated results. Here, we use the palaeolimnological proxy data to create hypotheses which can then be tested by modelling. For understanding the complexity of a system, palaeolimnology techniques have a distinct advantage because they can provide long term data (Dearing et al., 2010). Although a minimal mathematical model has always been considered a weak tool to fully understand a real system (Scheffer and Beets, 1994), the mutual authentication between palaeo- data and the minimal model, as shown in this study, provides a substantial improvement to the understanding of a real world, complex system.

The main conclusions are listed as follows:

1. The alternative stable states in the training set may affect the accuracy of diatom-based transfer functions. The reconstructions may have larger estimation errors in unstable sites. The idea of alternative stable states can also provide a good prospect for lake management as the lakes located between critical points may be easily shifted by small perturbations.
2. According to the comparison between fossil diatoms from Erhai Lake and diatoms in Yunnan training set, the lake's state was unstable between 1980 and 2001. The diatom *Fragiliaria crotonensis* dominated in the spring, and its high abundance could indicate algal blooming in the following summer and autumn. It can be used as an effective indicator to guide lake management. Meanwhile, the diatom-inferred TP is overestimated in Erhai lake, but the trends are similar to the instrumental TP during the recent two decades. The lake's reference TP value was around 11-12 µg/l.
3. The resilience of the lake's ecosystem is lost due to the intensification of land use and poor water management. The perturbations such as climate-induced low water level are also very important for the losses in resilience.
4. The main reason for the lake crossing the trophic boundary in around 2001

is the development of a new positive feedback system involving hypolimnetic anoxia and phosphorus release from the sediments. As the changes of the lake's resilience and feedback strengthened, the lake experienced different dynamical stages during the study period, culminating in a fold bifurcation and hysteresis loop between diatoms and lake nutrient status.

5. The lake is in a flickering state between 1980 and 2000 which can be demonstrated by a bimodal frequency distribution, short-lived algal blooming and changes in skewness. Rising variance in diatom communities could be considered as an indicator of EWS but it is most likely caused by flickering rather than CSD in this exogenous noise-induced situation. Meanwhile, it seems that decreases in autocorrelation are caused by the system becoming more asymmetric when the system is approaching a critical point in a flickering system.
6. The minimal model shows that the flickering states could be simulated, and the rising variance due to flickering can also predict the critical transitions in the system. The conclusions are robust and may be widely applied in other systems.

10.2 Future studies

Flickering shows potential as a good warning sign for the system within bistable states or an unstable state in the fold bifurcation dynamic system. Strong evidence shows bistability and hysteresis in the Erhai case, but fold bifurcation is not the only nonlinear change in the real world. The type of ecosystem dynamic is certain after the regime shift, but knowledge is still lacking about checking the types before tipping points, and effective warning indicators are still not available for other types of regime shifts.

The rising variance signals are in evidence in the case of regime shifts in Erhai Lake and the minimal model. The abrupt change is likely to correspond to rising variance when the system approaches a tipping point, but it is unlikely that rising variances will always precede critical transitions. The rising variance due to impending regime shifts is still difficult to distinguish from variance increasing

because of increasing perturbations (Carpenter and Brock, 2006). Therefore, it is assertive to consider all rising variance as EWS. In future, more studies should focus on finding the most robust way to show what kinds of rising variance could be used as warning signals.

1. Erhai Lake is a dynamic system with obvious alternative stable states and a very short transition period. Many systems, such as climate systems, may have much longer transition periods (like hundreds of years) so that the EWS in different time scales should be discussed in different complex systems.
2. The minimal model employed in this thesis simulated the P dynamic in the lake. It is actually the main driver for a lake's primary productions rather than the real indicator of its state. The feedbacks that control the availability of P for algae were not considered in the model. These key feedbacks should be considered in the model in the future.
3. Noise has different types in the real world, which may change the viability of EWS. Noise type 1 is 'white noise', which means the system contains random but equal mean power of perturbations. For instance, the noise from seasonal temperature and rainfall change could be considered as a type of this noise. However, some noise is amplified while processing due to gradually increasing variables, such as global warming. This will cause the noise type 2, which means the noise is continuously increasing, and it is liable to affect the pattern of EWS. Therefore, the various noise types should be considered in future studies of EWS.
4. EWS and flickering states in complex systems provide a method to evaluate the state of a system, so that it can be estimated whether or not a system is still in 'safe operating space'. Therefore, these conclusions could be applied in the studies of ecosystem services. In the future, more studies related to the way of using flickering signals and EWS in ecosystem service should be considered.

Reference

Abbaspour, K.C., Yang, J., Maximov, I., Siber, R., Bogner, K., Mieleitner, J., Zobrist, J., and Srinivasan, R., **2007**, Modelling hydrology and water quality in the pre-ailpine/alpine Thur watershed using SWAT. *Journal of Hydrology*, 333, 413-430.

Adler, S., Hubener, T., Dressler, M., Lotter, A.F., and Anderson, N.J., **2010**, A comparison of relative abundance versus class data in diatom-based quantitative reconstructions. *Journal of Environmental Management*, 91, 1380-1388.

Andersen, T., Carstensen, J., Hernandez-Garcia, E., and Duarte, C.M., **2009**, Ecological thresholds and regime shifts: approaches to identification. *Trends in Ecology & Evolution*, 24, 49-57.

Anderson, N.J., Bugmann, H., Dearing, J.A., and Gaillard, M.J., **2006**, Linking palaeoenvironmental data and models to understand the past and to predict the future. *Trends in Ecology & Evolution*, 21, 696-704.

Appleby, P.G., **2002**, Chronostratigraphic Techniques in Recent Sediments, *in* Last, W.M., and Smol, J.P., eds., Tracking Environmental Change Using Lake Sediments, Volume 1: *Developments in Paleoenvironmental Research*, Springer Netherlands, 171-203.

Arnold, J.G., Williams, J.R., Srinivasan, R., and King, K.W., **1996**, SWAT: Soil and Water Assessment Tool: 808 East Blackland Road Temple, TX 76502, *Soil and Water Research Laboratory*, 190.

Arquitt, S., and Johnstone, R., **2004**, A scoping and consensus building model of a toxic blue-green algae bloom. *System Dynamics Review*, 20, 179-198.

ASCE, **1996**, Hydrology handbook (2nd edition). ASCE Manuals and Reports on Engineering Practice No. 28.

Bailey, R.M., **2011**, Spatial and temporal signatures of fragility and threshold proximity in modelled semi-arid vegetation. *Proceedings of the Royal Society B-Biological Sciences*, 278, 1064-1071.

Bar-Yam, Y., **2003**, Dynamics of Complex Systems, *Westview Press*.

Barton, A.P., Fullen, M.A., Mitchell, D.J., Hocking, T.J., Liu, L.G., Bo, Z.W., Zheng, Y., and Xia, Z.Y., **2004**, Effects of soil conservation measures on erosion rates and crop productivity on subtropical Ultisols in Yunnan Province, China. *Agriculture Ecosystems & Environment*, 104, 343-357.

Battarbee, R.W., **1999**, The importance of palaeolimnology to lake restoration.

Hydrobiologia, 395, 149-159.

Battarbee, R.W., Anderson, N.J., Jeppesen, E., and Leavitt, P.R., **2005a**, Combining palaeolimnological and limnological approaches in assessing lake ecosystem response to nutrient reduction. *Freshwater Biology*, 50, 1772-1780.

Battarbee, R.W., Jones, V.J., Flower, R.J., Cameron, N.G., and Bennion, H., **2001**, Diatoms. Dordrecht ; Boston, *Kluwer Academic*, v.

Battarbee, R.W., Monteith, D.T., Juggins, S., Evans, C.D., Jenkins, A., and Simpson, G.L., **2005b**, Reconstructing pre-acidification pH for an acidified Scottish loch: A comparison of palaeolimnological and modelling approaches. *Environmental Pollution*, 137, 135-149.

Bayley, S.E., Creed, I.F., Sass, G.Z., and Wong, A.S., **2007**, Frequent regime shifts in trophic states in shallow lakes on the Boreal Plain: Alternative "unstable" states? *Limnology and Oceanography*, 52, 2002-2012.

Beaulac, M.N., and Reckhow, K.H., **1982**, An Examination of Land-Use - Nutrient Export Relationships. *Water Resources Bulletin*, 18, 1013-1024.

Beeton, A.M., **1965**, Eutrophication of the St. Lawrence Great Lakes. *Limnology and Oceanography*, 10, 240-254.

Beisner, B.E., Haydon, D.T., and Cuddington, K., **2003**, Alternative stable states in ecology. *Frontiers in Ecology and the Environment*, 1, 376-382.

Bennion, H., **1994**, A Diatom-Phosphorus Transfer-Function for Shallow, Eutrophic Ponds in Southeast England. *Hydrobiologia*, 275, 391-410.

Bennion, H., Appleby, P.G., and Phillips, G.L., **2001**, Reconstructing nutrient histories in the Norfolk Broads, UK: implications for the role of diatom-total phosphorus transfer functions in shallow lake management. *Journal of Paleolimnology*, 26, 181-204.

Bennion, H., Fluin, J., and Simpson, G.L., **2004**, Assessing eutrophication and reference conditions for Scottish freshwater lochs using subfossil diatoms. *Journal of Applied Ecology*, 41, 124-138.

Bennion, H., Johnes, P., Ferrier, R., Phillips, G., and Haworth, E., **2005**, A comparison of diatom phosphorus transfer functions and export coefficient models as tools for reconstructing lake nutrient histories. *Freshwater Biology*, 50, 1651-1670.

Bennion, H., Juggins, S., and Anderson, N.J., **1996**, Predicting epilimnetic phosphorus concentrations using an improved diatom-based transfer function and its application to lake eutrophication management. *Environmental Science & Technology*, 30, 2004-2007.

Biggs, R., Carpenter, S.R., and Brock, W.A., **2009**, Turning back from the brink:

Detecting an impending regime shift in time to avert it. *Proceedings of the National Academy of Sciences of the United States of America*, 106, 826-831.

Bigler, C., von Gunten, L., Lotter, A.F., Hausmann, S., Blass, A., Ohlendorf, C., and Sturm, M., **2007**, Quantifying human-induced eutrophication in Swiss mountain lakes since AD 1800 using diatoms. *Holocene*, 17, 1141-1154.

Bingner, R.L., Theurer, F.D., and Yuan, Y., **2009**, AnnAGNPS Technical Processes, Available at ftp://199.133.90.201/pub/outgoing/AGNPS/AGNPS_Web_Files/pdf_files/AnnAGNPS_Technical_Documentation.pdf.

Birks, H.H., and Birks, H.J.B., **2006**, Multi-proxy studies in palaeolimnology. *Vegetation History and Archaeobotany*, 15, 235-251.

Birks, H.J.B., **1998**, D.G. Frey & E.S. Deevey review #1 - Numerical tools in palaeolimnology - Progress, potentialities, and problems. *Journal of Paleolimnology*, 20, 307-332.

Birks, H.J.B., Heiri, O., Seppä, H., and Bjune, A.E., **2010**, Strengths and Weaknesses of Quantitative Climate Reconstructions Based on Late-Quaternary Biological Proxies. *The Open Ecology Journal*, 3, 68-110.

Birks, H.J.B., Line, J.M., Juggins, S., Stevenson, A.C., and Terbraak, C.J.F., **1990**, Diatoms and pH Reconstruction. *Philosophical Transactions of the Royal Society B-Biological Sciences*, 327, 263-278.

Blackmarr, W.A., **1995**, Documentation of Hydrologic, Geomorphic, and Sediment Transport Measurements on the Goodwin Creek Experimental Watershed, Northern Mississippi, for the Period 1982-1993, Preliminary Release. Channel and Watershed Processes Research Unit of the National Sedimentation Laboratory at Oxford, Mississippi, Research Report No. 3.

Boyle, J.F., **2007a**, Loss of apatite caused irreversible early-Holocene lake acidification. *Holocene*, 17, 543-547.

Boyle, J.F., **2007b**, Simulating loss of primary silicate minerals from soil due to long-term weathering using Allogen: Comparison with soil chronosequence, lake sediment and river solute flux data. *Geomorphology*, 83, 121-135.

Braak, C.J.F., and Looman, C.W.N., **1986**, Weighted averaging, logistic regression and the Gaussian response model. *Plant Ecology*, 65, 3-11.

Brock, W.A., and Carpenter, S.R., **2006**, Variance as a leading indicator of regime shift in ecosystem services. *Ecology and Society*, 11, -.

Brock, W.A., and Carpenter, S.R., **2010**, Interacting regime shifts in ecosystems: implication for early warnings. *Ecological Monographs*, 80, 353-367.

Carvalho, L., Miller, C., Spears, B.M., Gunn, I.D.M, Bennion, H., Kirika, A., May, L.,

2012, Water quality of Loch Leven: responses to enrichment,restoration and climate change. *Hydrobiologia*, 681, 35–47.

Carpenter, S., **1981**, Submersed Vegetation: An Internal Factor in Lake Ecosystem Succession. *The American Naturalist*, 118(3), 372-383.

Carpenter, S., Brock, W., and Hanson, P., **1999a**, Ecological and Social Dynamics in Simple Models of Ecosystem Management.

Carpenter, S.R., **2003**, Regime shifts in lake ecosystems : pattern and variation. Oldendorf/Luhe, Germany, *Ecology Institute*, xxviii, 199 p.

Carpenter, S.R., **2005**, Eutrophication of aquatic ecosystems: Bistability and soil phosphorus. *Proceedings of the National Academy of Sciences of the United States of America*, 102, 10002-10005.

Carpenter, S.R., Bolgrien, D., Lathrop, R.C., Stow, C.A., Reed, T., and Wilson, M.A., **1998a**, Ecological and economic analysis of lake eutrophication by nonpoint pollution. *Australian Journal of Ecology*, 23, 68-79.

Carpenter, S.R., and Brock, W.A., **2006**, Rising variance: a leading indicator of ecological transition. *Ecology Letters*, 9, 311-318.

Carpenter, S.R., Caraco, N.F., Correll, D.L., Howarth, R.W., Sharpley, A.N., and Smith, V.H., **1998b**, Nonpoint pollution of surface waters with phosphorus and nitrogen. *Ecological Applications*, 8, 559-568.

Carpenter, S.R., Cole, J.J., Pace, M.L., Batt, R., Brock, W.A., Cline, T., Coloso, J., Hodgson, J.R., Kitchell, J.F., Seekell, D.A., Smith, L., and Weidel, B., **2011**, Early Warnings of Regime Shifts: A Whole-Ecosystem Experiment. *Science*, 332, 1079-1082.

Carpenter, S.R., Kitchell, J.F., and Hodgson, J.R., **1985**, Cascading Trophic Interactions and Lake Productivity. *Bioscience*, 35, 634-639.

Carpenter, S.R., Ludwig, D., and Brock, W.A., **1999b**, Management of eutrophication for lakes subject to potentially irreversible change. *Ecological Applications*, 9, 751-771.

Carpenter, S.R., Mooney, H.A., Agard, J., Capistrano, D., DeFries, R.S., Diaz, S., Dietz, T., Duraiappah, A.K., Oteng-Yeboah, A., Pereira, H.M., Perrings, C., Reid, W.V., Sarukhan, J., Scholes, R.J., and Whyte, A., **2009**, Science for managing ecosystem services: Beyond the Millennium Ecosystem Assessment. *Proceedings of the National Academy of Sciences of the United States of America*, 106, 1305-1312.

Chen, J., and Xie, M., **2008**, The Analysis of regional Climate Change Features over Yunnan in Recent 50 Years. *Progress in Geography*, 27, 19-26.

Chisholm, R.A., and Filotas, E., **2009**, Critical slowing down as an indicator of transitions in two-species models. *Journal of Theoretical Biology*, 257,

142-149.

Cosby, B.J., Ferrier, R.C., Jenkins, A., and Wright, R.F., **2001**, Modelling the effects of acid deposition: refinements, adjustments and inclusion of nitrogen dynamics in the MAGIC model. *Hydrology and Earth System Sciences*, 5, 499-517.

Cosby, B.J., Wright, R.F., and Gjessing, E., **1995**, An Acidification Model (Magic) with Organic-Acids Evaluated Using Whole-Catchment Manipulations in Norway. *Journal of Hydrology*, 170, 101-122.

Coulthard, T.J., Macklin, M.G., and Kirkby, M.J., **2002**, A cellular model of Holocene upland river basin and alluvial fan evolution. *Earth Surface Processes and Landforms*, 27, 269-288.

Coulthard, T.J., and Van De Wiel, M.J., **2006**, A cellular model of river meandering. *Earth Surface Processes and Landforms*, 31, 123-132.

Dakos, V., Scheffer, M., van Nes, E.H., Brovkin, V., Petoukhov, V., and Held, H., **2008**, Slowing down as an early warning signal for abrupt climate change. *Proceedings of the National Academy of Sciences of the United States of America*, 105, 14308-14312.

Daniel, T.C., Sharpley, A.N., and Lemunyon, J.L., **1998**, Agricultural phosphorus and eutrophication: A symposium overview. *Journal of Environmental Quality*, 27, 251-257.

Dearing, J.A., **2008**, Landscape change and resilience theory: a palaeoenvironmental assessment from Yunnan, SW China. *Holocene*, 18, 117-127.

Dearing, J.A., Braimoh, A.K., Reenberg, A., Turner, B.L., and van der Leeuw, S., **2010**, Complex Land Systems: the Need for Long Time Perspectives to Assess their Future. *Ecology and Society*, 15, 21.

Dearing, J.A., Dann, R.J.L., Hay, K., Lees, J.A., Loveland, P.J., Maher, B.A., and OGrady, K., **1996**, Frequency-dependent susceptibility measurements of environmental materials. *Geophysical Journal International*, 124, 228-240.

Dearing, J.A., Jones, R.T., Shen, J., Yang, X., Boyle, J.F., Foster, G.C., Crook, D.S., and Elvin, M.J.D., **2008**, Using multiple archives to understand past and present climate-human-environment interactions: the lake Erhai catchment, Yunnan Province, China. *Journal of Paleolimnology*, 40, 3-31.

Di Toro, D.M., Fitzpatrick, J.J., Thomann, R.V., and Hydroscience, I., **1983**, Documentation For Water Quality Analysis Simulation Program (WASP) And Model Verification Program (MVP).

Dillon, P.J., and Kirchner, W.B., **1975**, The effects of geology and land use on the export of phosphorus from watersheds. *Water Research*, 9, 135-148.

Ditlevsen, P.D., and Johnsen, S.J., **2010**, Tipping points: Early warning and wishful thinking. *Geophysical Research Letters*, 37, -.

Ditoro, D.M., **1984**, Probability Model of Stream Quality Due to Runoff. *Journal of Environmental Engineering-Asce*, 110, 607-628.

Dobson, A., Lodge, D., Alder, J., Cumming, G.S., Keymer, J., McGlade, J., Mooney, H., Rusak, J.A., Sala, O., Wolters, V., Wall, D., Winfree, R., and Xenopoulos, M.A., **2006**, Habitat loss, trophic collapse, and the decline of ecosystem services. *Ecology*, 87, 1915-1924.

Dodds, W.K., Bouska, W.W., Eitzmann, J.L., **2009**, Eutrophication of U.S. freshwater: analysis of potential economic damages. *Environmental Science & Technology*, 43, 12-19.

Dong X.H., Bennion H., Battarbee R.W., Sayer C.D., **2012**, A multiproxy palaeolimnological study of climate and nutrient impacts on Esthwaite Water, England over the past 1200 years. *The Holocene*, 22(1), 107–118.

Drake, J.M., and Griffen, B.D., **2010**, Early warning signals of extinction in deteriorating environments. *Nature*, 467, 456-459.

Du, B., and Li, Y., **2001**, Danger Risk to Fish Diversity in Erhai Lake and Proposals to Dispel it. *Research of Environmental Sciences*, 14, 42-45.

Elvin, M., **2002**, The impact of clearance and irrigation on the environment in the Lake Erhai catchment from the ninth to the nineteenth century. *East Asian Hist (Canberra)*, 1-60.

Engel, B.A., Srinivasan, R., Arnold, J., Rewerts, C., and Brown, S.J., **1993**, Nonpoint-Source (Nps) Pollution Modeling Using Models Integrated with Geographic Information-Systems (Gis). *Water Science and Technology*, 28, 685-690.

Engstrom, D.R., Swain, E.B, **1986**,The chemistry of lakesediments in time and space. *Hydrobiologia,* 143, 37-44.

Flower, R.J., **1993**, Diatom Preservation - Experiments and Observations on Dissolution and Breakage in Modern and Fossil Material. *Hydrobiologia*, 269, 473-484.

Flower, R.J., Juggins, S., and Battarbee, R.W., **1997**, Matching diatom assemblages in take sediment cores and modern surface sediment samples: The implications for lake conservation and restoration with special reference to acidified systems. *Hydrobiologia*, 344, 27-40.

Flower, R.J., and Ryves, D.B., **2009**, Diatom preservation: differential preservation of sedimentary diatoms in two saline lakes. *Acta Botanica Croatica*, 68, 381-399.

Folke, C., Carpenter, S., Walker, B., Scheffer, M., Elmqvist, T., Gunderson, L., and

Holling, C.S., **2004**, Regime shifts, resilience, and biodiversity in ecosystem management. *Annual Review of Ecology Evolution and Systematics*, 35, 557-581.

Fritz, S.C., Juggins, S., Battarbee, R.W., and Engstrom, D.R., **1991**, Reconstruction of Past Changes in Salinity and Climate Using a Diatom-Based Transfer-Function. *Nature*, 352, 706-708.

Galman, V., Rydberg, J., de-Luna, S.S., Bindler, R., and Renberg, I., **2008**, Carbon and nitrogen loss rates during aging of lake sediment: Changes over 27 years studied in varved lake sediment. *Limnology and Oceanography*, 53, 1076-1082.

Gasse, F., Juggins, S., and Khelifa, L.B., **1995**, Diatom-Based Transfer-Functions for Inferring Past Hydrochemical Characteristics of African Lakes. *Palaeogeography Palaeoclimatology Palaeoecology*, 117, 31-54.

Genkai-Kato, M., and Carpenter, S.R., **2005**, Eutrophication due to phosphorus recycling in relation to lake morphometry, temperature, and macrophytes. *Ecology*, 86, 210-219.

Gibbs-Eggar, Z., Jude, B., Dominik, J., Loizeau, J.L., and Oldfield, F., **1999**, Possible evidence for dissimilatory bacterial magnetite dominating the magnetic properties of recent lake sediments. *Earth and Planetary Science Letters*, 168, 1-6.

Grasso, M., **1998**, Ecological–economic model for optimal mangrove trade off between forestry and fishery production: comparing a dynamic optimization and a simulation model. *Ecological Modelling*, 112, 131-150.

Gunderson, L.H., **2000**, Ecological resilience - in theory and application. *Annual Review of Ecology and Systematics*, 31, 425-439.

Guo, H.C., Liu, L., Huang, G.H., Fuller, G.A., Zou, R., and Yin, Y.Y., **2001**, A system dynamics approach for regional environmental planning and management: A study for the Lake Erhai Basin. *Journal of Environmental Management*, 61, 93-111.

Guttal, V., and Jayaprakash, C., **2008**, Changing skewness: an early warning signal of regime shifts in ecosystems. *Ecology Letters*, 11, 450-460.

Haith, D.A., and Shoemaker, L.L., **1987**, Generalized Watershed Loading Functions for Stream-Flow Nutrients. *Water Resources Bulletin*, 23, 471-478.

Håkanson, L., and Jansson, M., **2002**, Principles of lake sedimentology. Caldwell, N.J., *Blackburn Press*, 316 p.

Hanrahan, G., Gledhill, M., House, W.A., and Worsfold, P.J., **2001**, Phosphorus loading in the Frome catchment, UK: Seasonal refinement of the coefficient

modeling approach. *Journal of Environmental Quality*, 30, 1738-1746.

Hassan, G.S., De Francesco, C.G., and Peretti, V., **2012**, Distribution of diatoms and mollusks in shallow lakes from the semiarid Pampa region, Argentina: Their relative paleoenvironmental significance. *Journal of Arid Environments*, 78, 65-72.

Hastings, A., and Wysham, D.B., **2010**, Regime shifts in ecological systems can occur with no warning. *Ecology Letters*, 13, 464-472.

He, S.J., Pan, Y.H., Liu, E.K., Yan, C.R., Guo, Y.R., He, W.q., Liu, Q., and Liu, S., **2010**, Effect of different agronomic measures on soil erosion in sloping farmland of Erhai area. *Southwest China Journal of Agricultural Sciences*, 23, 1939-1943.

Heathwaite, A.L., Fraser, A.I., Johnes, P.J., Hutchins, M., Lord, E., and Butterfield, D., **2003**, The Phosphorus Indicators Tool: a simple model of diffuse P loss from agricultural land to water. *Soil Use and Management*, 19, 1-11.

Heiri O., Lotter A.F., Hausmann S., Kienast F., **2003**, A chironomid-based Holocene summer air temperature reconstruction from the Swiss Alps. *Holocene*, 13, 477–484.

Higgins, S.I., Azorin, E.J., Cowling, R.M., and Morris, M.J., **1997**, A dynamic ecological-economic model as a tool for conflict resolution in an invasive-alien-plant, biological control and native-plant scenario. *Ecological Economics*, 22, 141-154.

Higgins, S.N., Hecky, R.E., and Guildford, S.J., **2005**, Modeling the growth, biomass, and of Cladophora glomerata tissue phosphorus concentration in eastern Lake Erie: Model description and field testing. *Journal of Great Lakes Research*, 31, 439-455.

Hill, M.O., **1973**, Diversity and Evenness: A Unifying Notation and Its Consequences. *Ecology*, 54, 427-432.

Hirota, M., Holmgren, M., Van Nes, E.H., and Scheffer, M., **2011**, Global Resilience of Tropical Forest and Savanna to Critical Transitions. *Science*, 334, 232-235.

Hofmann, W., **1991**, Weichselian Chironomid and Cladoceran Assemblages from Maar Lakes. *Hydrobiologia*, 214, 207-211.

Holland, J.H., **1992**, Complex Adaptive Systems. *Daedalus*, 121, 17-30.

Holland, M.M., Bitz, C.M., and Tremblay, B., **2006**, Future abrupt reductions in the summer Arctic sea ice. *Geophysical Research Letters*, 33.

Holland, R.E., and Beeton, A.M., **1972**, Significance to Eutrophication of Spatial Differences in Nutrients and Diatoms in Lake-Michigan. *Limnology and Oceanography*, 17, 88-&.

Holling, C.S., **1973**, Resilience and stability of ecological systems. Laxenburg, Austria, *International Institute for Applied Systems Analysis*.

Howarth, R.W., Fruci, J.R., and Sherman, D., **1991**, Inputs of Sediment and Carbon to an Estuarine Ecosystem - Influence of Land-Use. *Ecological Applications*, 1, 27-39.

Hu, X., Jin, X., Du, B., and Zhu, J., **2005**, Submerged Macrophyte of Lake Erhai and its Dynamic Change. *Research of Environmental Sciences*, 18, 1-5.

Huang, G.H., Liu, L., Chakma, A., Wu, S.M., Wang, X.H., and Yin, Y.Y., **1999**, A hybrid GIS-supported watershed modelling system: application to the Lake Erhai basin, China. *Hydrological Sciences Journal-Journal Des Sciences Hydrologiques*, 44, 597-610.

Huang, H., Wang, Y., and Li, Q., **2010**, Evaporation variation from Erhai Lake and its controls under climatic warming. *Journal of Meteorology and Environment*, 26, 32-35.

Huang, J.L., and Hong, H.S., **2010**, Comparative study of two models to simulate diffuse nitrogen and phosphorus pollution in a medium-sized watershed, southeast China. *Estuarine Coastal and Shelf Science*, 86, 387-394.

Huang, Z.H., Xue, B., and Pang, Y., **2009**, Simulation on stream flow and nutrient loadings in Gucheng Lake, Low Yangtze River Basin, based on SWAT model. *Quaternary International*, 208, 109-115.

Little, J.L., Hall, R.I., Quinlan, R., Smol, J.P., **2000**, Past trophic status and hypolimnetic anoxia during eutrophicaton and remediation of Gravenhurst Bay, Ontario: comparison of diatoms, chironomids, and historical records. *Journal of Fisheries and Aquatic Science*, 57, 333–341.

Jeppesen, E., **1998**, The structuring role of submerged macrophytes in lakes. New York, *Springer*, xvii, 423 p.

James, T.R., Chimney, M.J., Sharfstein, B., Engstrom, D.R., Schottler, S.P., East, T., Jin, K.R., 2008, Hurricane effects on a shallow lake ecosystem, Lake Okeechobee, Florida (USA). Fundamental and Applied Limnology / Archiv für Hydrobiologie, 172(4), 273-287.

Jeppesen, E., Jensen, J.P., Sondergaard, M., Lauridsen, T., Pedersen, L.J., and Jensen, L., **1997**, Top-down control in freshwater lakes: The role of nutrient state, submerged macrophytes and water depth. *Hydrobiologia*, 342, 151-164.

Jeppesen, E., Leavitt, P., De Meester, L., and Jensen, J.P., **2001**, Functional ecology and palaeolimnology: using cladoceran remains to reconstruct anthropogenic impact. *Trends in Ecology & Evolution*, 16, 191-198.

Jeppesen, E., Sondergaard, M., Jensen, J.P., and Lauridsen, T.L., **2003**,

Restoration of eutrophic lakes: A global perspective. *Freshwater Management*, 135-151.

Jin, X., Xu, Q., and Huang, C., **2005a**, Current status and future tendency of lake eutrophication in China. *Science in China Series C: Life Sciences*, 48, 948-954.

Jin, X.C., Xu, Q.J., and Huang, C.Z., **2005b**, Current status and future tendency of lake eutrophication in China. *Science in China Series C-Life Sciences*, 48, 948-954.

Johnes, P.J., **1996**, Evaluation and management of the impact of land use change on the nitrogen and phosphorus load delivered to surface waters: The export coefficient modelling approach. *Journal of Hydrology*, 183, 323-349.

Johnes, P.J., and Burt, T.P., **1990**, Modeling the Impact of Agriculture Upon Water-Quality in the Windrush Catchment - an Export Coefficient Approach in a Representative Basin. *Hydrological Research Basins and the Environment*, 44, 245-252.

Johnes, P.J., and Heathwaite, A.L., **1997**, Modelling the impact of land use change on water quality in agricultural catchments. *Hydrological Processes*, 11, 269-286.

Johnson, P.T.J., and Carpenter, S.R., **2008**, Influence of eutrophication on disease in aquatic ecosystems: patterns, processes, and predictions, *in* Ostfeld, R.S., Keesing, F., and Eviner, V.T., eds., Infectious Disease Ecology: Effects of Ecosystems on Disease and of Disease on Ecosystems, Volume 1: New Jersey, *Princeton University Press*, 71-79.

Johnson, P.T.J., Townsend, A.R., Cleveland, C.C., Glibert, P.M., Howarth, R.W., McKenzie, V.J., Rejmankova, E., and Ward, M.H., **2010**, Linking environmental nutrient enrichment and disease emergence in humans and wildlife. *Ecological Applications*, 20, 16-29.

Jones, C.A., Cole, C.V., Sharpley, A.N., and Williams, J.R., **1984a**, A Simplified Soil and Plant Phosphorus Model .1. Documentation. *Soil Science Society of America Journal*, 48, 800-805.

Jones, C.A., Sharpley, A.N., and Williams, J.R., **1984b**, A Simplified Soil and Plant Phosphorus Model .3. Testing. *Soil Science Society of America Journal*, 48, 810-813.

Jongman, R.H., Braak, C.J.F.t., and Van Tongeren, O.F.R., **1995**, Data analysis in community and landscape ecology. Cambridge ; New York, *Cambridge University Press*, xxi, 299 p.

Kauppila, T., Moisio, T., and Salonen, V.P., **2002**, A diatom-based inference model for autumn epilimnetic total phosphorus concentration and its application to

a presently eutrophic boreal lake. *Journal of Paleolimnology*, 27, 261-273.

Kaushal, S., and Binford, M.W., **1999**, Relationship between C : N ratios of lake sediments, organic matter sources, and historical deforestation in Lake Pleasant, Massachusetts, USA. *Journal of Paleolimnology*, 22, 439-442.

Keatley, B.E., Douglas, M.S.V., and Smol, J.P., **2008**, Evaluating the influence of environmental and spatial variables on diatom species distributions from Melville Island (Canadian High Arctic). *Botany-Botanique*, 86, 76-90.

Kim, J.G., Park, Y., Yoo, D., Kim, N.W., Engel, B.A., Kim, S.J., Kim, K.S., and Lim, K.J., **2009**, Development of a SWAT Patch for Better Estimation of Sediment Yield in Steep Sloping Watersheds(1). *Journal of the American Water Resources Association*, 45, 963-972.

Knisel, W.G., **1980**, CREAMS: A field scale model for chemicals, runoff, and erosion from agricultural management systems, *in* Knisel, W.G., ed., Volume Number 26.

Korhola, A., Olander, H., and Blom, T., **2000**, Cladoceran and chironomid assemblages as qualitative indicators of water depth in subarctic Fennoscandian lakes. *Journal of Paleolimnology*, 24, 43-54.

Korhola, A., Weckstrom, J., Olander, H., and Blom, T., **1998**, Assessment of chironomid, cladoceran and diatom assemblages as markers of global change in subarctic Fennoscandian lakes. *Proceedings of the Second International Conference on Climate and Water, Vols 1-3*, 562-575.

Krammer, K., and Lange-Bertalot, H., **1988a**, Bacillariophyceae. 2 Teil, Bacillariaceae, Epithemiaceae, Surirellaceae. Stuttgart, *Gustav Fischer*, x, 596 p.

Krammer, K., and Lange-Bertalot, H., **1988b**, Bacillariophyceae. 2/1 Teil, Naviculaceae. Stuttgart, *Gustav Fischer*, vi, 876 p.

Krammer, K., and Lange-Bertalot, H., **1991a**, Bacillariophyceae. 3 Teil, Centrales, Fragilariaceae, Eunotiaceae. Stuttgart, *Gustav Fischer*, xiii, 576 p.

Krammer, K., and Lange-Bertalot, H., **1991b**, Bacillariophyceae. 4 Teil, Achnanthaceae, Kritische Ergänzungen zu Navicula (Lineolatae) und Gomphonema Gesamtliteraturverzeichnis Teil 1-4. Stuttgart, *Gustav Fischer*, vi, 437 p.

Krammer, K., and Lange-Bertalot, H., **2000**, Bacillariophyceae. Part 5, English and French translation of the keys. Heidelberg, *Spectrum*, xiv, 311 p.

Lam, Q.D., Schmalz, B., and Fohrer, N., **2010**, Modelling point and diffuse source pollution of nitrate in a rural lowland catchment using the SWAT model. *Agricultural Water Management*, 97, 317-325.

Langdon, P.G., Ruiz, Z., Brodersen, K.P., and Foster, I.D.L., **2006**, Assessing lake

eutrophication using chironomids: understanding the nature of community response in different lake types. *Freshwater Biology*, 51, 562-577.

Lansing, J.S., **2003**, Complex adaptive systems. *Annual Review of Anthropology*, 32, 183-204.

Last, W.M., Smol, J.P., and Birks, H.J.B., **2001a**, Tracking environmental change using lake sediments. Dordrecht ; Boston, *Kluwer Academic Publishers*, v. <1-4 >.

Last, W.M., Smol, J.P., and Birks, H.J.B., **2001b**, Tracking environmental change using lake sediments. Dordrecht ; Boston, *Kluwer Academic Publishers*, v. <1-4 >.

Lee, K.Y., Fisher, T.R., Jordan, T.E., Correll, D.L., and Weller, D.E., **2000**, Modeling the hydrochemistry of the Choptank River Basin using GWLF and Arc/Info: 1. Model calibration and validation. *Biogeochemistry*, 49, 143-173.

Lee, K.Y., Fisher, T.R., and Rochelle-Newall, E., **2001**, Modeling the hydrochemistry of the choptank river basin using GWLF and Arc/Info: 2. Model validation and application. *Biogeochemistry*, 56, 311-348.

Lei, K., and Wang, Z., **2008**, Emergy synthesis and simulation for Macao. *Energy*, 33, 613-625.

Lenton, T.M., **2011**, Early warning of climate tipping points. *Nature Clim. Change*, 1, 201-209.

Lenton, T.M., Held, H., Kriegler, E., Hall, J.W., Lucht, W., Rahmstorf, S., and Schellnhuber, H.J., **2008**, Tipping elements in the Earth's climate system. *Proceedings of the National Academy of Sciences of the United States of America*, 105, 1786-1793.

Lepš, J., and Šmilauer, P., **2003**, Multivariate analysis of ecological data using CANOCO. Cambridge, UK, *Cambridge University Press*, xi, 269 p.

Levin, S.A., **1998**, Ecosystems and the biosphere as complex adaptive systems. *Ecosystems*, 1, 431-436.

Levin, S.A., **2003**, Complex adaptive systems: Exploring the known, the unknown and the unknowable. *Bulletin of the American Mathematical Society*, 40, 3-19.

Li, H., and Shang, Y., **1989**, Aquatic vegetation in Lake Erhai, Yunnan. *Mountain Research*, 7, 166-174.

Li, J., **2001**, Research and Countermeasures for Erhai Lake Eutrophication. *Journal of Lake Sciences*, 13, 187-192.

Li, Q., **2008**, The characterization of precipitation and trends for Erhai catchment during recent 50 years. *http://www.wcb.yn.gov.cn/slsd/swzy/2370.html*.

Lin, B.Q., and Liu, J.H., **2010**, Estimating coal production peak and trends of coal

imports in China. *Energy Policy*, 38, 512-519.

Lin, Z., Radcliffe, D.E., Risse, L.M., Romeis, J.J., and Jackson, C.R., **2009**, Modeling Phosphorus in the Lake Allatoona Watershed Using SWAT: II. Effect of Land Use Change. *Journal of Environmental Quality*, 38, 121-129.

Liukkonen, M., Kairesalo, T., and Keto, J., **1993**, Eutrophication and Recovery of Lake Vesijarvi (South Finland) - Diatom Frustules in Varved Sediments over a 30-Year Period. *Hydrobiologia*, 269, 415-426.

Lotter, A.F., **1998**, The recent eutrophication of Baldeggersee (Switzerland) as assessed by fossil diatom assemblages. *Holocene*, 8, 395-405.

Lund, J.W.G., **1950**, Studies on Asterionella Formosa Hass: II. Nutrient Depletion and the Spring Maximum. *Journal of Ecology.* 38, 15-35.

Lv, X., Zhu, J., and Meng, L., **2010**, Pilot Study on Diversity of Cyanobacteria Bloom in Erhai Lake. *Environmental Science Survey*, 29, 32-35.

Ma, Y.S., Tan, X.C., and Shi, Q.Y., **2009**, The Simulation of Agricultural Non-Point Source Pollution in Shuangyang River Watershed. *Computer and Computing Technologies in Agriculture Ii, Vol 1*, 293, 553-561.

MacKinnon, J., Sha, M., Cheung, C., Carey, G., Xiang, Z., and Melville, D., **1996**, A Biodiversity review of China, *WWF International, Hong Kong*.

Maclsaac, H.J., Sprules, W.G., and Leach, J.H., **1991**, Ingestion of Small-Bodied Zooplankton by Zebra Mussels (Dreissena polymorpha): Can Cannibalism on Larvae Influence Population Dynamics? *Canadian Journal of Fisheries and Aquatic Sciences*, 48, 2051-2060.

Manson, S.M., **2001**, Simplifying complexity: a review of complexity theory. *Geoforum*, 32, 405-414.

Mattikalli, N.M., and Richards, K.S., **1996**, Estimation of surface water quality changes in response to land use change: Application of the export coefficient model using remote sensing and geographical information system. *Journal of Environmental Management*, 48, 263-282.

Meyers, P.A., **1994**, Preservation of Elemental and Isotopic Source Identification of Sedimentary Organic-Matter. *Chemical Geology*, 114, 289-302.

Moore, J.J., Hughen, K.A., Miller, G.H., and Overpeck, J.T., **2001**, Little Ice Age recorded in summer temperature reconstruction from vared sediments of Donard Lake, Baffin Island, Canada. *Journal of Paleolimnology*, 25, 503-517.

Mourguiart, P., Correge, T., Wirrmann, D., Argollo, J., Montenegro, M.E., Pourchet, M., and Carbonel, P., **1998**, Holocene palaeohydrology of Lake Titicaca estimated from an ostracod-based transfer function. *Palaeogeography Palaeoclimatology Palaeoecology*, 143, 51-72.

Ning, S.K., Jeng, K.Y., and Chang, N.B., **2002**, Evaluation of non-point sources pollution impacts by integrated 3S information technologies and GWLF modelling. *Water Science and Technology*, 46, 217-224.

Noy-Meir, I., **1975**, Stability of Grazing Systems: An Application of Predator-Prey Graphs. *Journal of Ecology*, 63, 459-481.

Nyström, M., Norström, A., Blenckner, T., de la Torre-Castro, M., Eklöf, J., Folke, C., Österblom, H., Steneck, R., Thyresson, M., and Troell, M., **2012**, Confronting Feedbacks of Degraded Marine Ecosystems. *Ecosystems*, 1-16.

Nystrom, M., Folke, C., and Moberg, F., **2000**, Coral reef disturbance and resilience in a human-dominated environment. *Trends in Ecology & Evolution*, 15, 413-417.

Odum, E.P., **1969**, The Strategy of Ecosystem Development. *Science*, 164, 262-270.

Oldfield, F., **1991**, Environmental Magnetism - a Personal Perspective. *Quaternary Science Reviews*, 10, 73-85.

Overpeck, J.T., Webb, T., and Prentice, I.C., **1985**, Quantitative Interpretation of Fossil Pollen Spectra - Dissimilarity Coefficients and the Method of Modern Analogs. *Quaternary Research*, 23, 87-108.

Pan, H., Wang, Y., and Dong, Y., **1999**, Factor analysis of Eutrophication in Erhai Lake. *Journal of Lake Sciences*, 11, 184-188.

Park, R.A., Clough, J.S., and Wellman, M.C., **2008**, AQUATOX: Modeling environmental fate and ecological effects in aquatic ecosystems. *Ecological Modelling*, 213, 1-15.

Park, R.A., Clough, J.S., Wellman, M.C., and Mauriello, D.A., **1997**, Estimating fate and effects with the aquatic ecosystems model, AQUATOX. *Abstracts of Papers of the American Chemical Society*, 213, 33-Cinf.

Parry, M.L., and Intergovernmental Panel on Climate Change. Working Group II., **2007**, Climate change 2007 : impacts, adaptation and vulnerability : contribution of Working Group II to the fourth assessment report of the Intergovernmental Panel on Climate Change. Cambridge, U.K. ; New York, *Cambridge University Press*, ix, 976 p.

Pascual, M., Roy, M., and Franc, A., **2002**, Simple temporal models for ecological systems with complex spatial patterns. *Ecology Letters*, 5, 412-419.

Patterson, T., Gulden, T., Cousins, K., and Kraev, E., **2004**, Integrating environmental, social and economic systems: a dynamic model of tourism in Dominica. *Ecological Modelling*, 175, 121-136.

Peterson, G., Allen, C.R., and Holling, C.S., **1998**, Ecological resilience,

biodiversity, and scale. *Ecosystems*, 1, 6-18.

Platt Bradbury, J., **1988**, A climatic-limnologic model of diatom succession for paleolimnological interpretation of varved sediments at Elk Lake, Minnesota. *Journal of Paleolimnology*, 1, 115-131.

Qian, W.H., and Zhu, Y.F., **2001**, Climate change in China from 1880 to 1998 and its impact on the environmental condition. *Climatic Change*, 50, 419-444.

Radcliffe, D.E., and Cabrera, M.L., **2007**, Modeling phosphorus in the environment. Boca Raton, *CRC Press*, 420 p.

Radcliffe, D.E., Lin, Z., Risse, L.M., Romeis, J.J., and Jackson, C.R., **2009**, Modeling Phosphorus in the Lake Allatoona Watershed Using SWAT: I. Developing Phosphorus Parameter Values. *Journal of Environmental Quality*, 38, 111-120.

Rockstrom, J., Steffen, W., Noone, K., Persson, A., Chapin, F.S., Lambin, E.F., Lenton, T.M., Scheffer, M., Folke, C., Schellnhuber, H.J., Nykvist, B., de Wit, C.A., Hughes, T., van der Leeuw, S., Rodhe, H., Sorlin, S., Snyder, P.K., Costanza, R., Svedin, U., Falkenmark, M., Karlberg, L., Corell, R.W., Fabry, V.J., Hansen, J., Walker, B., Liverman, D., Richardson, K., Crutzen, P., and Foley, J.A., **2009**, A safe operating space for humanity. *Nature*, 461, 472-475.

Rosen, P., Hall, R., Korsman, T., and Renberg, I., **2000**, Diatom transfer-functions for quantifying past air temperature, pH and total organic carbon concentration from lakes in northern Sweden. *Journal of Paleolimnology*, 24, 109-123.

Ryves, D.B., Juggins, S., Fritz, S.C., and Battarbee, R.W., **2001**, Experimental diatom dissolution and the quantification of microfossil preservation in sediments. *Palaeogeography Palaeoclimatology Palaeoecology*, 172, 99-113.

Saleh, A., Arnold, J.G., Gassman, P.W., Hauck, L.M., Rosenthal, W.D., Williams, J.R., and McFarland, A.M.S., **2000**, Application of swat for the Upper North Bosque River Watershed. *Transactions of the Asae*, 43, 1077-1087.

Sayer, C., Roberts, N., Sadler, J., David, C., and Wade, P.M., **1999**, Biodiversity changes in a shallow lake ecosystem: a multi-proxy palaeolimnological analysis. *Journal of Biogeography*, 26, 97-114.

Sayer, C.D., **2001**, Problems with the application of diatom-total phosphorus transfer functions: examples from a shallow English lake. *Freshwater Biology*, 46, 743-757.

Schelske, C.L., Hodell, D.L., **1995**, Using Carbon Isotopes of Bulk Sedimentary Organic Matter to Reconstruct the History of Nutrient Loading and

Eutrophication in Lake Erie, Limnology and Oceanography, 40(5), 918-929.

Scheffer, M., **1998**, Ecology of shallow lakes. Dordrecht ; Boston, *Kluwer Academic Publishers*, xx, 357 p.

Scheffer, M., **2009**, Critical transitions in nature and society. Princeton ; Oxford, *Princeton University Press*, xi, 384 p.

Scheffer, M., Bascompte, J., Brock, W.A., Brovkin, V., Carpenter, S.R., Dakos, V., Held, H., van Nes, E.H., Rietkerk, M., and Sugihara, G., **2009**, Early-warning signals for critical transitions. *Nature*, 461, 53-59.

Scheffer, M., and Beets, J., **1994**, Ecological Models and the Pitfalls of Causality. *Hydrobiologia*, 275, 115-124.

Scheffer, M., Carpenter, S., Foley, J.A., Folke, C., and Walker, B., **2001**, Catastrophic shifts in ecosystems. *Nature*, 413, 591-596.

Scheffer, M., and Carpenter, S.R., **2003**, Catastrophic regime shifts in ecosystems: linking theory to observation. *Trends in Ecology & Evolution*, 18, 648-656.

Scheffer, M., and Jeppesen, E., **2007**, Regime shifts in shallow lakes. *Ecosystems*, 10, 1-3.

Schindle, D., **1974**, Eutrophication and Recovery in Experimental Lakes - Implications for Lake Management. *Science*, 184, 897-899.

Schneider, S.H., **2004**, Abrupt non-linear climate change, irreversibility and surprise. *Global Environmental Change-Human and Policy Dimensions*, 14, 245-258.

Schneiderman, E.M., Pierson, D.C., Lounsbury, D.G., and Zion, M.S., **2002**, Modeling the hydrochemistry of the Cannonsville watershed with Generalized Watershed Loading Functions (GWLF). *Journal of the American Water Resources Association*, 38, 1323-1347.

Schriver, P., Bogestrand, J., Jeppesen, E., and Sondergaard, M., **1995**, Impact of Submerged Macrophytes on Fish-Zooplankton-Phytoplankton Interactions - Large-Scale Enclosure Experiments in a Shallow Eutrophic Lake. *Freshwater Biology*, 33, 255-270.

SCS, **1972**, Hydrology, Section 4: National Engineering Handbook, U.S. Soil Conservation Service, Washington, D.C., Government Printing Office.

Seppa, H., and Birks, H.J.B., **2001**, July mean temperature and annual precipitation trends during the Holocene in the Fennoscandian tree-line area: pollen-based climate reconstructions. *Holocene*, 11, 527-539.

Sharpley, A.N., Smith, S.J., Williams, J.R., Jones, O.R., and Coleman, G.A., **1991**, Water-Quality Impacts Associated with Sorghum Culture in the Southern Plains. *Journal of Environmental Quality*, 20, 239-244.

Shrestha, S., Babel, M.S., and Das Gupta, A., **2004**, Evaluation of AnnAGNPS

model for a watershed in the Siwalik Hills of Nepal. *Land and Water Management: Decision Tools and Practices, Vols 1 and 2*, 675-681.

Smith, V.H., **2003**, Eutrophication of freshwater and coastal marine ecosystems - A global problem. *Environmental Science and Pollution Research*, 10, 126-139.

Smith, V.H., and Schindler, D.W., **2009**, Eutrophication science: where do we go from here? *Trends in Ecology & Evolution*, 24, 201-207.

Smol, J.P., Pollution of Lakes and Rivers: A Paleoenvironmental Perspective, 2nd Edition, pp 369.

Smol, J., **1992**, Paleolimnology: an important tool for effective ecosystem management. *Journal of Aquatic Ecosystem Health*, 1, 49-58.

Smol, J.P., and Stoermer, E.F., **2010**, The diatoms : applications for the environmental and earth sciences. Cambridge ; New York, *Cambridge University Press*, xviii, 667 p.

Smol, J.P., Wolfe, A.P., Birks, H.J.B., Douglas, M.S.V., Jones, V.J., Korhola, A., Pienitz, R., Ruhland, K., Sorvari, S., Antoniades, D., Brooks, S.J., Fallu, M.A., Hughes, M., Keatley, B.E., Laing, T.E., Michelutti, N., Nazarova, L., Nyman, M., Paterson, A.M., Perren, B., Quinlan, R., Rautio, M., Saulnier-Talbot, E., Siitoneni, S., Solovieva, N., and Weckstrom, J., **2005**, Climate-driven regime shifts in the biological communities of arctic lakes. *Proceedings of the National Academy of Sciences of the United States of America*, 102, 4397-4402.

Snowball, I.F., **1994**, Bacterial Magnetite and the Magnetic-Properties of Sediments in a Swedish Lake. *Earth and Planetary Science Letters*, 126, 129-142.

Stanghellini, C., **1987**, Transpiration of greenhouse crops. An aid to climate management, Prof.dr.ir. J. Schenk (promotor), dr.ir. G.P.A. Bot (co-promotor). Wageningen (1987) 150 pp.

Sterman, J.D., **2002**, Systems dynamics modeling: tools for learning in a complex world. *Engineering Management Review, IEEE*, 30, 42-42.

Suding, K.N., Gross, K.L., and Houseman, G.R., **2004**, Alternative states and positive feedbacks in restoration ecology. *Trends in Ecology & Evolution*, 19, 46-53.

Sverdrup, H., and Warfvinge, P., **1993**, Calculating field weathering rates using a mechanistic geochemical model PROFILE. *Applied Geochemistry*, 8, 273-283.

Sverdrup, H., Warfvinge, P., Blake, L., and Goulding, K., **1995**, Modelling recent and historic soil data from the Rothamsted Experimental Station, UK using

SAFE. *Agriculture, Ecosystems & Environment*, 53, 161-177.

Swaney, D.P., Sherman, D., and Howarth, R.W., **1996**, Modeling water, sediment and organic carbon discharges in the Hudson-Mohawk basin: Coupling to terrestrial sources. *Estuaries*, 19, 833-847.

Swenson, W., Wilson, D.S., and Elias, R., **2000**, Artificial ecosystem selection. *Proceedings of the National Academy of Sciences of the United States of America*, 97, 9110-9114.

Telford, R.J., and Birks, H.J.B., **2009**, Evaluation of transfer functions in spatially structured environments. *Quaternary Science Reviews*, 28, 1309-1316.

ter Braak, C.J.F., **1986**, Canonical Correspondence-Analysis - a New Eigenvector Technique for Multivariate Direct Gradient Analysis. *Ecology*, 67, 1167-1179.

ter Braak, C.J.F., **1987**, The Analysis of Vegetation-Environment Relationships by Canonical Correspondence-Analysis. *Vegetatio*, 69, 69-77.

ter Braak, C.J.F., and Juggins, S., **1993**, Weighted Averaging Partial Least-Squares Regression (WA-PLS) - an Improved Method for Reconstructing Environmental Variables from Species Assemblages. *Hydrobiologia*, 269, 485-502.

ter Braak, C.J.F., Juggins, S., Birks, H.J.B., and Vandervoet, H., **1993**, Weighted Averaging Partial Least-Squares Regression (Wa-Pls) - Definition and Comparison with Other Methods for Species-Environment Calibration. *Multivariate Environmental Statistics*, 6, 525-560.

ter Braak, C.J.F., and Šmilauer, P., **2002**, CANOCO Reference Manual and CanoDraw for Windows User's Guide: Software for Canonical Community Ordination (version 4.5). Ithaca, NY, USA (www.canoco.com): Microcomputer Power.

Theurer, F.D., and Clarke, C.D., **1991**, Wash load component for sediment yield modeling. In Proceedings of the fifth federal interagency sedimentation conference, March 18-21, 1991, pg. 7-1 to 7-8.

Tian, Y.W., Huang, Z.L., and Xiao, W.F., **2010**, Reductions in non-point source pollution through different management practices for an agricultural watershed in the Three Gorges Reservoir Area. *Journal of Environmental Sciences-China*, 22, 184-191.

USEPA, **1996**, EPA method 3052: microwave assisted acid digestion of siliceous and organically based matrices, Test methods for evaluating solid waste, physical/chemical methods: Washington, D.C., *EPA office solid waste*, 3052-1-3052-20.

USFWS, **1984**, Instream water temperature model, part II. physical processes and

math models. Report FWS/OBS-84/15.

van Nes, E.H., and Scheffer, M., **2005a**, Implications of spatial heterogeneity for catastrophic regime shifts in ecosystems. *Ecology*, 86, 1797-1807.

Van Nes, E.H., and Scheffer, M., **2005b**, A strategy to improve the contribution of complex simulation models to ecological theory. *Ecological Modelling*, 185, 153-164.

van Nes, E.H., and Scheffer, M., **2007**, Slow recovery from perturbations as a generic indicator of a nearby catastrophic shift. *American Naturalist*, 169, 738-747.

Vitousek, P.M., **1994**, Beyond Global Warming - Ecology and Global Change. *Ecology*, 75, 1861-1876.

Vyverman, W., and Sabbe, K., **1995**, Diatom-Temperature Transfer-Functions Based on the Altitudinal Zonation of Diatom Assemblages in Papua-New-Guinea - a Possible Tool in the Reconstruction of Regional Paleoclimatic Changes. *Journal of Paleolimnology*, 13, 65-77.

Wade, A.J., Butterfield, D., Griffiths, T., and Whitehead, P.G., **2007**, Eutrophication control in river-systems: an application of INCA-P to the River Lugg. *Hydrology and Earth System Sciences*, 11, 584-600.

Wade, A.J., Whitehead, P.G., and Butterfield, D., **2002**, The Integrated Catchments model of Phosphorus dynamics (INCA-P), a new approach for multiple source assessment in heterogeneous river systems: model structure and equations. *Hydrology and Earth System Sciences*, 6, 583-606.

Wade, A.J., Whitehead, P.G., and Butterfield, D., **2004**, The Integrated Catchments Model of Phosphorus Dynamics (INCA-P), a new approach for multiple source assessment in heteorogenous river systems: model structure and equations (vol 6, pg 583, 2002). *Hydrology and Earth System Sciences*, 8, 859-859.

Walker, B., Hollin, C.S., Carpenter, S.R., and Kinzig, A., **2004a**, Resilience, adaptability and transformability in social-ecological systems. *Ecology and Society*, 9.

Walker, B., Holling, C.S., Carpenter, S.R., and Kinzig, A., **2004b**, Resilience, adaptability and transformability in social-ecological systems. *Ecology and Society*, 9.

Walker, B., and Meyers, J.A., **2004**, Thresholds in Ecological and Social-Ecological Systems: A Developing Database.

Wang, R., Yang, X.D., Langdon, P., and Zhang, E.L., **2011**, Limnological responses to warming on the Xizang Plateau, Tibet, over the past 200

years. *Journal of Paleolimnology*, 45, 257-271.

Wang, S., and Dou, H., **1998**, Lakes in China. Beijing, *Science Press*.

Wang, S.H., Huggins, D.G., Frees, L., Volkman, C.G., Lim, N.C., Baker, D.S., Smith, V., and Denoyelles, F., **2005a**, An integrated modeling approach to total watershed management: Water quality and watershed assessment of Cheney Reservoir, Kansas, USA. *Water Air and Soil Pollution*, 164, 1-19.

Wang, W.P., Hong, H.S., Zhang, L.P., Cao, W.Z., Jiang, Q.S., and Huang, J.L., **2005b**, Agricultural non-point source pollution information system of a mesoscale river watershed in southeast China. *Environmental Informatics, Proceedings*, 58-66.

Wang, Y., **2000**, Environmental Protection of Erhai Lake Source. *Yunnan Environmental Science*, 19, 35-36.

Wang, Y., Pang, H., Wu, Q., and Huang, Q., **1999**, Impacts of Human Activity on Erhai Lake and Countermeasures. *Journal of Lake Sciences*, 11, 123-129.

Weckstrom, J., Korhola, A., and Blom, T., **1997**, Diatoms as quantitative indicators of pH and water temperature in subarctic Fennoscandian lakes. *Hydrobiologia*, 347, 171-184.

Wetzel, R.G, **1970**, Recent and Postglacial Production Rates of a Marl Lake *Limnology and Oceanography,* 15, 491-503.

Williams, J.R., **1975**, SEDIMENT ROUTING FOR AGRICULTURAL WATERSHEDS1. *JAWRA Journal of the American Water Resources Association*, 11, 965-974.

Williams, J.W., Blois, J.L., and Shuman, B.N., **2011**, Extrinsic and intrinsic forcing of abrupt ecological change: case studies from the late Quaternary. *Journal of Ecology*, 99, 664-677.

Wischemier, W.H., and Smith, D.D., **1978**, Predicting rainfall erosion losses, A guide to conservation planning, *USDA*.

Wissel, C., **1984**, A universal law of the characteristic return time near thresholds. *Oecologia*, 65, 101-107.

World Bank, **2007**, China - Second Yunnan Urban Environmental Project (Vol. 5 of 5) : Erhai Lake Basin regional environmental assessment, Volume 5, *The World Bank*, 138.

Wright, R.F., Cosby, B.J., Hornberger, G.M., and Galloway, J.N., **1986**, Comparison of Paleolimnological with Magic Model Reconstructions of Water Acidification. *Water Air and Soil Pollution*, 30, 367-380.

Wu, J.L., Gagan, M.K., Jiang, X.H., Xia, W.L., and Wang, S.M., **2004**, Sedimentary geochemical evidence for recent eutrophication of Lake Chenghai, Yunnan, China. *Journal of Paleolimnology*, 32, 85-94.

Wu, Q., and Wang, Y., **1999**, On the Succession of Aquatic Communities in Erhai Lake. *Journal of Lake Sciences*, 11, 267-274.

Xu, J.C., and Wilkes, A., **2004**, Biodiversity impact analysis in northwest Yunnan, southwest China. *Biodiversity and Conservation*, 13, 959-983.

Yan, C.-z., Jin, X.-c., Zhao, J.-z., Shen, B., Li, N.-b., Huang, C.-z., and Xiong, Z.-h., **2005**, Ecological Protection and Sustainable Utilization of Erhai Lake, Yunnan. *Environmental Science (in Chinese)*, 26, 38-43.

Yan, C.Z., Lu, X., and Zhao, X.L., **2008**, Protection and sustainable utilisation of water resources in Lake Erhai basin. *International Journal of Sustainable Development and World Ecology*, 15, 357-361.

Yang, S., and Ni, X., **1999**, The status of agriculture Non-point pollution in watershed of Erhai lake. *Agro-Environment & Development*, 2, 65-70.

Yang, X.D., Anderson, N.J., Dong, X.H., and Shen, J., **2008**, Surface sediment diatom assemblages and epilimnetic total phosphorus in large, shallow lakes of the Yangtze floodplain: their relationships and implications for assessing long-term eutrophication. *Freshwater Biology*, 53, 1273-1290.

Yang, X.D., Kamenik, C., Schmidt, R., and Wang, S.M., **2003**, Diatom-based conductivity and water-level inference models from eastern Tibetan (Qinghai-Xizang) Plateau lakes. *Journal of Paleolimnology*, 30, 1-19.

Young, R.A., Onstad, C.A., Bosch, D.D., and Anderson, W.P., **1989**, Agnps - a Nonpoint-Source Pollution Model for Evaluating Agricultural Watersheds. *Journal of Soil and Water Conservation*, 44, 168-173.

Yu, G., Xue, B., Lai, G.Y., Gui, F., and Liu, X.M., **2007**, A 200-year historical modeling of catchment nutrient changes in Taihu Basin, China. *Hydrobiologia*, 581, 79-87.

Yuan, Y., Bingner, R.L., and Theurer, F.D., **2006**, Subsurface flow component for AnnAGNPS. *Applied Engineering in Agriculture*, 22, 231-241.

Yuan, Y.P., Bingner, R., Williams, R., Lowrance, R., Bosch, D., and Sheridan, J., **2007**, Integration of the models of AnnAGNPS and REMM to assess riparian buffer system for sediment reduction. *International Journal of Sediment Research*, 22, 60-69.

Zhang, Y.L., Zhang, E.L., Liu, M.L., Wang, X., and Qin, B.Q., **2007**, Variation of chromophoric dissolved organic matter and possible attenuation depth of ultraviolet radiation in Yunnan Plateau lakes. *Limnology*, 8, 311-319.

Appendix I Lake's environment variables in Yunnan datasets (A/D means the ratio of area and depth) (CODE is same as in Figure 3-1)

Name	CODE	LAKE	Depth (m)	Area km2	A/D	pH	LONG.	LAT.	Altitude (m)	SD (m)	NO_3-N mg/l	Na^+ mg/l	K^+ mg/l	Mg^{2+} mg/l	Ca^{2+} mg/l	Cl^- mg/l	SO_4^{2-} mg/l	Si mg/l	Chla ug/L	TN µg/l	TP µg/l	TSS mg/l	Cond. µs/cm	Salinity mg/l	Do mg/l
Qingshuihai	**9**	QSHL	21.0	5.8	0.3	7.2	25.6	103.1	2182.2	2.5	0.1	1.1	1.6	7.7	18.4	1.4	4.0	0.4	3.7	433.5	1.7	0.7	241	34.6	9.6
Changhu	**30**	CHAN	12.0	0.8	0.1	8.7	24.7	103.4	1870.0	2.7	0.0	0.5	0.2	18.1	17.3	0.7	1.5	0.8	2.4	350.8	1.8	2.9	229	39.1	1.4
Yuehu	**7**	YUEH	3.4	2.2	0.7	8.4	24.8	103.5	1893.0	0.6	0.1	1.3	2.1	5.3	36.6	4.1	10.0	1.0	2.3	329.9	2.1	4.0	232	60.5	1.6
Fuxianhu	**6**	FXHL	110.0	211.0	1.9	8.7	24.6	102.9	1720.0	4.1	0.0	6.8	2.4	20.9	24.0	3.4	10.4	0.3	4.4	259.6	3.9	0.4	245	68.2	8.5
Laojunshan	**2**	LJSL	2.0	0.2	0.1	7.4	26.6	99.7	3827.0	1.5	0.3	0.7	0.2	0.6	1.6	0.1	0.4	2.2	1.8	389.9	5.5	1.0	40	6.1	1.0
Bigutianchi	**16**	BGTC	1.5	0.2	0.1	8.2	27.6	99.6	3809.0	1.5	0.0	1.1	0.2	1.4	10.7	0.3	0.3	0.9	1.6	756.0	5.5	1.2	281	14.9	1.4
Lijiawa	**39**	LJAL	10.5	0.3	0.0	8.5	26.1	103.9	2025.0	3.0	0.2	0.8	0.4	1.6	38.6	1.1	15.0	1.2	2.2	299.6	8.5	1.3	237	58.9	6.1
Caohai	**28**	CAOH	2.3	0.9	0.4	8.4	26.6	100.2	2208.0	1.2	0.0	0.6	0.1	10.0	16.9	0.4	0.3	1.1	1.5	300.3	8.7	17.5	234	29.4	2.3
Yuanhu	**25**	YUAN	12.5	0.2	0.0	8.3	24.7	103.4	1902.0	2.2	0.1	1.3	2.1	13.4	35.9	2.4	4.5	0.6	1.6	449.4	8.7	3.1	227	60.2	1.1
Hunshuihai	**19**	HSHZ	2.3	0.9	0.4	8.3	25.5	100.6	2006.0	0.4	0.3	33.0	3.4	22.5	56.0	17.5	204.6	4.1	5.9	1238.8	10.2	24.1	232	341.4	4.3
Jianhu	**38**	JIAN	5.2	5.0	1.0	8.9	26.5	99.9	2201.0	2.3	0.0	5.0	1.0	9.7	9.3	1.5	6.7	1.8	0.0	558.9	10.7	28.5	235	35.0	3.4
Cibihu	**35**	CB07	17.0	8.2	0.5	8.1	26.2	99.9	2033.0	6.1	0.0	7.0	1.7	11.9	41.1	1.7	3.0	2.6	1.9	255.2	10.9	0.2	226	69.0	3.0
Yangzonghai	**34**	YZHL	20.0	31.4	1.6	8.7	24.9	103.0	1775.0	2.4	0.2	4.9	3.3	26.6	26.2	4.1	40.4	0.3	1.1	492.2	11.1	2.1	230	105.9	2.0
Pingdihai	**36**	PDHZ	2.0	0.3	0.2	8.7	25.9	104.1	2147.0	1.1	0.6	1.2	2.5	3.9	30.3	1.7	29.4	1.3	3.2	912.7	12.7	4.1	234	70.8	4.8
Haizibian	**27**	HZBL	6.0	2.4	0.4	8.7	23.7	104.1	1508.0	0.9	0.0	1.5	2.2	30.8	26.3	2.3	3.0	1.8	3.3	828.6	16.2	5.4	221	67.9	0.1
Bitahai	**11**	BT07	8.5	1.4	0.2	8.7	27.8	99.9	3568.0	1.5	0.0	1.5	0.2	1.5	10.3	0.3	0.8	3.5	4.8	458.3	18.8	1.4	252	18.2	2.0
Chaheihai	**14**	CHHL	2.0	2.9	1.5	8.7	23.7	103.9	1484.0	0.2	0.2	1.4	1.4	6.7	20.9	1.7	14.3	1.3	7.1	671.5	19.0	41.2	224	47.8	0.1
Shipohai	**32**	SPHZ	2.5	0.4	0.2	9.5	25.8	103.6	1957.0	0.6	0.1	0.4	0.3	5.8	11.5	1.6	3.8	0.5	1.5	687.1	19.9	7.9	232	23.9	4.4
Matangshuiku	**22**	MTSK	4.2	0.5	0.1	8.3	25.9	104.1	2113.0	0.6	1.4	1.0	1.0	2.7	48.2	2.0	21.3	1.9	1.6	1762.9	20.9	7.7	242	79.4	4.5
Chenhai	**4**	CHEN	18.0	76.4	4.2	9.2	26.5	100.7	1550.0	1.6	0.0	132.8	7.4	49.1	7.5	12.4	3.8	0.5	0.7	606.8	21.3	7.8	225	213.5	2.8
Wenbihai	**29**	WBHL	3.0	0.5	0.2	9.1	26.8	100.2	2374.0	1.5	0.0	3.6	0.8	17.3	10.5	1.5	2.1	3.4	2.3	546.8	23.5	19.6	233	39.3	3.3

Appendix I Continuous

Name	CODE	LAKE	Depth (m)	Area km2	A/D	pH	LONG.	LAT.	Altitude (m)	SD (m)	NO_3-N mg/l	Na^+ mg/l	K^+ mg/l	Mg^{2+} mg/l	Ca^{2+} mg/l	Cl^- mg/l	SO_4^{2-} mg/l	Si mg/l	Chla ug/l	TN µg/l	TP µg/l	TSS mg/l	Cond. µs/cm	Salinity mg/l	Do mg/l
Shuduhu	**31**	SDHL	8.0	1.7	0.2	8.7	27.9	100.0	3611.0	1.1	0.1	1.2	0.4	0.8	4.2	0.2	1.0	1.9	2.4	489.5	25.3	3.0	165	9.8	2.2
Haixihai	**5**	HXHL	11.0	4.2	0.4	8.5	26.3	100.0	2128.0	1.2	0.0	1.7	0.7	8.2	11.6	0.7	2.1	3.2	0.8	213.9	26.8	2.7	226	28.2	3.2
Haishaoshuiku	**18**	HSSK	13.5	3.3	0.2	8.9	25.7	100.6	1632.0	0.6	0.0	14.1	3.6	14.6	22.6	6.2	7.8	2.2	10.8	893.3	32.2	9.1	211	71.1	4.9
Xihu	**33**	XHLL	2.5	2.2	0.9	8.3	26.0	100.1	1979.0	0.8	0.1	15.9	1.4	21.3	24.3	11.2	8.2	2.1	4.0	995.2	32.6	14.7	224	84.5	3.2
Changqiaohai	**20**	CQHL	2.1	11.2	5.3	9.4	23.4	103.4	1291.0	0.5	0.1	15.1	5.1	17.3	19.5	24.7	47.7	2.3	11.1	1981.0	34.8	10.3	219	131.8	0.1
Lashihai	**37**	LSHL	1.2	9.9	8.3	8.8	26.9	100.1	2436.0	0.7	0.2	2.3	1.4	12.1	24.8	1.6	3.1	6.7	2.2	666.9	43.8	32.4	234	52.2	3.4
Erhai	**15**	EH05	8.9	249.0	28.0	8.6	25.9	100.1	1954.0	1.3	0.1	8.4	2.5	11.7	26.2	4.9	7.0	1.7	6.6	592.1	45.3	3.3	228	62.4	4.2
Sanjiaohai	**17**	SJHL	4.7	5.1	1.1	8.6	23.6	103.3	1316.0	0.5	0.1	5.2	2.8	13.8	40.1	9.8	69.6	1.4	6.4	1536.0	45.6	57.7	214	142.8	0.1
Yangpai	**13**	YPSK	8.9	4.5	0.5	8.9	25.5	101.2	1930.0	0.4	0.4	7.3	2.8	5.6	24.0	3.9	27.9	1.5	3.1	915.1	56.8	27.7	220	73.4	7.1
Qingjianmei	**24**	QMJL	2.0	1.0	0.5	8.6	25.7	100.7	1954.0	0.3	0.0	17.5	6.3	10.6	26.5	26.3	35.4	1.3	9.9	2634.4	61.3	23.2	227	124.0	3.9
Qinghai	**21**	QING	1.0	2.8	2.8	9.7	25.4	100.6	1980.0	1.0	0.1	24.6	5.5	25.7	15.9	41.4	86.8	6.5	2.3	1846.5	61.9	31.0	226	206.5	5.7
Qiluhai	**8**	QLHL	5.8	35.6	6.1	8.8	24.2	102.8	1801.0	0.5	0.6	23.2	15.2	34.8	20.6	43.9	69.5	0.9	84.2	3351.4	82.0	26.1	248	208.7	11.8
Wulanghai	**1**	WLHZ	3.6	1.1	0.3	8.3	24.6	103.9	1876.0	0.6	2.1	1.1	1.7	6.6	35.3	1.1	9.5	0.6	9.4	2686.9	85.1	29.0	231	58.0	0.7
Yiliangcaohai	**23**	YLCH	4.8	1.3	0.3	8.6	24.9	103.0	1853.0	0.6	0.1	4.7	4.7	16.6	25.3	6.1	30.8	1.6	14.2	1382.2	112.8	15.0	228	89.8	2.9
Yilonghu	**3**	YLHL	3.0	27.5	9.2	7.3	23.7	102.5	1405.0	0.5	1.2	15.4	14.9	21.7	53.4	20.9	71.4	3.7	14.2	4592.5	149.9	29.1	266	202.6	6.9
Xinyunhu	**12**	XY07	10.0	34.1	3.4	9.0	24.4	102.8	1732.0	0.3	0.0	17.1	8.7	25.3	24.2	17.6	23.4	0.5	105.6	3103.9	271.5	40.3	238	116.8	7.7
Tinghu	**10**	THXL	3.0	0.3	0.1	8.7	23.6	104.4	1516.0	0.2	0.1	11.7	7.3	11.3	47.3	16.1	28.6	1.3	133.2	3864.6	329.5	42.5	226	123.6	3.7
Qiantunsuiku	**26**	QTSK	2.0	1.8	0.9	8.2	26.2	104.1	2032.0	0.4	2.0	3.8	1.7	12.1	58.4	4.2	58.9	2.5	1.7	2504.7	1248.3	14.2	238	143.6	5.0

Appendix II Species descriptions in Yunnan datasets

CodeNum	Name	N non-zero values	Hill's N2	Minimum	Maximum	Optimum	Tolerance	SD.
1	*Karayevia clevei* (Grunow) Round & Bukhtiyarova	4	2.1	0.0	1.5	26.89	2.30	0.2
2	*Psammothidium curtissimum* (J.R.Carter) M.Aboal	11	4.8	0.0	10.9	8.56	2.36	2.4
3	*Achnanthes exigua* Grunow	5	2.5	0.0	2.9	21.59	1.51	0.5
4	*Planothidium rostratum* (Oestrup) Lange-Bertalot	11	4.9	0.0	5.9	9.61	3.24	1.1
5	*Achnanthidium minutissimum* (Kützing) Czarnecki	35	13.9	0.0	38.9	18.80	2.24	8.9
6	*Achnanthes saccula* Carter	8	4.9	0.0	4.2	9.91	1.74	0.9
7	*Psammothidium subatomoides* (Hustedt) L.Bukhtiyarova & Round	8	5.7	0.0	1.3	22.41	1.95	0.3
8	*Amphora libyca* Ehrenberg	8	7.1	0.0	1.0	21.22	1.85	0.2
9	*Amphora pediculus* (Kützing) Grunow	3	2.1	0.0	1.0	24.02	1.53	0.2
10	*Amphipleura pellucida* (Kützing) Kützing	2	1.5	0.0	1.5	11.32	1.14	0.2
11	*Brachysira vitrea* (Grunow) R.Ross	5	3.6	0.0	2.7	17.74	3.19	0.5
12	*Aulacoseira alpigena* (Grunow) Krammer	16	4.5	0.0	11.3	40.80	2.27	1.9
13	*Aulacoseira ambigua* (Grunow) Simonsen	18	5.8	0.0	75.9	62.66	2.01	16.1
14	*Aulacoseira granulata* (Ehrenberg) Simonsen	20	4.6	0.0	52.8	59.73	2.47	8.8
15	*Aulacoseira tenuior* (Grunow) Krammer	3	1.3	0.0	12.4	35.36	1.32	2.0
16	*Cocconeis placentula var. euglypta* (Ehrenberg) Grunow	13	2.4	0.0	30.2	44.50	2.66	4.8
17	*Cocconeis placentula* var. *lineata* (Ehrenberg) Van Heurck	5	3.8	0.0	2.9	20.22	1.99	0.7
18	*Cyclostephanos dubius* (Fricke) Round	22	3.4	0.0	79.4	50.34	4.14	14.7
19	*Cyclostephanos tholiformis* Stoermer, Håkansson & Theriot	16	3.1	0.0	73.9	62.89	2.06	15.1
20	*Cyclotella atomus Hustedt*	3	1.7	0.0	1.3	5.48	1.89	0.2

CodeNum	Name	N non-zero values	Hill's N2	Minimum	Maximum	Optimum	Tolerance	SD
21	*Cyclotella bodanica* var. *lemanica* (O. Müller) Bachmann	24	8.4	0.0	19.3	20.46	3.45	4.8
22	*Cyclotella michiganiana* Skvortzow	13	3.3	0.0	56.2	166.75	2.75	10.0
23	*Cyclotella ocellata* Pantocsek	21	8.2	0.0	68.2	10.60	2.14	19.0
24	*Cyclotella pseudostelligera* Hustedt	23	3.9	0.0	72.4	23.20	2.29	11.5
25	*Cyclotella schumannii* (Grunow) Håkansson	3	1.5	0.0	1.3	23.81	3.82	0.2
26	*Discostella stelligera* (Cleve & Grunow) Houk & Klee	21	12.2	0.0	4.1	28.27	3.15	1.1
27	*Cymbella affinis* Kützing	12	7.1	0.0	3.9	25.12	3.76	1.0
28	*Encyonopsis cesatii* (Rabenhorst) K.Krammer	2	1.5	0.0	1.3	9.72	1.02	0.2
29	*Cymbella cistula* (Ehrenberg) Kirchner	2	1.7	0.0	1.0	34.15	2.37	0.2
30	*Cymbella ehrenbergii* Kützing	12	7.6	0.0	2.4	18.17	2.45	0.5
31	*Cymbella falaisensis* (Grunow) Krammer & Lange-Bertalot	7	3.1	0.0	6.9	15.24	2.13	1.2
32	*Cymbella hustedtii* Krasske	6	2.9	0.0	11.9	22.01	2.12	2.1
33	*Cymbella naviculacea* Grunow	4	3.1	0.0	2.4	5.65	2.46	0.5
34	*Encyonopsis microcephala* (Grunow) Krammer	14	5.3	0.0	16.9	13.26	2.18	3.2
35	*Encyonema minutum* (Hilse) D.G.Mann	15	5.9	0.0	7.9	8.01	3.23	1.4
36	*Encyonema silesiacum* (Bleisch) D.G.Mann	14	6.7	0.0	6.0	12.38	2.52	1.1
37	*Diploneis oblongella* (Naegeli) Cleve-Euler	15	7.6	0.0	7.3	14.70	2.19	1.7
38	*Epithemia adnata* (Kützing) Brébisson	5	3.6	0.0	3.0	34.19	1.29	0.6
39	*Epithemia sorex* Kützing	13	3.8	0.0	24.1	24.46	2.92	3.9
40	*Eunotia bilunaris* var. *linearis* (Okuno) Lange-Bertalot	3	1.0	0.0	21.3	6.60	2.58	3.4
41	*Eunotia implicata* Nörpel et al.	2	1.5	0.0	1.5	17.95	1.45	0.2
42	*Pseudostaurosira brevistriata* (Grunow) D.M.Williams & Round	5	3.4	0.0	2.1	15.89	2.64	0.4

CodeNum	Name	N non-zero values	Hill's N2	Minimum	Maximum	Optimum	Tolerance	SD
43	*Fragilaria capucina subsp. rumpens* (Kützing) Lange-Bertalot	12	5.9	0.0	3.4	32.71	2.63	0.6
44	*Staurosira construens* Ehrenberg	14	5.3	0.0	50.3	7.72	3.01	8.8
45	*Staurosira venter* (Ehrenberg) H.Kobayasi	11	2.7	0.0	33.5	25.35	1.82	5.4
46	*Fragilaria crotonensis* Kitton	5	3.8	0.0	35.8	47.11	5.06	7.7
47	*Fragilariforma virescens* (Ralfs) D.M.Williams & Round	3	2.1	0.0	1.5	12.66	1.96	0.3
48	*Fragilaria nanana* Lange-Bertalot	9	4.9	0.0	24.7	33.65	1.82	5.3
49	*Synedrella parasitica* (W.Smith) Round & N.I.Maidana	5	2.8	0.0	2.9	31.94	1.69	0.5
50	*Staurosirella pinnata* (Ehrenberg) D.M.Williams & Round	26	11.6	0.0	46.3	13.11	2.59	12.1
51	*Fragilaria tenera* (W. Smith) Lange-Bertalot	14	4.8	0.0	16.4	10.33	4.79	2.8
52	*Ulnaria ulna* (Nitzsch) P.Compère	4	1.2	0.0	6.6	118.73	5.22	1.0
53	*Gyrosigma acuminatum* (Kützing) Rabenhorst	7	4.9	0.0	1.2	19.80	3.05	0.2
54	*Gomphonema vibrio var. intricatum* (Kützing) Playfair	6	5.3	0.0	5.0	21.63	1.39	1.2
55	*Gomphonema clavatum* Ehrenberg	3	2.7	0.0	1.9	72.08	1.96	0.4
56	*Gomphonema gracile* Ehrenberg	8	3.5	0.0	8.2	15.05	3.73	1.4
57	*Gomphonema minutum* (Agardh) Agardh	2	1.2	0.0	4.8	12.43	1.77	0.8
58	*Gomphonema parvulum* (Kützing) Kützing	9	3.3	0.0	18.3	6.88	2.63	3.3
59	*Gomphonema truncatum* Ehrenberg	5	2.0	0.0	5.4	64.65	6.18	0.9
60	*Gyrosigma acuminatum* (Kützing) Rabenhorst	13	5.4	0.0	10.4	19.25	1.62	2.0
61	*Mastogloia smithii* Thwaites	3	2.2	0.0	1.7	7.83	4.99	0.3
62	*Navicula cincta* (Ehrenberg) Ralfs	3	2.1	0.0	1.3	10.93	3.56	0.2

CodeNum	Name	N non-zero values	Hill's N2	Minimum	Maximum	Optimum	Tolerance	SD
63	*Navicula cryptocephala* Kützing	17	8.6	0.0	4.7	17.88	2.29	0.9
64	*Navicula cryptotenella* Lange-Bertalot	25	8.2	0.0	18.4	15.13	1.84	3.5
65	*Placoneis explanata* (Hustedt) Lange-Bertalot	2	1.7	0.0	1.3	26.30	2.47	0.2
66	*Navicula harderii* Hustedt	2	1.6	0.0	1.0	87.10	2.47	0.2
67	*Craticula halophila* (Grunow) D.G.Mann	3	1.7	0.0	1.5	24.47	6.21	0.2
68	*Navicula impexa* Hustedt	3	2.2	0.0	2.1	19.08	5.04	0.4
69	*Navicula lanceolata* (Agardh) Ehrenberg	4	2.4	0.0	3.5	47.24	1.74	0.7
70	*Eolimna minima* (Grunow) Lange-Bertalot	6	3.1	0.0	2.4	11.89	2.50	0.4
71	*Navicula pseudolanceolata* Lange-Bertalot	15	5.3	0.0	8.2	15.07	2.03	1.6
72	*Navicula pupula* Kützing var.*pupula*	19	7.3	0.0	11.4	14.20	2.34	2.1
73	*Navicula radiosa* Kützing	12	6.0	0.0	2.9	15.35	1.82	0.7
74	*Navicula subrotundata* Hustedt	3	1.9	0.0	4.2	14.93	1.41	0.7
75	*Navicula trivialis* Lange-Bertalot	21	5.3	0.0	21.8	18.50	2.12	3.5
76	*Navicula utermoehlii* Hustedt	3	2.1	0.0	2.3	49.48	2.58	0.4
77	*Navicula veneta* Kützing	7	2.3	0.0	18.6	27.22	3.21	4.1
78	*Sellaphora vitabunda* (Hustedt) D.G.Mann	4	2.3	0.0	2.1	4.51	2.72	0.4
79	*Navicula vulpina* Kützing	3	1.8	0.0	3.4	10.80	3.87	0.6
80	*Nitzschia amphibia* Grunow	4	2.7	0.0	13.5	25.29	4.97	2.7
81	*Tryblionella angustata* W.Smith	4	2.9	0.0	2.0	31.82	1.27	0.4
82	*Tryblionella calida* (Grunow in Cleve & Grunow) D.G.Mann	2	1.4	0.0	1.6	44.67	2.47	0.3
83	*Nitzschia dissipata* (Kützing) Grunowvar.*dissipata*	7	4.0	0.0	3.1	14.04	1.94	0.6
84	*Nitzschia draveillensis* Coste & Ricard	2	1.3	0.0	2.8	61.02	1.05	0.5

CodeNum	Name	N non-zero values	Hill's N2	Minimum	Maximum	Optimum	Tolerance	SD
85	*Nitzschia fonticola* Grunow	3	2.9	0.0	2.2	51.11	3.48	0.5
86	*Nitzschia gracilis* Hantzsch	13	6.2	0.0	5.0	44.54	2.98	1.0
87	*Nitzschia inconspicua* Grunow	3	1.4	0.0	2.9	54.23	4.72	0.5
88	*Nitzschia intermedia* Hantzsch	2	1.9	0.0	1.0	19.64	1.95	0.2
89	*Nitzschia lacuum* Lange-Bertalot	2	1.8	0.0	1.6	5.14	2.83	0.3
90	*Nitzschia palea* (Kützing) W. Smith	24	10.5	0.0	12.5	38.44	3.61	2.5
91	*Nitzschia paleacea* Grunow	12	5.9	0.0	6.8	43.19	2.46	1.4
92	*Nitzschia sigma* (Kützing) W. Smith	6	2.8	0.0	4.7	45.08	1.87	0.8
93	*Grunowia solgensis* (Cleve-Euler) M.Aboal	13	7.6	0.0	2.9	24.99	3.13	0.7
94	*Rhopalodia gibba* (Ehrenberg) O. Müller	7	3.1	0.0	7.3	23.79	1.70	1.3
95	*Stauroneis anceps* Ehrenberg	2	1.6	0.0	3.0	9.38	2.70	0.5
96	*Stephanocostis chantaicus* Genkal & Kuzmin	4	1.6	0.0	3.2	3.89	9.88	0.5
97	*Stephanodiscus hantzschii* Grunow	8	4.3	0.0	10.4	16.91	4.09	2.0
98	*Surirella angusta* Kützing	5	3.1	0.0	2.9	47.55	1.93	0.5
99	*Surirella bifrons* Ehrenberg	7	4.7	0.0	2.0	32.28	1.99	0.4
100	*Surirella splendida* (Ehrenberg) Kützing	2	1.5	0.0	1.7	20.88	1.16	0.3
101	*Tabellaria flocculosa* (Roth) Kützing	3	1.5	0.0	2.2	21.48	2.20	0.3
102	*Thalassiosira baltica* (Grunow) Ostenfeld	3	1.1	0.0	21.4	310.64	4.48	3.4

Appendix III Modelling equations

1 Runoff

Like the CREAMS model (Knisel, 1980), the runoff volume is estimated with the SCS (USDA Soil Conservation Service) curve number. The basin equation is as follows:

$$Q = \frac{(P-0.2S)^2}{P+0.8S} \quad [1]$$

where, Q is the runoff volume (mm), P is the rainfall (mm), and S is a retention parameter. The retention parameter S is calculated using the curve number methods, as follows:

$$S = \frac{1{,}000}{CN} \quad [2]$$

where, CN is the curve number which is an empirical parameter to predict runoff from rainfall. It is a parameter which combines land use, soil type, and the information from the soil's hydrological characters together. This method simply describes the main factors that affect the runoff process after rain, so it can be widely used in different hydrological models (Radcliffe and Cabrera, 2007).

An empirical relationship proposed by Smith and Williams (Young et al., 1989)is used to estimate the peak runoff rate. The equation is as follows:

$$Q_p = 3.79A^{0.7}CS^{0.16}(Q/25.4)^{(0.903A^{0.017})}LW^{-0.19} \quad [3]$$

where, Q_p is the peak runoff rate (m^3/s); A is the HRU area in this research (km^2); CS is the channel slope (m/km); Q is the runoff volume in mm which can be calculated by equation [2]; and LW is the watershed length-width ratio, calculated by L^2/A where L is the watershed length.

2 Soil erosion

Soil loss caused by rainfall is always estimated through Universal Soil Loss Equation (USLE) (Wischemier and Smith, 1978). Its improvement method, named MUSLE (Williams, 1975), is used to simulate soil erosion. The equation is :

$$\mathrm{SL} = \mathrm{RKLSCP} \quad [4]$$

where, SL is soil loss per unit area; R is the runoff factor (or rainfall factor if USLE is used). K is the soil erodibility factor. LS are factors about site's topography, whereL is the slope-length factor and S is the slope-steepness factor. C is the cover and management factor. P is the supporting practice factor, which is set as 1 in this research.

In order to calculate the runoff factor (R) in the Erhai catchment, an alternative equation (5) from Theurer and Clarke (1991) is used.

$$S_y = 0.22 * Q^{0.68} {Q_p}^{0.95} * KLSCP \quad [5]$$

where Sy is the sediment yield (Mg/ha). It should be noted that all three variables (Sy, Q, and Qp) are based on the unit area.

3 Potential Evapotranspiration and Soil moisture

Potential evapotranspiration (PE) is a very important factor in relation to the water balance and soil moisture. Soil moisture is one of the key factors for phosphorus transformation, so it is necessary to consider both PE and soil moisture when modelling phosphorus.

Similar to most hydrological simulations, the Penman equation (Radcliffe and Cabrera, 2007) is used to model the potential Evapotranspiration.

$$ET_P = \frac{1}{H_v}\left[\left(\frac{\Delta}{\Delta+\gamma}\right)(R-G) + \left(\frac{\gamma}{\Delta+\gamma}\right)W(e_{sat}-e)\right. \quad [6]$$

where:

ET_P=potential evapotranspiration (mm)

H_v=latent heat of vaporization (MJ/kg)

Δ =slope of saturation vapour pressure-temperature curve (kPa/°C)

γ=psychrometric constant (kPa/°C)

R =the net radiation (MJ/m2)

G =soil heat flux (MJ/m2)

W =wind function

e_{sat}=saturation vapour pressure (kPa)

e=actual vapour pressure (kPa)

The latent heat of vaporization, H_v, is calculated with the following equation:

$H_v = 2.501 - 0.0022T$ Where T is the temperature in degrees Celsius. [7]

The saturation vapour pressure is also a function of air temperature:

$e_{sat} = 0.1\exp\left(54.879 - 5.029 \ln T_k - \frac{6790.5}{T_k}\right)$ [8]

where T_k is the temperature in Kelvin. The actual vapour pressure 'e'is a function of the saturated vapour pressure (Eq 9).

$e = RHe_{sat}$ [9]

where, RH is the relative humidity (fraction), 0.6 in this research.

The slope of the saturation vapour pressure-temperature curve can be calculated using the following equation (Eq. 10):

$\Delta = \left(\frac{e_{sat}}{T_k}\right)\left(\frac{6790.5}{T_k} - 5.029\right)$ [10]

However, this equation's constant are not suitable for the Erhai Catchment as the results are close to zero. Therefore, an alternative equation is used, which is the Stanghellini equation (Stanghellini, 1987):

$\Delta = 0.004145e^{0.06088T}$ [11]

The psychrometric constant, γ ,is a function of elevation, Z_e (m), and is calculated as follows:

$\gamma = 6.6 \times 10^{-4}(101 - 0.0115Z + 5.44 \times 10^{-7}{Z_e}^2)$ [12]

The soil heat flux is calculated as a function of the air temperature for the current day and the three previous days:

$G = 0.12[T_0 - \frac{T_{-1}+T_{-2}+T_{-3}}{3}]$ [13]

where T_0 is the current day's air temperature, and the other subscripts on T refer to the number of days prior to the current day.

The original Penman wind function is employed here, as follows:

$W = 6.43 + 3.4079U$ [14]

where U is wind speed (m/s), a constant of 1 in this research.

Net radiation should also be calculated for the Potential Evapotranspiration. Net radiation to the ground surface can simply be calculated by the sum of net short wave radiation and net long wave radiation, as follows:

$R_N = R_{SN} + R_{LN}$ [15]

where, $\mathrm{R_N}$ is the net radiation; $\mathrm{R_{SN}}$ and $\mathrm{R_{LN}}$ are net short wave and net long wave respectively, the calculations for which are detailed below.

Incoming short wave radiation is a fraction of the extraterrestrial radiation that is received at the top of the earth's atmosphere. It is affected by dust, water vapour, clouds, and elevation. Therefore, several methods have been proposed to calculate the correction factors of incoming short wave radiation according to the effect of atmosphere or clouds, such as U. S. Fish and Wildlife Service (USFWS,

1984), American Society of Civil Engineers (ASCE, 1996). However, a limited comparison of these methods at the Goodwin Creek watershed in Mississippi (Blackmarr, 1995) showed that incoming short wave radiation in average values of 197, 209, and 206 W/m^2, respectively, with very little variation from year to year. In the current study we therefore set the value of R_{SN} to 200 W/m^2.

There are also several methods for calculating net long wave radiation. In this research, the USFWS method is used (Eq 16-18).

$$R_{LN} = \sigma(T + 273.16)^4[\left(0.61 + 0.05\sqrt{e}\right)(1 + 0.17C^2) - \varepsilon \qquad [16]$$

$$e = 6.11\exp\left(\frac{22.46T_D}{272.62+T_D}\right) \text{ (for air temperature below 0 ℃)} \qquad [17]$$

$$e = 6.11\exp\left(\frac{17.62T_D}{243.12+T_D}\right) \text{ (for air temperature above 0 ℃)} \qquad [18]$$

where, σ is Stefan-Bolzmann constant (5.672×10-8 W m^{-2}K^{-4}); and e is vapour pressure; ε is emissivity of the ground and vegetative surface which is set as 0.98.

Soil moisture is caculated using the water balance equation. In most hydrology models, such as AnnAGNPS, SWAT, RUSLE, EPIC and so on, multi soil layer would be considered in the model. Irrigation amounts and tillage conditions are always considered in the model. Only one soil layer is currently included in this STELLA model, and it does not take irrigation or tillage into account to simplify the process. Only precipitation, runoff, and potential evapotranspiration are considered.

$$SM = \frac{WI-Q-ET}{Z} \qquad [19]$$

where, SM is the soil moisture (fraction); WI is the water input replaced by the precipitation here (mm); Q is the surface runoff (mm); Z is the thickness of thesoil

layer (mm), which is set at 600 mm in this research.

4 Phosphorus Cycle

Phosphorus (P) cycling in the soil mainly refers to phosphorus cycling in the EPIC model. The pool of labile P directly receives phosphorus from fertilization, and dissolved P immediately balances with active inorganic P in soil. While active inorganic P slowly balances with stable inorganic P. Plant decomposition produces fresh organic P which will decrease during mineralization or increase during immobilization. Some amount of fresh organic P will transfer to stable organic P and stable organic P also provides labile P for the pant through mineralization. To calculate the plant decomposition rate, the soil organic pool and its decomposition rate must be calculated.

The detailed equations of phosphorus are found in Jones et al. (1984a). The export of phosphorus by runoff is treated separately here. The magnitude of the phosphorus export coefficient depends on the intensity of rainfall or runoff. Therefore, the export coefficient can be expressed as a function of runoff. The exponent function between runoff and phosphorus export was simplified for the primary research. Fig. a1 shows the loops of phosphorus in soil.

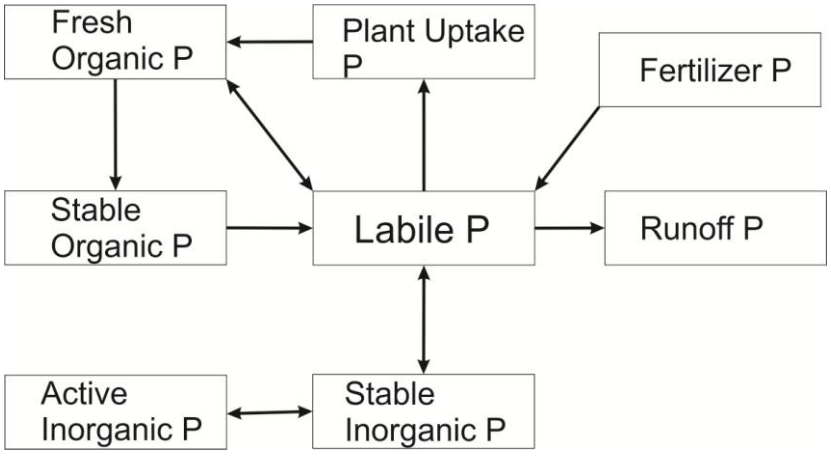

Figure a1 Pools and flows of Phosphorus (modified from (Jones et al., 1984a))

Plant uptake P is one of the important factors, which determine the P loss from the Labile P pool. In EPIC, the rate of P uptake is controlled either by plant demand or by its ability to take up P from the soil on a given day. Plant demand for P is the difference between the actual plant P content and the P content of a plant of identical biomass at optimum plant P content. The optimum P content is a function of plant growth stage (Jones et al., 1984a; Jones et al., 1984b). Several parts of plants should be considered, such as leaf, seeds, and roots. Undoubtedly, this increases the model's complexity, and requires lot of data. For longer period simulation, it is unnecessary to divide all crops into different stages, as most of the remains of crops are returned to the soil as fertilizer. Only seeds are removed from the system. Therefore, a mass balance is employed here to calculate P loss by plant uptake. Crop productions are employed to calculate the P uptake by crops. The records of crop productions were from Dali statistic yearbook. The ratio for phosphorus composition is about 0.000135 for the crop. Plant uptake P in each HRU is calculated as the following equation:

$$\mathrm{P_p} = \mathrm{PR_{plant}} * \mathrm{C_{prod}} * A \qquad [20]$$

where, $\mathrm{P_p}$ is the plant uptake P; $\mathrm{PR_{plant}}$ is the phosphorus ratio in plant; $\mathrm{C_{prod}}$ is the crop productions;A is the HRU area.

The organic residue pool cannot directly influence the abundance of P in the soil. But the rate of decomposition is used to calculate P gross immobilization from labile P pool to residue pool. Therefore, its value determines P loss from labile P pool. The organic content is calculated as the below:

$$\mathrm{O_c} = \mathrm{C_{prod}} * \mathrm{F_{pf}} * \mathrm{F_{Or}} \qquad [21]$$

where, $\mathrm{O_c}$ the organic matter from crop; $\mathrm{F_{pf}}$ is fraction of organic content in crop;

F_{Or} is the fraction of residue organic matter to seed.

Only the bioavailable particle P (BPP) is considered in the model. It always attaches at eroded sediment during runoff. An enrichment ratio is introduced for calculating BPP accumulations, which represents the P concentration in eroded sediments divided by the P concentration in the surface soil. Normally, the value of ER decreases as erosion increases (Sharpley et al., 1991). ER can be estimated through the following equation:

$$\ln \mathrm{ER} = 1.21 - 0.16 \ln(\text{soil loss}) \quad [22]$$

where, soil loss represent erosion in each HRU (kg/ha).

The BPP is estimated by following equation:

$$\mathrm{BPP} = \text{soil BP} * \text{Sediment in runoff} * \mathrm{ER} \quad [23]$$

where, soil BP is the bioavailable P in the soil (mg/kg) which is replaced by labile P from the model.

5 Phosphorus recycling from in lake

A differential equation (Carpenter et al., 1999b; Scheffer et al., 2001) was employed to simulate P dynamic in the lake. The equation is as follows:

$$\frac{dP}{dt} = a - b * P + r * \frac{P^8}{P^8 + h^8} + \sigma P dw \quad [24]$$

where P means phosphorus in lake; a represents phosphorus from catchment that promotes phosphorus dynamic in lake; b is the loss rate of phosphorus in lake, which is set as 1 in this case; r is the maximum internal phosphorus recycling rate (=1 in this case); h is a threshold, and is set as 0.85; noise is express as σPdw in the equation. dw is a white noise which is replaced by the function of random(-3, 3, 8) in STELLA. σ is the scaling factor which is set as 0.2.